Université catholique de Louvain

Faculté de Pharmacie et des Sciences Biomédicales

Institut de Recherche Expérimentale et Clinique

Pôle de Recherche Cardiovasculaire (CARD)

Exploring the role of AMPK-ACC signalling and lipid metabolism in platelet functions and thrombus formation

Sophie Lepropre

Thesis submitted in fulfillment of the requirements for the PhD degree in Pharmaceutical and Biomedical Sciences

Thesis supervisor: Pr. Sandrine Horman (IREC, CARD)

Thesis co-supervisor: Pr. Christophe Beauloye (IREC, CARD)

September 2018

Jury members

Thesis supervisor and co-supervisor

- Professor Sandrine Horman (Supervisor)

Pole of Cardiovascular Research (CARD), Institute of Experimental and Clinical Research (IREC), Université catholique de Louvain (UCL), Brussels, Belgium.

- Professor Christophe Beauloye (Co-supervisor)

Pole of Cardiovascular Research (CARD), Institute of Experimental and Clinical Research (IREC), Université catholique de Louvain (UCL), Brussels, Belgium.

UCL jury members

- Professor Etienne Marbaix (President)

Department of Pathological Anatomy, Cliniques universitaires Saint-Luc, Université catholique de Louvain (UCL), Brussels, Belgium.

- Professor Françoise Bontemps

Purine Research Group, de Duve Institute (DDUV), Université catholique de Louvain (UCL), Brussels, Belgium.

- Professor Stéphane Eeckhoudt

Department of Hematology, Cliniques universitaires Saint-Luc, Université catholique de Louvain (UCL), Brussels, Belgium.

- Professor Laurent Knoops

Department of Palliative Care, Cliniques universitaires Saint-Luc, Université catholique de Louvain (UCL), Brussels, Belgium.

- Professor Jean-Louis Vanoverschelde

Pole of Cardiovascular Research (CARD), Institute of Experimental and Clinical Research (IREC), Université catholique de Louvain (UCL), Brussels, Belgium.

External jury members

- Professor Pierre Fontana

Department of Haemostasis, Hôpitaux Universitaires Genève (HUG), Geneva, Switzerland.

- Professor Steve Watson

Institute of Cardiovascular Sciences, College of Medical and Dental Sciences, University of Birmingham, Birmingham, United Kingdom.

Remerciements

Ça y est ! Mon tour est venu de clôturer mon manuscrit de thèse mais surtout de prendre l'occasion de remercier toutes les personnes qui ont participé à ma formation, à l'aboutissement de ma thèse et à mon épanouissement professionnel et personnel.

Mes plus chaleureux remerciements s'adressent au Professeur Sandrine Horman. Merci Sandrine de m'avoir donné l'opportunité de me joindre à votre équipe et surtout de m'avoir proposé un projet si innovant et original. Je n'en doute pas que cela a grandement contribué au succès de mon travail. Merci pour votre soutien quotidien, pour les nombreuses heures de réunion et pour les multiples abstracts, présentations et posters revus et corrigés. Merci de m'avoir donné la précieuse opportunité de présenter nos travaux lors de congrès, cela a grandement contribué à mon apprentissage. Finalement, je voulais également vous remercier pour votre investissement envers le bon fonctionnement de tout le labo. Grâce à vous, il y a toujours une solution face aux problèmes administratifs, techniques et personnels. Je vous en suis très reconnaissante.

Je voudrais ensuite remercier le Professeur Christophe Beauloye pour son entrain, son intérêt et sa motivation pour la recherche. Merci Christophe pour vos nombreuses idées et hypothèses de travail. J'ai pu encore en témoigner au retour de l'ESC, il y a quelques jours, lors duquel une présentation « plaquette » vous a insufflé une nouvelle hypothèse « oxLDL-phosphoACC ». Ce qui a d'ailleurs suscité la remarque d'un jeune médecin : « mais comment faites-vous pour gérer toutes les idées de Christophe ? ». Eh oui, ce n'est pas toujours facile de faire la part des choses entre celles qui sont « super urgentes », « très urgentes » et « urgentes ». Mais au final, cela crée un environnement de travail très stimulant et enrichissant et je vous en remercie. Merci pour les discussions scientifiques, merci d'avoir valorisé autant notre projet et de nous avoir donné cette unique opportunité de le présenter devant les médias.

Un immense merci au Professeur Cécile Oury pour s'être investie dans nos projets. Merci pour votre accueil si chaleureux au sein de votre laboratoire, vos nombreux conseils, vos encouragements et votre optimisme. Cela fut une grande satisfaction de vous avoir à mes côtés. Merci également de nous avoir introduit à votre réseau de collaborateurs, qui nous ont, à leur tour,

permis d'améliorer grandement la qualité de notre travail. Merci pour votre bonne humeur, c'était toujours un plaisir de vous retrouver en congrès ou à Liège.

Je remercie également le Professeur Luc Bertrand pour ses précieux conseils scientifiques, aussi bien pour tester de nouvelles hypothèses que pour des mises au point expérimentales. Merci également pour votre esprit scientifique critique.

Je tiens à remercier les membres de mon comité d'encadrement, les Professeurs Etienne Marbaix, Françoise Bontemps, Stéphane Eeckhoudt, Laurent Knoops et Jean-Louis Vanoverschelde pour le temps consacré au suivi de ma thèse ainsi que pour leurs encouragements. I have had the privilege of having Professors Pierre Fontana and Steve Watson, two renowned experts in the field of platelets, as my thesis external members. Thank you for the enriching and stimulating discussion during my private defense and the judicious advice to improve my manuscript.

Un énorme merci à Marie, qui m'a soutenue et écoutée plus d'une fois. Cela m'a fait tellement du bien de pouvoir discuté de mes problèmes « plaquettes » avec toi. J'ai été très fière de pouvoir t'encadrer pour ton mémoire, lors duquel j'ai directement pû apprécier ta rigueur scientifique et technique. Un immense merci à toi et à Audrey pour votre support morale et scientifique lors de notre reviewing. Je n'aurai pas pû compter sur une meilleure équipe.

Je remercie également vivement toute l'équipe du Professeur Cécile Oury, merci pour votre accueil si chaleureux, à la « liégeoise », lors de mes visites au GIGA et lors des congrès! Un merci tout particulier à Céline, Alex et Odile. Céline, merci pour tes nombreux conseils qui ont été si précieux pour guider mes premiers pas dans le monde plaquette. Merci également à Odile et Alex pour votre accueil et votre expertise pour le thrombus *in vivo*.

Merci à Shakeel pour les nombreuses discussions médicales qui m'ont permis de me sentir beaucoup plus à l'aise avec la partie clinique du projet. Merci pour ta bonne humeur et ta compagnie lors des congrès.

J'adresse un immense merci à Flo, infirmière à Saint-Luc, qui a prélevé sans relâche des litres et des litres de sang, qui nous ont permis de mener à bien

nos projets de recherche. Un tout grand merci Flo pour ta gentillesse, ta disponibilité et ta bonne humeur.

Je remercie également Mini-Sophie pour ta joie de vivre, ton rire et ton sourire permanent. Cela a permis de détendre plusieurs fois l'atmosphère lors de discussion « oxLDL ».

Merci aussi à Marie-Blanche pour avoir guidé mes premiers pas au labo.

Quel bonheur d'avoir pu réaliser ma thèse entourée de collègues extraordinaires : Edith, Cécile, Flo, Anne, Carole, Marine A., Laura, Justine, Bubs, Sylvain, Marine D., Julien et Vangelis. Merci à tous pour votre soutien, votre écoute, votre bonne humeur, vos dons de sang et pour tous les moments hors labo passés ensemble. Grâce à vous, mes 5 années de thèse resteront véritablement mémorables. Et surtout, n'hésitez pas à me recontacter que ce soit pour une vente de boucle d'oreilles ou l'organisation d'une photo de labo. Merci également à Gauthier, Auré, Mag et Julien pour votre accueil au sein du labo. Un grand merci au NEDI sans qui les pauses de midi seraient beaucoup moins divertissantes. Un merci tout particulier à Delphine, pour son aide si précieuse dans les élevages de souris (même lors d'encombrement spatial). Tu es généreuse et toujours prête à rendre service à la communauté avec efficacité. Je t'en suis très reconnaissante.

Je remercie chaleureusement tous mes amis pour les sorties/voyages, pour votre bonne humeur et votre présence à mes côtés.

Merci à ma famille pour leur soutien au cours de ces années et d'être là pour moi.

Pour terminer, je remercie Ivan de m'avoir épaulé tout au long de ce parcours, merci pour ta patience, tes attentions quotidiennes et surtout pour toute la fierté que tu portes à mon égard.

Summary

Platelets are central actors in haemostasis and thrombosis. We previously showed that AMP-activated protein kinase (AMPK) α1 is activated in platelets upon thrombin or collagen stimulation and, as consequence, phosphorylates and inhibits its *bona-fide* substrate, the acetyl-CoA carboxylase (ACC). Since ACC is crucial for the synthesis of fatty acids, which are essential for platelet structure, energy storage and signalling, we hypothesized that this enzyme plays a central regulatory role in platelet function. We used a double knock-in (DKI) mouse model in which the AMPK phosphorylation sites Ser79 on ACC1 and Ser212 on ACC2 were mutated to prevent AMPK-signalling to ACC. Suppression of ACC phosphorylation promoted injury-induced arterial thrombosis *in vivo* and enhanced thrombus growth *ex vivo* on collagen-coated surfaces under flow. After collagen stimulation, loss of AMPK-ACC signalling was associated with amplified thromboxane generation and dense granule secretion. Interestingly, lipidomic analysis revealed that ACC DKI platelets had increased arachidonic acid-containing phosphatidylethanolamine plasmalogen lipids, which are major contributors of arachidonic acid and thromboxane generation following platelet stimulation. In conclusion, AMPK-ACC signalling is coupled to the control of thrombosis by specifically modulating thromboxane and dense granule release in response to collagen. It appears to achieve this by increasing platelet phospholipid content required for the generation of arachidonic acid, a key mediator of platelet activation.

In a second part of the work, we were interested in characterizing ACC phosphorylation (phosphoACC) state in coronary artery disease (CAD) patients, a pathological situation associated with thrombin generation. In addition, its impact on platelet lipid content in diseased patients was assessed. We performed a prospective clinical trial (ACCTHEROMA), in which 188 consecutive patients admitted for coronary angiogram were included. Circulating platelets in CAD patients demonstrated significant increased phosphoACC, which was highly related to acute coronary syndrome. In addition, triglycerides (TG)/HDL-cholesterol ratio, a well-known atherogenic marker, was importantly associated with increased phosphoACC, rather than markers of thrombin generation. Accordingly, oxidized LDL activated AMPK-ACC axis *in vitro*. Finally, lipidomic analysis revealed that increased phosphoACC led to a down-regulation of intraplatelet TG lipid species in CAD patients. In conclusion, platelet phosphoACC could therefore be a potential marker for early identification of high-risk patients with suspected CAD and impact their platelet functions through changes in TG content.

Table of content

Main Abbreviations

A

AA	arachidonic acid
AC	adenylate cyclase
ACC	acetyl-CoA carboxylase
ACP	acyl-carrier protein
ADAP	adhesion- and degranulation-promoting adaptor protein
ADP	adenosine diphosphate
AMPK	AMP-activated protein kinase
APT	acyl-protein thioesterase
Arf	ADP-ribosylation factor
ASA	acetylsalicylic acid
ATIII	antithrombin III
ATP	adenosine triphosphate

B

BC	biotin carboxylase
BCCP	biotin-carboxyl carrier protein

C

Ca^{2+}	calcium
CAD	coronary artery disease
CaMKKβ	Ca^{2+}/calmodulin-dependent protein kinase kinase β
cAMP	cyclic AMP
CalDAG-GEF1	Ca^{2+}-diacylglycerol guanine nucleotide exchange factor1
CCL5	RANTES
CD40L	CD40 ligand
CD62P	P-selectin
CEACAM1	carcinoembryonic antigen-related cell adhesion molecule1

cGMP	cyclic guanosine monophosphate
COX	cyclooxygenase
$cPLA_2$	Ca^{2+}-dependent cytosolic PLA_2
CPTI	carnitine palmitoyl transferase I
CPTII	carnitine palmitoyl transferase II
CT	carboxyl-transferase
CTS	computed tomography scan
Cu^{2+}	copper
CVDs	cardiovascular diseases
CXCL7	β-thromboglobulin

D

2DG	2-Deoxy-D-Glucose
DAG	1,2-diacylglycerol
DKI	double knock-in
DMS	demarcation membrane system
DNA	deoxyribonucleic acid
DOACs	direct oral anticoagulants
DTS	dense tubular system

E

ECM	extracellular matrix
ERK5	extracellular signal-regulated kinase 5
EC	enterochromaffin cells

F

F1.2	fragments 1+2
$FADH_2$	flavin adenine dinucleotide hydrogen
FAK	focal adhesion kinase
FAS	fatty acid synthase
FcR	Fc receptor
FGF	fibroblast growth factor
FV	factor V
FXII	factor XII
Fe^{3+}	iron

G

GDP	guanosine diphosphate
GEF	guanine-nucleotide exchange factor
GLUT1	glucose transporter 1
GLUT3	glucose transporter 3
GP	glycoprotein
GPCR	G-protein coupled receptor
GPS	Gray platelet syndrome
GTP	guanosine triphosphate

H

HDAC	histone deacetylase
HETE	hydroxy-eicosatetraenoic
HPS	Hermansky-Pudlak syndrome
HSC	haematopoetic stem cell

I

Ig	immunoglobulin
IL-1β	interleukin-1β
IL-8	interleukin-8
IP3	inositol 1,4,5-trisphosphate
$iPLA_2$	Ca^{2+}-independent cytosolic PLA_2
ITAM	immunoreceptor tyrosine-based activation motif

K

KAT	lysine acetyltransferase
KDAC	lysine deacetylase
KI	knock-in
Knl	kindlin

L

LDL	low-density lipoprotein
LKB1	liver kinase B1

M

MCD	malonyl-CoA decarboxylase
MKs	megakaryocytes
MLC	myosin light chain
MLCK	myosin light chain kinase
MLCP	myosin light chain phosphatase

N

NADH	nicotinamide adenine dinucleotide hydrogen
NADPH	nicotinamide adenine dinucleotide phosphate hydrogen
NAFLD	nonalcoholic fatty liver disease
NETs	neutrophils extracellular traps
NOX	NADPH oxydase

O

OCR	oxygen consumption rate
OCS	open canalicular system
oxLDL	oxidized LDL
oxPL	oxidized phospholipid

P

PAF	platelet activating factor
PAR	protease-activated receptor
PAT	palmitoyl acyl transferase
PC	phosphatidyl-choline
PDGF	platelet derived growth factor
PE	phosphatidyl-ethanolamine
PECAM-1	platelet endothelial cell adhesion molecule-1
PF4	platelet factor4
PG	prostaglandin

PH	pleckstrin homology
PI	phosphatidyl-inositol
PI3K	phosphoinositide-3 kinase
PIP2	phosphatidyl-inositol 4,5-bisphosphate
PIP3	phosphatidyl-inositol-3,4,5-trisphosphate
PKA	cAMP-dependent protein kinase
PKC	protein kinase C
PLC	phospholipase C
PPTs	proplatelets
PS	phosphatidylserine
PSGL1	P-selectin glycoprotein ligand1

R

RANTES	regulated on activation normal T-cell expressed and secreted
RIAM	Rap1-GTP-interacting adaptor molecule
ROCK	Rho-associated protein kinase
ROS	reactive oxygen species

S

S1P	sphingosine 1-phosphate
sCD40L	soluble CD40 ligand
sema4D	semaphorin 4D
Ser	serine
SERCA	sarco-endoplasmic Ca^{2+} ATPase
SFK	src family of kinase
SIRT	sirtuin deacetylase
SM	sphingomyelin
SNAP-23	synaptosome-associated protein of 23 kDa
SNP	single nucleotide polymorphism
$sPLA_2$	secreted PLA_2

T

TATc	thrombin-antithrombin complex
TCA	tricarboxylic acid
TCIPA	tumor cell-induced platelet aggregation
TF	tissue factor
TFPI	tissue factor pathway inhibitor
TG	triglycerides
TGF-β	transforming growth factor-β
TLR	Toll-like receptor
TMAO	trimethylamine N-oxide
TMEM-16F	transmembrane protein-16F
TNF-α	tumor necrosis factor-α
TP	thromboxane /prostaglandin
tPA	tissue plasminogen activator
TPO	thrombopoietin
t-SNAREs	t- Soluble NSF(N-ethylmaleimide-sensitive factor) attachment protein receptor
TXA_2	thromboxane A_2

U

uPA	urokinase plasminogen activator

V

VEGF	vascular endothelial growth factor
VSMCs	vascular smooth muscle cells
vWF	von Willebrand factor

W

WHO	World Health Organization

INTRODUCTION

1. PLATELET OVERVIEW AND FORMATION

Platelets are cytoplasmic fragments of megakaryocytes (MKs) that circulate in the blood. They are central players in haemostasis and wound repair. Following vascular injury, collagen and proteins of the sub-endothelial extracellular matrix (ECM) are exposed to the blood stream, leading to platelet activation and the formation of a haemostatic plug at the site of injury. Platelets are therefore essential to prevent blood loss. However, if they are excessively activated, such as in a pathological situation, they constitute a threat to the human body as they will form a thrombus which may result in blood vessel obstruction. As a consequence, tight regulation of platelet activation is needed to prevent pathological thrombus formation.

Platelets are produced by the cytoplasmic division of the MKs (Figure 1), which are large, polyploid cells that originate from the haematopoetic stem cell (HSC).

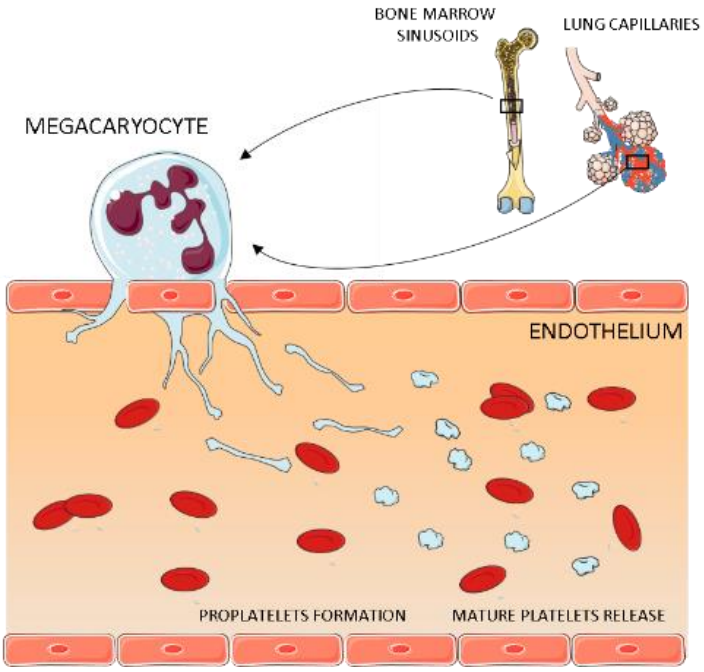

Figure 1. Thrombopoiesis. MKs, which are large and polyploid cells, migrate from their bone marrow niche to the bone marrow sinusoids or to lung capillaries, where they emit long pseudopods, called proplatelets. The latter fragment in mature platelets, acquiring all their constituents from the MKs.

Megakaryopoiesis is the process by which the HSC differentiate into MKs, a mechanism dependent on the hormone thrombopoietin (TPO) [1] and various transcription factors [2]. MKs must undergo various processes of maturation to release functional platelets. These maturation steps include the formation of polyploid MKs via endomitosis, a process consisting of several rounds of chromosomal duplication without cell division [3], the increase in platelet-specific organelles and the generation of a demarcation membrane system (DMS), which constitutes a membrane reservoir for the future released platelets [4]. Once mature, MKs are able to release platelets

via a mechanism called thrombopoiesis (Figure 1) [5]. The latter involves the migration of MKs from their bone marrow niche to the bone marrow sinusoids or to the lung capillaries [6] into which the DMS extends to form long pseudopodial extensions called proplatelets (PPTs) that fragment into platelets, inheriting granule and organelle content from the MKs. Each MK releases approximately 5000-10,000 platelets. Platelets concentration ranges from 150-400 x 10^9 per liter for a human adult whereas their concentration in mice is approximately 1000 x 10^9 per liter [7]. Platelets survive between 8-12 days in the human circulation while it is reduced to 3-4 days in mice.

2. PLATELET STRUCTURE

Platelets are discoid, anucleated cell fragments that constitute the smallest of the blood cells with a diameter of approximately 2 µm. They contain a number of distinguishable structural elements that contribute to platelet physiological role, including: a plasma membrane and the Open Canalicular System (OCS), the Dense Tubular System (DTS), a highly sophisticated cytoskeletal organization, different secretory granules and typical cellular organelles (Figure 2).

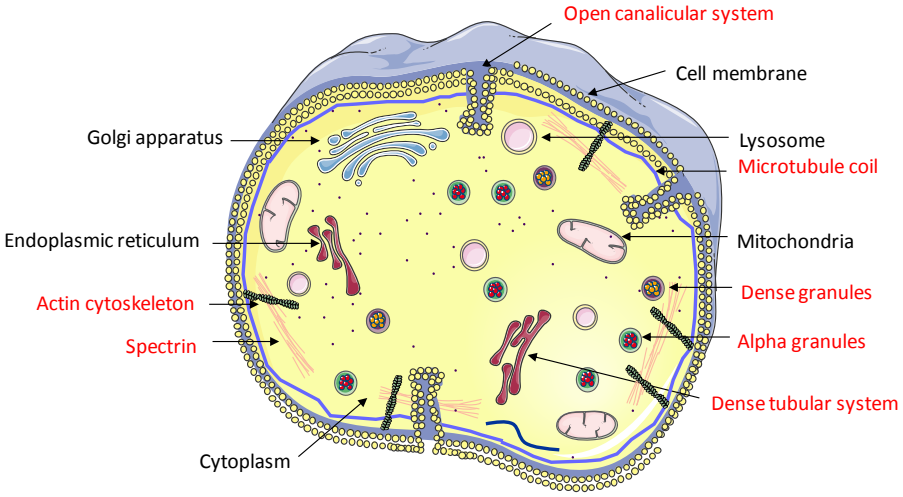

Figure 2. Platelet structure. Platelets are anuclear cell fragments that contain, in addition to elements found in other cell types, specific structures (highlighted in red) such as the open canalicular system, the dense tubular system, a highly organized cytoskeleton and different types of granules. All of these constituents are necessary for the proper execution of platelet physiological role.

2.1 Plasma membrane and the open canalicular system

Platelets are delimited by a typical phospholipid bilayer plasma membrane. A detailed description of membrane lipids composition and functions will be made on point 6.1.2. Platelet plasma membrane exhibits extensions and invaginations into the cytoplasm which form the OCS, unique to platelets. The OCS constitutes an extensive plasma membrane reservoir required when platelets spread on a surface and form plasma membranes protrusions, called filipodia and lamellipodia, that tremendously increase platelet surface area [8]. In addition, the OCS supports granules secretion and facilitates the uptake of plasma components into the platelet [9].

2.2 Dense tubular system

The DTS is a reticular membrane network originating from the endoplasmic reticulum of the MKs and constitutes a major reservoir for intraplatelet releasable Ca^{2+}.

2.3 Cytoskeleton

In the resting state, platelets have a smooth discoid shape that is maintained by a well-organized and robust cytoskeleton to withstand high shear forces in the blood stream. Upon activation, structural changes occur leading to shape change and platelet spreading. Platelet cytoskeleton consists of 3 major elements:

(1) A peripheral microtubule coil composed of polymerized α-β tubulin dimers that form a rigid tubular structure allowing platelets to maintain their discoid shape [10].
(2) A spectrin-based membrane skeleton that associates with actin filaments to provide structural support to the plasma membrane.
(3) A cytoplasmic actin cytoskeleton formed by the action of filamin and α-actinin, 2 proteins that promote actin filaments branching, organizing them into a densely packed network.

2.4 Platelet secretory granules

Platelets contain two major types of secretory granules: the alpha and dense granules. These structures store a large number of biologically

active molecules that are released upon platelet activation due to the fusion of the granules with the plasma membrane.

2.4.1 Alpha granules

Alpha granules are the most abundant platelet granules, ranging from 50 to 80 per platelet. They contain a large variety of molecules involved in various physiological/pathological processes. These include:

(1) adhesive proteins (fibrinogen, fibronectin, von Willebrand factor (vWF), vitronectin and thrombospondin) that allow platelets adhesion on the injured endothelium.

(2) chemo-and cytokines (interleukin-8 (IL-8), β-thromboglobulin (CXCL7), regulated on activation normal T-cell expressed and secreted (RANTES/CCL5) and platelet factor4 (PF4)) that recruit neutrophils and thereby influence inflammation.

(3) pro- (vascular endothelial growth factor (VEGF)) and anti-angiogenic factors (angiostatin, endostatin and thrombospondin-1) which regulate microvascular integrity.

(4) growth factors (platelet derived growth factor (PDGF), transforming growth factor-β (TGF-β)) involved in infarct healing or tumor metastasis and stability.

(5) anti-coagulants (antithrombin, tissue factor pathway inhibitor (TFPI), protein S) and coagulation factors (factor V, factor XI, factor XIII) to regulate haemostasis and thrombosis.

Alpha granules acquire their molecular content via two mechanisms: either some molecules (vWF, CXCL7 and PF4) are synthesized in the MKs and are redistributed in the newly formed platelets or they are endocytosed from the plasma via a mechanism involving the αIIbβ3 integrins [11].

Importantly, degranulation leads to the exposure on platelet surface of granule membrane markers. Among these proteins, P-selectin (CD62P) is the most highly expressed and its detection on platelet surface is used as a marker of alpha granules secretion. One of the role of P-selectin on platelet membrane is to recruit neutrophils which express the P-selectin glycoprotein ligand1 (PSGL1) receptor.

The essential role of alpha granules secretion in haemostasis is well illustrated by the mild bleeding disorders of patients suffering from the Gray platelet syndrome (GPS), characterized by a lack of alpha granules [12]. In addition, the Nbeal2-deficient mice, which recapitulate the features of GPS patients, display impaired platelet aggregation and adhesion, and decreased arteriolar thrombosis [13]. These observations highlight the critical role of alpha granules secretion in haemostasis and thrombosis.

2.4.2 Dense granules

Dense granules number is about 10 times less than alpha granules ranging from 3 to 8 per platelet [14]. They belong to a family of lysosome-related organelles and contain non-protein small molecules that mainly play a role in amplifying platelets response in a positive feedback mechanism. These include Ca^{2+} (which contributes to the electron opaque appearance of

dense granules), the nucleotides adenosine diphosphate (ADP) and adenosine triphosphate (ATP), pyrophosphates, polyphosphates and serotonin. ADP and serotonin play a crucial role in “secondary” platelet activation by binding to their receptor $P2Y_{12}$ and 5HTR2A, respectively, and in platelet recruitment to the growing thrombus (see point 3.1.5.) [15-17]. Polyphosphate, a negatively charged polymer of inorganic phosphates, contributes to thrombus formation and fibrin clot structure by modulating the coagulation cascade. Among its many roles, it initiates the contact activation pathway of blood coagulation by triggering factor XII (FXII) activation, it promotes the activation of factor V (FV) by thrombin and inhibits the anticoagulant function of TFPI [18, 19]. In contrast, it has been proposed that pyrophosphates antagonize the effects of polyphosphates [20]. However, further studies are needed to clarify its precise role.

Defects in dense granules secretion have been described in humans. Among these, the Hermansky-Pudlak syndrome (HPS) is characterized by an absence of dense granules leading to impaired platelet aggregation and therefore bleeding diathesis [21]. Similarly, mouse models of HPS display impaired platelet functions resulting in decreased thrombus formation [22, 23].

2.5 Platelet organelles

Platelets contain classical cellular organelles such as the endoplasmic reticulum, lysosomes, the Golgi apparatus and mitochondria. Among these, the mitochondria play a crucial role not only in providing energy needed for

platelet activation [24] but also in regulating platelet procoagulant activity and apoptosis [25].

3. PLATELET PHYSIOLOGICAL ROLES

3.1 Haemostasis

The major physiological role of platelets is to prevent excessive blood loss from an injured vessel by contributing to the haemostatic plug, which formation requires a well-coordinated series of events. Following injury of the vessel wall, circulating platelets become exposed to the sub-endothelial ECM, which triggers platelet adhesion and activation, resulting in the recruitment of additional platelets to the growing thrombus. Haemostatic plug formation is accelerated and stabilized by thrombin generated from the coagulation cascade. The various steps leading to thrombus formation are represented on Figure 3 and are summarized below.

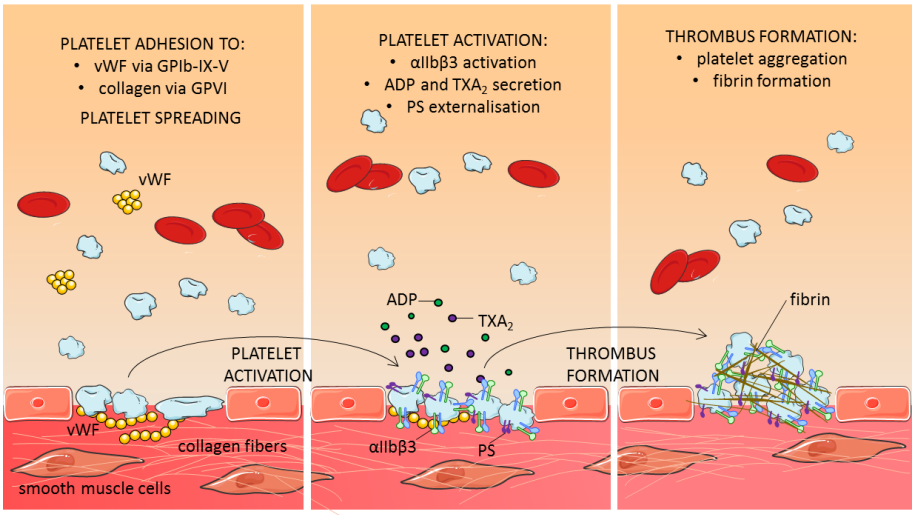

Figure 3. Steps leading to platelet activation and thrombus formation. Following vessel injury, sub-endothelial components, such as collagen fibers and the vWF binding protein, which allows circulating vWF attachment and unfolding, become exposed to circulating platelets. Collagen and vWF bind to their specific platelet receptor, respectively GPVI and GPIb-IX-V, which initiate platelets adhesion, activation and spreading. Activated platelets (1) release ADP and generate TXA_2, (2) express active αIIbβ3 fibrinogen receptor and (3) externalise PS, which respectively, recruit and activate additional platelets, allow platelet aggregation and contribute to thrombin generation. All of these factors induce the formation of a thrombus which is stabilized by fibrin formation, resulting from coagulation cascade activation. vWF: von Willebrand factor; TXA_2: thromboxane A_2; PS: phosphatidylserine.

3.1.1 Rolling and adhesion

The major mechanism of platelet rolling and adhesion on the endothelium is mediated by the interaction of platelet glycoprotein (GP) Ib-IX-V and the high molecular weight plasma protein vWF bound to the exposed collagen. This pathway is mostly involved in platelet adhesion under

elevated shear conditions (>500 sec^{-1}) as found in small arteries, which induce a conformational change of vWF, allowing its tight binding to the GPIb-IX-V. However, in conditions of low shear stress (<500 sec^{-1}) as in large veins/arteries, the contribution of vWF/ GPIb-IX-V is not essential. Instead, $\alpha_2\beta_1$ and GPVI (binding to collagen), $\alpha_5\beta_1$ (binding to fibronectin), αIIbβ3 (binding to vWF, fibrinogen and fibronectin), $\alpha_6\beta_1$ (binding to laminin), all constitute platelet membrane receptors that bind to their respective ECM-associated protein [26, 27].

The engagement of vWF/ GPIb-IX-V and GPVI/collagen axis triggers platelet activation, especially, the binding of collagen to GPVI which induces a strong and sustained platelet stimulation.

3.1.2 Spreading

Following platelet activation, major reorganization of platelet cytoskeleton occurs, leading to important morphological changes, including the formation of filopodia and lamellipodia. Filopodia are long finger-like structures that extend from the platelet cytoplasm and lamellipodia are actin-rich sheets that maximize platelet surface area to induce strong platelet adherence and stabilize the aggregate [28]. Our lab specifically showed the involvement of the AMP-activated protein kinase (AMPK) pathway and the downstream phosphorylation of cytoskeletal targets in this process (see point 9.6.) [29].

3.1.3 Integrin αIIbβ3 activation

Platelet activation induces a conformational change of the αIIbβ3, from a low affinity to a high affinity state for fibrinogen (see point 4.3.). This new conformation strongly binds to plasma- or platelet-derived fibrinogen which leads to stable platelet adhesion and aggregation.

3.1.4 Secretion

Platelet activation leads to the release of the secondary mediators (ADP, serotonin, fibrinogen,…) contained in the alpha and dense granules, which further potentiate thrombus growth by recruiting additional platelets and promoting their activation (see point 3.1.5.). Even though both granules are released upon platelet activation, the mechanisms leading to either alpha or dense granules secretion differ [14]. Indeed, treatments affecting alpha granule release do not necessarily modulate dense granule secretion or vice-versa, indicating that these events are independent of each other. Among others, the involvement of the actin cytoskeleton [30], the different proteins of the exocytosis machinery [23, 31] and the various protein kinase C (PKC) isoforms [32, 33], all explain the differential secretory responses between dense and alpha granules.

3.1.5 Thrombus formation

Platelet activation and accumulation at the lesion site lead to thrombus formation. Strong evidences indicate that, both in mice [34] and human [35], the thrombus is composed of a heterogeneous population of activated platelets forming a very hierarchical structure (Figure 4).

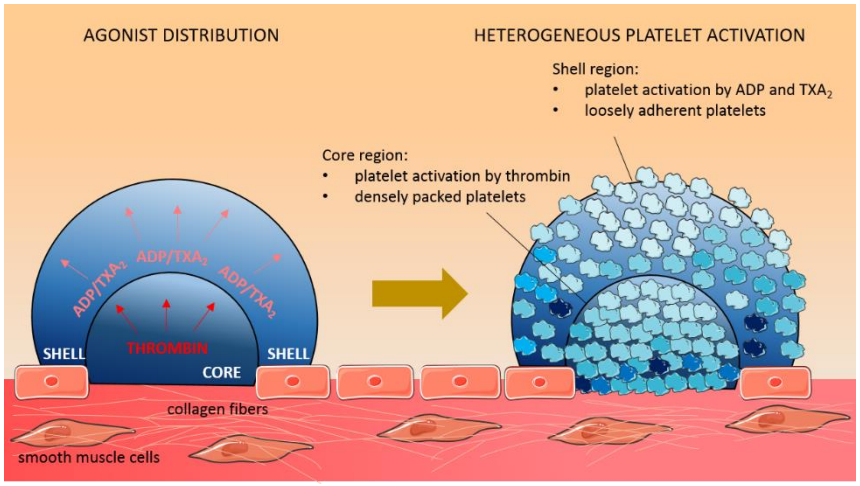

Figure 4. Hierarchical organization of the haemostatic plug. A thrombus is composed of two different regions, a core and a shell, distinguished by their agonist content and the level of platelet activation. The core region, which is in close contact with the injured endothelium, where thrombin concentration is the highest, contains highly activated and packed platelets. They release ADP and TXA_2, generating a gradient of secondary agonists, which recruit and activate additional platelets into the shell region. TXA_2: thromboxane A_2.

The haemostatic plug is composed of two distinct regions defined by the level of platelet activation and packing density which depend on the nature of the agonist and its distribution. The core region, in close contact with thrombin generated at the site of injury, is composed of tightly packed and highly activated platelets. It is surrounded by a shell composed of loosely attached platelets mainly recruited by the action of ADP and thromboxane (TXA_2) secreted by the activated platelets in the core. While ADP signalling plays a role in initial platelet deposition and secondary aggregation, TXA_2 is only important for the latter [15]. Accordingly, treatment of platelets with acetylsalicylic acid (ASA, aspirin), a cyclooxygenase (COX)-1 inhibitor

preventing TXA_2 generation, and ADP-receptor antagonists reduce platelet deposition and aggregate formation [15, 36-38].

TXA_2 and ADP release contributes to thrombus growth not only by promoting platelet aggregation but also by recruiting circulating platelets in the thrombus, bringing them in sufficiently close contact to allow platelet surface molecules to interact with each other and induce a contact-dependent signalling [39]. For example, semaphorin 4D (sema4D) which is found on the surface of platelets, allows their close contact and potentiates collagen/GPVI signalling [40]. Accordingly, sema4D$^{-/-}$ mice display decreased intra-thrombus platelet deposition [34]. In addition, various adhesion/junction proteins, such as the platelet endothelial cell adhesion molecule-1 (PECAM-1) and the carcinoembryonic antigen-related cell adhesion molecule 1 (CEACAM1), modulate platelet aggregation through contact dependent events [39, 41].

3.1.6 Thrombus stabilization

Thrombus stability is enhanced by the formation of a dense fibrin network that prevents thrombus disaggregation and consequently its embolization. Fibrin is generated from fibrinogen cleavage by thrombin, the resulting product of the coagulation cascade (Figure 5).

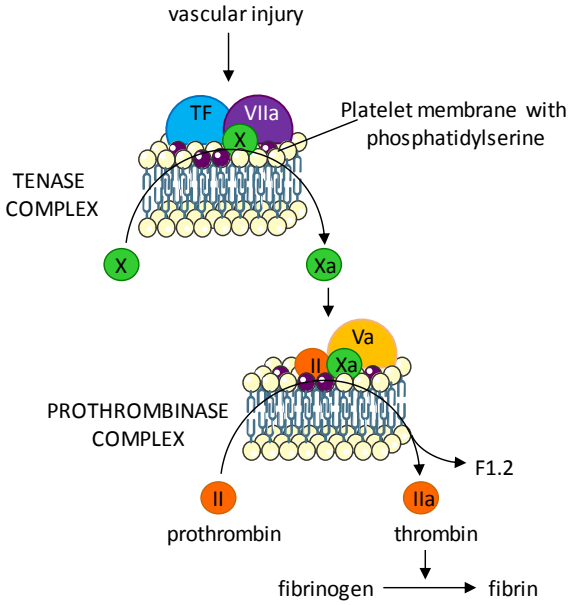

Figure 5. Roles of platelet phosphatidylserine in the extrinsic pathway of coagulation. The extrinsic pathway of coagulation is triggered by TF, released from injured endothelium. TF associates with factors IX and VIIa on negatively charged PS of activated platelets to form the tenase complex. The latter activates factor X, which, in addition to factor Va, binds to PS, generating the prothrombinase complex which cleaves prothrombin into thrombin and F1.2. Finally, thrombin converts fibrinogen into fibrin which stabilizes the clot. TF: tissue factor; PS: phosphatidylserine; F1.2: fragments 1+2.

The extrinsic pathway of coagulation is triggered by the tissue factor (TF) present on the injured endothelial cells and the smooth muscle cells of the vessel wall. The cascade activation is largely dependent on phosphatidylserine (PS) exposed on the outer membrane of activated platelets. PS constitute a platform for the Ca^{2+}-dependent assembly of coagulation factors complexes, the tenase and prothombinase. The extrinsic tenase complex is composed of the TF and the coagulation factor VIIa which

activate the factor X whereas the prothrombinase complex, consisting of factors Xa and Va, converts prothrombin (factor II) to thrombin (factor IIa) and the prothrombin fragments 1+2 (F1.2), both produced in equimolar concentrations. This leads to a strong increase in thrombin generation on the surface of PS-exposing platelets [42]. Finally, thrombin, besides being a strong platelet activator and further enhancing the coagulation cascade through positive feedback, converts the soluble fibrinogen into insoluble fibrin.

The activation of the coagulation cascade is tightly regulated to prevent excessive thrombin generation which is deleterious. Among the mechanisms involved, antithrombin III (ATIII) is a very effective thrombin inhibitor by sequestering it in a complex called the thrombin–antithrombin complex (TATc) [43]. In clinical practice, the dosage of TATc [44], in addition to F1.2 assay, is used as an indicator of thrombin generation.

3.1.7 Clot retraction

The interaction of fibrinogen with its receptor αIIbβ3 induces the "outside-in signalling" (see point 4.3.2.) which triggers an important platelet cytoskeletal remodelling that contracts the thrombus. Mice displaying a selective impairment in αIIbβ3 outside-in signalling show defective clot retraction [45].

3.1.8 Fibrinolysis

The last step of haemostasis, called fibrinolysis, involves the dissolution of the fibrin network, constituted by the cross-linking of fibrin monomers, each composed of one E and two D domains (Figure 6).

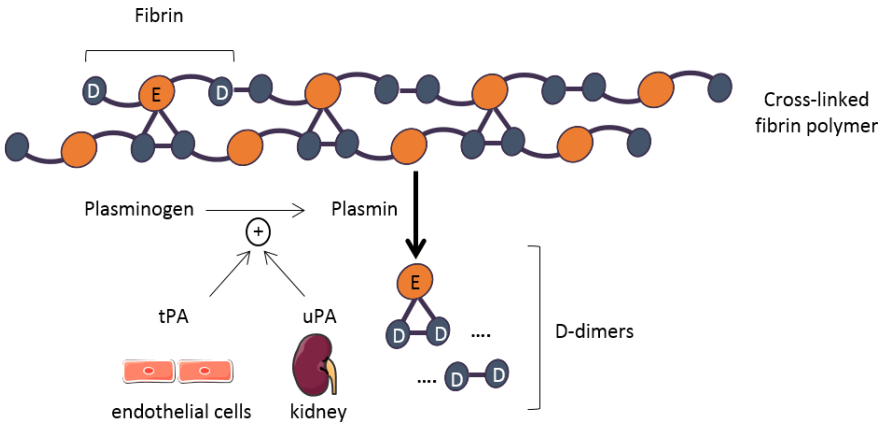

Figure 6. Fibrinolysis. Fibrin is formed by the cross-linking of fibrin monomers, composed of one central E and two lateral D domains. Fibrin is degraded by plasmin into D-dimers. Plasmin is generated following plasminogen activation by tPA or uPA, released by endothelial cells or the kidney, respectively. tPA: tissue plasminogen activator; uPA: urokinase plasminogen activator.

Fibrinolysis requires plasminogen activation which is initiated by its binding, on a fibrin surface, to the tissue plasminogen activator (tPA), released from endothelial cells, or to the urokinase plasminogen activator (uPA), generated by the kidney. Activated plasminogen is converted to plasmin which cleaves fibrin resulting in the formation of fragments

composed of two D domains, called D-dimers, which can be assayed clinically as indirect markers of thrombin generation.

3.2 Other emerging roles

In addition to their well-described role in haemostasis, platelets participate in other crucial processes including angiogenesis and inflammation, two major characteristics which inevitably involve them in carcinogenesis [46].

3.2.1 Platelets interfere with cancer cells proliferation and death and induce angiogenesis

Platelets alpha granules contain growth factors such as PDGF and TGF-β which are released upon platelet activation. Among them, TGF-β has been shown to stimulate the proliferation of ovarian cancer cells [47]. In addition, platelets microparticles induce the propagation of lung carcinoma cells [48]. Platelets do not only increase tumor cell proliferation but also enhance their resistance to apoptosis. Indeed, platelet lysates incubated with leukemia cells inhibit Bax oligomerization, a crucial step in apoptosis induction [49]. The important role played by platelets on cell proliferation and death is highlighted by the observation that platelet depletion reduces tumor size and increases the efficacy of chemotherapy [50]. Platelets also release numerous pro-angiogenic factors including VEGF, PDGF, fibroblast growth factor (FGF) and insulin-like growth factor [46], which all participate in platelet-induced blood vessel formation, allowing tumor cells dissemination. In addition, platelet microparticles induce proliferation and survival of

endothelial cells [51]. Finally, platelet-derived angiopoietin-1 and serotonin promote vessels stabilization [52].

3.2.2 Platelets promote tumor invasion, metastasis and extravasation

CCL5 is a chemokine crucially involved in tumor invasion. It is secreted both by mesenchymal stem cells within the tumor and activated platelets. Following its release, it binds to CCR5 on cancer cells to promote their invasion. In addition, by directly interacting with tumor cells and providing a procoagulant surface, platelets are involved in a mechanism known as tumor cell–induced platelet aggregation (TCIPA), a process by which tumor cells do not only trigger platelet aggregation but also associate with them via various receptors. TCIPA is essential for cell metastasis as it protects circulating tumor cells from membrane damage but also prevents their recognition and elimination by the immune system [46]. Once metastasis have been transported in the circulation, they invade remote organs by binding to their endothelium and being internalized in a process called extravasation. Platelets favor tumor arrest at the endothelium since they promote endothelial activation by releasing soluble factors, such as cytokines, extracellular vesicles and proteases, which induce endothelial cells receptor expression [46].

3.2.3 Platelets, inflammation and the immune system

Clearly, by promoting inflammation, platelets exacerbate tumor microenvironment. They contain a multitude of pro-inflammatory mediators

such as TXA_2, CD40L, chemokines and cytokines, which are released upon activation [53]. In addition, they do not only induce leukocytes adhesion to the endothelium but also interact with neutrophils, initiating neutrophils extracellular traps (NETs) formation, which strongly support tumor progression [54]. Platelets also directly interact with the immune system, which plays a key role in tumor suppression. They have been shown to promote cancer cell evasion from immunosurveillance by preventing tumor cell lysis by natural killer cells but also by inhibiting tumor-infiltrating lymphocytes [46].

3.2.4 Antiplatelets agents against cancer

Given the involvement of platelets in cancer progression, various antiplatelet agents have been found to have a beneficial impact on cancer prevention.

3.2.4.1 Aspirin

By inhibiting COX, aspirin interferes with eicosanoids production and thereby has been found to reduce the risk of colorectal cancer especially [55] but also of gastrointestinal cancers [56]. Aspirin is considered as a promising cancer prevention agent and the US Preventive Services Task Force has therefore recommended the prophylaxis administration of low dose aspirin for colorectal cancer in patients at increased cardiovascular risk [57]. Even though the preventive effect of aspirin on cancer progression was attributed to its inhibitory action on COX-2, it was later shown that the antiplatelet effect of aspirin was sufficient and necessary for its anticancer action [46]. The beneficial impact of aspirin is attributed to its effect on eicosanoids

production, which have been found to promote the transformation of cells to cancer cells, to participate in angiogenesis and to be involved in TCIPA formation [58].

3.2.4.2 $P2Y_{12}$ antagonists

Another antiplatelet therapy potentially used to limit cancer growth concerns $P2Y_{12}$ antagonists. Platelets express $P2Y_{12}$ receptors which trigger a signalling cascade upon ADP binding, leading to platelet activation (see 4.2.2). It was recently shown that cancer cells release ADP to induce platelet activation, which in turn promote tumor growth [59], creating a vicious cycle. As a consequence, ticagrelor, a $P2Y_{12}$ inhibitor, reduces tumor growth in a mouse model of ovarian cancer [59]. In addition, $P2Y_{12}$ deficiency reduces the weight of lung metastasis and decreases the invasiveness of lung carcinoma cells [60]. Despite the fact that these preclinical studies indicate a beneficial impact of $P2Y_{12}$ inhibition on cancer progression, there is no clinical data available to date [61]. At this stage, it is therefore difficult to draw conclusions on their use as anticancer treatment.

4. PLATELET SURFACE RECEPTORS AND THEIR DOWNSTREAM SIGNALLING PATHWAYS

Platelets respond to environmental stimuli via a multitude of receptors on their membranes, which, when activated, trigger tightly regulated signalling cascades that crosstalk. They also express receptors for autocrine agonists, allowing positive feedback loop and a rapid burst in platelet activation. Major platelet receptors will be detailed in order of their

involvement in the growing thrombus: (1) adhesion, (2) soluble agonists and (3) fibrinogen receptors. Highlighting their importance in haemostasis, genetic mutations, leading to deficient or dysfunctional receptors, trigger bleeding disorders.

4.1 Adhesion receptors

The signalling cascades downstream of GPIb-IX-V, GPVI and integrin $\alpha_2\beta_1$ are summarized below and the two most important (GPIb-IX-V and GPVI) are represented on Figure 7.

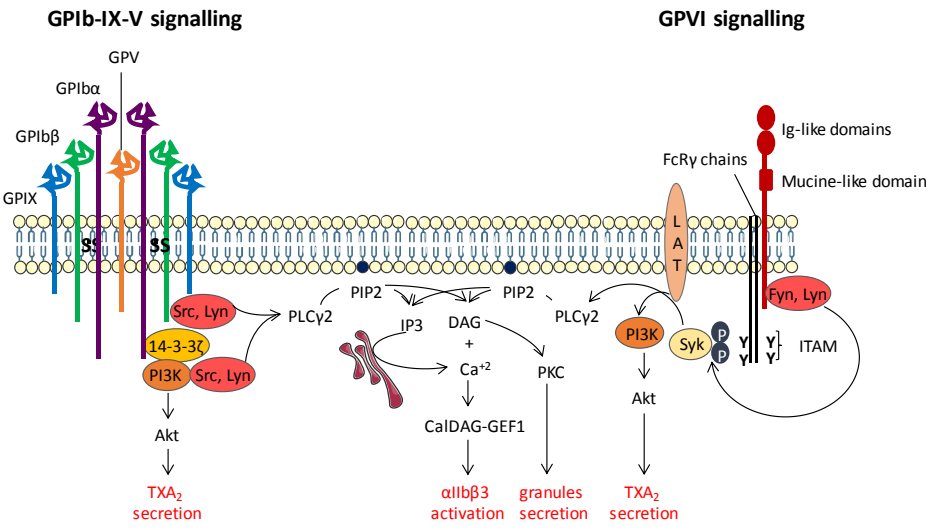

Figure 7. Signalling pathways of two major platelet adhesion receptors. Platelets adhere to the subendothelial matrix via two main receptors, GPIb-IX-V and GPVI, which trigger a signalling cascade, activating platelets. Following vWF binding to GPIb-IX-V, Src, Lyn and PI3K are activated which leads on the one hand to Akt stimulation and TXA_2 generation and on the other hand to PLCγ2 activation. The latter cleaves PIP2 into IP3 and DAG, which both contribute to αIIbβ3 activation, via CalDAG-GEF1 stimulation and to granules secretion via PKC. Collagen binding to GPVI induces phosphorylation of its FcRγ chains ITAM motifs by Fyn and Lyn. ITAM phosphorylation recruits the LAT signalosome via Syk, which finally leads to PI3K and PLCγ2 stimulation that activate platelets similarly to the GPIb-IX-V signalling pathway. PI3K: phosphoinositide-3 kinase; PLCγ2: phospholipase Cγ2; PIP2: phosphatidylinositol 4,5-bisphosphate; IP3: inositol 1,4,5-trisphosphate; DAG: 1,2-diacylglycerol; CalDAG-GEF1: Ca^{2+}-diacylglycerol guanine nucleotide exchange factor1; PKC: protein kinase C; ITAM: immunoreceptor tyrosine-based activation motif; TXA_2: thromboxane A_2.

4.1.1 vWF receptor - GPIb-IX-V complex

VWF is a highly complex protein, composed of various domains with distinct functions and structures, that is exclusively produced by MKs and endothelial cells. Before its secretion in the plasma, vWF monomers assemble into a multimeric structure of varying monomers length. Under

high shear forces only, circulating vWF multimers unfold, resulting in efficient binding to subendothelial collagen and platelet GPIbα, a subunit of the GPIb-IX-V complex, allowing the capture of circulating platelets on the injured endothelium [62, 63]. The GPIb-IX-V complex is highly expressed with 25.000 copies/platelet [64] and contains four distinct leucine-rich repeats: the two disulfide-linked subunits of GPIb (GPIbα and GPIbβ), GPIX and GPV, present at a ratio of 2:2:2:1 [64]. Following binding of vWF to the GPIb-IX-V complex, Src and Lyn associate with GPIb-IX and phosphoInositide-3 kinase (PI3K), which is bound to GPIbα via 14-3-3ζ. Src, Lyn and PI3K activation triggers a signalling cascade, including the stimulation of phospholipase C (PLC) γ2 and Akt activation, which contributes to TXA_2 generation, granule secretion as well as αIIbβ3 activation [63]. Phospholipase stimulation is a mechanism common to many intracellular signalling pathways and has therefore a central impact on platelet activation. Once activated, PLC cleaves membrane phosphatidylinositol 4,5-bisphosphate (PIP2) into inositol 1,4,5-trisphosphate (IP3) and 1,2-diacylglycerol (DAG). IP3 activates its receptor in the endoplasmic reticulum membrane, increasing cytosolic Ca^{2+}, a master regulator of platelet activation. On the other hand, DAG activates several PKC isoforms, which actively participate in platelet stimulation [65]. The combined increase in Ca^{2+} and DAG finally activates CalDAG-GEF1 (Ca^{2+}-diacylglycerol guanine nucleotide exchange factor1), which induces the small Rap1 GTPase activation and subsequent αIIbβ3-mediated aggregation (detailed on point 4.3.) [66].

In addition to binding vWF, GPIb-IX-V also interacts with E- and P-selectin, present on activated endothelial cells and platelets respectively [67], with the coagulation factors FXII and FXI and with thrombin [68].

Functional deficiency or absence of GPIbα, GPIbβ or GPIX subunits, causes an autosomal recessive disorder, called Bernard-Soulier syndrome, characterized by thrombocytopenia, large platelets and a bleeding phenotype [69].

4.1.2 Collagen receptors - GPVI and $\alpha_2\beta_1$

Collagen is a crucial component of the ECM that lines all vessel walls. The most active form includes its fibrillar rather than monomeric configuration [70] and the subtypes I and III, found in the majority of sub-endothelial matrix. Collagen is composed of GXY repeats (where G is a glycine, X and Y are frequently proline (P) and hydroxyproline (O)). Two major collagen receptors are expressed by platelets: GPVI and the integrin $\alpha_2\beta_1$. Not only do they differ by the collagen sequence recognized, with GPVI binding to GPO and $\alpha_2\beta_1$ to GFOGER, but also in their binding affinity, with GPVI having a low and $\alpha_2\beta_1$ a high affinity [71]. GPVI mainly participates in platelet activation while $\alpha_2\beta_1$ is involved in platelet adhesion.

4.1.2.1 Collagen receptor - GPVI/FcR γ-chain complex

In addition to its two well-established ligands collagen and laminin, GPVI also binds fibrin which potentiates thrombin generation and platelet recruitment to the clot [72, 73]. GPVI is composed of an extracellular domain, consisting of two immunoglobulins (Ig)-like domains and a mucine-

like part, followed by a transmembrane region and a cytoplasmic tail. The transmembrane region contains a crucial amino acid, the arginine, which allows a non-covalent interaction with the homodimeric Fc receptor (FcR) γ chains, which are vital elements of GPVI signalling. Binding of collagen fibrils on GPVI induces receptor clustering and cross-linking, leading to phosphorylation of the immunoreceptor tyrosine-based activation motif (ITAM) of the FcR γ-chain by the two Src kinases, Fyn and Lyn, which are permanently associated to GPVI cytoplasmic tail. ITAM phosphorylation triggers the binding and activation of Syk, which induces the formation of the "LAT signalosome", a complex protein network that activates PI3K and PLCγ2, leading to complete platelet activation.

Impairment of GPVI signalling due to receptor absence, has been reported to cause a mild mucocutaneous bleeding in humans [74]. In the same line, a moderate thrombocytopenia and mild bleeding are observed in the presence of anti-GPVI antibodies [75].

4.1.2.2 Collagen receptor - integrin $\alpha_2\beta_1$

Each α_2, β_1 subunit is composed of an extracellular head that assembles to form the ligand binding site. $\alpha_2\beta_1$ is almost exclusively considered as an adhesion receptor even though it also increases collagen binding to GPVI. $\alpha_2\beta_1$ and GPVI are therefore regarded as complementary for maximal platelet adhesion and activation in response to collagen. Similar to other integrins, $\alpha_2\beta_1$ conformation changes from a low to a high affinity state, following collagen binding and "inside-out" signalling [76]. It triggers a signalling pathway involving many proteins of the GPVI-FcR γ -chain

cascade (Src, Syk, and PLCγ2) [77]. Patients with low expression or reduced signalling of $\alpha_2\beta_1$, display mild bleeding and defective response to collagen [78, 79].

4.2 Soluble agonists receptors

Once activated by sub-endothelial matrix components, platelet stimulation is further potentiated by the presence of soluble agonists in their surrounding environment for which they express membrane receptors. The majority of these agonists are secondary auto- or paracrine mediators, generated by platelets themselves (thrombin, ADP, ATP and TXA_2) that transduce signal via binding to their respective receptors, which are mostly G-protein coupled receptors (GPCR), except the ATP-receptor which is a channel (Figure 8).

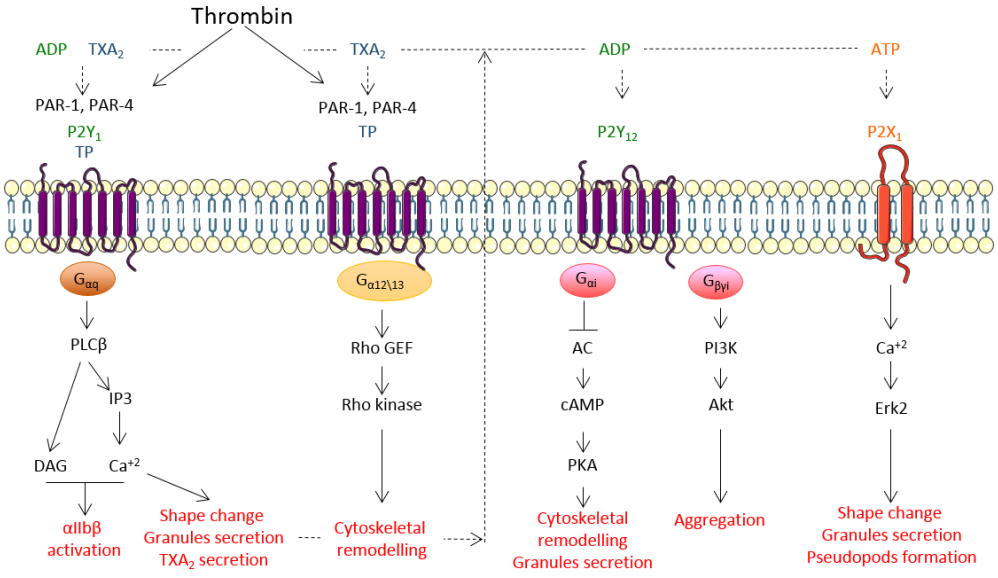

Figure 8. Signalling pathways of soluble agonists receptors. Thrombin, as well as the secondary mediators ADP and TXA_2, binds to GPCRs. In human platelets, thrombin binds to PAR-1 and PAR-4, which are coupled to Gαq and Gα12/13. Gαq activates the PLCβ, leading to IP3 and DAG generation, αIIbβ activation, granules secretion and TXA_2 generation. On the other hand, Gα12/13 induces cytoskeletal remodelling via Rho kinase. The secondary mediator TXA_2 binds to Gαq and Gα12/13 coupled receptors, similar to PARs. ADP, in addition to stimulating Gαq via its $P2Y_1$ receptor, also binds to $P2Y_{12}$ which is coupled to Gαi, inhibiting the AC, thereby decreasing PKA activity, a negative regulator of platelet activation. In addition, Gβγi promotes platelet aggregation via PI3K. ATP binding to its Ca^{2+} channel $P2X_1$, triggers Ca^{2+} entry and platelet activation. PAR: protease-activated receptor; TXA_2: thromboxane A_2; PLCβ: phospholipase Cβ ; IP3: inositol 1,4,5-trisphosphate; DAG: 1,2-diacylglycerol; GEF: guanine-nucleotide exchange factor; AC : adenylate cyclase; cAMP: cyclic AMP; PKA: protein kinase A; PI3K: phosphoinositide-3 kinase.

GPCRs are composed of seven transmembrane domains, with an extracellular N-terminal and intracellular C-terminal, which associate with a heterotrimeric G-protein, consisting of α, β and γ subunits. The latter two are inseparable, forming a Gβγ dimer, while the α subunit is bound to

guanosine diphosphate (GDP) when the receptor is inactive. Following ligand binding, GDP is replaced by guanosine triphosphate (GTP) which destabilizes the three subunits complex and leads to Gα dissociation from Gβγ. Even though both the Gα and the Gβγ subunits can all individually induce a signalling cascade, the nature of the activation pathway mostly depends on the Gα subunit. The activation signal ends when Gα hydrolyzes GTP to GDP, leading to Gα and Gβγ reassembly. Various sub-classes of Gα have been characterized. Among them, platelets express the Gαs, Gαq, Gα12/13 and Gαi.

4.2.1 Thrombin Receptors - Protease Activated Receptors (PARs)

Thrombin is a soluble plasma serine protease that is generated via the coagulation cascade on the surface of activated platelets. It is a major platelet agonist that leads to strong stimulation [80] but also contributes to endothelial cells activation (vWF release and E-selectin expression) [81] via its binding to the protease-activated receptor (PAR). Four PARs members have been characterized: PAR-1, PAR-2, PAR-3, and PAR-4, with PAR-2 exceptionally not binding thrombin. Among these, human platelets express PAR-1, their major thrombin receptor [82], and PAR-4, being secondary, while the role of the latter is predominant in mice platelets. In addition to PAR-4, mice platelets also express PAR-3 which does not trigger a signalling cascade but rather acts as a co-factor that binds thrombin and localizes it in proximity to PAR-4 [80]. Thrombin mediates PAR activation via a proteolytic cleavage of its N terminal extracellular loop that contains a thrombin cleavage site LDPR/S [83]. Following thrombin cleavage, a new N-terminus is

generated that constitutes the receptor ligand. Both PAR-1 and PAR-4 are coupled to the G proteins Gαq and Gα12/13, which respectively lead to PLCβ activation, triggering IP3 and DAG generation as detailed above, and Rho kinase stimulation, inducing cytoskeletal remodelling and platelet activation [80, 84]. Tight regulation of signalling is essential to prevent excessive platelet stimulation. Regarding PARs, the activating signal is switched off due to receptor desensitization following the phosphorylation of its cytoplasmic tail or its internalization and degradation in lysosomes [85].

Given thrombin's strong effect on platelet activation and its pleiotropic impact on blood cells and vessels, drugs that target the coagulation cascade (anticoagulants) are widely used in clinical practice. For many years, warfarin, a vitamin K (an essential co-factor of the coagulation cascade) antagonist, and heparin, which potentiates the inhibitory action of ATIII, were the most widely used anticoagulants. More recently, direct oral anticoagulants (DOACs) have been developed and are used for the treatment of thrombosis. They either directly inhibit thrombin (dabigatran), preventing stable clot formation, or inhibit factor Xa (rivaroxaban, apixaban and edoxaban), interfering with the prothrombinase activity, thereby blocking prothrombin cleavage to thrombin [86].

4.2.2 ADP receptors - $P2Y_1$ and $P2Y_{12}$

In addition to being secreted by injured endothelial cells and red blood cells, ADP is released from platelet dense granules, one of the earliest event of platelet activation. Even though ADP is weaker than thrombin, it leads to complete platelet activation and is crucial for thrombus shell build-

up as explained on point 3.1.5. The two ADP receptors expressed on platelets are $P2Y_1$ and $P2Y_{12}$, which are associated with Gαq and Gαi, respectively. In order to regulate platelet reactivity towards ADP, both receptors are submitted to endocytic trafficking, which allows platelets to become desensitized (receptor internalized) and resensitized (receptor is recycled back to the membrane) after agonist disappearance [87]. $P2Y_{12}$ is approximately four times more expressed in platelets as compared to $P2Y_1$ [88]. Both receptors are crucial for a complete and coordinated platelet response to ADP, with $P2Y_1$ being involved in the early stages of platelet aggregation and shape change, while $P2Y_{12}$ allows potentiation of platelet function and strong aggregation [88].

4.2.2.1 $P2Y_1$

$P2Y_1$ is associated with Gαq, which as explained above, activates the PLCβ, which induces the release of IP3 and DAG, increasing intracellular Ca^{2+} and PKC activity, allowing platelet shape change and granule secretion.

4.2.2.2 $P2Y_{12}$

By binding to ADP, $P2Y_{12}$ potentiates platelet response to secondary mediators. $P2Y_{12}$ activates Gαi which inhibits the adenylate cyclase (AC), leading to decreased cyclic AMP (cAMP) generation and therefore to attenuation of the protein kinase A (PKA) activity. PKA is a negative regulator of platelet activation by inhibiting Ca^{2+} mobilization, aggregation, granules secretion and cystoskeletal remodelling [89]. In addition to relieving PKA

inhibition on platelet function via Gαi, $P2Y_{12}$ coupling to Gβγi leads to PI3 kinase, Akt and Rap1b activation, increasing platelet aggregation.

Given its crucial role on platelet function, $P2Y_{12}$ irreversible inhibition by thienopyridines (ticagrelor, clopidogrel, cangrelor, elinogrel and prasugrel) constitutes an important therapeutic strategy to reduce/prevent platelet over-activation such as in the acute coronary syndrome.

4.2.3 ATP receptor - $P2X_1$

ATP released by activated platelets binds, in an autocrine way, to $P2X_1$, a ligand-gated Ca^{2+} channel that belongs to a large family of P2X channels. They are formed by the homo-or heterotrimeric assembly of various subunits, for which seven isoforms have been described ($P2X_{1-7}$). Each P2X subunit is composed of a large extracellular ligand-binding loop, two transmembrane domains, a N-terminal and C-terminal short intracellular tails. ATP binding triggers a conformational change of the extracellular loop which is transmitted to the transmembrane region, allowing channel opening and ion entry [90]. Platelets only express the $P2X_1$ homotrimer, which is responsible for the rapid Ca^{2+} entry following ATP binding. This increase in intracellular Ca^{2+} mediates Ca^{2+}-calmodulin-dependent Erk2 activation which amplifies myosin light chain phosphorylation in response to collagen, leading to cytoskeletal remodelling, shape change, granule secretion and pseudopods formation [91, 92]. One of the difficulty of studying $P2X_1$ receptor is its rapid desensitization to ATP, even in the presence of spontaneously secreted ATP under basal condition.

4.2.4 Thromboxane A_2 receptor - TP

TXA_2 is synthesized by activated platelets in response to collagen or thrombin and it stimulates and recruits additional platelets to the thrombus, similarly to ADP. Its synthesis starts with the generation of arachidonic acid (AA) (Figure 9) from membrane AA-containing phospholipid cleavage by PLA_2.

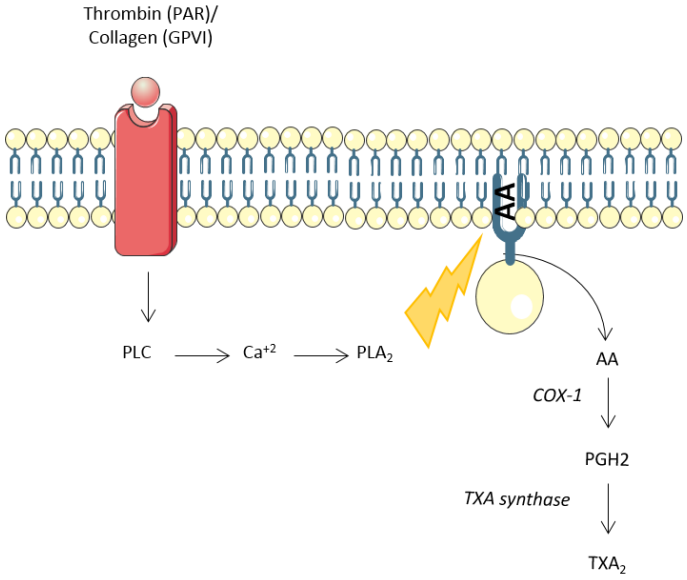

Figure 9. Mechanism of TXA_2 generation. Thrombin or collagen binding to their respective receptor, PAR or GPVI, leads to PLC activation, Ca^{2+} increase and PLA_2 stimulation. PLA_2 cleaves, among others, AA-containing phospholipids at the sn-2 acyl bond, releasing AA which is metabolized to TXA_2 via the sequential action of COX-1 and TXA synthase. PLC: phospholipase C; PLA_2: phospholipase A_2; AA: arachidonic acid; COX-1: cyclooxygenase-1; PGH2: prostaglandin; TXA synthase: thromboxane synthase; TXA_2: thromboxane A_2.

The synthesis of TXA_2 from AA includes the sequential metabolization of AA into prostaglandin (PG) H2, via the COX-1, and of PGH2 into TXA_2 via the TXA synthase. Due to its high polarity, TXA_2 freely crosses the plasma membrane and activates platelets in the vicinity in an auto- or paracrine way. TXA_2 is extremely unstable, has therefore a very short half-life and is rapidly converted to TXB_2. The latter binds to the TP (Thromboxane/Prostaglandin) receptor which has two isoforms, TP_α and TP_β, which are associated with Gαq and Gα12/13, and are both expressed on platelets [93].

The wide use of aspirin, an irreversible COX-1 inhibitor, as a major antiplatelet drug, indicates the crucial contribution of TXA_2 to platelet activation.

4.3 Fibrinogen receptor - integrin αIIbβ3

Fibrinogen and vWF, two soluble plasma proteins, and fibronectin, which exists both as insoluble protein in the ECM and soluble protein in the plasma, all represent endogenous ligands of αIIbβ3, which mediates platelet aggregation. Integrins are composed of two subunits, α and β, linked by a non-covalent interaction, each consisting of an extracellular domain containing the ligand-binding site, a single transmembrane region and a cytoplasmic tail. Mammals have 18 different α subunits and 8 β subunits, creating an important number of α- β combinations [94]. Platelets express six different integrins of which αIIbβ3 is by far the most abundant. It is expressed both on the plasma membrane but also on alpha granules, which considerably increases their surface expression when platelets are activated

due to granules fusion with the plasma membrane [95]. Following ligand binding, similarly to other integrins, αIIbβ3 switches from a low- to a high-affinity state, a conformational change induced by a signalling pathway referred as "inside-out" signalling. In addition, fibrinogen binding induces "outside-in" signalling, which participates in filopodia and lamellipodia formation, secretion and clot retraction, stabilizing the growing thrombus (Figure 10).

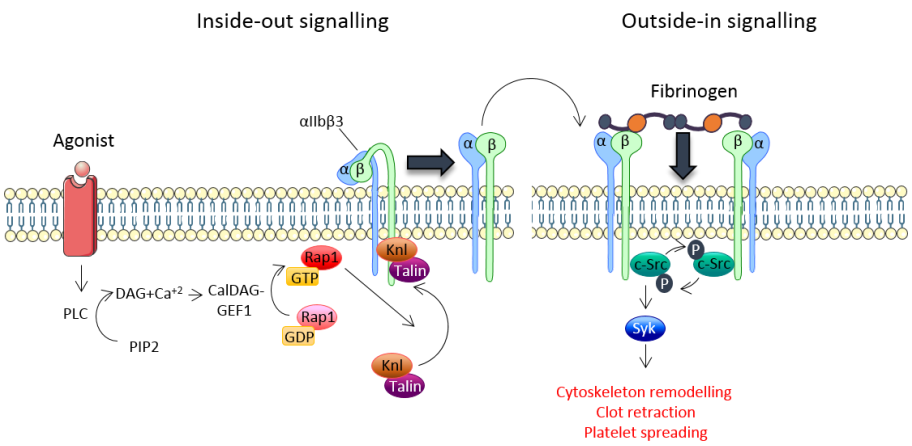

Figure 10. Inside-out and outside-in signalling. Agonist binding to its receptor triggers the formation of DAG and an increase in Ca^{2+} concentration, which both act as co-factors for the CalDAG-GEF1. The latter activates Rap1 which recruits talin and kindlin (Knl) to the β3 cytoplasmic tail of αIIbβ3, inducing its conformational change to a high-affinity state for fibrinogen. This pathway is referred as inside-out signalling. Fibrinogen binding to active αIIbβ3 induces integrin clustering and trans-autophosphorylation of c-Src. Phophorylated c-Src activates Syk which mediates cytoskeleton remodelling, clot retraction and platelet spreading. This process is referred as outside-in signalling. PLC: phospholipase C; PIP2: phosphatidylinositol 4,5-bisphosphate; DAG: 1,2-diacylglycerol; CalDAG-GEF1: Ca^{2+}-diacylglycerol guanine nucleotide exchange factor1; Knl: kindlin.

The essential involvement of αIIbβ3 in platelet aggregation is highlighted in Glanzmann thrombasthenia, a disorder caused by a genetic defect of αIIbβ3, leading to its complete absence or impaired signalling, and characterized by severe bleeding [96].

In addition, αIIbβ3 is the target of eptifibatide, abciximab and tirofiban that inhibit its ligand-binding site. These drugs are used in clinics as antithrombotic agents. However, their field of application is limited due to significant bleeding risks [97].

4.3.1 Inside-out signalling

Inside-out signalling, leading to αIIbβ3 conformational change from a low- to high-affinity state in response to platelet activation, involves a succession of activation steps that ultimately lead to talin and kindlin binding to the β3 cytoplasmic domain. Platelet agonist binding to their receptors leads to DAG generation and increase in intracellular Ca^{2+} content, two activating factors of the guanine nucleotide exchange factor CalDAG-GEF1. The latter catalyzes the exchange of GDP to GTP bound to the small Rap1 GTPase. Active Rap1-GTP promotes the interaction of talin and kindlin, two structural proteins, with αIIbβ3 cytoplasmic domain, inducing its conformation change to a high-affinity state for its ligand. The adaptor protein RIAM (Rap1-GTP-interacting adaptor molecule) was initially described as linking Rap1-GTP to αIIbβ3-talin [98]. However, recent evidence from RIAM-null mice shows that they display unaltered αIIbβ3 activation and platelet aggregation, indicating that RIAM is dispensable for integrin conformational change [99].

4.3.2 Outside-in signalling

When αIIbβ3 is in a high conformation state, c-Src, a member of the Src family of kinases (SFKs), associates with the β3 cytoplasmic tail via its SH3 domain. Ligand binding, such as fibrinogen, to αIIbβ3 induces integrin clustering and trans-autophosphorylation of c-Src, which is essential for its complete activation [100]. Active c-Src in turn phosphorylates and stimulates the tyrosine kinase Syk, which finally activates an array of proteins involved in signalling and cytoskeleton remodelling (PLCγ2, focal adhesion kinase (FAK) and adhesion- and degranulation-promoting adaptor protein (ADAP)), allowing platelet spreading and thrombus stability [100].

4.4 Novel mechanisms of platelet activation

4.4.1 CD36 receptor-oxLDL

In the last few decades, the role of platelet CD36 has been investigated, especially in the context of atherosclerosis. CD36 is one of the major glycoproteins expressed on the surface of mouse and human platelets, with ≤ 25 000 copies/platelet [101]. It belongs to the Scavenger Receptor Type B family and it is composed of two transmembrane domains, a large extracellular domain and two short cytoplasmic tails [102]. The extracellular domain can be heavily glycosylated due to the presence of 9 N-linked glycosylation sites [103]. Glycosylation is necessary for proper trafficking of CD36 to the plasma membrane [103].

CD36 possesses a wide range of ligands, which can be classified in three categories: modified phospholipids, proteins containing a thrombospondin

type I repeat and free fatty acids [101]. Among them, the signalling induced by modified phospholipids, including oxidized LDL (oxLDL), has been well described given their importance in atherosclerosis. OxLDL are formed following the oxidation of their phospholipid component or their protein ApoB-100 either by metal ions, such as Fe^{3+} or Cu^{2+}, present in atherosclerotic lesions or by enzymes, mainly the myeloperoxidase, released by macrophages or activated white blood cells [104].

OxLDL binding to CD36 activates various pathways which contribute to platelet aggregation and granules secretion (Figure 11) [105-107].

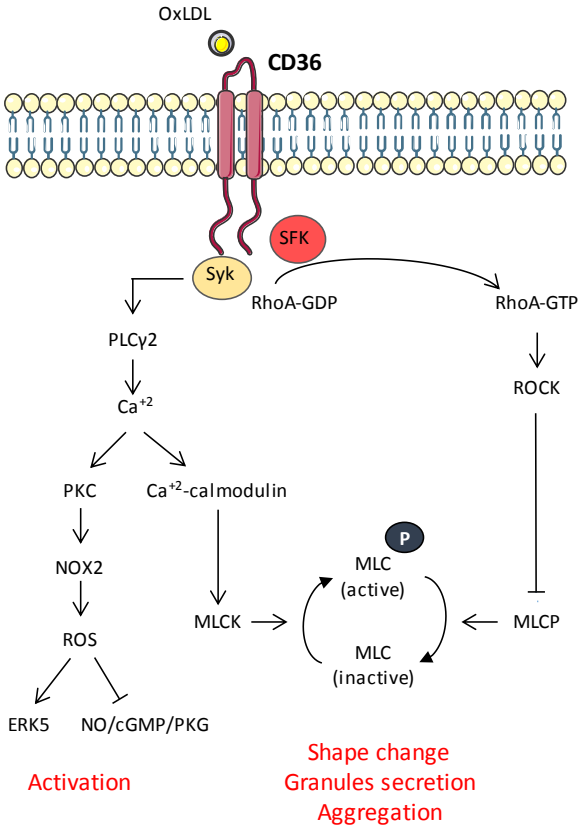

Figure 11. Signalling pathways triggered by oxLDL binding to CD36. OxLDL binding to CD36 triggers the activation of both SFK and Syk. SFK-dependent signalling leads to MLCP inhibition, resulting in increased MLC phosphorylation. On the other hand, Syk stimulates the MLCK, contributing to the potentiation of MLC phosphorylation, leading to platelet activation. Simultaneously, Syk stimulates PKC, NOX2 and ROS production which activate ERK5 and inhibit the NO/cGMP/PKG signalling, contributing to platelet hyperactivity. SKF: src family of kinase; PLCγ2: phospholipase Cγ2; PKC: protein kinase C; NOX2: NADPH oxidase 2; ROS: reactive oxygen species; ERK5: extracellular signal-regulated kinase 5; NO: nitrogen monoxide; cGMP: cyclic GMP; PKG: protein kinase G; MLCK: myosin light chain kinase; MLC: myosin light chain; ROCK: Rho-associated protein kinase; MLCP: myosin light chain phosphatase.

Wraith et al. describe the activation of two kinases downstream of CD36: Syk and SFKs [107]. On the one hand, Syk activates the PLCγ2, leading to increased Ca^{2+} concentration, similarly to GPVI signalling (see point 4.1.2). The Ca^{2+}-calmodulin complex is therefore activated and stimulates the myosin light chain kinase (MLCK), which phosphorylates the myosin light chains (MLC), enhancing shape change, granule secretion and platelet aggregation [108]. On the other hand, activated SFKs induce the formation of RhoA-GTP which stimulates the Rho-associated protein kinase (ROCK), an inhibitor of the myosin light chain phosphatase (MLCP), thereby contributing to enhanced MLC phosphorylation. Others showed the involvement of reactive oxygen species (ROS) in oxLDL-mediated CD36 signalling. Following PLCγ2 activation [106], and Ca^{2+} increase, PKC are activated, leading to NADPH oxidase (NOX) 2 stimulation and ROS generation [109]. ROS production in turn desensitizes platelets to cyclic guanosine monophosphate (cGMP) inhibitory signalling, resulting in platelet hyperactivity. In addition, ROS activate the extracellular signal-regulated kinase 5 (ERK5), which contributes to integrin activation, aggregation and thrombus formation [105].

4.4.2 The microbiota regulates platelet functions

Recently, a link between dietary nutrients, gut microbes and platelet functions has been highlighted. It was shown that trimethylamine N-oxide (TMAO), a waste product of phosphatidylcholine, choline, and carnitine-rich diet, generated by the gut microbes, leads to platelet hyperresponsiveness and increased *in vivo* thrombosis [110]. As a consequence, alteration of

TMAO metabolizing enzyme similarly affects platelet reactivity [111]. By binding to a still undefined receptor, TMAO potentiates agonist-induced Ca^{2+} release from intracellular store. Interestingly, cecal transplantation of TMAO-producing bacteria led to enhanced platelet activation and thrombosis in the recipient mice, indicating that thrombosis potential is transmissible [110]. Finally, Zhu et al. showed that elevated TMAO levels are independently associated with incident risk for thrombotic events in patients [110].

In addition to regulating TMAO levels, gut microbes produce metabolites which stimulate enterochromaffin cells (ECs) -dependent serotonin secretion [112]. Serotonin is subsequently taken up by the platelets, which promotes platelet activation and aggregation [112].

Finally, gut microbes release Toll-like receptor (TLR) ligands in the portal circulation, which reach the liver and trigger TLR2 signalling in the hepatic endothelium [113]. As a consequence, liver endothelial cells synthesize vWF, which is released in the circulation and promotes platelet adhesion. In the absence of gut microbes, vWF production is reduced, impairing platelet deposition on the endothelial matrix and thrombus formation [113].

5. PLATELETS IN CORONARY ARTERY DISEASE

In pathological conditions, excessive platelet activation triggers the formation of a thrombus that can lead to vessel occlusion, in a process called

thrombosis, which involves similar pathways as in haemostasis, except that they are exacerbated.

When platelets are exposed to a pro-thrombotic environment, such as inflammation, they are inappropriately activated, which leads to the formation of a thrombus that obstructs the veins (venous thrombosis) or the arteries (arterial thrombosis). Depending on the site of thrombosis, the structure of the clot will be different, being fibrin-rich in the veins due to the main involvement of the coagulation cascade, or platelet-rich in the arteries given the important contributions of platelet activation and aggregation. While different thrombus localization sites exist, the following section will focus on thrombosis in coronary arteries, a major consequence of coronary artery disease (CAD).

5.1 Global burden of coronary artery disease

Cardiovascular diseases (CVDs) are a global medical problem and represent the number one cause of death globally. According to the World Health Organization (WHO), 17.7 million people died from CVDs in 2015, representing 31 % of all global deaths. Among these, about 7.4 million were due to CAD and subsequent myocardial infarction or ischemic stroke.

5.2 Pathophysiology of coronary artery disease

CAD is caused by the presence of atherosclerotic plaques that form inside the intima of the vessel (Figure 12).

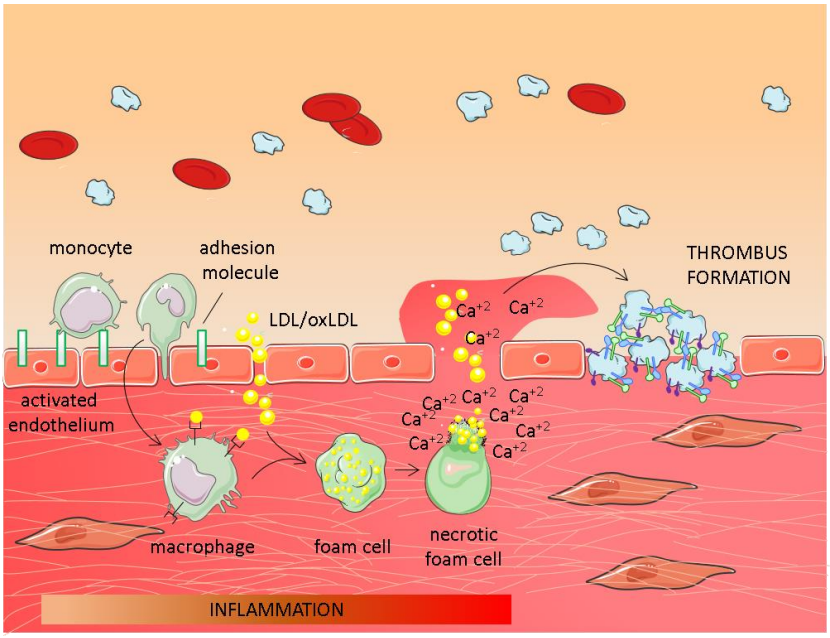

Figure 12. Pathophysiology of coronary artery disease. Pathological conditions such as hypercholesterolemia or hyperglycaemia induce endothelial cells activation, leading to adhesion molecule expression and the loss of vascular barrier integrity. These alterations induce monocyte adhesion and the infiltration of LDL/oxLDL. Once in the intima, monocytes differentiate into macrophages which express scavenger receptors, internalizing surrounding lipids, leading to foam cell formation. The presence of macrophages and monocytes inside the intima creates a highly inflammatory environment leading to cell necrosis, calcifications, extracellular matrix degradation and eventually endothelial rupture. This leads to the release of pro-thrombotic molecules in the circulation which trigger thrombus formation. LDL: low-density lipoprotein; oxLDL: oxidized LDL.

The pathway leading to plaque development is complex and involves many cellular processes. The first trigger is endothelial dysfunction, resulting from its exposure to several risk factors including hypertension, hyperglycaemia, smoking and especially hypercholesterolemia. This pro-

inflammatory environment activates endothelial cells, inducing the expression on their surface of adhesion molecules, and disrupting intercellular junctions, especially in regions of disturbed flow, where arteries divide or curve sharply [114]. These modifications do not only potentiate attachment and infiltration of leukocytes and monocytes/macrophages in the subendothelial space, but also promote the accumulation of plasma low-density lipoprotein (LDL) and/or oxLDL in the intima [115]. Once in the intima, monocytes differentiate in macrophages which express different classes of scavengers receptors that recognize and internalize LDL and/or oxLDL, leading to their cytosolic accumulation and to the formation of foam cells. Inside the plaque, activated leucocytes and macrophages release a multitude of inflammatory cytokines, chemokines and ROS that propagate inflammation [115]. This inflammatory environment promotes the proliferation and migration of vascular smooth muscle cells (VSMCs) which are responsible for the formation of fibrosis and calcifications in the arterial intima, a process highly dependent on the tumor necrosis factor-α (TNF-α) [116]. Coronary artery calcification is a hallmark of atherosclerosis and participates in the progression of the disease. Macrophages eventually undergo necrosis and form a necrotic core. The composition of the plaque largely influences the probability of its rupture. Vulnerable plaques are highly inflammatory and composed of a thin fibrotic cap, calcified nodules and a large necrotic core. The local massive inflammation, along with metalloproteinase secretion by macrophages, progressively degrades the ECM, promotes plaque erosion, which under high blood pressure, eventually ruptures. This induces the release and exposure of highly pro-thrombotic

elements in the blood lumen leading to strong platelet activation and thrombus formation which may obstructs the vessel. If more than 80 % of the coronary artery is occluded, lack of oxygen and nutrient supply lead to tissue ischaemia, and eventually myocardial infarction.

5.3 Clinical detection of coronary artery disease

5.3.1 Coronary angiogram

When CAD is suspected, based on patient complaints and the presence of risk factors, patients undergo a coronary angiogram, which allows the detection and localization of a vessel narrowing or blockage due to the presence of atherosclerotic plaques. The physician inserts a small catheter in large arteries or veins, usually in the arm, that he guides through the vessel until the tip reaches one of the coronary arteries. At this precise localization, an X-ray dye is injected via the catheter and mixes with the flowing blood in the coronary arteries, making it visible for 3-5 seconds as the radiocontrast agent is rapidly eliminated. The X-ray images analysis allows to determine which artery is affected and the percentage of luminal stenosis that determines the severity of the disease.

5.3.2 Computed tomography scan

Computed tomography scan (CTS) represents an additional tool to assess atherosclerotic burden as it specifically reveals the importance of coronary and extra-coronary arteries calcifications, which, as explained, on point 5.2., is a clinical hallmark of atherosclerosis. Calcifications appear on the images as hyperdense (bright) structures and can be quantified using a

calcium scoring software, allowing to calculate the Agatston score, which defines the severity of the calcifications [117].

5.4 Platelet involvement in coronary artery disease

Platelets do not only contribute to end-stage atherothrombosis, where they constitute the major element of the thrombus, but they also strongly participate in the progression of the disease as they modulate vessel properties and environment, rendering them more thrombotic.

It has been clearly described that CAD is associated with increased and persistent thrombin generation [118], leading to exacerbated platelet activation via PARs. Interestingly, in this pathological context, PARs can also bind molecules released from neutrophils, such as cathepsin G and elastase [119]. Increased levels of oxLDL, typical of patients suffering from atherosclerosis, can also alter platelet activation following their binding to platelet CD36 [120]. However, the current link between platelets and oxLDL is not clear yet and has to be studied in more depth.

5.4.1 Secretion of pro-inflammatory molecules

Once activated, platelets strongly participate in the progression of inflammation as they release inflammatory mediators into their surrounding environment, which mainly modify the chemotactic and adhesive characteristics of endothelial cells (Figure 13).

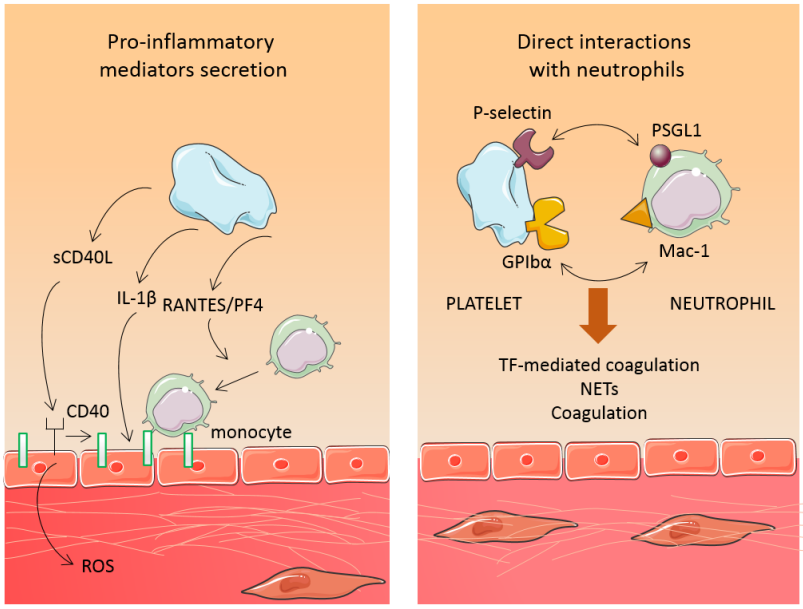

Figure 13. Platelet involvement in the pathophysiology of coronary artery disease. Platelets actively participate in the development of coronary artery disease by (1) releasing pro-inflammatory molecules (left panel) and (2) by directly interacting with and stimulating neutrophils (right panel). Left panel: platelets secrete sCD40L and IL-1β, which mainly induce adhesion receptor expression on endothelial cells. RANTES and PF4, released by activated platelets, recruit monocytes to the endothelium. Right panel: platelets directly interact with neutrophils via their P-selectin and GPIbα, which respectively bind to PSGL1 receptor and to Mac-1 on neutrophils. This interaction contributes to TF-dependent coagulation and to NETs formation, which promote thrombus formation. sCD40L: soluble CD40 ligand; IL-1β: interleukin-1β; RANTES: regulated on activation normal T-cell expressed and secreted; PF4: platelet factor4; ROS: reactive oxygen species; PSGL1: P-selectin glycoprotein ligand1; TF: tissue factor; NETs: neutrophils extracellular traps.

CD40 ligand (CD40L) is a pro-atherogenic protein stored in resting platelets and released following activation, becoming soluble. Once in the

plasma, soluble CD40L (sCD40L) binds to its receptor, CD40, expressed on endothelial cells, and modifies endothelial (1) release of ROS, chemokines, TF and matrix metalloproteinases, and (2) expression of neutrophil and monocyte adhesion molecules. The deleterious effect of sCD40L is highlighted by the correlation between the increased risk of vascular events and the high plasma levels of sCD40L [121]. Interleukin-1β (IL-1β) is synthesized by activated platelets [122] and, has similar effects as those induced by sCD40L [123]. Recent evidences suggest that platelet microparticles, which are small membrane vesicles released by activated platelets, also contribute to platelet-dependent increase in chemoattractant and adhesive properties of the endothelium [124].

Platelets also secrete molecules such as RANTES and PF4 which, in addition to attracting monocytes, also induce their differentiation into macrophages [123].

5.4.2 Interaction with inflammatory cells

Platelets bind to neutrophils and potentiate their activation (Figure 13). Platelets adhesion to neutrophils includes two main mechanisms: (1) platelet P-selectin binding PSGL1 on neutrophils and (2) platelet GPIbα binding to Mac-1 on neutrophils [119]. These platelet-neutrophils interactions propagate thrombosis by at least three mechanisms [119]. First of all, they contribute to coagulation cascade activation since neutrophils have been shown to transfer TF, the trigger of coagulation cascade, to platelets [125]. Secondly, they induce the generation of NETs, which are released upon neutrophils activation and are composed of neutrophil DNA

attached to proteins such as histones. NETs participate in thrombus formation by multiple mechanisms, including coagulation cascade stimulation, platelet adhesion, red blood cells recruitment and fibrinolysis inhibition [119]. Thirdly, activated neutrophils release various molecules that promote coagulation [126] and prevent vWF degradation by endogenous proteases [127].

6. PLATELET LIPIDS: MAJOR ACTORS IN PLATELET FUNCTION

Platelet activation, as detailed in Chapter 4, induces a profound lipid remodelling which is essential for platelet response to agonists. Platelets exhibit a complex array of over 5000 distinct lipid species with over 700 responding to thrombin activation. Lipids contribute to 16-19 % of platelets dry matter and include 65 % of phospholipids, 25 % of neutral lipids (glycerides, cholesteryl ester and free cholesterol) and about 8 % of glycosphingolipids [128]. Lipids are either incorporated from circulating plasma LDL [129], actively synthesized by platelets or generated following phospholipid cleavage by phospholipases. They are essential components of platelet structure, intracellular signalling and energy store. In addition, increasing evidences also indicate that they participate in protein post-translational modifications, thereby affecting platelet functions [130, 131].

Among the various lipid species found in platelets, phospholipids, besides from being the most abundant class, are major actors of platelet activation as they fulfill three main roles by contributing to platelet structure and providing substrates for platelet signalling and energy.

6.1 Overview of lipid metabolism

A fatty acid is a carboxylic acid linked to a long hydrocarbon chain, which is either saturated (carbon atoms linked by a single bond) or unsaturated (carbon atoms linked by double or triple bonds). This particular structure confers them a polar, hydrophilic head and a non-polar, hydrophobic tail. Fatty acids are generated either via their *de novo* synthesis or by phospholipids cleavage. Conversely, when energy needs to be mobilized, fatty acids are degraded via their β-oxidation which occurs in the mitochondria and generates the high energy-containing molecules, flavin adenine dinucleotide (reduced form) ($FADH_2$) and nicotinamide adenine dinucleotide (reduced form) (NADH).

6.1.1 *De novo* lipogenesis

Platelets contain all the essential machinery for synthesizing fatty acids *de novo* [132, 133]. *De novo* lipogenesis can be sub-divided into three steps; (1) palmitate synthesis from acetyl-CoA, (2) palmitate elongation and (3) palmitate desaturation yielding oleic acid, considered as the end product of *de novo* lipogenesis.

6.1.1.1 Palmitate synthesis

Palmitate synthesis occurs in the cytosol and consists of a cycle of elongation steps that starts with acetyl-CoA on which two-carbon units from malonyl-CoA are added at each cycle which ends when the fatty acid has reached 16 carbons (palmitate). The various steps of palmitate synthesis are illustrated in Figure 14.

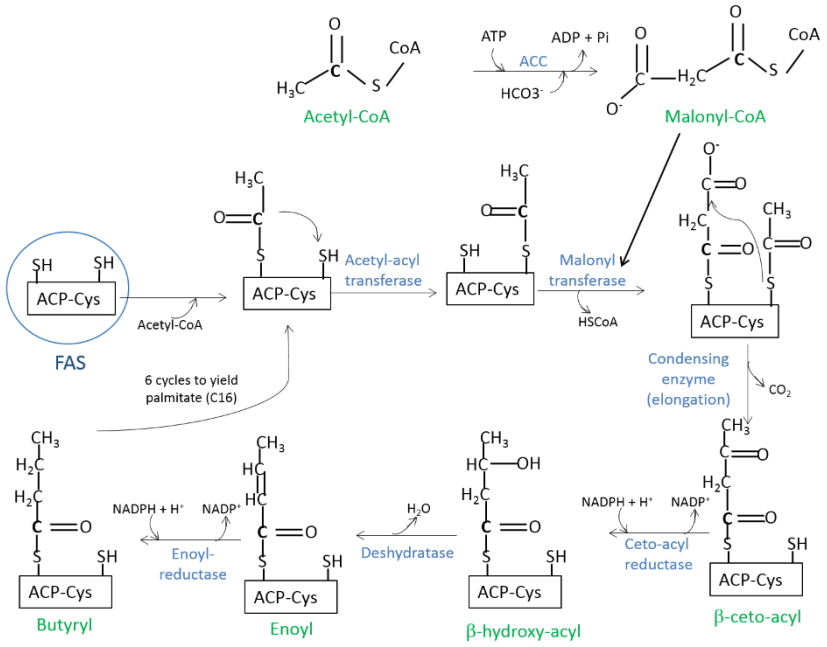

Figure 14. Palmitate synthesis. Palmitate synthesis starts with the carboxylation of acetyl-CoA into malonyl-CoA, which is catalyzed by the ACC. Malonyl-CoA then associates with the ACP domain of the FAS which uses acetyl-CoA as a primer. After 6 cycles of malonyl-CoA incorporation, reduction and dehydration reactions, palmitoyl-ACP is produced, cleaved and released as palmitate. ACC: acetyl-CoA carboxylase; ACP: acyl-carrier protein; FAS: fatty acid synthase.

The first rate-limiting step of palmitate synthesis, is the conversion of acetyl-CoA to malonyl-CoA catalyzed by the acetyl-CoA carboxylase (ACC). The next four reactions are catalyzed by the fatty acid synthase (FAS), a complex enzyme, containing a small polypeptide called acyl-carrier protein (ACP), on which the two-carbon unit of malonyl-CoA associates at each cycle, using acetyl-CoA as a primer and nicotinamide adenine dinucleotide phosphate hydrogen (NADPH) as a reducing equivalent. After six cycles of reaction, palmitoyl-ACP is produced and cleaved by the palmitoyl thioesterase yielding palmitate and ACP.

6.1.1.2 Palmitate elongation

Once released by the FAS, palmitate can be elongated to form long- or very-long-chain fatty acids. The elongation reaction involves elongases, which are localized on the cytosolic side of the endoplasmic reticulum. They catalyze a four step reaction in which malonyl-CoA is used as the two-carbon unit donor and NADPH as reducing equivalent.

6.1.1.3 Palmitate desaturation

Fatty acids of varying carbon lengths can be converted to unsaturated products by fatty acyl-CoA desaturase.

6.1.2 Phospholipids cleavage

The major structural lipids of platelets are phospholipids which are composed of a hydrophobic fatty acid tail attached to a hydrophilic head consisting of a phosphate group (Figure 15).

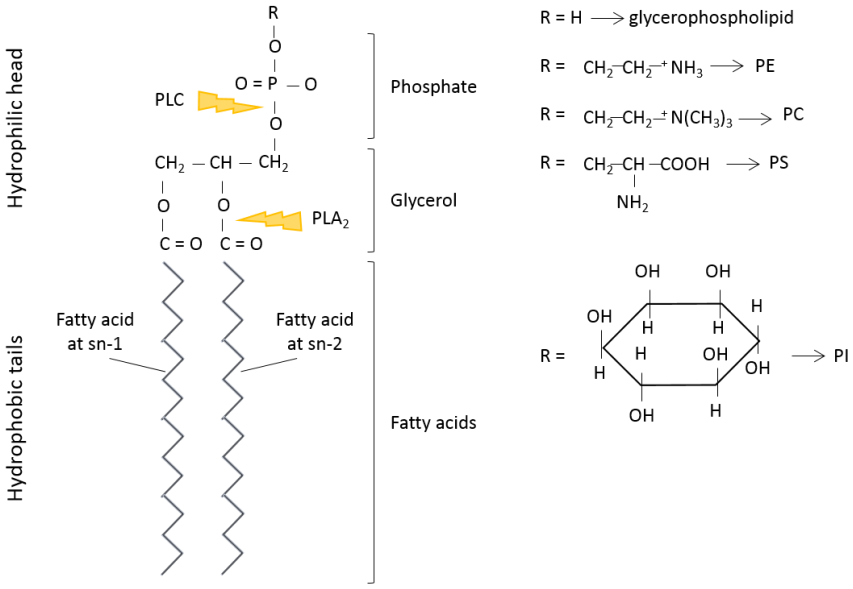

Figure 15. General glycerophospholipid structure. Phospholipids contain a hydrophilic head, composed of a phosphate group, and a hydrophobic tail containing two fatty acids, linked to carbon 1 (sn-1 position) and 2 (sn-2 position) of the glycerol backbone. Different classes of phospholipids exist, depending on the nature of the group attached to the phosphate (R). Phospholipids are the substrates of PLC and PLA_2 which respectively cleave the bond between the glycerol and the phosphate moiety (for PLC) and the sn-2 acyl bond (for PLA_2). PLC: phospholipase C; PLA_2: phospholipase A_2; PE: phosphatidylethanolamine; PC: phosphatidylcholine; PS: phosphatidylserine; PI: phosphatidylinositol.

This particular structure gives them the essential property of being amphipathic which triggers spontaneous aggregation of the hydrophobic tails when placed in water to minimize contact with the aqueous medium. Two principal classes of phospholipids exist: glycerophospholipids and sphingomyelin. Glycerophospholipids are lipids in which two fatty acids molecules are linked to carbon 1 (sn-1 position) and 2 (sn-2 position) of the glycerol backbone, while phosphoric acid is attached to the carbon 3 (Figure

15). Furthermore, the phosphate moiety can be linked to an additional group which is either an amino acid, such as ethanolamine, choline or serine, generating the sub-classes phosphatidylethanolamines (PE), phosphatidylcholines (PC) or PS respectively, or a carbohydrate such as inositol, making phosphatidylinositol (PI) (Figure 15). Sphingomyelin (SM), although also considered a phospholipid, has a different structure which is composed of a hydrophilic phosphocholine headgroup linked to a sphingosine and a fatty acid, making the hydrophobic tail. In platelets, PC and PE represent the major pool of phospholipids accounting for ±40 % and 28 % of total phospholipids, respectively, followed by SM (18 %), PS (10 %) and finally PI which represents 3-5 % [134].

While glycerophospholipids constitute an important reservoir of signalling and energetic lipid molecules, sphingomyelin does not, even though sphingomyelinase is expressed in platelets [135].

Phospholipid-derived fatty acids are generated via the action of PLC which hydrolyzes PIP2, by cleaving the bond between the glycerol and the phosphate moiety to yield IP3 and DAG and of PLA_2, which hydrolyzes the sn-2 acyl bond of phospholipids, releasing fatty acids from the second carbon group of the glycerol (Figure 15).

6.1.2.1 Cleavage by phospholipase C

PLCs are classified into 6 subfamilies: PLCβ, PLCγ, PLCδ, PLCε, PLCζ and PLCη, each expressing various isoforms. Human platelets express PLCβ (PLCβ1-β4) and PLCγ (PLCγ1 and PLCγ2) [136]. PLCβ is activated following its

binding to Gβγ subunit of the active GPCR in response to soluble agonists such as thrombin and TXA_2, whereas PLCγ is activated by immobilized ligands, such as collagen, which triggers a signalling cascade that ultimately leads to PLCγ stimulation (see Chapter 4).

6.1.2.2 Cleavage by phospholipase A_2

Phospholipase A_2 are subdivided into various subclasses, which include the low-molecular-weight secreted PLA_2 ($sPLA_2$), the Ca^{2+}-dependent cytosolic PLA_2 ($cPLA_2$) and the Ca^{2+}-independent cytosolic PLA_2 ($iPLA_2$), each having various isoforms [137]. Even though platelets express each of these three subclasses, $cPLA_2$ has been shown to be the exclusive phospholipase responsible for releasing fatty acids in response to thrombin. Indeed, its inhibition totally prevented any thrombin-induced increase in fatty acid while $sPLA_2$ or $iPLA_2$ inhibitors did not have any impact [138]. Supporting this data, mice deficient for $iPLA_2$ display normal TXA_2 generation in response to thrombin [139]. In contrast, collagen-induced TXA_2 generation is dependent on the three phospholipases, $cPLA_2$, $sPLA_2$ and $iPLA_2$. Indeed, platelets isolated from $cPLA_2$/$sPLA_2$ double-deficient mice [140] or from $iPLA_2$ knock-out mice [139], display a partial reduction in TXA_2 generation in response to collagen, indicating the redundancy between these phospholipases. Finally ADP-dependent TXA_2 production relies on the $iPLA_2$ as $cPLA_2$/$sPLA_2$ deficiency does not prevent any decrease in TXA_2 synthesis [140] while it is reduced in $iPLA_2$ knock-out mice [139].

It has been shown that $cPLA_2$ comprises 6 members ($cPLA_2\alpha$, $cPLA_2\beta$, $cPLA_2\gamma$, $cPLA_2\delta$, $cPLA_2\varepsilon$ and $cPLA_2\zeta$) and contains an N-terminal C2 domain

for Ca^{2+} binding. Following platelet stimulation, Ca^{2+} concentration increases, binds to the C2 domain and induces $cPLA_2$ translocation to the plasma membrane, positioning it in close proximity with phospholipids [137]. In addition, phosphorylation of its Ser505 residue, which is essential for maximal lipase activation, is induced by Erk1/2 [141] and p38 [142] in thrombin-stimulated platelets.

6.1.3 β-oxidation

β-oxidation is the catabolic process by which fatty acids are degraded in the mitochondria to generate energy. The first step consists in fatty acids activation by the acyl-CoA synthetase to generate acyl-CoA esters, the substrates of the β-oxidation. This pathway can be divided into two parts; the first involves acyl-CoA transfer into the mitochondria, and the second concerns fatty acid degradation by oxidative removal of two-carbon units.

6.1.3.1 Mitochondrial entry of acyl-CoA

Because the mitochondrial inner membrane is impermeable to heavy polar molecules like CoA, the acyl group needs to be cleaved from the acyl-CoA and transported into the mitochondria following its association with carnitine. The acyl-carnitine formed by the carnitine palmitoyl transferase I (CPTI) on the outer mitochondrial membrane is transported across the inner mitochondrial membrane via the carnitine acylcarnitine translocase and then reconverted to acyl-CoA by the carnitine palmitoyl transferase II (CPTII). Fatty acid entry in the mitochondria is a major regulatory point of β-oxidation.

6.1.3.2 Carbon chain shortening

Mitochondrial β-oxidation consists of a repeated sequence of four reactions (two dehydrogenations, one hydration and one thiolytic cleavage) leading to complete lipid breakdown into acetyl-CoA, NADH and $FADH_2$. Palmitate oxidation, a 16 carbon fatty acid, yields 8 acetyl-CoA, 7 NADH and 7 $FADH_2$. The resulting acetyl-CoA is finally degraded in the tricarboxylic acid (TCA) cycle which generates additional NADH and $FADH_2$, substrates of the oxidative phosphorylation, the final reaction converting high-energy molecules into ATP, in the presence of O_2.

6.2 Structural roles

Membrane phospholipids play a central structural role in almost all steps of platelet activation. They do not only serve as a scaffold for shape change and spreading, but are also required for platelet secretion, a process requiring the fusion of two membranes, and finally for appropriate signalling of receptors, which experience lateral movements and clustering in the plasma membrane, a process mediated by lipid rafts (Figure 16).

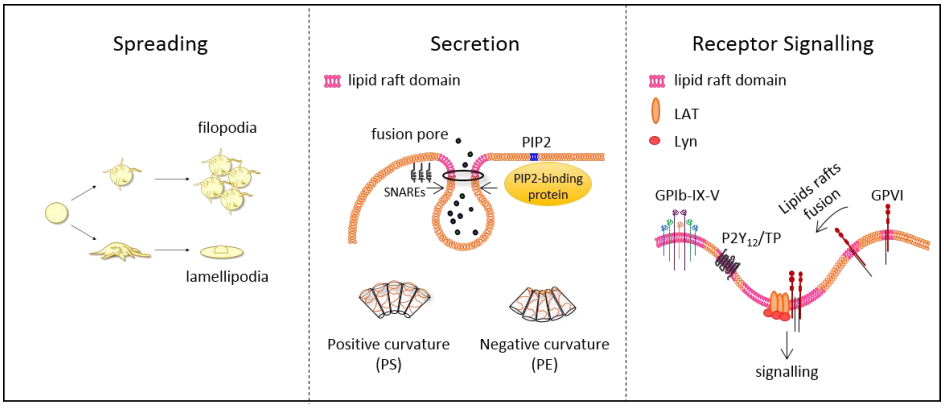

Figure 16. Structural roles of platelet membrane lipids. Platelet membrane lipids play a crucial role in platelet architecture, secretion and signalling. They provide substrates for platelet spreading, filopodia and lamellipodia formation. In addition, their nature, which influences their curvature, dictates the formation of the fusion pore, necessary for secretion. Finally, they provide protein binding sites and are major constituents of lipid rafts, which are essential for platelet secretion and receptor signalling. Indeed, several receptors are anchored in lipid rafts which cluster following activation, triggering a signalling pathway. PIP2: phosphatidylinositol 4,5-bisphosphate; SNAREs: soluble NSF(N-ethylmaleimide-sensitive factor) attachment protein receptor; PS: phosphatidylserine; PE: phosphatidylethanolamine; TP: thromboxane-prostaglandin receptor.

6.2.1 Role in platelet spreading and adhesion

When platelets adhere on the injured endothelium, they undergo irreversible morphological changes such as spreading, with the formation of lamellipodia and filopodia, which do not only require cytoskeletal remodelling but also an important lipid membrane reorganization to allow increase in platelet surface area. In this context, the role of the OCS to supply additional membrane is crucial. Indeed, bovine platelets, which lack the OCS, display defective spreading [143]. On the other hand, addition of

extracellular phospholipids, leading to their accumulation in the outer leaflet, increases platelet filopodia formation and actin polymerization [144]. These structural changes are mediated by PI3K activation, which is triggered by the physical and mechanical constraints of phospholipid excess [144].

6.2.2 Role in platelet secretion

Phospholipids have been described to modulate platelet secretion in three ways. First of all, they serve as a matrix for the fusion of two opposing membranes, secondly their nature influences membrane fluidity and curvature and thirdly they provide binding sites for exocytic machinery proteins (Figure 16).

Granule secretion occurs via the formation of a fusion pore between two membranes. Clearly the lipid composition of the two opposing membranes influences the secretion process. It has been shown that exocytosis mainly occurs in cholesterol and sphingolipid-rich microdomains, called lipid rafts [145]. Indeed, they do not only stabilize the fusion pore but they also allow the concentration of specific proteins involved in platelet secretion (t-SNAREs, SNAP-23 and syntaxin-11).

Given its degree of saturation, the length of its fatty acid chains and the nature of its polar headgroup, each phospholipid adopts a specific geometry and a preferential curvature that influence fusion pore formation and stability. Conical lipids (larger tail), such as PE, tend to form negative membrane curvature while inverted conical lipids (larger head), such as PS,

preferentially support positive curvature (Figure 16). The fusion pore is an extremely curved structure in which lipids associated with positive curvature assemble on the outer leaflet whereas negatively curved lipids are present in the inner leaflet. Platelets incubation with PS increases fusion pore stability, probably by providing additional lipids supporting positive curvature [146].

Several proteins involved in platelet signalling and cytoskeletal remodelling, essential for platelet secretion, contain a PIP2-binding site, for which at least five different domains have been described [147]. Among these proteins, talin involved in αIIbβ3 activation and a vast majority of cytoskeletal-binding proteins (including gelsolin, vinculin, Arf (ADP-ribosylation factor) and filamin) all bind PIP2 which potentiates their respective role in platelet secretion [148-150].

6.2.3 Role in receptor signalling via lipid rafts

Lipid rafts are very small membrane domains enriched in sphingolipids, cholesterol and proteins, which are involved in signalling due to their association with GPCRs and their ability to cluster signalling proteins. As a consequence, platelet rafts are critical for mediating platelet activation in response to agonists. They have been shown to be essential for GPIb-IX-V, GPVI, $P2Y_{12}$ and TP signalling as well as for clot retraction as they constitute a platform for fibrin concentration.

When isolated, platelet rafts appear as round vesicles ranging from 20 to 500 nm in size [151], containing less than 1 % of total protein content,

among which membrane receptors (CD36, GPIb, GPVI, $P2Y_{12}$ and TP), signal transduction partners (the transmembrane protein complex LAT and members of the Src family kinases) and enzymes (PI3K and PLCγ2) are specifically enriched [151]. Regarding platelet rafts lipid content, their cholesterol/phospholipid molar ratio is 1.2, while it is 0.5 in the remaining plasma membrane, indicating the strong cholesterol enrichment of rafts. Sphingomyelin is the most abundant phospholipid, accounting for 57 % of total lipid rafts.

Thrombin or collagen platelet stimulation induces cholesterol rearrangement, the lateral movements of lipid rafts and their fusion [151]. Since these domains are enriched in many signalling molecules, this lateral clustering has a great impact on receptor activation. Among them, GPVI signalling has been shown by several authors to involve lipid rafts. Following activation, GPVI translocates to lipid rafts where it is anchored via its FcR γ-chains. This association does not only trigger FcR γ-chain phosphorylation, since Lyn, one of its major kinase is enriched in these domains, but also favors downstream signalling pathway due to the high LAT content of lipid rafts [152]. In the same line, GPIb-IX-V signalling, triggered by vWF binding and which shares a number of similarities with GPVI pathway, also relocates to lipid rafts upon stimulation, a necessary step for complete platelet activation [153].

Regarding the involvement of lipid rafts in GPCRs signalling, a role has been highlighted for $P2Y_{12}$, which Gαi subunit association with lipid rafts is

essential for platelet response to ADP [154] and for TP, of which 40 % are localized in lipid rafts [155].

Finally, lipid rafts have been shown to constitute a platform connecting extracellular fibrin and intracellular actomyosin cytoskeleton via αIIbβ3, which promotes “outside-in” signalling and clot retraction [156].

6.3 Signalling and energy storage roles

The signalling and energy storage roles of lipids are intrinsically linked, as the majority of lipids involved in these functions needs to be cleaved from membrane phospholipids. As a result, certain lipid classes, such as eicosanoids, both play an energetic and signalling role. In this context, phospholipases (PLA_2 and PLC) are essential for generating phospholipid-derived signalling and energetic lipids (Figure 17).

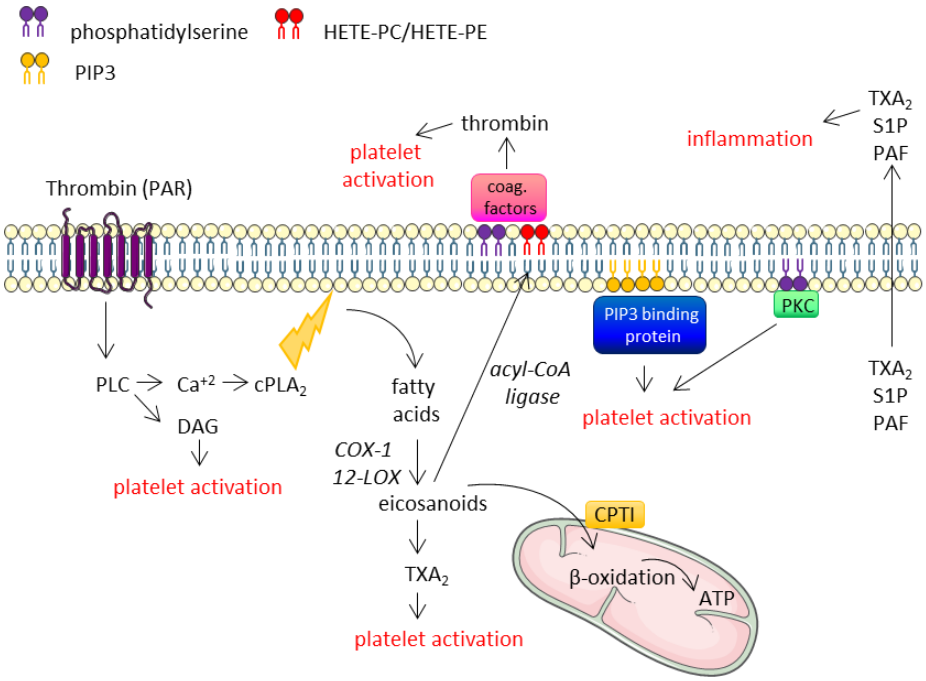

Figure 17. Signalling and energy storage roles of lipids. By providing protein binding sites, membrane lipids such as PIP3, recognized by PIP3 binding protein, or PS, by serving as PKC docking site, contribute to platelets activation. In addition, agonist binding to its receptor, activates phospholipases which generate an array of lipid-derived signalling molecules such as DAG, TXA_2 and oxidized phospholipids, potentiating platelet stimulation. Among them, the oxidized phospholipids HETE-PC/HETE-PE promote coagulation factors binding, thereby stimulating the coagulation cascade and thrombin generation. Following activation, platelets also secrete bioactive lipids such as TXA_2, S1P and PAF, which modulate platelets neighbouring environment. Finally, eicosanoids constitute an important source of energy as they are oxidized in the mitochondria, thereby contributing to platelets bioenergetics. HETE: hydroxy-eicosatetraenoic ; PC: phosphatidylcholine; PE: phosphatidylethanolamine; PAR: protease-activated receptor; PLC: phospholipase C ; DAG: 1,2-diacylglycerol; $cPLA_2$: Ca^{2+}-dependent cytosolic PLA_2; COX-1: cyclooxygenase-1; 12-LOX: 12-lipoxygenase; TXA_2: thromboxane A_2; PIP3: phosphatydilinositol-3,4,5-trisphosphate; PKC: protein kinase C; S1P: sphingosine 1-phosphate; PAF: platelet activating factor; CPTI: carnitine palmitoyl transferase I.

As a consequence, phospholipase genetic deficiency or pharmacological inhibition profoundly impacts platelet activation. Patients with a genetic deficiency of PLCβ suffer from a mild bleeding disorder due to defective platelet aggregation and secretion, highlighting the important role of PLC-derived lipids [157]. In line with this, PLCγ2 deficient mice display reduced platelet spreading, collagen-induced aggregation and thrombus formation [158]. Regarding PLA_2, an inherited deficiency of $cPLA_2$, leading to decreased phospholipase activity [159], as well as pharmacological inhibition of $cPLA_2$ [160], reduce platelet aggregation and secretion.

6.3.1 Signalling roles

Signalling bioactive lipids can either have an intracellular or extracellular role, when they are secreted by platelets. In general, these lipids are enzymatically synthesized from phospholipids, however, some intracellular lipids do not need any processing to contribute to platelet function. The following sections will focus on signalling lipids that have been described as significant contributors of platelet function rather than providing a detailed description of all lipid species present in platelets.

6.3.1.1 Intracellular platelet lipids

6.3.1.1.1 Phosphatidylserine

In the resting state, phospholipids are asymmetrically organized, with PC in the outer leaflet, and PS and PE facing the cytoplasm. This distribution is maintained by the action of flippase and floppase. Following agonist stimulation or energy depletion, this structure is perturbed with PS

and PE being externalized via the action of a Ca^{2+}-activated phospholipid scramblase, TMEM-16F, or via apoptosis-related mechanisms [161]. Studies indicate that two PS and five PE, accounting for 4 % of total cellular PS/PE pool, are being translocated to the outer membrane [162]. As explained on point 3.1.6., PS mainly provide a platform for coagulation factors binding, thereby participating in thrombin generation on platelet surface. In addition, PS exposure can also induce platelet clearance by macrophages [163, 164]. Finally, PS, when facing the cytoplasm, are essential co-factors for PKC as they constitute a membrane docking site for the kinase, which is an essential step in its activation [165].

6.3.1.1.2 Phosphatydilinositol-3,4,5-trisphosphate

Phosphatydilinositol-3,4,5-trisphosphate (PIP3) is a phosphatidylinositide that represents an essential bioactive lipid species generated from PIP2 phosphorylation by PI3K, following GPCRs activation. It binds to a region of ≈120 amino acids, known as a pleckstrin homology (PH) domain, which is present on a multitude of proteins involved in cytoskeleton remodelling, signalling, aggregation, adhesion, integrin activation and Ca^{2+} mobilization [134]. PIP3 recruits these proteins to the plasma membrane and contributes to their activation.

6.3.1.1.3 Oxidized phospholipids

Human platelets generate significant quantities of oxidized phospholipids (oxPL) via enzymatic mechanisms involving $cPLA_2$ -dependent AA generation, AA oxidation by 12-lipoxygenase or COX-1, and its re-

esterification by an acyl-CoA ligase, forming hydroxy-eicosatetraenoic (HETE)-PC or HETE-PE [166]. These oxPL have been shown to promote coagulation factors binding, via alteration of membrane charge, and therefore to enhance thrombin generation [166].

6.3.1.1.4 1,2-diacylglycerol

As detailed on point 4.1.1., DAG, generated from PIP2 by PLC cleavage in response to platelet stimulation, is a master regulator of platelet activation as it does not only activate several PKC isoforms but is also an important co-factor for signalling molecules such as CalDAG-GEF1.

6.3.1.2 Extracellularly secreted platelet-derived lipids

Platelets also synthesize lipids that will be passively, due to their high polarity, or actively secreted following platelet activation. These include TXA_2, sphingosine 1-phosphate (S1P) and platelet activating factor (PAF). Besides having auto- or paracrine effects on platelets, they also modulate neighboring cells such as endothelial and immune cells thereby contributing to the progression of inflammatory diseases.

6.3.1.2.1 Thromboxane A_2

Among the bioactive lipids generated by platelets but secreted in the medium, TXA_2 is abundantly produced and released following platelet activation. TXA_2 derives from AA-containing phospholipids which are cleaved by PLA_2 upon platelet activation by various agonists (as described in paragraph 6.1.2.2. and illustrated in Figure 8). TXA_2 potentiates platelet activation by binding to its platelet receptor TP, which activates a signalling

cascade that ultimately leads to dense granule secretion (Figure 8) [167]. As a consequence, a defect in TXA_2 generation results in impaired dense granule secretion [168]. In addition, TXA_2 induces the expression of adhesion molecules on endothelial cells, which favors leukocyte-endothelial interactions and activates VSMCs, contributing to vasoconstriction.

6.3.1.2.2 Sphingosine 1-phosphate

S1P is a bioactive lysosphingolipid, generated from sphingosine phosphorylation by sphingosine kinase, which is highly expressed in platelets. Once synthesized, S1P is stored in two major pools; near the plasma membrane and in granules [169], before being secreted upon platelet activation. Plasmatic S1P exerts pleiotropic effects on platelets production but also on their surrounding cellular environment to regulate physiological and pathophysiological processes. S1P plays a role in thrombopoiesis as MKs express various S1P receptors and preferentially form proplatelets under conditions of high S1P concentration [169]. In addition, it activates a multitude of cellular pathways leading to endothelial cells migration and proliferation, macrophages and T-lymphocytes migration and finally neutrophils activation [169]. Since all these processes are involved in inflammatory diseases, such as atherosclerosis and sepsis, S1P is a central actor in the progression of inflammation and is therefore considered as a promising tool to fight chronic inflammatory disease [169].

6.3.1.2.3 Platelet activating factor

Platelet activation leads to the acetylation of 1-alkyl-glyceryl-3-phosphorylcholine which generates the PAF that is released in the plasma. PAF binds to a unique GPCR present on a large variety of cells and, similarly to S1P, exerts pleiotropic effects on platelet aggregation, neutrophils, leucocytes adhesion and activation [170].

6.3.2 Energy storage role

In addition to platelet signalling, eicosanoids generated by $cPLA_2$ are the exclusive β-oxidation substrates used by platelets mitochondria following their activation [138]. However, even though their oxidation increases in response to thrombin [24, 138], the energy provided by lipid degradation is not a major contributor of platelet functions. This point is detailed in Chapter 7, along with the contributions of other energetic pathways to platelet metabolism and function.

7. OVERVIEW OF PLATELET METABOLISM

Platelets are one of the most metabolically active circulating elements in the blood, a state under which they mainly rely on mitochondrial oxidative phosphorylation and to a lesser extent on aerobic glycolysis [171]. In resting platelets, ATP is mainly needed to control Ca^{2+} homeostasis. The sarco-endoplasmic Ca^{2+} ATPase (SERCA) uses ATP to pump cytosolic Ca^{2+} in the DTS, maintaining a Ca^{2+} gradient between the cytosol (100 nM) and the

intracellular stores (1 mM) [172]. In addition, Ca^{2+} homeostasis is further controlled by the Ca^{2+}-ATPases on the plasma membrane, which transport Ca^{2+} out of the platelet in the presence of ATP [173]. These two processes are particularly important for platelets as a slight increase in cytosolic Ca^{2+} concentration would activate them.

In contrast, glycolysis, rather than oxidative phosphorylation, supplies most of the energy used for platelet activation. Indeed, impairment of glucose uptake or glycolysis inhibitors induce a profound reduction in platelet activation while inhibiting oxidative phosphorylation has a minimal impact. Platelet metabolism is summarized below (Table 1 and Figure 18).

7.1 Glycolysis

Glucose enters the cell via glucose transporters. Among them, platelets express the glucose transporter 1 (GLUT1) and the glucose transporter 3 (GLUT3) which allow glucose entry via facilitative diffusion. GLUT1 is a ubiquitously expressed transporter but, in contrast to GLUT3, only traces are found in platelets [174] and it has a minimal role on glucose uptake following platelet activation [164]. Under basal condition, ~ 85 % of GLUT3 is localized on the alpha granules membrane whereas the rest is expressed on the plasma membrane [174]. GLUT3 has a K_m for glucose of ~ 1.5 mM which indicates that under physiological glycaemic conditions (5 mM), the transporter is saturated. Following platelet stimulation with thrombin, the alpha granules fuse with the platelet membrane, which considerably increases GLUT3 availability, and glucose entry, which is stimulated by 2-fold [174]. In addition, thrombin induces a decrease in the

K_m for glucose, contributing to enhanced glycolytic flux following platelet activation [175]. GLUT3 deficiency decreases basal glycolytic flux and prevents any increase in glycolysis following thrombin stimulation [164]. Regarding the impact on platelet function, mice deficient for either GLUT3 [176] or both GLUT3 and GLUT1 [164] display decreased *in vivo* thrombosis, platelet activation and degranulation. In addition, the combined deficiency of GLUT3 and GLUT1 impairs PPTs formation from the MKs and reduces platelet half-life due to increased PS externalization. The latter is partially rescued by the addition of alternative metabolic substrates (pyruvate and glutamate), indicating the energy dependence of this process. In agreement with these data, treatment of human platelets with 2-deoxy-D-glucose (2DG), an inhibitor of glycolysis, reduces platelet aggregation [24], clot retraction [177], platelet spreading [178] and strongly increases PS externalization [138].

7.2 Glycogenolysis

Glucose uptake also allows platelet to constitute an important glycogen store, as illustrated with GLUT1 and GLUT3 transporters deficient mice which display strongly reduced platelet glycogen content [164]. Upon platelet stimulation, glycogen is rapidly degraded to provide glucose, due to the activation of glycogen phosphorylase [176, 179]. Treatment of human and mice platelets with an inhibitor of the glycogen phosphorylase prevents alpha granules release [176].

7.3 Mitochondrial oxidative phosphorylation

Among oxidized substrates, lipid, glutamine and glucose contribute for 37 %, 7 % and 4 %, respectively, to total ATP turnover under basal condition [180]. Following platelet stimulation, oxidative phosphorylation increases, largely due to enhanced lipid and glutamine oxidation [24]. However, the impact of inhibiting metabolic substrates oxidation has a much less profound impact on platelet function than interfering with glycolysis. Platelets treated with antimycin-A, an inhibitor of the cytochrome c reductase, a central enzyme in the electron transport chain of the oxidative phosphorylation, does not affect platelet spreading [178] nor aggregation [181, 182]. Nevertheless, several studies demonstrate the necessity to inhibit both glycolysis and mitochondrial oxidative phosphorylation to strongly impact platelet functions [24, 138, 182-184]. This is probably due to the fact that platelets have the capacity to switch between ATP-providing pathways to compensate the inhibition of one of the two processes.

7.3.1 Lipids

Lipids enter mitochondria via CPTI, where they are oxidized to generate acetyl-CoA for the TCA cycle. Interestingly, exogenous lipids do not contribute to platelet basal and thrombin-stimulated oxygen consumption rate (OCR) [24]. Oxidation of endogenous lipids is the main ATP provider. Accordingly, treatment of platelets with etomoxir, a CPTI inhibitor, decreases platelet basal and thrombin-stimulated mitochondrial respiration reflected by the OCR [24, 185]. However, it does not influence aggregation [24, 186], while slightly increasing PS exposure [138] and procoagulant

activity. Similar observations are made with a $cPLA_2$ inhibitor, preventing phospholipids breakdown and eicosanoids generation [138].

7.3.2 Glutamine

Glutamine, the most abundant amino acid in plasma, is an important substrate for oxidative metabolism following its conversion to glutamate and then alpha-ketoglutarate, which fuels the TCA cycle, through a pathway known as glutaminolysis. It has been shown that glutamine enters platelets via two glutamine transport systems which have been partially characterized [187] and that it is effectively metabolized by platelets [188]. Under resting condition, glutaminolysis is operating [188] and contributes to basal platelet oxidative phosphorylation as removal of glutamine from the medium decreases mitochondrial OCR [24]. In addition, glutamine breakdown is strongly accelerated by thrombin [188] and significantly supports the thrombin-dependent increase in OCR [24]. However, removing glutamine from the medium does not impact platelet aggregation [24].

7.3.3 Glucose

Glucose oxidation does not significantly contribute to thrombin-dependent increase in OCR and therefore to ATP supply, which contrasts with the crucial role of aerobic glycolysis to provide energy [24].

	RESTING PLATELETS			ACTIVATED PLATELETS		
ATP source	**Relative contribution to total ATP generation**	**Regulation of platelet functions**	**Ref.**	**Relative contribution to total ATP generation**	**Regulation of platelet functions**	**Ref.**
Aerobic glycolysis	intermediate	none	[171]	high (++)	-activation -secretion -production -aggregation -clot retraction -spreading -*in vivo* thrombosis	[24, 138, 164, 176-178]
Glycogeno-lysis	low	none	[176]	intermediate	-secretion	[176]
Mitochondrial oxidation	high	-Ca^{2+} homeostasis	[172, 173]	high	none	[24, 138, 178, 181, 182, 186]

Table 1. Overview of resting and activated platelet metabolism. Three main ATP generating pathways co-exist in platelets, glycolysis, glycogenolysis and mitochondrial oxidation, which differently contribute to energy generation, depending on platelet activation state. Under resting conditions, platelets are mostly oxidative and less glycolytic. The energy generated is mainly used to maintain Ca^{2+} homeostasis. However, under activated conditions, the three pathways are stimulated, with a major impact on glycolysis. Surprisingly, even though they all provide energy, glycolysis has been shown to be the major regulator of platelet functions following activation. Indeed, inhibition of glycogenolysis or mitochondrial oxidation affects alpha granules secretion only or none of the platelet activation marker, respectively.

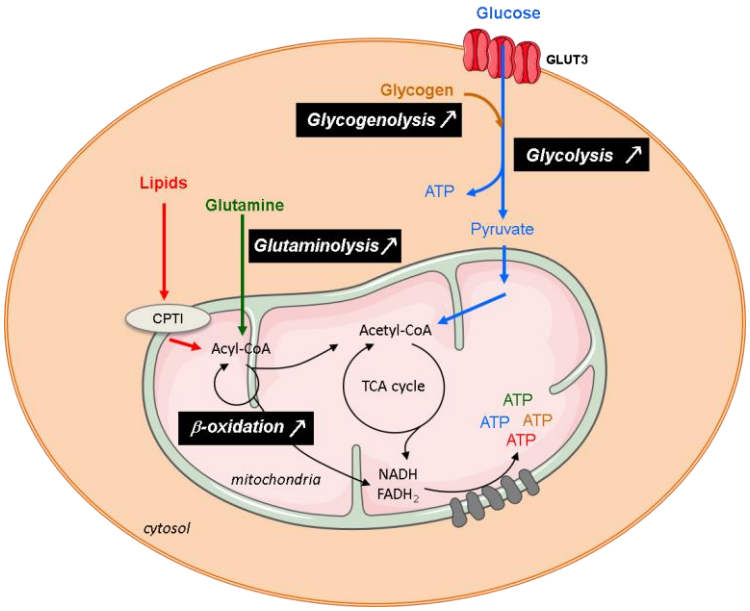

Figure 18. Overview of activated platelet metabolism. Following platelet stimulation with thrombin, glycogenolysis, glycolysis, glutaminolysis and β oxidation are activated to supply energy. Of these pathways, glycolysis-dependent ATP generation is crucial to allow proper platelet activation. CPTI: carnitine palmitoyl transferase I; TCA: tricarboxylic acid; GLUT3: glucose transporter 3; $FADH_2$: flavin adenine dinucleotide hydrogen; NADH: nicotinamide adenine dinucleotide hydrogen.

8. PROTEINS ACYLATION

Post-translational attachment of lipids to proteins constitutes an important regulatory mechanism of various cellular functions and biological processes. The most frequent lipids attached to proteins are palmitic acid (16-carbon fatty acid), usually via a thioester bond linked to a cysteine residue, or myristic acid (14-carbon fatty acid) most frequently via an amide linkage to glycine, leading to protein *S*-palmitoylation or *N*-myristoylation respectively [189] (Figure 19).

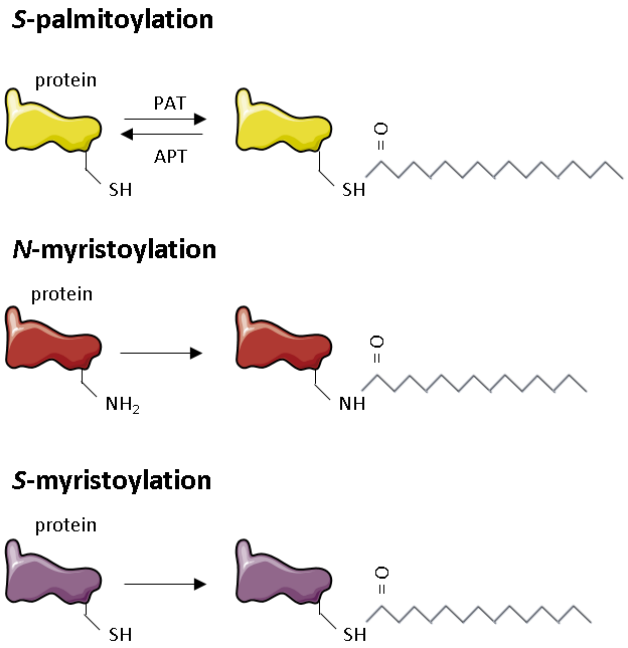

Figure 19. Protein palmitoylation and myristoylation. Protein palmitoylation and myristoylation constitute important post-translational protein modifications induced by lipids. *S*-palmitoylation consists in the binding of palmitic acid to a cysteine residue of the protein. It is mediated by PAT and cleaved by APT. *N*-myristoylation and *S*-myristoylation involve the binding of a myristic acid to a N-terminal glycine or to a cysteine residue, respectively. PAT: palmitoyl-acyl transferase; APT: acyl-protein thioesterase.

Among modified amino acid, cysteine is unique as its binding to palmitic acid, leading to *S*-palmitoylation, is reversible, leading to a dynamic balance of palmitoylated and depalmitoylated proteins, similarly to phosphorylation. Past and recent studies indicate that palmitoylation and myristoylation are occurring in platelets and that they are essential regulators of platelet functions.

8.1 Palmitoylation

Palmitoylation involves the binding of a palmitic acid to a protein, usually to a cysteine residue, which is catalyzed by the palmitoyl-acyl transferases (PATs). In addition, specifically for *S*-palmitoylation, the S-acyl linkage can be cleaved by acyl-protein thioesterases (APT). Platelets express at least 13 PATs isoforms and have an active palmitoylation machinery [130], leading to over 200 palmitoylated proteins, the majority of them being involved in signal transduction [190]. Protein palmitoylation occurs both under resting and stimulated conditions, the latter leading to increased and more rapid palmitate incorporation [191, 192]. Since protein palmitoylation enhances their incorporation in lipid rafts, affects protein-protein interaction, regulates their stability and activity, its inhibition affects platelet functions. In this regard, it has been shown that inhibiting platelet palmitoylation decreases their aggregation, dense and alpha granules secretion as well as their accumulation into a thrombus [130, 131, 193].

8.2 Myristoylation

Protein myristoylation usually occurs through attachment of a myristic acid to N terminal glycine via an amide bond catalyzed by N-myristoyltransferase, leading to *N*-myristoylation. However, myristic acid can also be linked to a cysteine residue via a thioester bond, leading to *S*-myristoylation, being less frequent. In contrast to palmitoylation, myristoylation occurs at a much lower rate in platelets [194] and has been much less studied. Platelet myristoylation mainly involves *S*-myristoylation as only 5 % of myristate linked to proteins is found in amide linkage [194],

suggesting that *N*-myristoylation is hardly active in platelets. Few proteins have been reported to be myristoylated in platelets. Among these, GPIX subunit of the vWF receptor is myristoylated in MKs, but its role has not been investigated [195].

9. ACETYL-COA CARBOXYLASE: A KEY PLAYER IN LIPOGENESIS

ACC catalyzes the carboxylation of acetyl-CoA to malonyl-CoA using bicarbonate as a CO_2 donor and ATP as energy source. It is a crucial enzyme for *de novo* lipogenesis, as it synthesizes the first rate-limiting step of this complex process. In addition, malonyl-CoA, the resulting product of ACC-catalyzed reaction, is a powerful CPTI inhibitor, which controls fatty acids entry in the mitochondria for their oxidation, giving ACC the dual role of being both involved in lipid synthesis and oxidation.

9.1 Acetyl-CoA carboxylase structure

ACC belongs to the family of biotin-dependent carboxylases which are characterized by a common structure consisting of three subunits: the biotin carboxylase (BC), the carboxyltransferase (CT), and the biotin-carboxyl carrier protein (BCCP), giving it a high molecular weight of ~250 kDa (Figure 20).

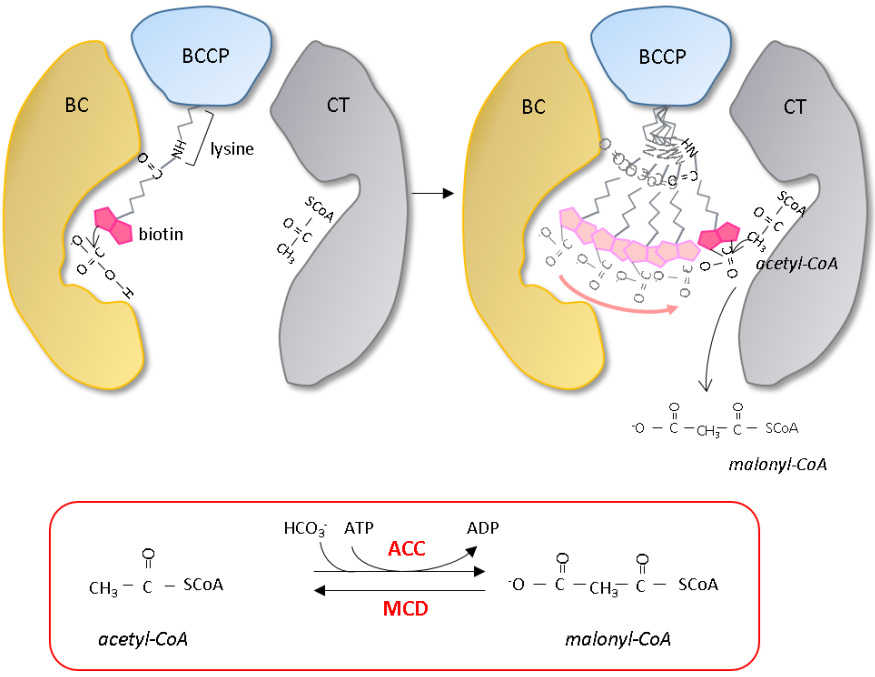

Figure 20. Acetyl-CoA carboxylase structure and reaction. ACC is composed of three subunits: the BC and the CT domains, and the BCCP. The latter plays a crucial role in the catalysis as it binds biotin, via a lysine residue, which is carboxylated by HCO_3^- and transferred to acetyl-CoA, which is converted to malonyl-CoA. The net reaction catalyzed by ACC consists in the carboxylation of acetyl-CoA into malonyl-CoA in the presence of HCO_3^- and ATP. The decarboxylation of malonyl-CoA into acetyl-CoA is catalyzed by the MCD. ACC: acetyl-CoA carboxylase; BC: biotin carboxylase; CT: carboxyltransferase; BCCP: biotin-carboxyl carrier protein; MCD: malonyl-CoA decarboxylase.

The BC and CT domains are responsible for carrying out the enzymatic activity of ACC while BCCP has a crucial structural role since it carries a lysine residue that forms an amide bond with biotin, an essential co-factor for ACC catalysis. The structures of the BC and the CT domains have been particularly well characterized. The BC subunit, which can dimerize, contains three

domains: A, B and C. While A and C domains constitute the active site, the B domain closes the active site during catalysis [196]. The CT domain contains the N and C sub-domains. In order to be catalytically active, CT must dimerize as its active site is formed at the interface of two CT domains dimers [196].

9.2 Acetyl-CoA carboxylase reaction

ACC catalysis proceeds in a two-step reaction, involving the BC and CT domains which have two distinct enzymatic activities (Figure 20). The first step involves the BC domain which carboxylates biotin, in the presence of MgATP, using HCO_3^- as the CO_2 donor, and forming carboxybiotin. In the second step, the CT domain catalyzes the CO_2 transfer from carboxybiotin to the acceptor molecule which is usually acetyl-CoA [196]. Acetyl-CoA carboxylation results in malonyl-CoA synthesis. Biotin therefore needs to be transferred from the BC to the CT domain between the two-steps of the reaction. This is occurring through the swinging arm model which requires biotin to be linked via a flexible arm that can rotate between the two domains. In ACC, the nature of the bond between biotin and BCCP makes it extendable and flexible, allowing biotin to swing between the two catalytic domains [196].

9.3 Acetyl-CoA carboxylase isoforms and roles

Mammals express two ACC isoforms, known as ACC1 and ACC2, which have different tissue distributions, cellular localizations and roles, even though they catalyze the same reaction. ACC1 and ACC2 are highly conserved and share 73 % amino acid sequence identity. ACC1 is cytoplasmic

and mainly expressed in lipogenic tissues such as the liver and adipose tissue. On the other hand, ACC2 is more common in oxidative tissues such as the heart and skeletal muscle and is associated with the outer mitochondrial membrane. Indeed, as compared to ACC1, ACC2 has an extra N-terminal of 140 residues, of which the 20 first amino acids are highly hydrophobic, allowing its attachment to the mitochondrial membrane [197]. In view of these different cellular localizations, it has been suggested that two different pools of malonyl-CoA co-exist and it was therefore shown that the two isoforms have distinct roles [198, 199]. While malonyl-CoA produced from ACC1 is mostly involved in *de novo* lipogenesis [198], malonyl-CoA generated from ACC2 inhibits CPTI [199], the essential enzyme allowing fatty acids entry in the mitochondria for their oxidation. In this regard, $ACC1^{+/-}$ hepatocytes display no differences in fatty acid oxidation [198], while $ACC2^{/-}$ hepatocytes continuously oxidize fatty acids and show normal *de novo* lipogenesis [199].

Due to its central role in lipid metabolism, ACC has been shown to be involved not only in metabolic syndrome, such as obesity and diabetes [200], but also in cancer progression [201].

9.4 Regulation of acetyl-CoA carboxylase activity

ACC activity, like many metabolic enzymes, is tightly controlled both by allosteric and covalent (phosphorylation) modifications. Under resting conditions, ACC exists as a homodimer of 500 kDa that can possibly undergo extensive polymerization. Accordingly, the most important allosteric regulator is citrate which activates the enzyme by promoting its

polymerization [202]. In contrast, covalent modifications inhibit the enzyme. Both ACC isoforms contain up to eight phosphorylated residues. Among these, Ser79, Ser1200, Ser1215, all located in the N-terminal extension of the BC domain, have been shown to be phosphorylated by the AMPK and Ser77 and Ser1200 by the PKA [203]. Of these phosphorylated residues, only Ser77 and Ser79 phosphorylation lead to ACC inhibition [204]. While PKA-mediated Ser77 phosphorylation only induces modest changes of ACC activity [204], it has been shown that the AMPK-induced ACC inhibition is only dependent upon Ser79 phosphorylation. Indeed, the single mutation of Ser79 to alanine totally prevents ACC inactivation by AMPK [205]. Ser79 phosphorylation decreases ACC Vmax [206] by preventing the polymerization of the BC domains, crucial for ACC activity [207] . Ser79 residue is found on ACC1 isoform sequence while its corresponding residue is Ser212 on ACC2 [208]. Therefore, AMPK-dependent ACC inactivation is mediated both by Ser79 and Ser212 phosphorylation on ACC1 and ACC2, respectively.

9.5 AMPK-ACC signalling: role in metabolic homeostasis

9.5.1 Role in lipid homeostasis and insulin sensitivity

The essential role of AMPK-dependent ACC phosphorylation in the control of lipid homeostasis and insulin sensitivity has been highlighted in ACC double knock-in (DKI) mice carrying alanine mutations in both ACC1 (at Ser79) and ACC2 (at Ser212) [209]. Along with increased liver ACC1 and ACC2 activity, ACC DKI mice display increased hepatic *de novo* lipogenesis and lower fatty acid oxidation. As a result, ACC DKI liver DAG and triglycerides

(TG) contents are increased, leading to clinical signs of nonalcoholic fatty liver disease (NAFLD), such as hepatic fibrosis. Similarly, muscle DAG and TG content is increased in ACC DKI mice. This excessive lipid accumulation consequently renders ACC DKI mice hyperglycaemic, hyperinsulinemic, glucose and insulin intolerant compared to ACC WT. These observations indicate that AMPK-induced ACC phosphorylation controls lipid homeostasis which, if unregulated, directly affects insulin sensitivity.

9.5.2 Role in lipid oxidation

The heart and skeletal muscles are two highly oxidative tissues which oxidize fatty acids to provide energy for maintaining their functions. The importance of AMPK-ACC axis in the regulation of fatty acid oxidation has therefore also been investigated in these tissues.

9.5.2.1 Skeletal muscle

Resting skeletal muscles of ACC2 knock-in (KI) mice, carrying a single alanine mutation in Ser212 of ACC2, display decreased lipid oxidation, associated with an increase in TG and ceramides levels, leading to skeletal muscle insulin resistance [210]. In contrast to resting state, ACC2 KI mice had normal rates of fatty acid oxidation during muscle contractions or treadmill exercise, indicating that ACC2 phosphorylation is not essential for controlling lipid oxidation during exercise [211].

9.5.2.2 Heart

The impact of a lack of ACC phosphorylation on heart function was studied in ACC DKI mice. Unexpectedly, their heart display normal cardiac

functions, morphology and myocardial fatty acid oxidation under basal conditions, during elevated workloads, as well as after a myocardial ischaemia, a condition known to strongly activate the AMPK [212]. These results indicate that other mechanisms, besides AMPK-ACC, exist for maintaining cardiac fatty acid oxidation rates.

9.6 Acetyl-CoA carboxylase in platelet

It has been known for a long time that platelets express ACC [132] but its role in the regulation of platelet function has never been investigated. We [29] and others [213, 214] reported that ACC is phosphorylated on its Ser79/Ser212 by AMPK in response to platelet agonists (Figure 21).

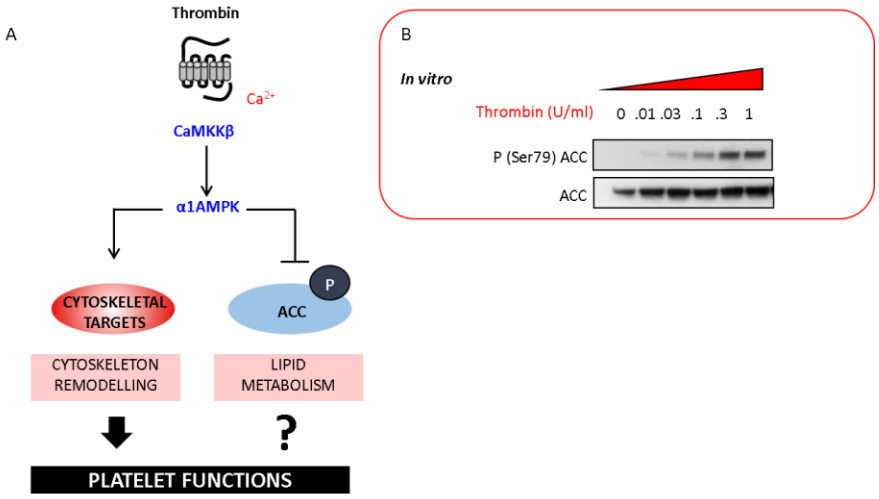

Figure 21. α1AMPK controls platelet functions. (A) We previously showed that thrombin stimulates the CaMKKβ, leading to α1AMPK activation and the phosphorylation of its *bona fide* substrate, the ACC (B). By phosphorylating its cytoskeletal targets, AMPK regulates platelets cytoskeleton remodelling, thereby controlling their functions. The impact of ACC phosphorylation on platelet functions was not analyzed in this study [29]. CaMKKβ : Ca^{2+}/calmodulin-dependent protein kinase kinase β; AMPK: AMP-activated protein kinase; ACC: acetyl-CoA carboxylase.

Among platelet agonists, thrombin is the most powerful, leading to strong and sustained ACC phosphorylation in human and murine platelets both in a time- and dose-dependent manner [29, 214]. In addition, collagen [29] and lipid-derived mediators, such as 2-arachydonoylglycerol [213], have been reported to induce ACC phosphorylation.

In these studies, ACC phosphorylation was only used as a readout of AMPK activation in this work and its impact on platelet functions was not investigated.

In agreement with the *ex vivo* data, platelet ACC phosphorylation is also detectable *in vivo*, during clinical circumstances characterized by a significant activation of the coagulation cascade (and therefore a massive thrombin generation): the post-operative status following a major surgery [29].

9.7 AMPK-ACC signalling in platelet

The mechanisms leading to Ser79 phosphorylation in agonist-stimulated platelets have been elucidated. We reported that thrombin, by stimulating the Ca^{2+}/calmodulin-dependent protein kinase kinase β (CaMKKβ), an AMPK-activating kinase, induces AMPK activation and subsequent Ser79/Ser212 phosphorylation [29]. We showed that human platelets exclusively express the AMPKα1 subunit, while both subunits α1 and α2 are found in mice platelets. In addition, AMPKα1 is the main isoform controlling platelet functions by modulating the phosphorylation of its downstream cytoskeletal targets, thereby impacting actin cytoskeletal remodelling which is crucial for platelet activation (Figure 21).

The role played by AMPK in platelets has also been elucidated in another study. The authors show that the AMPKα2 subunit is the main regulator of platelet functions as compared to AMPKα1 [214]. While we cannot exclude the possibility that both AMPKα isoforms control murine platelet functions, only AMPKα1 was present in highly purified human platelets extracts. In addition, our data are supported by a transcriptomic and proteomic analysis demonstrating the exclusive presence of AMPKα1 transcript or proteins in human platelets [215, 216]. Accordingly, in a second

study led by the same authors, they finally demonstrated the presence of AMPKα1 in human platelets [217].

Randriamboavonjy et al. reported that the liver kinase B1 (LKB1) was responsible for AMPK activation by demonstrating increased AMPK-dependent phosphorylation of LKB1 [214]. However, it is known that LKB1 is constitutively active and that its activity is solely regulated by the relative levels of its partner, STRAD and MO25 [218]. We therefore evaluated LKB1 activity after coimmunoprecipitation of the enzymatic complex from platelet extracts after thrombin stimulation and show no differences. Analysis of ACC phosphorylation in LKB1 (or CaMKKβ) knock-out platelets could resolve this discrepancy.

AIMS

1 EVALUATING THE IMPACT OF ACC PHOSPHORYLATION ON PLATELET FUNCTIONS IN A GENETICALLY MODIFIED MOUSE MODEL

AMPKα1 is activated in platelets upon thrombin or collagen stimulation, and as consequence, phosphorylates and inhibits ACC which is crucial for the synthesis of fatty acids. Given the key roles of lipids in platelets, namely structural, signalling and energy storage, we hypothesized that this enzyme plays a central regulatory role in platelet function. To investigate this, we used the ACC DKI mouse model in which the AMPK phosphorylation sites Ser79 on ACC1 and Ser212 on ACC2 were mutated to prevent AMPK-signalling to ACC.

Our main research objectives were:

a) Evaluate the effect of ACC phosphorylation/inhibition on platelet functions, structure, lipidomics and bioenergetics.
b) Determine the *in vivo* importance of ACC phosphorylation on haemostasis and arterial thrombosis.

Results are described in a manuscript published in Blood (DOI: 10.1182/blood-2018-02-831503) “AMPK-ACC signalling modulates platelet phospholipids content and potentiates platelet function and thrombus formation.” By Sophie Lepropre*, Shakeel Kautbally*, Marie Octave, Audrey Ginion, Marie-Blanche Onselaer, Gregory R. Steinberg, Bruce E. Kemp, Alexandre Hego, Odile Wéra, Sanne Brouns, Frauke Swieringa, Martin Giera,

Victor M. Darley-Usmar, Jérôme Ambroise, Bruno Guigas, Johan Heemskerk, Luc Bertrand, Cécile Oury, Christophe Beauloye and Sandrine Horman.
*Contributed equally to the work

2 CLINICAL EVALUATION OF ACC PHOSPHORYLATION IN CAD PATIENTS (ACCTHEROMA CLINICAL TRIAL)

Given the role of AMPK-ACC signalling on platelet lipid metabolism and function, this pathway could be affected in platelets of patients suffering from CAD, where the atherogenic environment has an impact on platelet biology. Our objective was here to determine whether platelet AMPK-ACC signalling is activated by atherogenic lipids and could be considered as a potential marker for risk assessment in patients with suspected CAD
Our main research objectives in this second part of the work were:

a) Evaluate prospectively ACC phosphorylation state in platelets from patients with CAD or atherosclerosis, as a marker of atherothrombotic disease.
b) Determine the factors influencing ACC phosphorylation state, in addition to known thrombin generation markers, in diseased patients.
c) Study the impact of ACC phosphorylation on platelet lipid content in diseased patients.

Manuscript submitted in the Journal of American College of Cardiology: “Platelet acetyl-CoA carboxylase phosphorylation: A risk stratification marker evidencing platelet-lipid interplay in CAD patients.” By Shakeel Kautbally*, Sophie Lepropre*, Marie-Blanche Onselaer, Astrid Le Rigoleur, Audrey Ginion, Christophe De Meester de Ravenstein, Jerome Ambroise, Karim Z.Boudjeltia, Marie Octave, Odile Wera, Philippe Lesnik, Martin Giera, Bernhard Gerber, Anne-Catherine Pouleur, Bruno Guigas; Jean-Louis Vanoverschelde, Luc Bertrand, Cecile Oury, Sandrine Horman and Christophe Beauloye.

*Contributed equally to the work

Elucidating the impact of ACC phosphorylation on platelet functions from a fundamental perspective does not only contribute to platelet lipid metabolism understanding, which is poorly documented, but might also have far-reaching clinical relevance in the context of CAD.

RESULTS-1

Part 1

AMPK-ACC signalling modulates platelet phospholipids content and potentiates platelet function and thrombus formation

Sophie Lepropre[1,*], Shakeel Kautbally[1,*], Marie Octave[1], Audrey Ginion[1], Marie-Blanche Onselaer[1,2], Gregory R. Steinberg[3], Bruce E. Kemp[4,5], Alexandre Hego[6], Odile Wéra[6], Sanne Brouns[7], Frauke Swieringa[7], Martin Giera[8], Victor M. Darley-Usmar[9], Jérôme Ambroise[10], Bruno Guigas[8,11], Johan Heemskerk[7], Luc Bertrand[1], Cécile Oury[6], Christophe Beauloye[1,12,#] and Sandrine Horman[1,#]

[1]Pôle de Recherche Cardiovasculaire, Institut de Recherche Expérimentale et Clinique, Université catholique de Louvain (UCL), Brussels, Belgium [2]Institute of Cardiovascular Sciences, College of Medical and Dental Sciences, University of Birmingham, Birmingham, United Kingdom [3]Division of Endocrinology and Metabolism, Departments of Medicine and Biochemistry and Biomedical Sciences, McMaster University, Hamilton, Ontario, Canada [4]St. Vincent's Institute of Medical Research and Department of Medicine, University of Melbourne, Fitzroy, VIC, 3065, Australia [5]Mary MacKillop Institute for Health Research, Australian Catholic University, Fitzroy, VIC, 3065, Australia [6]Laboratory of Thrombosis and Haemostasis and Valvular Heart Disease, GIGA-Cardiovascular Sciences, Department of Cardiology, Université de Liège, CHU Sart-Tilman, Liège, Belgium [7]Department of Biochemistry, Cardiovascular Research Institute Maastricht, University of Maastricht, Maastricht, the Netherlands [8]Center for Proteomics and Metabolomics, Leiden University Medical Center, Leiden, the Netherlands [9]Department of Pathology, UAB Mitochondrial Medicine Laboratory, Center for Free Radical Biology, University of Alabama at Birmingham, Birmingham, AL, USA[10]Centre de Technologies Moléculaires Appliquées, Institut de Recherche Expérimentale et Clinique, UCL, Brussels, Belgium [11]Department of Molecular Cell Biology and Department of Parasitology, Leiden University Medical Center, Leiden, the Netherlands [12]Division of Cardiology, Cliniques Universitaires Saint-Luc, UCL, Brussels, Belgium

[*] S.L. and S.K. contributed equally and are joint first authors.

[#]C.B. and S.H. contributed equally and are joint last authors.

Published in **Blood**, 2018 Jul 17. pii: blood-2018-02-831503.
DOI: 10.1182/blood-2018-02-831503.

1. ABSTRACT

AMP-activated protein kinase (AMPK) α1 is activated in platelets upon thrombin or collagen stimulation, and as consequence phosphorylates and inhibits acetyl-CoA carboxylase (ACC). Since ACC is crucial for the synthesis of fatty acids, which are essential for platelet activation, we hypothesized that this enzyme plays a central regulatory role in platelet function. To investigate this, we used a double knock-in (DKI) mouse model in which the AMPK phosphorylation sites Ser79 on ACC1 and Ser212 on ACC2 were mutated to prevent AMPK-signalling to ACC. Suppression of ACC phosphorylation promoted injury-induced arterial thrombosis in vivo and enhanced thrombus growth ex vivo on collagen-coated surfaces under flow. After collagen stimulation, loss of AMPK-ACC signalling was associated with amplified thromboxane generation and dense granule secretion. ACC DKI platelets had increased arachidonic acid-containing phosphatidylethanolamine plasmalogen lipids. In conclusion, AMPK-ACC signalling is coupled to the control of thrombosis by specifically modulating thromboxane and granule release in response to collagen. It appears to achieve this by increasing platelet phospholipid content required for the generation of arachidonic acid, a key mediator of platelet activation.

2. INTRODUCTION

A growing body of evidence shows that lipids are essential in regulating platelet functions. Indeed, the platelet exhibits a complex array of over 5000 distinct lipid species with over 700 responding to thrombin

activation[138]. Given this increased focus on the role of lipid species in platelet function, it is imperative to understand the molecular basis of their regulation during platelet activation. Acetyl-CoA carboxylase (ACC) is a good candidate because of its established role as a central regulator of fatty acid metabolism [209]. ACC catalyzes acetyl-CoA carboxylation to form malonyl-CoA. Its two isoforms, ACC1 and ACC2, have distinct cellular distributions [219]. ACC1 is present in the cytosol and synthesizes malonyl-CoA for *de novo* lipogenesis [198], while ACC2 is localized on the outer mitochondrial membrane and generates malonyl-CoA which inhibits fatty acid transport into mitochondria for oxidation [197, 200]. ACC is a *bona fide* substrate of AMP-activated protein kinase (AMPK) and its phosphorylation is typically used as a marker of AMPK activation in cells and tissues, including platelets [29, 213, 214]. AMPK phosphorylates ACC1/2 on serine residues (Ser79/212), leading to suppression of ACC activity [206, 220]. We have previously reported that AMPKα1 is activated in platelets upon thrombin stimulation, and increases the phosphorylation of myosin regulatory light chains (MLCs), cofilin, and vasodilator-stimulated phosphoprotein (VASP) [29]. These cytoskeletal proteins are critical for triggering platelet shape change and the centralization of secretory granules during platelet activation [221]. However, the impact of AMPK-mediated ACC phosphorylation on platelet function has never been investigated.

Fatty acids fulfil at least three main roles: structural, signalling and energy storage. Phospholipids (PL) are the major structural lipids in platelets. Upon platelet activation, reorganization of the plasma membrane PL facilitates shape change, filopodia and lamellipodia formation [144] as well

as granule secretion [146] or microvesicle formation. In addition to this structural role, PL provide substrates for phospholipases A (PLA) or C (PLC) to generate bioactive species, including phosphatidylinositides, 1,2-diacylglycerol (DAG), inositol 1,4,5-trisphosphate, and eicosanoids/prostaglandins [138]. These secondary mediators are crucial for the tight regulation of platelet activation [66, 222, 223].

Finally, lipids contribute to platelet energy metabolism. In the basal state, platelets are more oxidative than glycolytic [180, 224] and lipid oxidation contributes to at least one-third of the total oxygen consumed by mitochondria [24, 180, 225]. Mitochondrial lipid oxidation increases upon thrombin stimulation, to cope with the energetic demands of platelet activation [24, 226], a process which is supported by the enhanced availability of eicosanoids released from the membrane PL through the action of Ca^{2+}-dependent cytosolic phospholipase A_2 ($cPLA_2$) [138].

Clearly, the signalling needed to coordinate these diverse functions of PL metabolism is important to define. In the current study, we hypothesized that ACC controls key aspects of platelet function using mice with alanine knock-in mutations in both ACC1 (at Ser79) and ACC2 (at Ser212) (ACC double knock-in (ACC DKI) mice). These mice harbor functional ACC and AMPK but express a mutant form of ACC that can no longer be inhibited by AMPK phosphorylation resulting in a persistent active form of the enzyme [209].

Here, we report that blood from ACC DKI mice have increased thrombus formation on collagen-coated surfaces or after vascular injury.

The underlying mechanisms involve elevated levels of arachidonic acid (AA)-containing phosphatidylethanolamine plasmalogen (PEP) lipids in ACC DKI platelets compared to wild type (WT), increasing thromboxane A_2 (TXA_2) generation and granule secretion after platelet stimulation with collagen. Although mitochondrial fatty acid oxidation is important in thrombin-dependent platelet activation, we found that AMPK-ACC signalling had no effect on platelet bioenergetics.

These findings highlight a novel metabolic regulatory pathway in platelets that influences thrombus formation by modulating the content of specific PL which generate key mediators of platelet activation.

3. MATERIEL AND METHODS

3.1 Mice

ACC1/2 DKI mice have been described previously [209]. WT mice served as controls. Eight- to sixteen- week-old male mice were studied. Animal procedures and protocols were approved by local authorities (*Comité d'éthique facultaire pour l'expérimentation animale*, 2012/UCL/MD/003 and 2016/UCL/MD/027) and performed in accordance with the Guide for the Care and Use of Laboratory Animals, published by the US National Institutes of Health (NIH Publication No. 85-23, revised 1996).

3.2 Platelet preparation

Murine platelet Mice were bled under ketamine and xylazine anesthesia from the retro-orbital plexus. Blood was collected in 1/6 citrate-

dextrose (ACD) solution with apyrase 1 U/ml. PRP was obtained by centrifugation at 800 g for 5 s, followed by 5 min at 100 g. It was washed by adding 2 volumes of ACD with apyrase 1 U/ml. The platelets were pelleted by centrifugation at 400 g for 5 min and re-suspended to a density of 2.5 x 10^5/µl (unless stated otherwise) in modified Tyrode's buffer. Platelets were counted with Cell-Dyn Emerald. They were stimulated with agonists in the presence of 2 mM $CaCl_2$.

3.3 Flow chamber assay

Blood was collected from the retro-orbital plexus into 48 µM D-Phenylalanyl-prolyl-arginyl Chloromethyl Ketone (PPACK), 5 U/ml heparin and 40 U/ml fragmin. Samples of 400 µl were flowed over type I collagen-coated (100 µg/ml), vWF-binding protein (BP) (12.5 µg/ml) and laminin (50 µg/ml)- or vWF-BP (12.5 µg/ml), laminin (50µg/ml) and rhodocytin (250 µg/ml)-coated coverslips mounted on a transparent, parallel plate flow chamber (50 µm depth, 3 mm width and 20 mm length), at a shear rate of 1,000 s^{-1} for 3.5 min, as described [227]. Alternatively, samples were pre-incubated with 20 µM Ticagrelor for 10 min or the corresponding vehicle (DMSO) and flowed over type I collagen-coated coverslips, as described above. Activated platelets in thrombi were post-stained with FITC-labeled anti-P-selectin Ab (1:40), PE-labeled JON/A Ab against the active conformation of αIIbβ3 (1:20) or Alexa Fluor 647-annexin A5 (1:200), all diluted in Tyrode's buffer. Labeling was undertaken for 2 min (stasis), after which unbound Abs were removed by perfusion with Tyrode's buffer. Brightfield phase-contrast and fluorescence images were recorded by a non-

confocal 2-camera system. Surface coverage was analyzed by ImagePro software (Media Cybernetics) [228].

3.4 Ferric chloride-induced thrombosis

Carotid arteries were injured in anesthetized mice by topical application of 10% ferric chloride ($FeCl_3$) for 5 min, as described previously [229]. Briefly, exogenous Carboxyfluorescein Succinimidyl Ester (CFSE)-labeled platelets were injected into the jugular vein of anesthetized mice, and fluorescence was recorded by BX61WI microscope (Olympus). Digital images were captured every 2 min for a total of 24 min.

3.5 Untargeted lipidomics

Lipidomics analysis was carried out on the commercial Lipidyzer platform, according to the manufacturer's instructions (Sciex) [230]. The amount of platelets needed to obtain consistent results was evaluated before application of the commercial platform. Lipid analysis was performed in flow-injection mode, separating lipid classes by differential mobility spectroscopy [230], followed by tandem mass spectrometry of lipid species with QTrap 5500 in multiple reaction monitoring mode. Lipid species were identified and quantified on the basis of characteristic mass spectrometric transitions. Commercial Lipidyzer software automatically calculated lipid species concentrations. All samples were analyzed in a randomized fashion. Control plasma samples as well as fortified plasma samples were assessed daily as quality controls. Relative standard deviations (RSD) of quality control

samples were below 15% for all lipid classes, except for sphingomyelin where a RSD of 25% was noted.

A detailed description of the reagents and the methods is provided in *supplemental Methods*, available on the Blood Web site.

4. RESULTS

4.1 Lack of AMPK-ACC phosphorylation does not impact AMPK signalling or cytoskeletal protein phosphorylation

ACC WT and ACC DKI mice have comparable erythrocyte, leukocyte and platelet counts in whole blood (Table S1). Expression levels of the major platelet surface receptors, αIIbβ3, GPIbα, the collagen receptor GPVI, and the Protease-Activated Receptor-3 (PAR-3) and PAR-4, were equivalent in ACC WT and ACC DKI platelets (Figures S1A and S1B).

ACC1, but not ACC2, was detected in both human and murine platelets (Figure 1A). Consistent with previous observations [29], 0.2 U/ml thrombin (Figure 1B) or 5 μg/ml collagen (Figure 1C) induced phosphorylation on Ser79 of ACC in platelets from WT mice with maximal effects after 1 min and 5 min, respectively. As expected, no Ser79 ACC phosphorylation was detected in either basal or thrombin- or collagen-treated ACC DKI platelets (Figures 1B and 1C). ACC1 mutation did not influence AMPK activation, reflected by Thr172 phosphorylation (Figures 1D and 1E). In addition, thrombin- or collagen-induced phosphorylation of known AMPK cytoskeletal targets, MLC, cofilin and VASP, were similar

between ACC DKI and ACC WT platelets (Figures 1D and 1E), as well as platelet-spreading and lamellipodia/filopodia formation after platelet immobilization on fibrinogen-coated coverslips (Figures S1 C-H). These data confirm that, although ACC phosphorylation was impaired, AMPK signalling was unaltered in ACC DKI platelets.

Figure 1. Lack of AMPK-ACC phosphorylation does not impact AMPK signalling or phosphorylation of cytoskeletal proteins. (A) Washed murine and human platelets were lysed and subjected to Western blotting for ACC1 or ACC2 isoform expression analysis. Isolated rat cardiomyocytes (CM) and mouse liver extracts served as positive controls for the detection of ACC2 and ACC1, respectively. (B-E) ACC WT and ACC DKI platelets were stimulated with 0.2 U/ml thrombin (B, D) or 5 µg/ml collagen (C, E) for the indicated time points. Whole platelet lysates were subjected to Western blotting and probed with Ser79 phosphorylated ACC Ab (B, C), Thr172 phosphorylated AMPK, Ser19 phosphorylated myosin light chain (MLC), Ser3 phosphorylated cofilin and Thr278 phosphorylated vasodilator-stimulated phosphoprotein (VASP) Abs (D, E). Gelsolin and β-actin were used as loading controls. Quantification and representative Western blotting are systematically shown. The solid lines on the Western blots indicate that samples were run on the same gel but were not contiguous. The results are expressed as means ± SEM (at least 3 experiments for each condition). *indicates values statistically different from respective untreated platelets, P≤0.05. Analysis was performed by 2-way ANOVA. See also Figure S1 and Table S1.

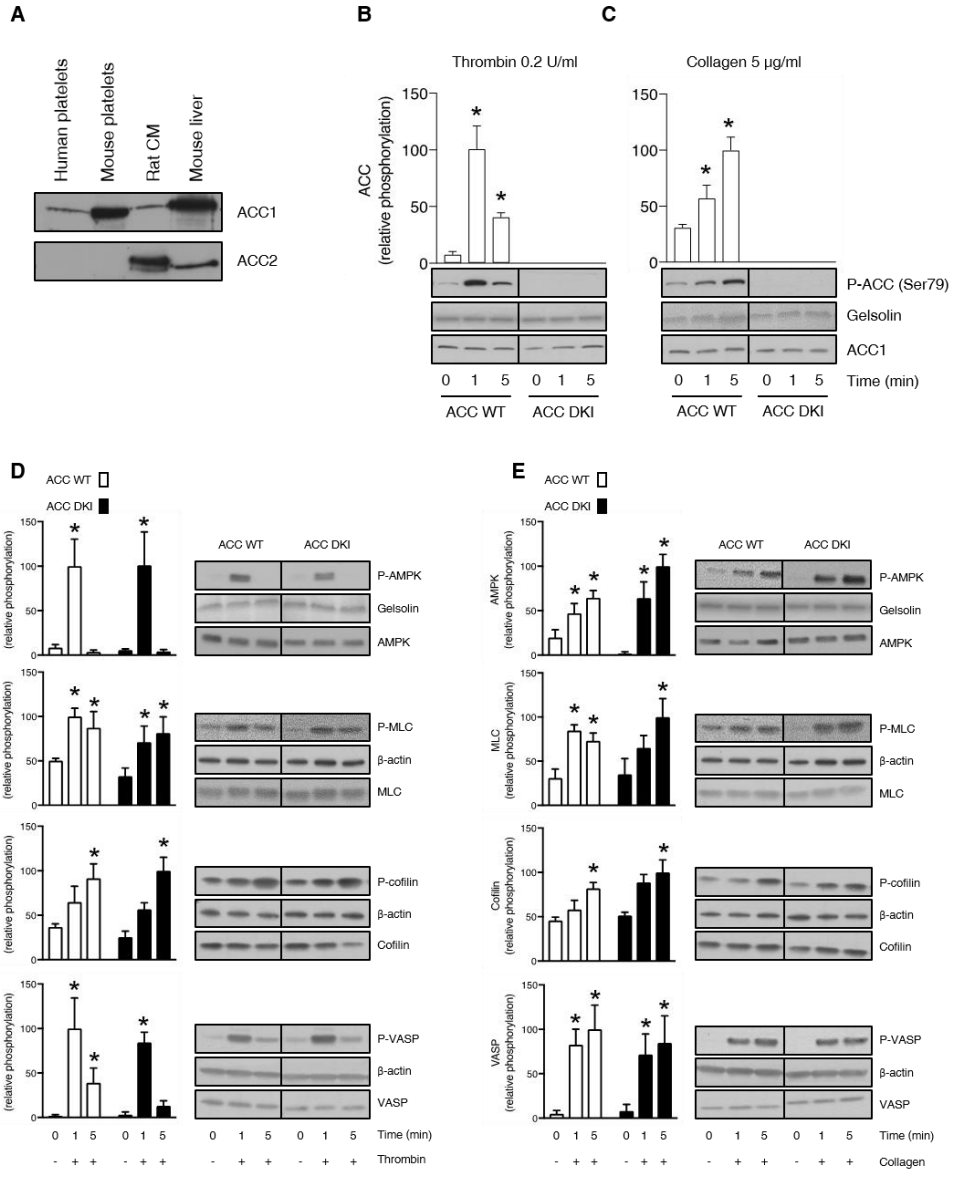
A
Human platelets
Mouse platelets
Rat CM
Mouse liver
ACC1
ACC2
B
C
Thrombin 0.2 U/ml
Collagen 5 µg/ml
ACC (relative phosphorylation)
P-ACC (Ser79)
Gelsolin
ACC1
Time (min)
ACC WT
ACC DKI
D
E
ACC WT
ACC DKI
AMPK (relative phosphorylation)
MLC (relative phosphorylation)
Cofilin (relative phosphorylation)
VASP (relative phosphorylation)
P-AMPK
AMPK
P-MLC
MLC
β-actin
P-cofilin
Cofilin
P-VASP
VASP
Thrombin
Collagen

4.2 ACC DKI mice display enhanced primary haemostasis and thrombosis

The impact of AMPK-mediated ACC phosphorylation on haemostasis and thrombosis was evaluated *in vivo*. No spontaneous bleeding or thrombotic event was observed in 91 ACC DKI young mice (up to 4 months) or 19 ACC DKI older mice (at least 9 months old). However, median tail bleeding time was significantly shorter in ACC DKI mice than in their WT counterparts (ACC DKI: 82 ± 42 s vs. ACC WT: 188 ± 51 s, $P<0.05$) (Figure 2A). We then investigated the role of ACC phosphorylation on arterial thrombosis *in vivo*, in the collagen-dependent carotid artery thrombosis model, in response to a 10% $FeCl_3$ application. Arterial thrombus formation was monitored in real time by intravital fluorescence microscopy (Figures 2B and 2C). The rate of thrombus growth was significantly increased in ACC DKI mice compared to the WT animals. The fold change increase in thrombus growth over a 20-min period of time after arterial injury was 62.4 ± 17.4 for ACC DKI mice vs. 31.3 ± 8.2 for ACC WT mice relative to baseline (Figure 2B). These data demonstrate that AMPK-ACC signalling is a key mechanism regulating primary haemostasis and arterial thrombosis *in vivo*.

4.3 Lack of AMPK-ACC signalling favours thrombus formation during perfusion on collagen in flow conditions

We next examined thrombus formation *ex vivo*, using a flow chamber system. Whole blood from ACC WT and DKI mice was perfused at an intermediate shear rate of 1,000 s^{-1}, on 3 different coated surfaces containing either collagen, laminin or vWF-binding peptide (vWF-BP) in the

absence or presence of rhodocytin[228]. Brightfield images were captured to assess overall platelet adhesion and thrombus formation. Platelet activation was simultaneously monitored by infusing fluorescently-labelled anti-CD62P antibody (Ab) as a marker of α-granule secretion, JON/A Ab to measure αIIbβ3 activation, and annexin V to analyze phosphatidylserine (PS) externalization, reflecting platelet pro-coagulant activity.

On collagen-coated coverslips, the surface area covered (SAC) by adherent platelets and their activation state (Figures 2D-F) were similar between the 2 genotypes. However, buildup of multilayered platelet thrombi was increased with ACC DKI blood compared to WT (Figure 2G), indicating that AMPK-ACC signalling affects mechanisms involved in the secondary formation of platelet aggregates on collagen. Of note, no differences in platelet adhesion and activation processes were observed between ACC DKI and WT blood perfused on laminin and vWF-BP, in the absence or presence of rhodocytin (data not shown).

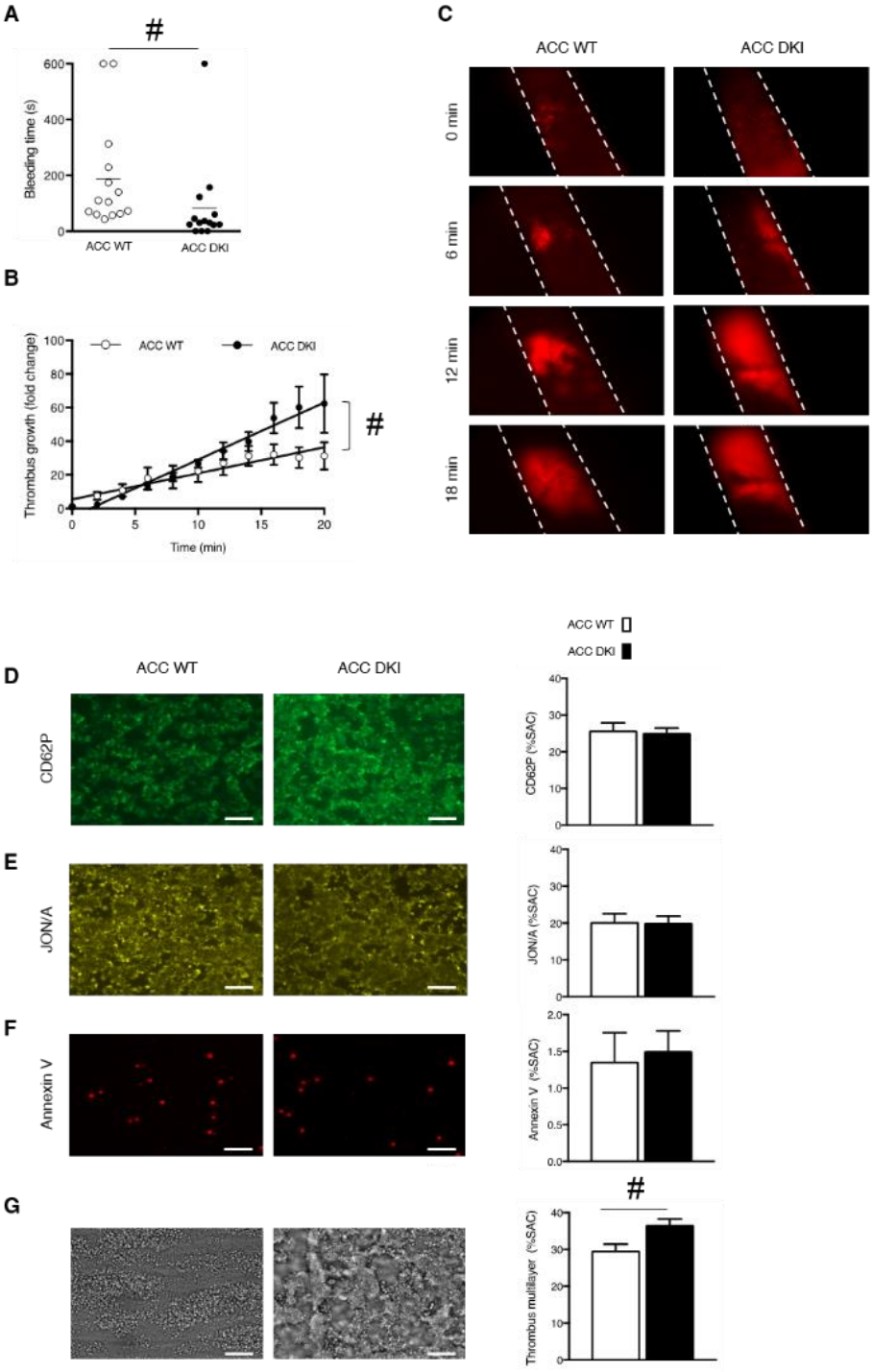
A
#
Bleeding time (s)
600
400
200
0
ACC WT
ACC DKI
B
Thrombus growth (fold change)
ACC WT
ACC DKI
100
80
60
40
20
0
0
5
10
15
20
Time (min)
#
C
ACC WT
ACC DKI
0 min
6 min
12 min
18 min
D
ACC WT
ACC DKI
CD62P
E
JON/A
F
Annexin V
G
ACC WT
ACC DKI
CD62P (%SAC)
JON/A (%SAC)
Annexin V (%SAC)
#
Thrombus multilayer (%SAC)

Figure 2. ACC DKI mice display enhanced primary haemostasis and thrombosis. (A) Tail bleeding times of ACC WT and ACC DKI mice in saline at 37°C. Individual values are plotted on the graph (n=14 in each group). Bars indicate means. #P≤0.05. Data were analyzed by the Mann-Whitney test. (B, C) ACC WT and ACC DKI mice were subjected to *in vivo* $FeCl_3$-induced thrombosis of carotid arteries (10% $FeCl_3$, 5 min). Thrombus formation was monitored by analyzing exogenous carboxyfluorescein succinimidyl ester-labeled platelet accumulation by intravital microscopy and recording videos (fluorescence) of microscopic images every 2 min. (B) Thrombus growth kinetics was evaluated by dividing the area of the thrombus at time (*t*) by the area of the same thrombus at time 0, defined as the time point at which the thrombus first reaches 100 µm. Thrombus growth is expressed as means ± SEM per group at different time points with fitted regression lines (at least 6 mice/group). Slopes are statistically different on the basis of significant interaction (#P≤0.05) between slope and group in a linear model, with group, time and their interaction as covariates. (C) Representative fluorescence microscopy images at 0, 6, 12 and 18 min after $FeCl_3$ application. (D-G) Whole blood from ACC WT and ACC DKI mice was perfused over collagen-coated surfaces (100 µg/ml) at a shear rate of 1,000 s^{-1}. Exposure of P-selectin was evaluated by staining with CD62P Ab (D), αIIbβ3 integrin activation by JON/A Ab (E) and phosphatidylserine externalization by Annexin V (F). Thrombus formation was assessed on brightfield images taken 3.5 min after initial blood perfusion (G). Representative images appear on the left. Scale bars represent 20 µm. Histograms indicate quantification of surface area covered (SAC) by P-selectin (D), activated αIIbβ3 (E), Annexin V (F)-positive platelets or multilayered platelet thrombi (G). The results are expressed as means ± SEM (at least 4 mice/group). #P≤0.05. Data were analyzed by the Mann-Whitney test.

4.4 ACC DKI platelets display increased dense granule secretion and thromboxane generation upon collagen stimulation

To further decipher the mechanisms responsible for the gain-of-function phenotype of ACC DKI mice on thrombus formation, we studied the impact of a lack of AMPK-mediated ACC phosphorylation on washed platelet reactivity. First, we investigated the effect of thrombin or collagen on αIIbβ3 inside-out activation by analyzing platelet aggregation. ACC DKI platelets aggregated normally at low and high concentrations of thrombin or collagen (Figures 3A and S2A). Accordingly, thrombin- or collagen-induced activation of αIIbβ3, detected by JON/A Ab, was normal (Figure 3B). Integrin αIIbβ3-mediated clot retraction consistently showed no differences between ACC WT and ACC DKI platelets after thrombin stimulation (Figures S2B and S2C).

Besides αIIbβ3 activation, TXA_2 generation and ADP released from dense granules are important players in collagen-induced platelet aggregate formation under flow [36, 37] and in thrombus formation *in vivo* [23, 231]. Interestingly, the lack of AMPK-ACC signalling amplified dense granule release, specifically in response to collagen. Indeed, a significant 30% increase of ATP (Figures 3C and 3D) and serotonin secretion (Figure 3E) was detected after collagen stimulation in ACC DKI platelets compared to WT, but not in response to thrombin (Figures 3C and 3E). To further conclude that this increase was related to secretion rather than to augmented packaging of dense granules, we measured total ADP, ATP and serotonin content in platelet extracts and found no difference between genotypes (Figure 3F and 3G). Regarding α-granule secretion, P-selectin surface exposure was similar between ACC WT and ACC DKI platelets (Figure S3A). However, platelet factor 4 (PF4) secretion was potentiated upon collagen stimulation in ACC DKI platelets (Figure S3B), while total PF4 levels in α-granules showed no change (Figure S3C), indicating that the ACC DKI phenotype seems also associated with increased α-granule secretion, at least those containing PF4.

Lack of AMPK-ACC signalling potentiated TXA_2 generation in response to collagen (Figure 3H), independently of any change in basal cyclooxygenase 1 (COX-1) expression or activity (Figure S4A and S4B). To evaluate the connection between ACC DKI-related increased TXA_2 generation and dense granule secretion, collagen-stimulated ACC DKI platelets were pre-treated with 1 mM aspirin (ASA) before assessment of serotonin secretion. As expected, COX-1 inhibition by aspirin almost

completely abolished collagen-induced TXA_2 generation (Figure 3H). In this condition, collagen failed to further enhance serotonin secretion in ACC DKI compared to WT platelets (Figure 3I), demonstrating that the increase in dense granule secretion observed in ACC DKI platelets depends on TXA_2 synthesis. The increased TXA_2 generation in ACC DKI platelets did not result from the enhanced dense granule release induced by collagen, as Ticagrelor, a $P2Y_{12}$ inhibitor, preserved TXA_2 potentiation in ACC DKI platelets (Figure 3J).

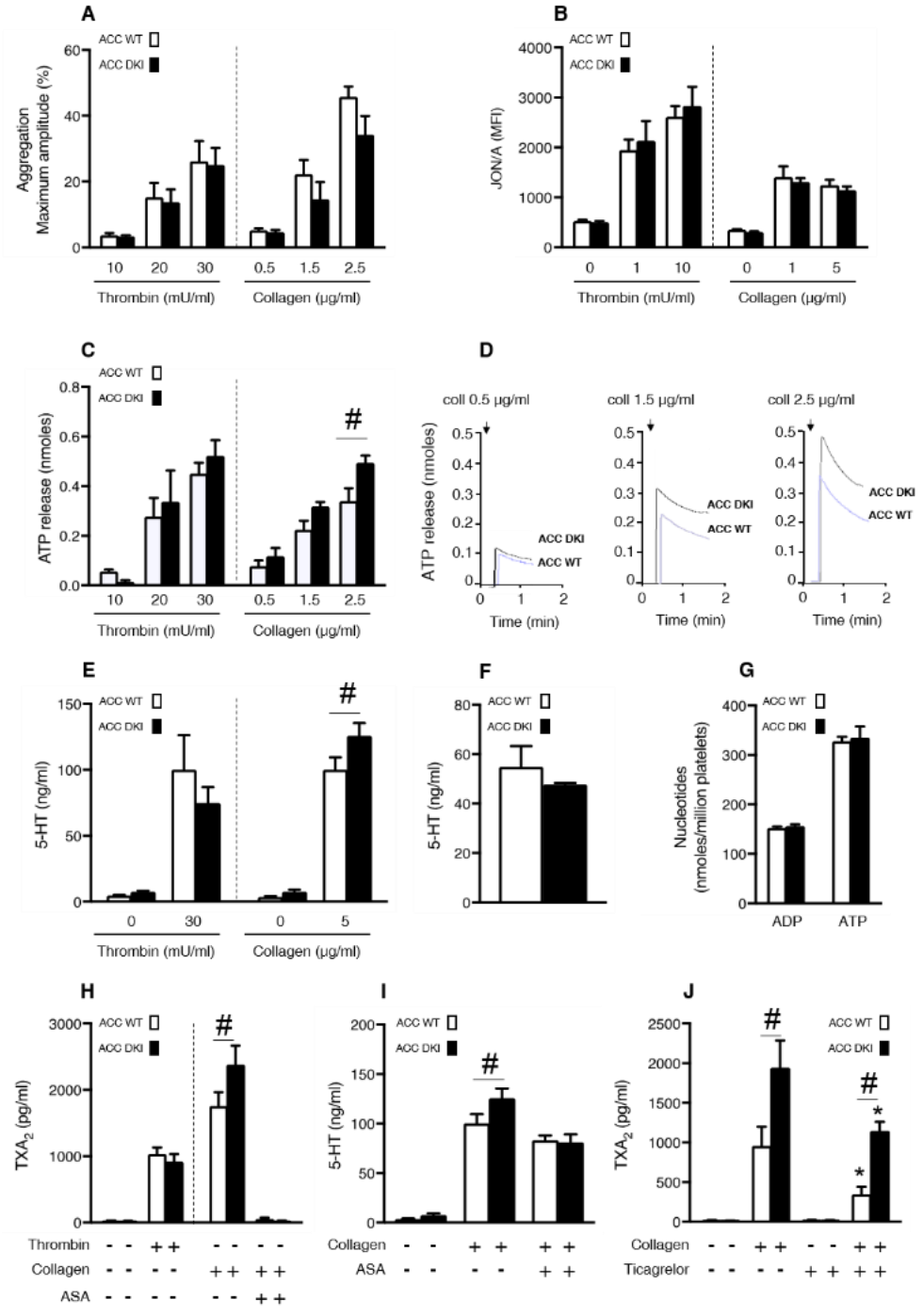
A
ACC WT
ACC DKI
Aggregation Maximum amplitude (%)
60
40
20
0
10 20 30
Thrombin (mU/ml)
0.5 1.5 2.5
Collagen (µg/ml)
B
ACC WT
ACC DKI
JON/A (MFI)
4000
3000
2000
1000
0
0 1 10
Thrombin (mU/ml)
0 1 5
Collagen (µg/ml)
C
ACC WT
ACC DKI
ATP release (nmoles)
0.8
0.6
0.4
0.2
0.0
#
10 20 30
Thrombin (mU/ml)
0.5 1.5 2.5
Collagen (µg/ml)
D
coll 0.5 µg/ml
coll 1.5 µg/ml
coll 2.5 µg/ml
ATP release (nmoles)
ACC DKI
ACC WT
Time (min)
E
ACC WT
ACC DKI
5-HT (ng/ml)
150
100
50
0
#
0 30
Thrombin (mU/ml)
0 5
Collagen (µg/ml)
F
ACC WT
ACC DKI
5-HT (ng/ml)
80
60
40
20
0
G
ACC WT
ACC DKI
Nucleotides (nmoles/million platelets)
400
300
200
100
0
ADP
ATP
H
ACC WT
ACC DKI
TXA2 (pg/ml)
3000
2000
1000
0
#
Thrombin - - + + - - - -
Collagen - - - - + + + +
ASA - - - - - - + +
I
ACC WT
ACC DKI
5-HT (ng/ml)
200
150
100
50
0
#
Collagen - - + + + +
ASA - - - - + +
J
ACC WT
ACC DKI
TXA2 (pg/ml)
2500
2000
1500
1000
500
0
#
#
*
*
Collagen - - + + - - + +
Ticagrelor - - - - + + + +

Figure 3. ACC DKI platelets display increased dense granule secretion and thromboxane generation upon collagen stimulation. (A) Washed platelets were stimulated with thrombin or collagen at the indicated concentrations, and light transmission was measured (Chrono-Log). Aggregation is expressed as the maximal percentage of light transmitted. The dashed line represents separate analyses. The results are expressed as means ± SEM (at least 4 experiments for each condition). (B) αIIbβ3 activation (binding of JON/A) was analyzed by flow cytometry in washed ACC WT and DKI platelets stimulated with thrombin for 8 min or collagen for 30 min at the indicated concentrations. The dashed line represents separate analyses. The results are expressed as mean fluorescence intensity (MFI) ± SEM (at least 4 experiments for each condition). (C, D) Washed ACC WT and DKI platelets were stimulated with thrombin or collagen at the indicated concentrations in the presence of Luciferase-Luciferin reagent, and ATP release was measured in a Lumi-aggregometer. (C) The dashed line represents separate analyses. The results are expressed as mean amount of ATP released (nmoles) ± SEM (at least 4 experiments for each condition). $^{\#}$P≤0.05 between ACC WT and DKI platelets. The data underwent 2-way ANOVA. (D) Representative traces of ATP secretion after 0.5 µg/ml, 1.5 µg/ml and 2.5 µg/ml collagen stimulation. (E) Washed platelets (30 x 10^3/µl) were stimulated with 30 mU/ml thrombin or 5 µg/ml collagen for 5 min, and serotonin (5-HT) was measured in the supernatant by ELISA kit. The dashed line represents separate analyses. The results are normalized to ACC WT-stimulated platelets and are expressed as means ± SEM (at least 3 experiments for each condition). $^{\#}$P≤0.05 between ACC WT and DKI platelets. The data underwent 2-way ANOVA. (F) Washed platelets (7.5 x 10^3/µl) were centrifuged, the pellet was lysed, and serotonin (5-HT) was assayed in the lysate. The results are expressed as means ± SEM (n=3). (G) Washed platelets were centrifuged, the pellet was lysed, and ADP and ATP content assayed in the lysate by reverse-phase high-performance liquid chromatography (HPLC). Results are expressed as means ± SEM (n=3). (H) Washed platelets were stimulated with 100 mU/ml thrombin alone or pre-incubated or not for 45 min with 1 mM aspirin (ASA), and stimulated with 5 µg/ml collagen. TXA_2 was measured in the supernatant by ELISA. The dashed line represents separate analyses. The results are expressed as means ± SEM (at least 3 experiments for each condition). $^{\#}$P≤0.05 between ACC WT and DKI platelets. The data underwent 2-way ANOVA. (I) Washed platelets were pre-incubated or not for 45 min with 1 mM ASA and stimulated with 5 µg/ml collagen. Serotonin (5-HT) was measured in the supernatant by ELISA. The results are expressed as means ± SEM (at least 3 experiments for each condition). $^{\#}$P≤0.05 between ACC WT and DKI platelets. The data were assessed by 2-way ANOVA. (J) Washed platelets were pre-incubated with 30 µM Ticagrelor or the corresponding vehicle (DMSO) for 30 min and stimulated with 5 µg/ml collagen for 5 min. TXA_2 was measured in the supernatant by ELISA. The results are expressed as means ± SEM (n=4). *P≤0.05 relative to respective untreated platelets, $^{\#}$P≤0.05 between ACC WT and ACC DKI platelets. The data underwent 2-way ANOVA. See also Figures S2-S5.

More interestingly, whole-blood flow perfusion experiments over type I collagen showed that Ticagrelor completely abolished the increased thrombus buildup in ACC DKI blood compared to WT, demonstrating the key implication of dense granule secretion in the enhanced thrombus formation (Figures 4A and 4B).

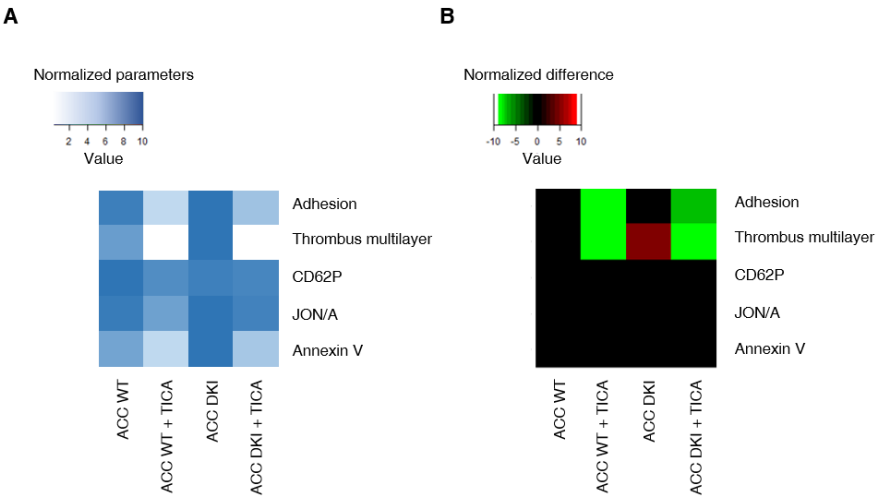

Figure 4. Increased thrombus formation in ACC DKI mice is prevented by $P2Y_{12}$ inhibition. (A-B) Whole-blood flow perfusion experiments were performed with collagen type I as platelet-adhesive substrate. Where indicated, autocrine effects were blocked by pre-incubation with 20 µM Ticagrelor (TICA) or vehicle (DMSO) for 10 min. Microscopic images were analyzed for indicated parameters, and per parameter normalized on scale 0-10 *[228]*. (A) Heatmap of normalized parameters. (B) Subtraction heatmap of normalized differences compared to WT mice, filtered for changes with P≤0.05.

In addition to thrombin and collagen, ACC WT and ACC DKI platelets were also treated with increasing concentrations of ADP, U46619, rhodocytin, an agonist of the C-type lectin like receptor-2, or collagen-related peptide (CRP), a specific GPVI agonist. For all agonists and concentrations tested, ACC DKI platelets aggregated normally (Figures S5A and S5B) and there was no difference in ATP released from dense granules (Figure S5C). These data reinforce the conclusion that the impact of AMPK-ACC signalling on TXA_2 generation and dense granule secretion is specific to platelet response to collagen. Moreover, these results reveal that collagen increases TXA_2 generation in ACC DKI platelets most likely through a mechanism involving the α2β1 integrin, which is compatible with the

enhancing role of this integrin in GPVI-dependent thrombus stability via TXA_2 production [232].

Taken together these results indicate that the absence of AMPK-ACC signalling in collagen-stimulated platelets elicits increased TXA_2 generation and, subsequently, enhanced granule secretion. These events might contribute to exacerbated thrombus growth via a mechanism that is independent of an altered αIIbβ3 activation.

4.5 Lack of AMPK-ACC signalling does not affect lipid oxidation but results in an increased AA-containing PL pool

To test whether persistent activation of ACC in platelets may affect platelet bioenergetics, we measured the thrombin- or collagen- dependent increase in mitochondrial function in ACC WT and ACC DKI platelets. As illustrated in Figure 5A-F, extracellular flux analysis showed that platelet basal oxygen consumption rate (OCR) was similar between ACC WT and DKI mice, and similar to reported studies in the literature [24, 138]. As expected, thrombin stimulated OCR (Figures 5A and 5B), which has been shown to be due to increased mitochondrial lipid oxidation [24, 138]. The oxidative phosphorylation component was further assessed by injecting oligomycin, a complex V inhibitor, which led to an expected decrease in OCR. ATP-linked respiration was not different in ACC DKI platelets compared to WT platelets. Carbonyl cyanide p-trifluoromethoxyphenylhydrazone (FCCP), a proton-ionophore, then induced maximal OCR and a corresponding decrease in maximal respiration and reserve capacity upon thrombin stimulation, owing to the mobilization of endogenous metabolic substrates to cope with

increased energetic demands. This occurred to a similar extent in platelets from both genotypes (Figures 5A and 5B). Finally, antimycin A and rotenone, complex III/I inhibitors totally inhibited mitochondrial-induced OCR. Proton leak was unchanged in all groups (Figures 5A and 5B). It has not been previously reported that collagen also stimulates mitochondrial function using this approach. As shown in Figures 5C and 5D, collagen stimulates OCR with similar characteristics to thrombin. Taken together, these data indicate that in platelets, AMPK-ACC signalling is not playing a major role in mitochondrial respiration, both basally and in the presence of thrombin or collagen. The comparable impact of Etomoxir, a carnitine palmitoyltransferase-1 inhibitor, on the ACC WT and ACC DKI platelet mitochondrial bioenergetics further supports the conclusion that platelets from both genotypes similarly rely on fatty acids to produce ATP (Figures 5E and 5F).

Figure 5. Lack of ACC phosphorylation does not impact oxidative metabolism. (A-F) Oxygen consumption rate (OCR) was measured in washed platelets pre-treated or not with Etomoxir (25 μM) (E, F) for 1 h prior to bioenergetic measurements. OCR was assessed under basal conditions, after injection of media alone or 1 U/ml thrombin (A, B) or 0.25 μg/ml collagen (C, D) or followed by treatment with 1 μM oligomycin (O), 0.1 μM FCCP (F) and a mix of 1 μM antimycin A (AA) and 1 μM rotenone (R). (A, C, E) Representative OCR profiles with thrombin (A) and collagen stimulation (C) or Etomoxir treatment (E). (B, D) Mitochondrial function was assessed by calculating basal, thrombin (B)- or collagen (D)-induced, ATP-linked, maximal, non-mitochondrial, reserve capacity and proton leak OCR. In addition, bioenergetics measurements were assessed in Etomoxir-treated platelets (F). The results are expressed as means ± SEM (at least n=3). *P≤0.05 relative to respective untreated platelets, #P≤0.05 between ACC WT and ACC DKI platelets. The data underwent 2-way ANOVA.

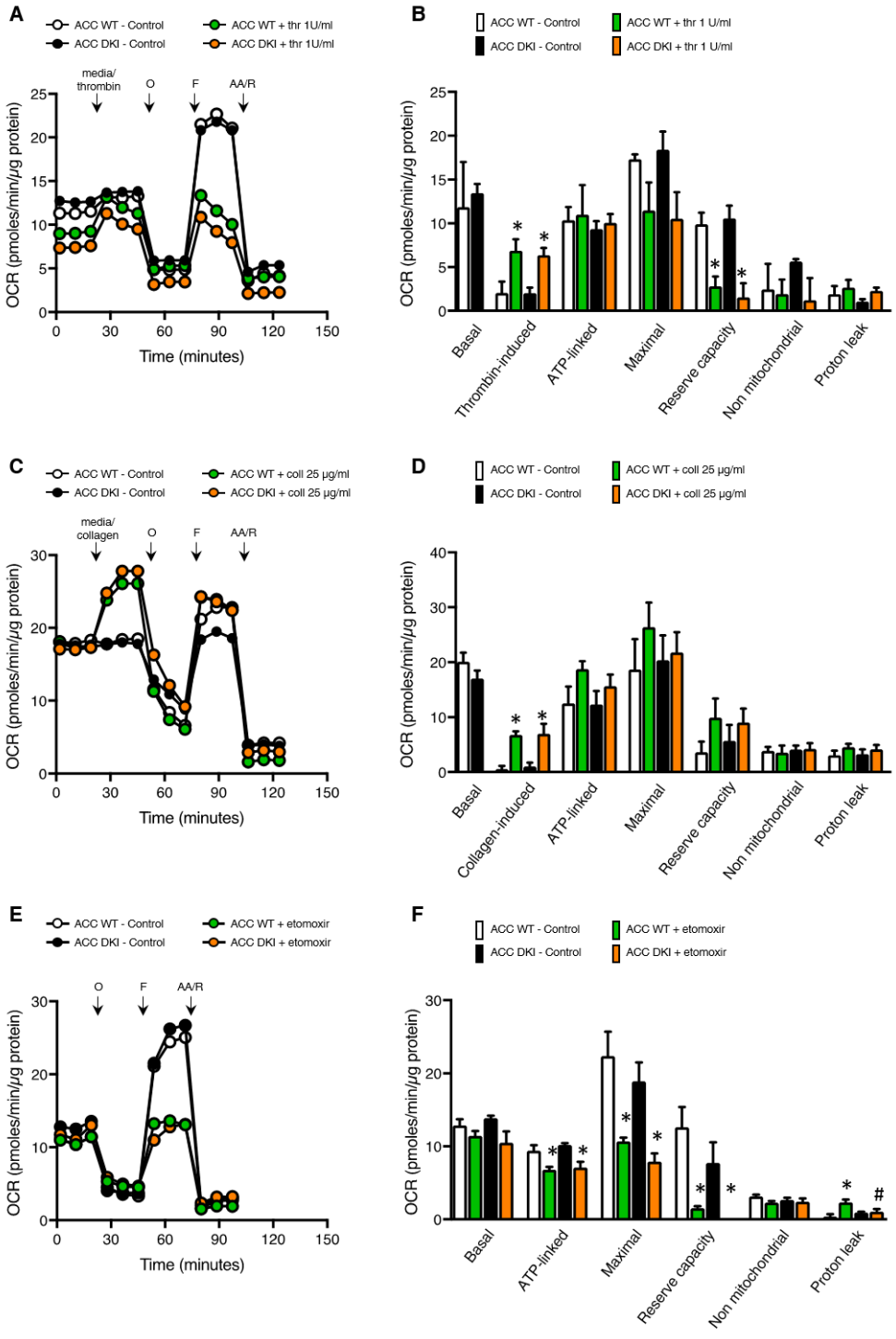
A
ACC WT - Control
ACC DKI - Control
ACC WT + thr 1U/ml
ACC DKI + thr 1U/ml
media/
thrombin
O
F
AA/R
OCR (pmoles/min/µg protein)
Time (minutes)
B
ACC WT - Control
ACC DKI - Control
ACC WT + thr 1 U/ml
ACC DKI + thr 1 U/ml
OCR (pmoles/min/µg protein)
Basal
Thrombin-induced
ATP-linked
Maximal
Reserve capacity
Non mitochondrial
Proton leak
C
ACC WT - Control
ACC DKI - Control
ACC WT + coll 25 µg/ml
ACC DKI + coll 25 µg/ml
media/
collagen
O
F
AA/R
OCR (pmoles/min/µg protein)
Time (minutes)
D
ACC WT - Control
ACC DKI - Control
ACC WT + coll 25 µg/ml
ACC DKI + coll 25 µg/ml
OCR (pmoles/min/µg protein)
Basal
Collagen-induced
ATP-linked
Maximal
Reserve capacity
Non mitochondrial
Proton leak
E
ACC WT - Control
ACC DKI - Control
ACC WT + etomoxir
ACC DKI + etomoxir
O
F
AA/R
OCR (pmoles/min/µg protein)
Time (minutes)
F
ACC WT - Control
ACC DKI - Control
ACC WT + etomoxir
ACC DKI + etomoxir
OCR (pmoles/min/µg protein)
Basal
ATP-linked
Maximal
Reserve capacity
Non mitochondrial
Proton leak

To investigate whether the gain-of-function of ACC DKI platelets relies on a modified lipid content, we undertook a quantitative lipidomic analysis of resting and stimulated platelets. Isolated ACC DKI and ACC WT platelets were either left unstimulated or activated with 25 µg/ml collagen, 0.3 U/ml thrombin or a mix of both. The lipids classes analyzed included different PL (phosphatidylethanolamine [PE], PEP, plasmenyl phosphatidylethanolamine [PEO], phosphatidylcholine [PC], lysophosphatidylethanolamine [LPE], lysophosphatidylcholine [LPC]), sphingomyelin [SM], cholesteryl esters [CE], free fatty acids [FFA], DAG and triglycerides [TAG] [233].

In agreement with previous data [234], class enrichment analysis indicated that collagen significantly up-regulated lipid species among FFA (31%), LPC (57%), LPE (38%) and DAG (21%) lipid classes, in both ACC WT and ACC DKI platelets (Figure 6A, Table S2). Enrichment of FFA and DAG was also observed in response to thrombin alone (Figure S6A) and to a combination of thrombin and collagen (Figure S6B). More importantly, loss of AMPK-ACC signalling resulted in enrichment of upregulated lipid species among PEP lipid classes (28%), independently of the basal or simulated condition (Figure 6B, Table S3). Indeed, an increase in lipid species among PEP was strongly associated with lack of ACC phosphorylation (OR: 48 [14-217], Figure 6B). ACC DKI also displayed an increment of down-regulated lipid species among CE (38%) and PC (14%) (Figure 6B). Given that ACC DKI platelets show increased TXA_2 generation, we specifically focused our data analysis on AA-containing PEP and PC, the 2 PL classes particularly containing differentially-regulated lipids. Relevant PEP species with side-chains 16:0/20:4 and

18:1/20:4 were significantly increased in ACC DKI platelets (Figure 6C). We showed that they respectively contributed 18.9% and 7.3% to the total reservoir of AA-containing PL (Figure 6D). In contrast, PC species with side-chains 18:2/20:4 and 14:0/20:4 were decreased (Figure 6C) and marginally accounted for 0.8% and 0.4%, respectively, of all AA-containing PL (Figure 6D). Taken together, up-regulated AA-containing PEP in ACC DKI platelets clearly supports the enhanced TXA_2 formation observed in this condition. Of note, the AMPK-ACC signalling did not influence platelet palmitate uptake (Figure S7A). Moreover, collagen-induced TXA_2 production was not modulated by extracellular fatty acids availability in ACC WT or ACC DKI platelets (Figure S7B).

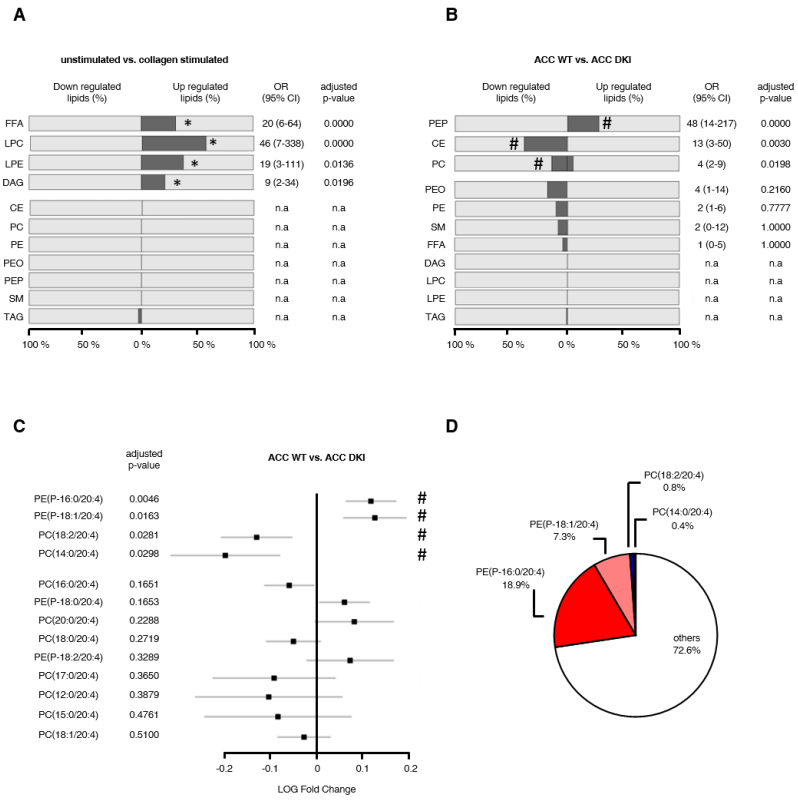

Figure 6. Lack of AMPK-ACC signalling results in an increased AA-containing PL pool. (A, B) The percentage (dark grey bar) of down- or up-regulated lipid species relative to the whole lipid class was calculated in collagen-stimulated platelets relative to unstimulated platelets (A) or ACC DKI relative to ACC WT platelets (B). The different lipid classes are arranged from top down in order of increasing adjusted P values. (A) *Adjusted P≤0.05 between collagen-stimulated platelets and unstimulated platelets (n=3). (B) #P≤0.05 between ACC DKI and WT platelets (n=3). Multivariate regression analysis was performed. OR: odds ratio, CI: confidence interval, n.a.: not applicable (if no change or if change is OR <1). (C) Comparison of arachidonic acid (AA)-containing PEP and PC between ACC DKI and WT platelets. The data are presented as log fold change (squares) relative to ACC WT platelets and with 95% CI (horizontal lines). Statistical significance was based on false discovery rate (FDR) P values (adjusted P values). The different lipid species are arranged from top down in order of increasing adjusted P-values. Multivariate regression analysis was performed. #P≤0.05 between ACC WT and ACC DKI platelets. (D) Proportions of PE(P-16:0/20:4), PE(P-18:1/20:4), PC(18:2/20:4) and PC(14:0/20:4) relative to all AA-containing PL were evaluated in ACC WT platelets. See also Figures S6 and S7, Tables S2 and S3.

5. DISCUSSION

Lipids play fundamental roles in platelets, but little is known about the impact of endogenous lipid metabolism on platelet functions and subsequent thrombosis. To assess the importance of endogenous lipid synthesis on platelet function, we characterized a mouse model carrying a genetic mutation that prevents the AMPK-induced phosphorylation of ACC, the first rate-limiting enzyme of lipid synthesis [209]. We have shown that ACC1 is the predominant isoform in murine and human platelets. These data are consistent with transcriptomic and proteomic analyses that demonstrate ACC1 but not ACC2 transcript and protein expression in platelets [215, 216]. In accordance with the primary role of ACC1 in lipogenesis, ACC DKI platelets display modified PL content rather than altered lipid oxidation. Indeed, no difference in oxygen consumption, which relies on endogenous lipid oxidation [24], is observed between ACC WT and ACC DKI platelets under both basal conditions and upon thrombin or collagen treatment. Consistent with our results, liver-specific inactivation of ACC1 resulted in reduced *de novo* fatty acid synthesis without alteration of fatty acid oxidation [235].

In the first series of experiments, we demonstrated that bleeding time is shorter in ACC DKI mice and thrombosis is increased *in vivo* and *ex vivo* under flow on collagen. Second, platelet functions were analyzed and the results indicate that ACC DKI platelets exhibit enhanced dense granule secretion in response to collagen, attributed to exacerbated TXA_2 generation. Finally, untargeted lipidomics revealed that lack of AMPK-ACC

signalling was associated with an increase in some AA-containing PEP, leading to TXA_2 enrichment. Our findings highlight the critical role of platelet endogenous lipid synthesis in thrombosis and haemostasis, a concept which is supported by a recent study showing that a genetic deletion of acid sphingomyelinase, which converts sphingomyelin to ceramide, leads to an alteration of platelet lipidome, which in turn causes dysregulated granule secretion and *in vitro* thrombus formation [236].

Thrombosis induced by $FeCl_3$ in the carotid artery is a widely used model which can provide valuable information about the impact of genetic modifications on platelet functions. However, it has a number of limitations regarding the underlying mechanisms that induce thrombus formation, notably about the relative roles of tissue factor and thrombin [237-240]. Recently, several studies reported that plasma proteins and blood cells, including platelets, aggregate because their negatively charged proteins bind to positively charged iron species [241, 242]. Altogether, these results indicate that $FeCl_3$-induced thrombosis relies on complex multifaceted, incompletely elucidated, mechanisms.

Collectively, the data presented here demonstrate that AMPK-induced ACC1 phosphorylation in platelets does not control lipid oxidation but rather regulates cellular lipid content. Intriguingly, we expect that an increase in AA-containing PL, as observed in ACC DKI platelets, would provide more substrates for mitochondrial respiration in response to thrombin [138]. However, we could not find any modifications of platelet mitochondrial oxygen consumption, indicating some degree of

compartmentalization and suggesting that increased PEP16:0/20:4 and 18:1/20:4 in ACC DKI platelets do not significantly contribute to overall platelet bioenergetics.

The view that TXA_2 and dense granules are of central importance in triggering thrombus formation but not platelet activation on collagen surfaces has been advanced in previous studies [36, 37]. In addition, the relationship between TXA_2 and dense granule secretion has been clearly established [66, 168, 243]. Our work not only confirms this link in ACC DKI platelets but also underlines that excessive thrombus formation is not systematically associated with an alteration of αIIbβ3-dependent platelet aggregation. This disconnection has been recently reported [236] and supports the notion that additional cell surface molecules participate in platelet/platelet interactions and support thrombus growth [236, 244, 245]. Therefore, based on the core-shell thrombosis model of [34, 246], we postulate that lack of AMPK-ACC signalling might potentiate platelet recruitment to the shell structure through increased TXA_2 and ADP secretion, augmenting thrombosis through mechanisms independent of αIIbβ3. In addition, increased PF4 secretion might possibly contribute to a rise in thrombus growth in ACC DKI mice.

Interestingly, the impact of AMPK-ACC signalling on TXA_2 generation and platelet dense granule secretion is collagen-specific. This is in agreement with previous data showing that different mechanisms of AA-containing PL breakdown are operating in response to collagen or thrombin. Indeed, while AA release by thrombin is dependent on $cPLA_2$

[138, 139], collagen-induced AA generation involves $cPLA_2$, the low-molecular-weight secreted PLA_2 ($sPLA_2$) and the Ca^{2+}-independent cytosolic PLA_2 ($iPLA_2$) [140]. In line with these observations, thrombin and collagen differentially degrade AA-containing PL, depending on the nature of the PL [236, 247]. For instance, thrombin is more potent at cleaving AA-containing PI and PS than collagen, while the latter is 2 times more efficient towards AA-containing PEP [247]. These data reinforce our observations and help us to understand the specific response(s) of ACC DKI platelets to collagen.

Importantly, ACC phosphorylation could be detected, even in the absence of any agonist stimulation, in platelets from both healthy mice and volunteers [29]. This has been confirmed by comparing ACC phosphorylation between ACC WT and ACC DKI platelets under basal conditions. A sustained change in basal ACC phosphorylation was sufficient to induce a decrease in PL, suggesting that ACC phosphorylation already impacts lipid composition in resting platelets, prior to activation.

In conclusion, our work provides new insights into the contribution of endogenous lipid synthesis to platelet functions. It reveals that sustained modulation of ACC phosphorylation in platelets can modify specific AA-containing PL content and influence platelet reactivity to collagen. This finding might have far-reaching clinical relevance in the pathological context of diseases such as atherosclerosis. Indeed, this is now being tested in a clinical trial demonstrating that basal ACC phosphorylation dramatically increases in platelets of patients with

coronary artery disease (ACCTHEROMA Clinical Trial NCT03034148). How and whether such a pathway is involved in regulating platelet function in this context remain to be determined.

6. SUPPLEMENTAL MATERIALS

6.1 Supplemental Methods

6.1.1 Reagents

Thrombin from bovine plasma (#T6634), citrate-dextrose solution (ACD) (#C3821), apyrase (#A6132), fibrinogen (#F4129), fluorescein isothiocyanate (FITC)- conjugated phalloidin (#P5282), Dulbecco's Modified Eagle's Medium (DMEM, #D5030), acetylsalicylic acid (#A5376), Etomoxir (#E1905), palmitic acid (#P0500), oleic acid (#O1008) and anti-phospho-MLC (Ser19) (#M6068), horse radish peroxidase (HRP)- conjugated anti-rabbit (#A0545) antibodies (Abs) were purchased from Sigma. Eptifibatide was obtained from GlaxoSmithKline. Bovine serum albumin (BSA) (#8076) was purchased from Roth, fatty acid-free BSA (#126575) and ADP (#1171) were from Millipore. Anti-phospho-VASP (Thr278) Ab (#VP2781) was sourced from ECM Bioscience. Collagen (equine tendon type I) came from ABP (#ABP-COL-1) for all experiments except for flow chamber assays, in which case it derived from Nycomed (#10345787). Carboxyfluorescein succinimidyl ester (CFSE) (#C34554), Alexa Fluor 647-conjugated annexin A5 (#A23204), BODIPY-palmitate (#D3821), anti-VASP (#MA5-14982) Ab were purchased from Thermo-Fisher Scientific. cOmplete, Mini Protease Inhibitor Cocktail (#11836153001) was obtained from Roche. Platelet factor 4 (PF4) ELISA Kit

(#ab100735) was from Abcam. Luciferin-luciferase reagent (#CH395) was from Stago BNL, and Cell Tak (#354240) was from Corning. Oligomycin, FCCP, antimycin-A and rotenone were from Agilent (Mito Stress Test Kit, #103015-100). Serotonin ELISA kit (#ADI-900-175) and thromboxane (TXA_2) ELISA kit (#ADI-900-002) came from Enzo Life Science. COX activity assay kit (#700200-2) and Ticagrelor (#15425) were from Sanbio. Anti-phospho-ACC (Ser79) (#3661), anti-ACC1 (#4190), anti-ACC2 (#8578), anti-phospho-AMPK (Thr172) (#2535), anti-AMPKα (#2532), anti-phospho-cofilin (Ser3) (#3313), anti-cofilin (#3312), anti-MLC2 (#3672), anti-COX-1 (#4841) and anti-gelsolin (#12953) Abs were obtained from Cell Signaling. Phycoerythrin (PE)-conjugated anti-αIIbβ3 (#M025-2), FITC-conjugated anti-GPVI (#M011-1), PE- conjugated anti-GPIbα (#M040-2) and PE-conjugated anti-active αIIbβ3 (clone JON/A) (#M023-2) Abs were from Emfret Analytics. FITC-conjugated anti-CD62P (P- selectin) (#553744) and HRP-conjugated anti-mouse (#554002) Abs were purchased from BD Bioscience. Anti-β-actin (#sc-69879) and anti-protease-activated receptor-3 (PAR-3) (#sc-5598) Abs were obtained from Santa Cruz Biotechnologies. Anti- protease-activated receptor-4 (PAR-4) (#APR-034) Ab was from Alomone Labs. U46619 (#1932) was purchased from Tocris. Rhodocytin and collagen-related peptide (CRP) were kind gifts from J. Heemskerk (Masstricht, the Netherlands) and C. Oury (Liège, Belgium), respectively. Palmitate and oleate coupled to BSA were made by dissolution of the fatty acid into a solution containing in 0.01 N NaOH, 0.9 % NaCl and 12.25 % fatty acid-free BSA, pH 7.4.

6.1.2 Human platelet preparation

Blood was collected from consenting healthy adults and drawn from the vein with a 21-gauge butterfly needle into tubes containing one-tenth volume of citrated solution (citrate, phosphate, dextrose, adenine). The platelet-rich plasma (PRP) was collected by centrifugation at 330 g for 20 min at 22 °C. After addition of eptifibatide (4 µg/ml) and apyrase (1 U/ml), PRP was subsequently centrifuged at 800 g for 10 min at 22 °C. The platelets pellet was washed in modified Tyrode's buffer (135 mM NaCl, 12 mM $NaHCO_3$, 3 mM KCl, 0.3 mM Na_2HPO_4, 1 mM $MgCl_2$, 5 mM D-glucose, 10 mM Hepes, 0.35 % BSA, pH 7.4, 37 °C) containing eptifibatide (4 µg/ml) and apyrase (1 U/ml). Platelets were finally isolated by centrifugation at 1000 g for 10 min at 22 °C, re-suspended in modified Tyrode's buffer, their concentration counted with Cell-DYN Emerald (Abbott Diagnostics) and adjusted to 2.5 x 10^5 platelets/µl.

6.1.3 Western blotting

For lysate preparation, platelets were centrifuged and the pellet lysed in SDS- Laemmli sample buffer 1x (25 mM Tris-HCl, pH 6.8, 12.5 % (w/v) glycerol, 3 % (w/v) SDS, 0.01 % (w/v) Bromophenol blue, 6.25 % (v/v) β-mercaptoethanol). Whole platelet lysates were subjected to Western blotting. Abs dilutions in 5 % BSA were 1:1,000 for all primary Abs except for anti-gelsolin (1:50,000) and anti-β-actin (1:50,000) Abs. HRP-conjugated anti-rabbit (1:20,000) and HRP-conjugated anti-mouse (1:30,000) Abs were diluted in 5 % BSA. Band intensities were quantified by Image J, and those obtained with anti-phospho Abs were normalized to

those of loading controls on the same gel. Respective total protein analyses were performed on different gels.

6.1.4 Platelet spreading

Coverslips were coated overnight at 4 °C with either 100 µg/ml fibrinogen or 100 µg/ml collagen and blocked with 5 mg/ml phosphate buffer saline (PBS)-BSA for 1 h at room temperature. After washing with PBS, washed platelets (20 x 10^3/µl) were stimulated or not ("resting") with 0.5 U/ml thrombin in the presence of 2 mM $CaCl_2$ and were immediately placed on coverslips for 45 min at 37°C. After rinsing with PBS, adherent platelets were fixed with 1 % formaldehyde for 30 min at room temperature. After washing formaldehyde with PBS, the platelets were permeabilized with 0.1 % Triton and stained with FITC-conjugated phalloidin (1:300) for 45 min at room temperature. After washing with PBS, platelets were visualized with a Zeiss (x 100 oil immersion) fluorescence microscope (Carl Zeiss) equipped with ApoTome (AxioImager). The area covered by adherent platelets and the number of adherent platelets were quantified by Image J. Platelet surface area represents the surface covered by adherent platelets divided by their number.

6.1.5 Tail bleeding time

Mice were anesthetized with isoflurane, and 3 mm of tail tip was cut with scalpel. The tail was immediately immersed in 0.9 % NaCl (37 °C). Time until cessation of bleeding (no blood flow for 1 min) was recorded. Bleeding was quantified for a maximum of 10 min.

6.1.6 Platelet aggregation and ATP secretion

Light transmission during aggregation of washed platelets was recorded at 37 °C, with constant stirring (1,200 rpm), in an aggregometer (Chrono-Log). ATP secretion was monitored in parallel to platelet aggregation by adding Luciferase-Luciferin reagent and comparing the luminescence generated by platelet ATP release with an ATP standard (Chrono-Lume, Stago, The Netherlands).

6.1.7 Flow cytometry analysis

For CD62P and JON/A analysis, washed platelets (6.25×10^6), re-suspended in modified Tyrode's buffer supplemented with 1.5 % BSA, were incubated with respective Abs at saturating concentrations (1:12.5) for 15 min at room temperature. Platelets were stimulated with thrombin or collagen at 37 °C at the indicated concentrations and time points. To stop the reaction, platelets were fixed in 4 % formaldehyde supplemented with 5 % BSA. For platelet receptor expression, washed platelets (10^6) were incubated with respective Abs (1:40) for 15 min at room temperature and diluted with 0.1 % BSA-0.1 % Azide- PBS before analysis.

Samples were analyzed by BD Canto II flow cytometer, and 10,000 events were recorded. When necessary, appropriate compensation controls were included.

For analysis of palmitate uptake, washed platelets (6.25 x 10^6) were re-suspended in modified Tyrode's buffer supplemented with 1 % fatty acid-free BSA, incubated with 10 µM BODIPY-palmitate or the corresponding vehicle (DMSO) and either left untreated or stimulated with 5 µg/ml collagen for 10, 20, 40 or 60 min at 37 °C. To stop the reaction, platelets were diluted in 1.5 ml PBS and fluorescence was immediately analyzed by the BD Calibur flow cytometer (10,000 events were recorded).

6.1.8 Serotonin and TXA_2 assays

Serotonin and TXA_2 were assessed by enzyme immunoassay kit (see Reagents and materials). Washed platelets (30 x 10^3/µl) were stimulated with 5 µg/ml collagen, 30 mU/ml or 100 mU/ml thrombin for 5 min at 37 °C. For some conditions, platelets were pre-incubated with 1 mM aspirin for 45 min, 200 µM BSA-oleate/palmitate for 1 h or 30 µM Ticagrelor for 30 min. After the samples were centrifuged for 15 s at 11,700 g, the supernatant was removed and stored at -80 °C for serotonin and TXA_2 analysis according to the manufacturer's instructions. Serotonin content was also determined in platelet lysates (7.5 x 10^3/µl) after 4 freeze-thaw cycles.

6.1.9 PF4 assay

Washed platelets (60 x 10^3/µl), re-suspended in modified Tyrode's buffer not supplemented with BSA, were stimulated with 2.5, 5 or 10 µg/ml

collagen for 5 min at 37 °C. To stop the reaction, samples were centrifuged for 15 s at 11,700 g, the supernatant was removed and stored at -80 °C. Supernatant was diluted 30 x and PF4 assayed according to the manufacturer's instructions. Total PF4 content was also determined after platelet (180 x 10^3/µl) lysis in 0.1 M Tris-HCl, pH 7.5, in the presence of protease inhibitor cocktail (cOmplete, mini) and sonication 3 x 10 sec. Supernatant was diluted 240 x before analysis.

6.1.10 COX activity

Washed murine platelets (700 x 10^3/µl), re-suspended in modified Tyrode's buffer not supplemented with BSA, were lysed in 0.1 M Tris-HCl, pH 7.5, in the presence of protease inhibitor cocktail (cOmplete, mini) and sonicated 3 x 10 sec. Samples were cleared by centrifugation (16,000 g for 10 min at 4 °C) and supernatants pre-incubated or not with 1 mM ASA for 45 min. COX activity was assayed by a fluorescent assay kit according to the manufacturer's instructions.

6.1.11 Measurements of ADP and ATP

Washed platelets (100 x 10^6) were lysed in ice-cold 10 % (v/v) perchloric acid, 25 mM EDTA for 20 min before sonication for 30 sec. Samples were centrifuged at 10,000 g for 10 min at 4 °C and supernatant neutralized with 2 N KOH and 0.3 M MOPS. After centrifugation at 10,000 g for 10 min at 4 °C, ATP and ADP were analyzed in the supernatant by reverse-phase high performance liquid chromatography (HPLC), as already described [1].

6.1.12 Clot retraction

Washed platelets (500 x 10^3/µl) were incubated with 2 mg/ml fibrinogen, 2 mM $CaCl_2$ and 1 U/ml thrombin in the presence of 1.5 µl of erythrocytes. Subsequent clot retraction was monitored at 37 °C under non-stirring conditions, and pictures were taken at different time points by digital camera for up to 240 min. Clot surface area was quantified by Image J, and retraction was expressed as percentages of total surface area.

6.1.13 Extracellular flux analysis of mitochondrial respiration

Mitochondrial respiration was assessed by monitoring the real-time oxygen consumption rate (OCR) of individual platelets, with the Mito Stress Test Kit, and the Seahorse extracellular flux analyzer (Seahorse Bioscience), according to the manufacturer's instructions. Washed platelets were re-suspended in DMEM (supplemented with 5 mM glucose, 1 mM pyruvate, 4 mM glutamine and 20 mM HEPES for collagen stimulation). Platelets (30 x 10^6/well) were then loaded into each well of a XF96 microplate pre-coated with Cell Tak (150 µg/ml).

Plates were subsequently centrifuged (1 min at 148 g and 1 min at 213 g), DMEM was replaced by fresh medium and incubated in a CO_2-free incubator at 37 °C for 1 h in the absence or presence of Etomoxir 25 µM. OCR was measured in the presence of DMEM alone and after consecutive treatments with thrombin (1 U/ml) or collagen (25 µg/ml), oligomycin (1 µM), FCCP (0.45 µM) and a mix of rotenone (1 µM) and antimycin A (1 µM). 3 basal measurements, followed by 3 assessments after each injection, were

recorded per assay. Mitochondrial functional parameters were assessed via (1) basal OCR, (2) agonist-induced OCR, estimated by subtracting basal OCR from OCR after thrombin or collagen addition, (3) ATP-linked OCR, calculated by subtracting OCR after oligomycin from baseline, (4) maximal OCR, (5) reserve capacity, evaluated by subtracting basal OCR from OCR after FCCP, (6) non-mitochondrial respiration, and (7) proton leak, computed by subtracting OCR after antimycin A/rotenone from OCR after oligomycin.

6.1.14 Lipid extraction

Lipids were extracted according to the methyl-tert-butyl ether (MTBE) method [2,3]. 250 x 10^6 platelets were transferred to 2-ml Eppendorf vials, followed by the addition of 100 µl water and 100 µl of Internal Standard Mix (Sciex, Nieuwekerk aan den ljsel, the Netherlands). Next, 160 µl of methanol and 500 µl of MTBE were added. The extracts were then shaken at room temperature for 30 min. Subsequently, 200 µl of water was added, after which the samples were vortexed briefly and then centrifuged at 16,100 g for 3 min.

The upper organic layer (400 µl) was transferred to fresh glass vials. 500 µl MTBE, 100 µl methanol and 100 µl water were added to the original Eppendorf vials, and extraction was repeated. Combined organic extracts were concentrated under a gentle nitrogen stream and reconstituted in 250 µl of running buffer (10 mM ammonium acetate in 50:50 dichloromethane:methanol).

6.1.15 Lipidomics statistical analysis

Lipid species concentrations were analyzed using R.3.4.2 according to the following bioinformatics pipeline. Missing data were imputed by a probabilistic principal component analysis (PPCA) approach implemented in the pcaMethods Bioconductor package. Data were normalized with total lipid abundance, and log2 transformation was applied on normalized concentrations.

The Limma Bioconductor package [4] was used to build a multivariate regression model for each lipid species with 2 predictors, including ACC DKI status (i.e., ACC WT vs ACC DKI) and treatment group (control, collagen, thrombin, collagen and thrombin). Fold-change estimates and corresponding P values were derived from regression models for each lipid species and for each predictor. To control for multiple testing, all P values were further adjusted for the Benjamini- Hochberg false discovery rate (FDR) [5], and FDR ≤0.05 was considered as significant. As 865 lipid species belong to 11 lipid classes (CE, DAG, FFA, LPC, LPE, PC, PE, PEO, PEP, SM, TAG), enrichment analysis was performed with Fisher's exact tests to find lipid classes involving a high proportion of differentially-regulated lipid species.

6.1.16 Statistical analysis

All values are expressed as means ± SEM. Statistical analyses were performed by the Mann-Whitney test for the comparison of 2 different experimental groups, or 2-way ANOVA followed by Sidak's multiple comparison post hoc test for multiple testing comparisons. P≤0.05 values

were considered to be statistically significant. All statistical analyses were performed using GraphPad Prism (GraphPad Software).

6.2 Supplemental Figures and Tables

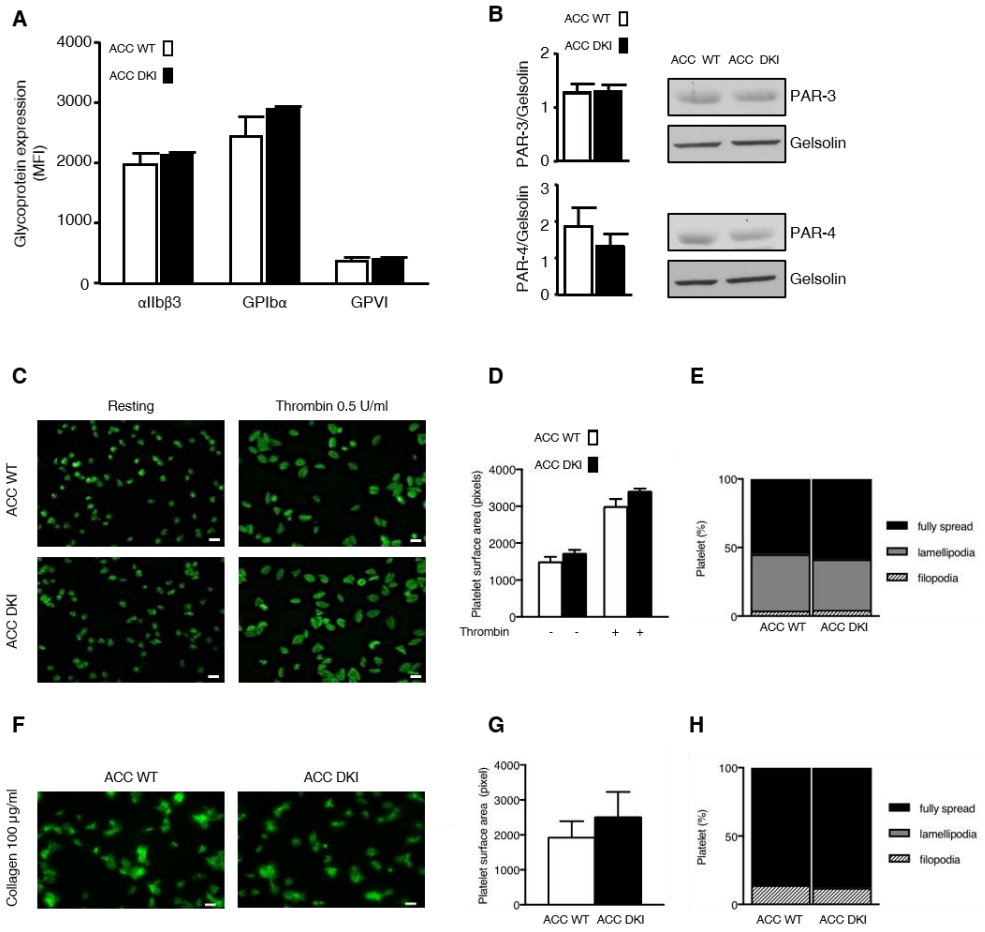

Figure S1. Lack of ACC phosphorylation does not impact platelet surface receptor expression, spreading, filopodia and lamellipodia formation on fibrinogen or collagen. Related to Figure 1. (A) Surface expression of glycoproteins on ACC WT or DKI platelets was analyzed by flow cytometry. The results are expressed as mean fluorescence intensity (MFI) ± SEM (n=3). (B) ACC WT and DKI platelets were lysed and subjected to Western blotting for PAR-3 and PAR-4 expression analysis. Gelsolin was used as a loading control. Representative Western blotting of PAR-3 and PAR-4 (right panel) and corresponding quantification (left panel) are shown. The results are expressed as means ± SEM (n=3). (C-H) Washed ACC WT and DKI platelets were allowed to spread for 45 min on fibrinogen (100 µg/ml) in the absence (resting) or presence of 0.5 U/ml thrombin (C-E) or on collagen (100 µg/ml) (F-H) and were stained with FITC-phalloidin. Representative fluorescence microscopy images of platelets are shown on fibrinogen (C) and collagen (F): scale bars represent 5 µm. Quantification of platelet surface area on fibrinogen (D) and collagen (G): the results are expressed as means ± SEM (n=4). Evaluation of percentages of platelet spread on fibrinogen (E) or collagen (H) at different spreading stages: filopodia, lamellipodia and totally spread platelets (n=4).

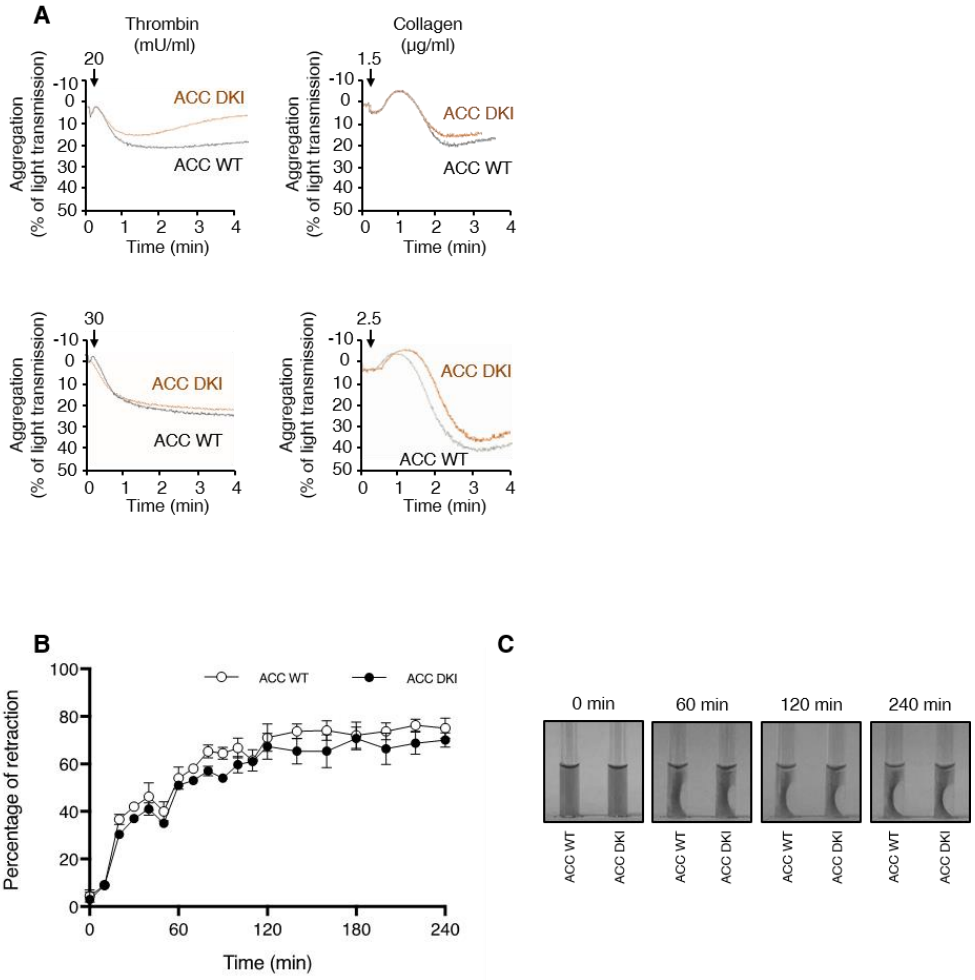

Figure S2. Normal αIIbβ3 signalling in ACC DKI platelets. Related to Figure 3. (A) Representative aggregation traces induced by 20 mU/ml or 30 mU/ml thrombin and 1.5 µg/ml or 2.5 µg/ml collagen. Arrows indicate addition of the respective agonist. (B, C) Clot retraction was induced in washed ACC WT and DKI platelets by adding 2 mg/ml fibrinogen, 2 mM $CaCl_2$ and 1 U/ml thrombin. Pictures of the clot were taken at different time points, and the extent of clot retraction was quantified by measuring clot area. (B) Quantification of time-dependent clot retraction. The results are expressed as means ± SEM (n=3). (C) Representative pictures of clots at 0, 60, 120 and 240 min after thrombin addition.

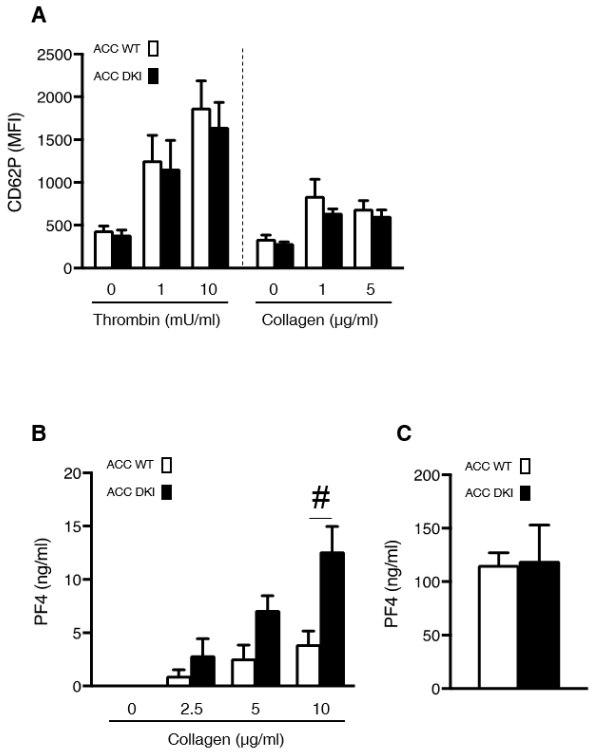

Figure S3. Increased PF4 secretion in response to collagen in ACC DKI platelets. Related to Figure 3. (A) P-selectin (CD62P) exposure was analyzed by flow cytometry in washed ACC WT and DKI platelets stimulated with thrombin for 8 min or collagen for 30 min at the indicated concentrations at 37 °C. The dashed line represents separate analyses. The results are expressed as mean fluorescence intensity (MFI) ± SEM (at least n=4). (B) Washed platelets were stimulated with the indicated concentrations of collagen for 5 min, and PF4 was measured in the supernatant by ELISA. Results are expressed as means ± SEM (n=4). $^{\#}P \leq 0.05$ between ACC WT and DKI platelets. The data were analyzed by 2-way ANOVA. (C) Washed platelets were centrifuged, the pellet was lysed, and total PF4 assayed. Results are expressed as means ± SEM (n=3).

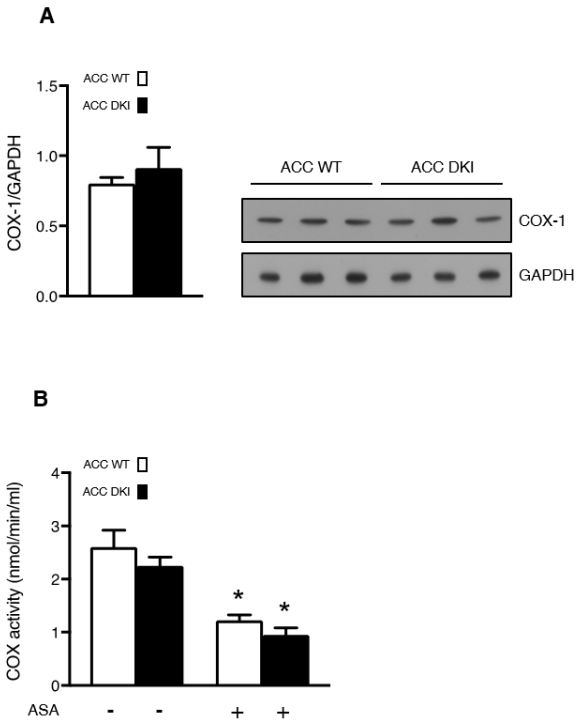

Figure S4. COX activity is similar between ACC WT and ACC DKI platelets. Related to Figure 3. (A) Washed murine platelets were lysed and subjected to Western blotting for cyclooxygenase-1 (COX-1) expression. GAPDH was used as a loading control. Quantification and Western blotting are shown. The results are expressed as means ± SEM (n=3). (B) COX activity was measured by a fluorescent assay kit in platelets lysates pre-incubated or not with 1 mM aspirin (ASA) for 45 min. The results are expressed as means ± SEM (n=4). *indicates values statistically different from respective untreated platelets, P≤0.05. Analysis was performed by 2-way ANOVA.

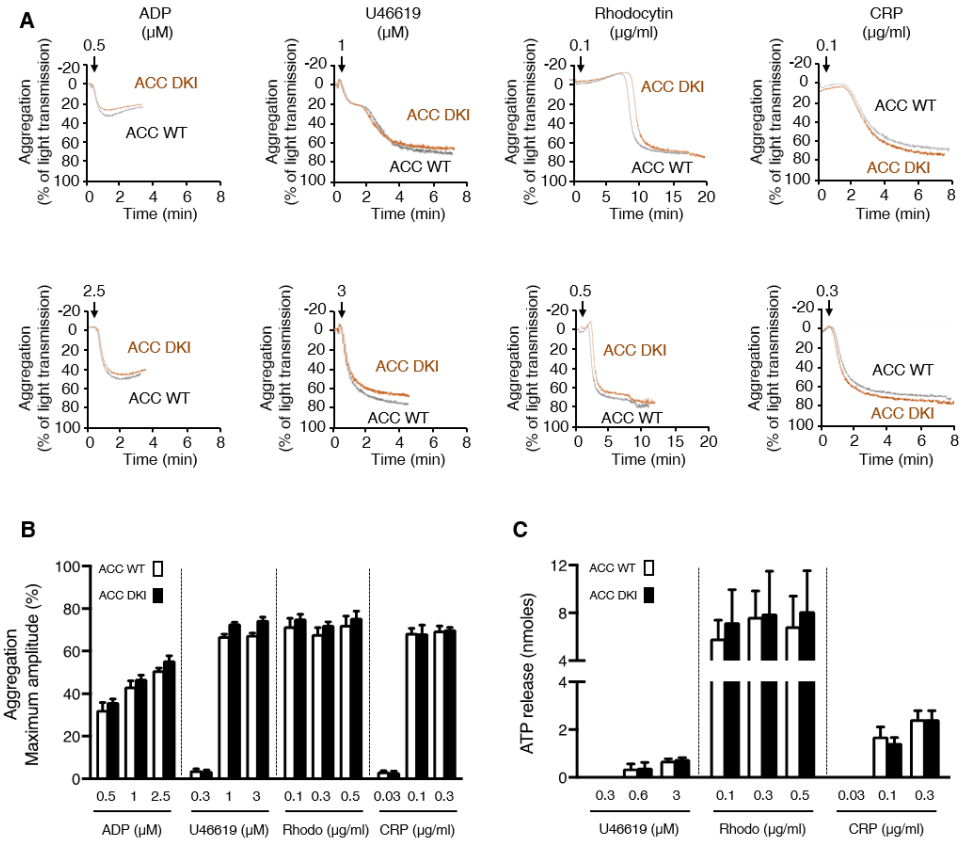

Figure S5. ACC WT and ACC DKI platelets display similar aggregation and dense granules secretion in response to ADP, U46619, rhodocytin or CRP. Related to Figure 3. (A-C) Washed platelets were stimulated with ADP, U46619 (TXA_2 analogue), rhodocytin or collagen-related peptide (CRP) at the indicated concentrations in the presence of Luciferase-Luciferin reagent, and light transmission was measured (Chrono-Log). (A) Representative aggregation profiles are represented. Arrows indicate addition of the respective agonist. (B) Aggregation expressed as the maximal percentage of light transmitted, and (C) quantification results of ATP release. The dashed lines represent separate analyses. Results are expressed as means ± SEM (n=3).

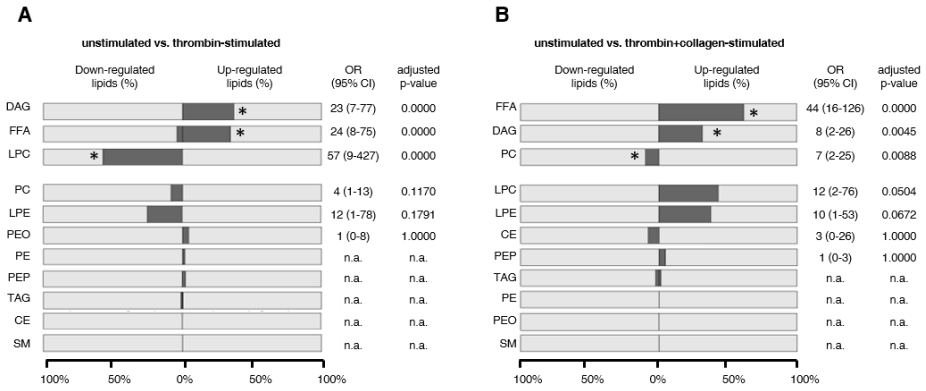

Figure S6. Analysis of lipid change in response to thrombin alone or to thrombin and collagen. Related to Figure 6. (A, B) Washed platelets were stimulated for 15 min with thrombin alone (0.3 U/ml) (A) or thrombin (0.3 U/ml) and collagen (25 µg/ml) (B), and the percentages (dark grey bar) of down- or up-regulated lipid species in both ACC WT and DKI platelets relative to unstimulated platelets are represented for each lipid class. The different lipid classes are arranged from top down in order of increasing P values. *P≤0.05 between stimulated and unstimulated conditions (n=3). Multivariate regression analysis was performed. OR: odds ratio, CI: confidence interval, n.a.: not applicable (if no change or if change is OR <1).

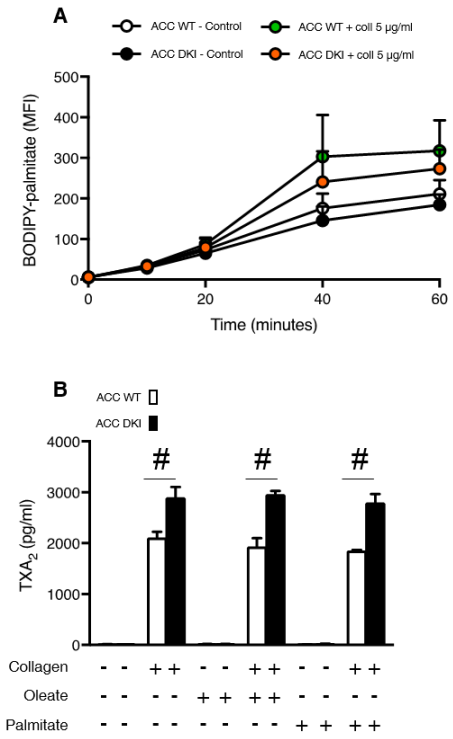

Figure S7. Extracellular fatty acids availability does not influence intra-platelet lipid transport and collagen-induced TXA_2 production in ACC DKI platelets. Related to Figure 6. (A) Murine platelets were incubated with 10 µM BODIPY-palmitate and either left untreated (Control) or stimulated with 5 µg/ml collagen for the indicated time points and fluorescence was immediately analyzed. Results are expressed as means ± SEM (n=3). (B) Washed platelets were pre-incubated for 1 h with 200 µM BSA-oleate, 200 µM BSA-palmitate or the corresponding vehicle (BSA) and stimulated with 5 µg/ml collagen for 5 min. Thromboxane A_2 (TXA_2) was measured in the supernatant by ELISA. Results are expressed as means ± SEM (n=3). $^{\#}P \leq 0.05$ between ACC WT and DKI platelets. The data were analyzed by 2-way ANOVA.

	ACC WT	ACC DKI	P
Erythrocytes, 10^6/µl	6.73 ± 0.15	6.98 ± 0.08	n.s.
Leukocytes, 10^3/µl	6.78 ± 0.29	7.41 ± 1.09	n.s.
Platelets, 10^6/µl	0.62 ± 0.03	0.69 ± 0.03	n.s.
Mean platelet volume, fl	4.72 ± 0.05	4.83 ± 0.04	n.s.

Table S1. ACC DKI mice show normal hematologic parameters. Related to Figure 1. Platelets as well as their mean volume, leukocytes and erythrocytes counts were analyzed by blood cell counter (Cell Dyn Emerald). fl.: femtoliter; n.s.: non-significant (n=10).

	n	log fc	Adjusted P value
FFA(22:2)	24	1.520	6.12E-14
FFA(20:5)	24	1.078	8.07E-11
DAG(16:0/20:4)	24	1.595	8.07E-11
LPC(16:0)	24	0.836	8.07E-11
LPE(16:0)	24	0.868	1.44E-10
LPE(18:0)	24	0.950	4.25E-10
LPC(18:0)	24	0.948	6.86E-09
LPE(18:1)	24	0.745	2.81E-07
FFA(22:4)	24	0.512	1.77E-06
LPC(18:1)	24	0.649	1.94E-06
FFA(20:4)	24	0.719	0.00001
FFA(18:2)	24	0.485	0.00013
LPC(18:2)	24	0.622	0.00030
DAG(16:0/18:2)	24	0.477	0.00139
TAG(48:0/FA16:0)	24	-0.715	0.00159
FFA(18:0)	24	0.368	0.00278
TAG(50:0/FA16:0)	24	-0.522	0.00278
TAG(56:8/FA18:3)	24	-0.482	0.00386
TAG(52:0/FA16:0)	24	-0.398	0.00404
TAG(50:0/FA18:0)	24	-0.555	0.00983
FFA(20:1)	24	0.309	0.01365
FFA(20:3)	24	0.295	0.01614
DAG(16:0/20:3)	17	0.537	0.02556
TAG(55:7/FA15:0)	24	-0.372	0.02687
DAG(18:1/20:4)	20	0.938	0.04050
TAG(54:0/FA16:0)	23	-0.441	0.04499

Table S2. Complete list of significantly modified lipids in collagen stimulated platelets relative to unstimulated platelets. Related to Figure 4. Differentially regulated lipids between collagen stimulated platelets and unstimulated platelets. Statistical significance was evaluated based on the false discovery rate (FDR) P values (adjusted P value). The different lipid species are arranged from top down in order of increasing adjusted P values and only those lipids having an adjusted P value≤0.05 are represented (n=3). Analysis was performed by multivariate regression model. n: number of condition analysed, fc: fold change.

.

	n	Log fc	Adjusted P value
PE(P-16:0/18:2)	24	0.261	0.00017
PC(16:0/14:0)	24	-0.221	0.00027
PC(14:0/18:2)	24	-0.212	0.00027
PE(O-18:0/22:6)	24	-0.223	0.00032
PE(P-16:0/18:1)	24	0.227	0.00032
PC(20:0/18:1)	24	0.273	0.00040
PC(16:0/20:2)	24	-0.194	0.00114
PE(P-18:1/18:2)	24	0.271	0.00166
CE(18:0)	22	-0.426	0.00166
PE(16:0/18:3)	24	-0.329	0.00166
PE(O-16:0/22:4)	24	-0.242	0.00193
PC(18:2/18:2)	24	-0.234	0.00225
PE(P-18:0/20:5)	24	0.189	0.00244
PE(P-16:0/20:5)	24	0.235	0.00247
PE(P-18:1/18:1)	24	0.224	0.00298
PC(18:0/20:5)	24	0.246	0.00307
PC(16:0/20:5)	24	0.167	0.00308
PE(P-18:0/18:2)	24	0.181	0.00313
PE(P-16:0/20:4)	24	0.119	0.00454
PE(O-18:0/22:4)	24	-0.248	0.00483
PC(18:0/18:1)	24	0.104	0.00499
PC(18:0/14:0)	24	-0.252	0.00772
CE(18:1)	24	-0.546	0.00799
SM(16:0)	24	-0.089	0.00971
PE(18:0/22:4)	24	-0.168	0.01165
PC(18:2/20:2)	24	-0.257	0.01304
PE(O-16:0/22:6)	24	-0.140	0.01454
PE(P-18:1/16:0)	24	0.161	0.01605
PE(P-18:1/20:4)	24	0.126	0.01625
PE(P-16:0/16:0)	24	0.185	0.01632
CE(18:3)	24	-0.455	0.01686
PC(16:0/22:4)	24	-0.231	0.01859
CE(16:0)	24	-0.480	0.02026
TAG(54:6/FA18:3)	24	-0.345	0.02071
PE(18:0/18:3)	24	-0.227	0.02123
PC(18:2/20:4)	24	-0.131	0.02812
PE(P-16:0/22:5)	24	0.150	0.02911
PC(14:0/20:4)	24	-0.200	0.02976
PE(16:0/22:4)	24	-0.209	0.03196
CE(20:4)	24	-0.349	0.03461
PE(18:1/22:4)	24	-0.164	0.04307
PC(18:1/18:2)	24	-0.100	0.04870
FFA(18:2)	24	-0.175	0.04920
PE(18:2/18:2)	24	-0.143	0.04920
TAG(58:9/FA22:6)	24	-0.215	0.04942

Table S3. Complete list of significantly modified lipids in ACC DKI platelets relative to WT platelets. Related to Figure 4. Differentially regulated lipids between ACC DKI and WT platelets. Statistical significance was evaluated based on the false discovery rate (FDR) P values (adjusted P value). The different lipid species are arranged from top down in order of increasing adjusted P values and only those lipids having an adjusted P value≤0.05 are represented (n=3). Analysis was performed by multivariate regression model. n: number of condition analysed, fc: fold change.

RESULTS-2

Part 2

Platelet acetyl-CoA carboxylase phosphorylation: A risk stratification marker evidencing platelet-lipid interplay in CAD patients.

Shakeel Kautbally, MD, [a,*], Sophie Lepropre, [a,*], Marie-Blanche Onselaer, PhD, [a], Astrid Le Rigoleur, [a], Audrey Ginion, [a], Christophe De Meester de Ravenstein, PhD, [a], Jerome Ambroise, PhD, [b], Karim Z.Boudjeltia, PhD, [c], Marie Octave, [a], Odile Wera, [d] , Philippe Lesnik, PhD, [e], Martin Giera, PhD, [f], Bernhard L.Gerber, MD, PhD, [a,g], Anne-Catherine Pouleur, MD, PhD, [a,g], Bruno Guigas, PhD, [f], Jean-Louis Vanoverschelde, MD, PhD, [a,g], Luc Bertrand, PhD,[a], Cecile Oury, PhD, [d], Sandrine Horman, PhD, [a,#], Christophe Beauloye, MD, PhD, [a,g,#]

[a] Institut de Recherche Expérimentale et Clinique (IREC), Pôle de Recherche Cardiovasculaire, Université Catholique de Louvain, Brussels, Belgium. [b] Institute de Recherche Expérimentale et Clinique (IREC), Center for Applied Molecular Technologies (CTMA), Université Catholique de Louvain, Brussels, Belgium. [c] Laboratory of Experimental Medecine (ULB 222 unit), Centre Hospitalier Universitaire de Charleroi, Université Libre de Bruxelles, Charleroi, Belgium. [d] Laboratory of Thrombosis and Haemostasis, GIGA-Cardiovascular Sciences, Université de Liège, Liège, Belgium. [e] INSERM UMR_S 1166, Integrative Biology of Atherosclerosis Team, Université Pierre et Marie Curie-Paris 6 and Institute of Cardiometabolism and Nutrition (ICAN), Pitié-Salpêtrière Hospital, Paris, France. [f] Center for Proteomics and Metabolomics, Leiden University Medical Center, Leiden, The Netherlands. [g] Division of Cardiology, Cliniques universitaires Saint Luc, Brussels, Belgium

[*] S.K. and S.L. contributed equally and are joint first authors.

[#] C.B. and S.H. contributed equally and are joint last authors.

1. ABSTRACT

Background. Activation of the adenosine monophosphate (AMP)-activated protein kinase (AMPK) leads to the inhibition and phosphorylation (on serine 79) of acetyl-CoA carboxylase (phosphoACC), its *bona fide* substrate. Given the role of AMPK-ACC signalling in platelet lipid metabolism and function, this pathway could be affected in the platelets of patients with coronary artery disease (CAD), where the atherogenic environment has an impact on platelet biology.

Aims. We hypothesized that platelet AMPK-ACC signalling is activated by atherogenic lipids and could be considered as a metabolic signature in high-risk CAD patients. We also explored the consequences of platelet phosphoACC on platelet lipid metabolism.

Methods. Blood samples from 188 consecutive patients admitted for coronary angiography were processed. Lipid extracts from the platelets of 31 patients were subjected to lipidomic analysis.

Results. The circulating platelets of CAD patients demonstrated a significant increase in phosphoACC that highly correlated with acute coronary syndrome (OR: 6.71, 95% CI: 2.06-21.91; P=0.002). The triglyceride (TG)/high-density lipoprotein ratio, a well-known atherogenic marker, was strongly associated with increased phosphoACC in our CAD cohort. Hence oxidized low-density lipoprotein (oxLDL) activated AMPK-ACC signalling through a CD36-dependent pathway. Lipidomic analysis revealed that

increased phosphoACC led to a down-regulation of intraplatelet TG, particularly of those containing C14:0 fatty acid chains.

Conclusion. Platelet phosphoACC is a potential marker for risk stratification in suspected CAD patients and reveals an interaction between platelets and lipids. Inhibitory phosphoACC impacts platelet lipid content by down-regulating TG, which in turn may affect platelet function (ACCTHEROMA, NCT03034148).

2. INTRODUCTION

Platelets are key players in atherothrombosis. In acute coronary syndrome (ACS), coagulation cascade activation upon plaque rupture leads to thrombin generation (ThG), a crucial platelet agonist enhancing platelet-mediated thrombus formation [248]. The association between increased ThG and ischemic risk in coronary artery disease (CAD) patients renders the coagulation cascade an interesting therapeutic target [249, 250].

We previously established the adenosine monophosphate (AMP)-activated protein kinase (AMPK) to be crucial for platelet activation. In human platelets, thrombin is the major agonist leading to AMPK activation through a calcium-dependent mechanism [29]. Once activated, AMPK contributes to platelet secretion, platelet aggregation, and clot retraction by controlling the actin cytoskeleton. AMPK activation likewise leads to phosphorylation of acetyl-CoA carboxylase (ACC) on serine 79, its *bona fide* substrate, typically used as a marker of AMPK activation in cells and tissues, including platelets [29]. It is tempting to speculate that ThG affects platelet

AMPK signalling and ACC phosphorylation (phosphoACC) in CAD. However, although thrombin is crucial for thrombus formation at the plaque rupture site in ACS, its impact on circulating platelets remains unclear. In CAD patients, the atherogenic environment influences platelet biology and reactivity, mainly through CD36 [101, 251]. Oxidized low-density lipoprotein (oxLDL) binds to CD36, inducing platelet activation and shape changes via a calcium-dependent mechanism [107]. Yet, other factors besides thrombin may affect AMPK-ACC signalling in the circulating platelets of CAD patients.

ACC is the first committed enzyme of the fatty acid biosynthesis pathway, while its phosphorylation on serine 79 by AMPK inhibits its activity [252]. We demonstrated that AMPK-ACC signalling is a key pathway in controlling platelet lipid content, thereby modulating platelet function and thrombus formation [253]. However, ACC contribution to platelet lipid metabolism in CAD, where atherogenic lipids interact with circulating platelets [254], remains unexplored.

We report herein platelet phosphoACC as a potential risk stratification marker in suspected CAD patients. In consecutive patients admitted for coronary angiography, phosphoACC was significantly increased in circulating platelets of CAD patients and highly associated with acute coronary events. We identified an interplay between platelets and lipids, with oxLDL as a central contributor to increased platelet phosphoACC. Interestingly, the lipidomic data show that sustained phosphoACC regulates triglyceride (TG) lipids in circulating platelets of CAD patients.

3. MATERIALS AND METHODS

Methods and reagents are described in the supplemental material.

3.1 Clinical Cohort

3.1.1 Study design

From March 2015 to February 2016, 188 consecutive patients admitted for coronary angiography were included in the ACCTHEROMA study (NCT03034148), with at least two patients prospectively screened per day, regardless of the indication for angiography. Based on indication and coronary angiography results analyzed by two experienced cardiologists, patients were classified into four groups. Patients undergoing angiography for chest pain or valvular disease investigation with normal coronary vessels were classed as non-CAD (N-CAD, reference population). The presence of at least one lesion but less than 50% luminal stenosis was classed as non-significant CAD (NS-CAD). Patients angiographied for stable disease with significant stenosis (>50%) were classed as stable CAD (S-CAD). ACS comprised unstable angina (n=30), non-ST segment elevation myocardial infarction (NSTEMI) (n=22), and ST segment elevation myocardial infarction (STEMI) (n=4). Further details on patient classifications are provided in the supplemental material, and study flow chart in Figure 1. The study was approved by the institutional ethics committee (2015/08JAN/010) and complied with the Declaration of Helsinki and good clinical practice guidelines. All participants provided written informed consent.

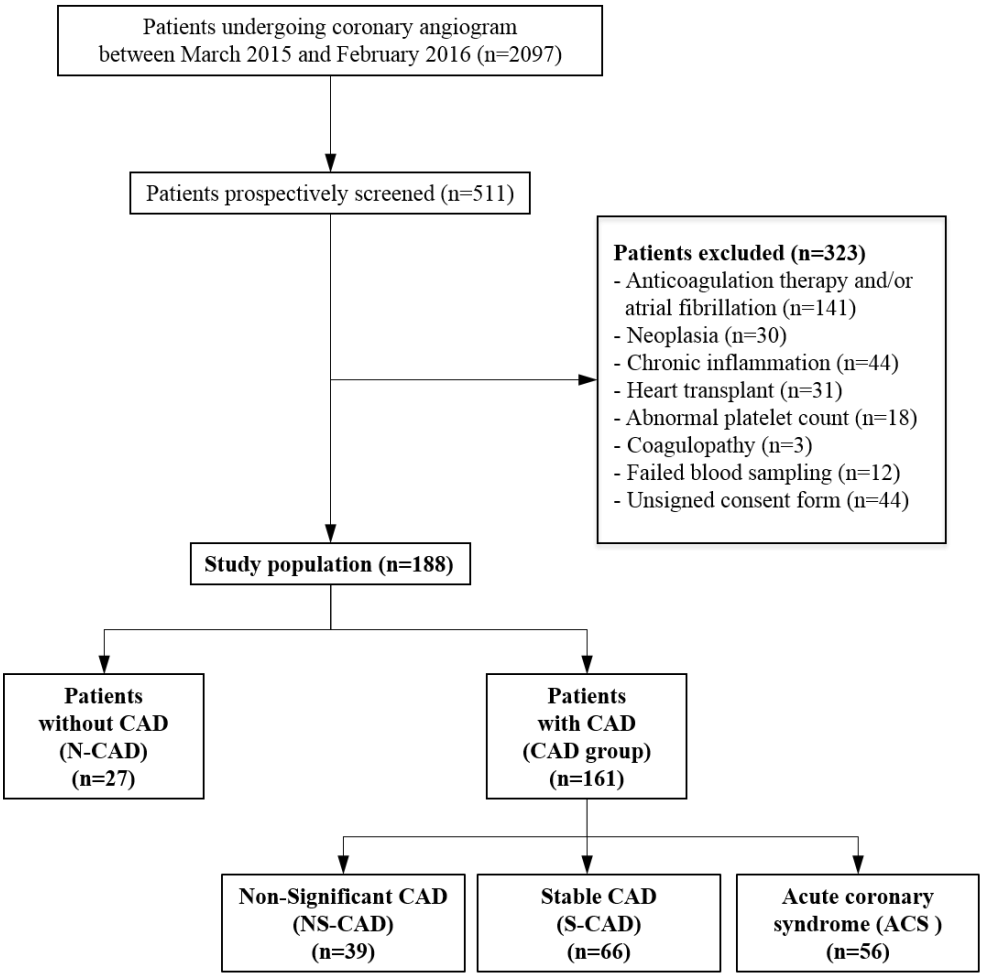

Figure 1. Flow chart of the study population. ACS: acute coronary syndrome, CAD: coronary artery disease, N-CAD: absence of coronary artery disease, NS-CAD: coronary artery disease without significant stenosis, S-CAD: coronary artery disease with at least one lesion >50%.

3.1.2 Blood sampling and phosphoACC analysis

All patients had been fasting for at least 6 hours prior to angiography, except for four STEMI patients. Blood samples drawn from the arterial sheath were collected in citrated tubes before any drug administration in

the catheterization laboratory, while avoided heparin injection before blood sampling. Samples were directly processed for platelet isolation. Platelets were lyzed in Laemmli buffer prior to phosphoACC analysis by western blotting. A standard positive control was prepared with washed platelets isolated from a healthy volunteer and stimulated with a high dose of thrombin (0.5 U/mL) for 2 minutes. This standard positive control was used for all the western blots, placed four times on each gel to validate the signal reproducibility. For each patient, band intensities were normalized to corresponding loading controls (gelsolin) on the same gel. The normalized phosphoACC value was compared against the standard positive control. Western blot analyses were confirmed by electrochemiluminescence immunoassay (ECLIA, Meso Scale Discovery).

3.1.3 Multidetector computed tomography

Thoraco-abdominal multidetector computed tomography (MDCT) was performed in randomly selected patients (n=68) to assess global atherosclerotic plaque burden. Coronary artery and extra-coronary calcification were measured as detailed in the supplemental material.

3.1.4 Platelet lipidomics

To characterize the phosphoACC impact on regulating platelet lipid metabolism, we performed a quantitative lipidomic study on 31 samples from patients with the lowest (n=12) and highest (n=19) platelet phosphoACC values. Lipids were extracted from a platelet pellet by the

methyl-tert-butylether method and injected into direct infusion-tandem mass spectrometry (DI-MS/MS) (Sciex, Redwood City, California, USA).

3.2 Statistical Analysis

3.2.1 Clinical cohort

Analyses were conducted using SPSS 24 (IBM Corp. 2011, IBM SPSS Statistics for Windows, Armonk, NY, USA). Continuous variables were expressed as mean ± one standard deviation (SD) or median with interquartile range (IQR) depending on data distribution, and categorical variables as number and percentage. Values were log10-transformed when appropriate. Categorical variables were analyzed using the chi-squared test or Fisher's exact test, and continuous variables using an unpaired t-test or the Mann-Whitney *U*-test, as appropriate. Data were subjected to the Kolmogorov-Smirnov normality test and Bartlett's test for homogeneity of variance. Group comparisons were made using either one-way ANOVA with the F-test (Bonferroni correction) or Kruskal-Wallis test. Correlations were presented as Pearson or Spearman coefficients. Multivariate logistic regression analysis (backward elimination) included variables with P value <0.10 on univariate analysis, with odds ratios (OR) and 95% confidence intervals (95%CI) calculated to determine independent factors associated with ACS. With the receiver operating characteristic (ROC) curve, we determined a threshold phosphoACC value for CAD by maximizing sensitivity and specificity. C-statistics were used to describe diagnostic discrimination.

3.2.2 Lipidomics

Lipid species concentrations obtained from DI-MS/MS were analyzed using R.3.4.2 according to the following bioinformatics pipeline. Missing DI-MS/MS data were imputed using probabilistic principal component analysis from pcaMethods Bioconductor package [255]. The data were normalized using total lipid abundance, with a log2 transformation applied to normalized concentrations. The limma Bioconductor package was used to build a multivariate regression model for each lipid species with predictors including platelet phosphoACC, diabetes and plasma TG levels. Fold-change estimates and corresponding P values were derived from regression models for each lipid species and each predictor. To control for multiple testing, all P values were further adjusted for Benjamini-Hochberg false discovery rate (FDR), with a FDR <0.05 considered statistically significant [256]. Considering that 865 lipid species belong to 11 lipid classes, namely cholesterol ester (CE), diacylglycerol (DAG), free fatty acid (FFA), lysophosphatidylcholine (LPC), lysophosphatidylethanolamine (LPE), phosphatidylcholine (PC), phosphatidylethanolamine (PE), plasmenyl phosphatidylethanolamine (PEO), plasmalogen phosphatidylethanolamine (PEP), sphingomyelin (SM), and TG, lipid class enrichment analysis was performed using Fisher's exact tests to identify lipid classes with a high proportion of differentially regulated lipid species.

4. RESULTS

4.1 Population baseline characteristics and global atherosclerotic plaque burden

The study population comprised 188 individuals (69.7% men, 30.3% women), aged 65±12 years, admitted for coronary angiography. They were divided into four groups according to clinical presentation and coronary anatomy (Table 1). The N-CAD group contained 27 (14.4%) patients with normal coronary arteries, with about 41% undergoing angiography for valvular disease. In the CAD group (n=161), 122 patients (76%) had significant coronary stenosis above 50 %, 46% of whom had ACS. Most ACS patients (93%) were taking aspirin at enrolment, with only 36% of them on dual antiplatelet therapy, as most unstable angina and NSTEMI patients did not receive $P2Y_{12}$ inhibitors before angiography. Accordingly, mean platelet reactivity assessed using the Multiplate® Analyzer showed decreased platelet aggregation in response to arachidonic acid in ACS patients. Laboratory parameters revealed significantly increased platelet counts in CAD patients, yet within the normal range. As previously reported, our data confirmed a significant increase in ThG, assessed by D-dimer levels, in ACS patients.

Table 1. Baseline characteristics of the ACCTHEROMA cohort

	Overall Population n = 188	N-CAD n = 27	CAD			P value
			NS-CAD n = 39	S-CAD n = 66	ACS n = 56	
Clinical Characteristics						
Age, yrs	65 ± 12	59 ± 9	68 ± 11	66 ± 12	66 ± 14	0.029*
Male sex, n (%)	131 (69.7)	15 (55.6)	23 (59.0)	48 (72.7)	45 (80.4)	0.046
BMI, kg/m²	27.6 ± 4.9	27.4 ± 4.0	28.0 ± 5.3	27.4 ± 5.5	27.6 ± 4.2	0.94
Hypertension, n (%)	119 (63.3)	8 (29.6)	21 (53.8)	52 (78.8)	38 (67.9)	<0.001
Smoking, n (%)	104 (55.3)	12 (44.4)	17 (43.6)	39 (59.1)	36 (64.3)	0.13
Diabetes, n (%)	43 (22.9)	1 (3.7)	9 (23.1)	14 (21.2)	19 (33.9)	0.022
Prior history of CAD, n (%)	62 (33.0)	0 (0)	0 (0)	36 (54.5)	26 (46.4)	<0.001
- MI, n (%)	35 (18.6)	0 (0)	0 (0)	19 (28.8)	16 (28.6)	<0.001
- PCI, n (%)	47 (25.0)	0 (0)	0 (0)	26 (39.4)	21 (37.5)	<0.001
- CABG, n (%)	16 (8.5)	0 (0)	0 (0)	10 (15.2)	6 (10.7)	0.017
Aortic valve disease, n (%)	34 (18.1)	4 (14.8)	14 (35.9)	16 (24.2)	0 (0)	<0.001
Mitral valve disease, n (%)	12 (6.4)	7 (25.9)	3 (7.7)	2 (3.0)	0 (0)	<0.001
Lab results						
Hemoglobin, (g/dL)	14.1 ± 1.6	13.7 ± 1.3	14.1 ± 1.5	14.2 ± 1.4	14.0 ± 1.9	0.62
Fasting blood glucose, (mg/dL)	100 (92-114)	98 (92-105)	99 (91-123)	101 (93-108)	105 (95-134)	0.61
Creatinine, (mg/dL)	1.0 (0.8-1.1)	0.9 (0.8-1.1)	1.0 (0.8-1.0)	1.0 (0.9-1.2)	0.9 (0.8-1.1)	0.22
CRI, n (%)	22 (11.7)	2 (7.4)	3 (7.7)	12 (18.2)	5 (8.9)	0.24
Total cholesterol, (mg/dL)	171 ± 48	177 ± 57	180 ± 40	162 ± 50	171 ± 46	0.28
LDL, (mg/dL)	96 ± 41	104 ± 46	98 ± 34	90 ± 41	99 ± 42	0.43
HsCRP, (mg/L)	1.4 (0.6-3.4)	0.9 (0.5-2.1)	1.2 (0.6-3.0)	1.3 (0.5-3.6)	1.7 (0.8-5.6)	0.13
Platelet count (x10³)/µL	244 ± 61	211 ± 38	268 ± 65	248 ± 66	240 ± 54	0.002*†
Multiplate® analysis						
- ASPI test (AU*min)	515 ± 278	549 ± 319	631 ± 258	507 ± 287	427 ± 228	0.004 ‡
- ADP test (AU*min)	638 ± 217	626 ± 163	692 ± 132	643 ± 243	601 ± 249	0.24
- TRAP test (AU*min)	1101 ± 255	1007 ± 258	1177 ± 232	1057 ± 226	1146 ± 280	0.011*
D-dimers, (ng/mL)	407 (281-686)	282 (250-435)	398 (288-573)	407 (290-775)	443 (349-706)	0.018§
Medication						
ACEi/ARB, n (%)	86 (45.7)	6 (22.2)	16 (41.0)	43 (65.2)	21 (37.5)	<0.001
Beta blokers, n (%)	97 (51.6)	9 (33.3)	15 (38.5)	39 (59.1)	34 (60.7)	0.022
Lipid lowering treatment, n (%)	111 (59.0)	13 (48.1)	16 (41.0)	48 (72.7)	34 (60.7)	0.008
Aspirin, n (%)	141 (75.0)	13 (48.1)	21 (53.8)	55 (83.3)	52 (92.9)	<0.001
Dual antiplatelet therapy, n (%)	30 (16.0)	0 (0)	0 (0)	12 (18.2)	20 (35.7)	<0.001
- Clopidogrel, n (%)	15 (8.0)	0 (0)	0 (0)	6 (9.1)	9 (16.1)	0.013
- Ticagrelor, n (%)	13 (6.9)	0 (0)	0 (0)	3 (4.5)	10 (17.9)	<0.001
- Prasugrel, n (%)	4 (2.1)	0 (0)	0 (0)	3 (4.5)	1 (1.8)	0.35

Table 1. Values are mean ± SD, n (%) or median (interquartile range). ACEi/ARB: angiotensin converting enzyme inhibitor/angiotensin receptor blocker, BMI: body mass index, CABG: coronary artery bypass graft, CRI: chronic renal insufficiency, hsCRP: high sensitivity C-reactive protein, LDL: low-density lipoprotein, MI: myocardial infarction, PCI: percutaneous coronary intervention. Statistical differences between groups are denoted as * between NS-CAD and N-CAD, † between S-CAD and N-CAD, ‡ between ACS and NS-CAD, and § between ACS and N-CAD.

Thoraco-abdominal MDCT with prospective ECG-gating in randomly selected patients (n=68) was aimed to evaluate global atherosclerotic plaque burden, including coronary (CAC Agatston) and extra-coronary (AoC) calcification scores. We confirmed that N-CAD patient (reference population) classification based on angiographic data was consistent with low CAC Agatston scores (median [IQR]: 7.0 [0.0-33.9]) (Figure 2A). Although N-CAD patients had low CAC Agatston scores, their AoC scores were fairly high (median [IQR]: 543 [107-2001]) (Figure 2B). Accordingly, we observed a modest correlation between CAC and AoC calcification scores ($R=0.42$, $P<0.001$), indicating a heterogeneous atherosclerotic development (Figure 2C).

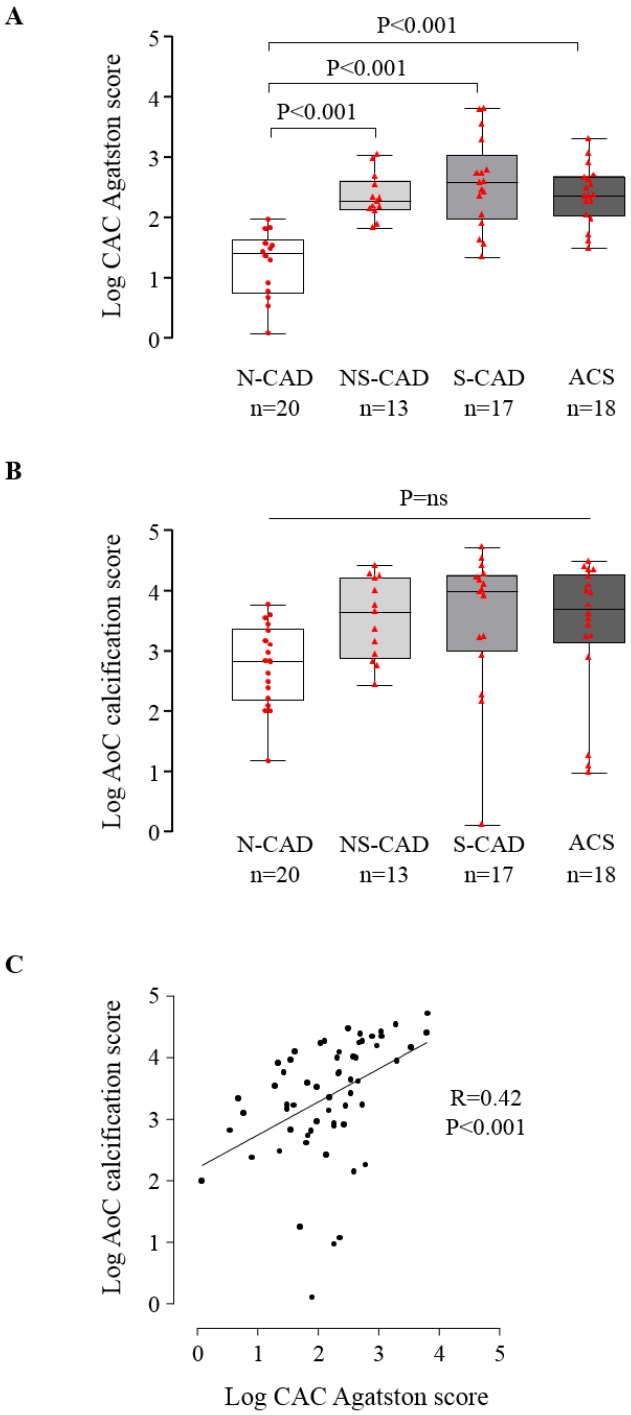
A
P<0.001
P<0.001
P<0.001
Log CAC Agatston score
0
1
2
3
4
5
N-CAD
n=20
NS-CAD
n=13
S-CAD
n=17
ACS
n=18
B
P=ns
Log AoC calcification score
0
1
2
3
4
5
N-CAD
n=20
NS-CAD
n=13
S-CAD
n=17
ACS
n=18
C
Log AoC calcification score
R=0.42
P<0.001
0
1
2
3
4
5
Log CAC Agatston score

Figure 2. Assessment of coronary and extra-coronary atherosclerotic plaque burden by prospective ECG-gated MDCT. Box-plot representation of log-transformed (A) CAC Agatston and (B) AoC scores in the N-CAD and CAD subgroups of patients. Red dots (N-CAD, reference population) and triangles (CAD patients) represent individual values. (C) Correlation between log-transformed CAC Agatston and AoC scores. ACS: acute coronary syndrome, AoC: aortic calcification, CAC: coronary artery calcification, N-CAD: absence of coronary artery disease, NS-CAD: coronary artery disease without significant stenosis, S-CAD: coronary artery disease with at least one lesion >50%.

4.2 Identification of high-risk coronary artery disease patients by platelet phosphoACC

Platelet phosphoACC was studied in consecutive patients by western blotting (Figure 3A). Based initially on visual phosphoACC assessment, patients were divided into three groups: high, intermediate, or low phosphoACC signal. High signal corresponded to phosphoACC greater than or equal to our standard positive control, and low signal to nearly undetectable phosphoACC. Hence, 36% of CAD group patients (*vs.* 7% in N-CAD, P<0.001) displayed a high phosphoACC signal (Figure 3B). Band intensities were then quantified for each patient. PhosphoACC was significantly increased in circulating platelets of CAD compared to N-CAD patients (median [IQR]: 0.48 [0.29-0.73] *vs.* 0.22 [0.11-0.45], P<0.001) (Figure 3C). Platelet phosphoACC in N-CAD patients was almost never >0.5 AU, a threshold value estimated from ROC analysis (Online Figure 1) with a 96% positive predictive value for CAD. Importantly, phosphorylation of protein kinase C (PKC) substrates, a read-out of platelet activation, was nearly undetectable in the platelets of CAD patients (Online Figure 2), indicating that phosphoACC occurred independently of platelet activation.

The western blot results were confirmed by quantitative ECLIA. Platelet phosphoACC was analyzed twice to test inter-experiment reproducibility (ICC), found to be high (0.90) with a bias of -0.03 (95%CI: -0.10-0.04) (Online Figure 3A). Furthermore, phosphoACC correlated with western blot results, confirming that it was significantly increased in circulating platelets of CAD patients (Online Figures 3B and 3C).

Among the CAD subgroups, the highest platelet phosphoACC level was found in ACS patients (median [IQR]: 0.55 [0.29-0.76]) (Figure 3D). Indeed, quartile analysis of platelet phosphoACC demonstrated that the 4th quartile included 98% of CAD patients, with a large proportion of high-risk ACS patients (45%) (P<0.02) (Figure 3E). Multivariate logistic regression results coincided with this, showing that, in addition to D-dimer levels (OR: 5.45, 95%CI: 1.50-19.81, P<0.05) and the TG/high-density lipoprotein-cholesterol ratio (TG/HDL-C) (OR: 8.59, 95%CI: 1.90-38.95, P<0.01), platelet phosphoACC (OR: 8.90, 95%CI: 2.30-34.53, P=0.002) was highly associated with ACS (Table 2).

Figure 3. PhosphoACC correlates with atherosclerotic plaque burden severity and identifies high-risk ACS patients. (A) Representative western blot of platelet phosphoACC in 17 consecutive patients from the ACCTHEROMA trial. +, positive control corresponding to washed platelets from healthy volunteers stimulated with thrombin (0.5 U/mL) for 2 minutes. (B) Distribution of patients according to visual assessment of phosphoACC signal intensity across N-CAD and CAD groups. (C) PhosphoACC quantification in N-CAD and CAD patients. Dotted line represents the threshold value of 0.5 AU estimated from ROC curve analysis for discriminating between N-CAD and CAD patients. Positive predictive values of this threshold for CAD are indicated on the graph. Red dots (N-CAD, reference population) and triangles (CAD patients) represent individual values. Medians and corresponding IQR are presented. (D) Box-plot representation of platelet phosphoACC quantifications in N-CAD and CAD subgroups. (E) Clinical and angiographic characteristics of patients across the different quartiles of platelet phosphoACC. Distribution of platelet phosphoACC quartiles across CAC Agatston score groups (F) and AoC score tertiles (G). The statistical differences between the groups were determined using the Mann-Whitney *U*-test in (C), Kruskal-Wallis test in (D) and chi-squared test in (B, E-G). ACS: acute coronary syndrome, AU: arbitrary units, M: molecular weight marker, N-CAD: absence of coronary artery disease, NS-CAD: coronary artery disease without significant stenosis, PPV: positive predictive value, Q: quartile, S-CAD: coronary artery disease with at least one lesion >50%.

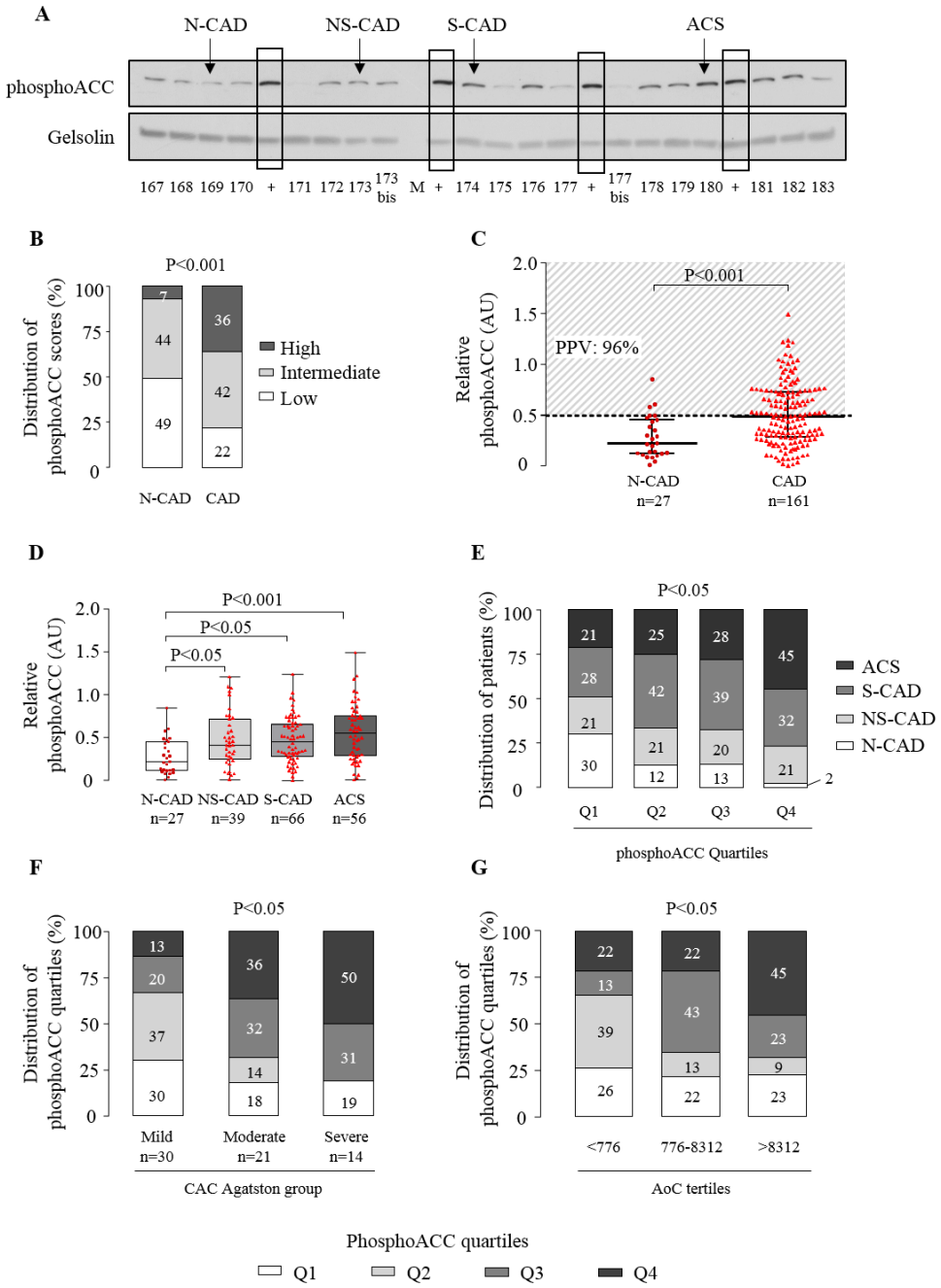
A
N-CAD
NS-CAD
S-CAD
ACS
phosphoACC
Gelsolin
167 168 169 170 + 171 172 173 173 bis M + 174 175 176 177 + 177 bis 178 179 180 + 181 182 183
B
P<0.001
Distribution of phosphoACC scores (%)
High
Intermediate
Low
N-CAD CAD
C
P<0.001
PPV: 96%
Relative phosphoACC (AU)
N-CAD n=27
CAD n=161
D
P<0.001
P<0.05
P<0.05
Relative phosphoACC (AU)
N-CAD n=27
NS-CAD n=39
S-CAD n=66
ACS n=56
E
P<0.05
Distribution of patients (%)
ACS
S-CAD
NS-CAD
N-CAD
Q1 Q2 Q3 Q4
phosphoACC Quartiles
F
P<0.05
Distribution of phosphoACC quartiles (%)
Mild n=30
Moderate n=21
Severe n=14
CAC Agatston group
G
P<0.05
Distribution of phosphoACC quartiles (%)
<776
776-8312
>8312
AoC tertiles
PhosphoACC quartiles
Q1 Q2 Q3 Q4

Table 2. Univariate and multivariate models of factors associated with ACS				
Variable	Univariate		Multivariate	
	OR (95% CI)	P value	OR (95% CI)	P value
Age	1.01 (0.98-1.03)	0.640		
Sex (male=1)	2.19 (1.03-4.63)	0.041		
BMI	1.00 (0.94-1.07)	0.980		
Hypertension (yes=1)	1.44 (0.74-2.82)	0.280		
Smoking (yes=1)	1.69 (0.89-3.23)	0.110		
Diabetes (yes=1)	2.31 (1.14-4.69)	0.020		
Positive family history (yes=1)	1.20 (0.63-2.30)	0.580		
Total cholesterol (mg/dL)	1.00 (0.99-1.01)	0.947		
TG/HDL-C ratio (log-transformed)	**7.57 (2.32-24.72)**	**0.001**	**8.59 (1.90-38.95)**	**0.005**
HsCRP (log-transformed)	1.99 (1.11-3.55)	0.020		
D-dimer (log-transformed)	**3.14 (1.16-8.51)**	**0.024**	**5.45 (1.50-19.81)**	**0.010**
Platelet phosphoACC	**4.02 (1.39-11.56)**	**0.010**	**8.90 (2.30-34.53)**	**0.002**

Table 2. Statistical significance when P<0.05. OR: odds ratio, CI: confidence interval, BMI: body mass index, HsCRP: high sensitivity C-reactive protein, TG/HDL-C ratio: triglyceride/high-density lipoprotein cholesterol ratio.

4.3 Relationship between platelet phosphoACC, atherosclerotic plaque burden severity, and thrombin generation markers

In patients who underwent MDCT, increased platelet phosphoACC was highly associated with coronary calcification severity. As depicted in Figure 3F, 50% of patients with high phosphoACC (4th quartile) exhibited severe CAC Agatston scores (P<0.05). AoC scores were positively associated with increased platelet phosphoACC (P<0.05) (Figure 3G). These observations were confirmed in SR-B1$^{flox/flox}$/ApoE$^{-/-}$ hypercholesterolemic mice, as these animals develop spontaneous atherosclerosis, which is enhanced by a Western diet (Online Figures 4A and 4B). As in human platelets, phosphoACC levels drastically increased with the severity of atherosclerotic plaque burden (Online Figure 4C). These results thus highlight the potential of

platelet phosphoACC for identifying disease severity and high-risk CAD patients.

ThG markers correlated with the severity of global atherosclerotic plaque burden, given that D-dimer levels ($P<0.05$), thrombin anti-thrombin complex (TATc) ($P<0.05$), and fragment 1.2 (F1.2) ($P< 0.01$) had a significant positive association with the severity of both CAC Agatston (Online Figure 5A) and AoC calcification score (Online Figure 5B). However, we did not find any correlation between ThG markers (D-dimer levels) and platelet phosphoACC across the entire population (Online Figure 5C), though thrombin is a major agonist leading to phosphoACC in platelets *in vitro*. Therefore, other factors besides thrombin contribute to platelet phosphoACC in atherosclerosis.

4.4 Contribution of inflammation and atherogenic oxLDL to phosphoACC in platelets

Since inflammatory cytokines may affect platelets [257] and are established atherosclerosis mediators, we explored whether interleukin-1beta, interleukin-6, interleukin-10, interleukin-17A, and tumor necrosis factor-alpha impacted phosphoACC in washed platelets from healthy volunteers. Although their respective receptors are present in human platelets [215], none of these cytokines affected platelet phosphoACC (Figure 4A).

We continued our analysis to identify biological predictors of increased platelet phosphoACC in the CAD group (>0.5 AU, Figure 3C). In

agreement with the above results, whereas hsCRP and ThG markers were not associated with increased phosphoACC, we identified a striking positive association between TG/HDL-C and phosphoACC, suggesting atherogenic lipids to affect phosphoACC in circulating platelets (OR: 3.97, 95%CI: 1.25-12.61, P=0.019) (Table 3). TG/HDL-C, a well-known atherogenic marker, indicates LDL particle size [258], while TGs were shown to correlate with plasma oxLDL levels [259]. We thus studied the effect of oxLDL on AMPK-ACC signalling. PhosphoACC was assessed in platelets from healthy volunteers treated with copper-oxidized LDL (CoxLDL) and myeloperoxidase-oxidized LDL (MoxLDL). Both induced a time- and dose-dependent increase in platelet phosphoACC (Figures 4B-D and Online Figure 6A). MoxLDL-induced phosphoACC was prevented by anti-CD36 antibodies (Figure 4E). Accordingly, oxidized choline glycerophospholipids ($OxPC^{CD36}$), a specific high-affinity ligand for CD36, increased platelet phosphoACC (Figure 4F). In line with *ex vivo* data, platelet phosphoACC correlated with oxLDL levels in statin-free CAD patients (R=0.28, P<0.05) (Online Figure 6B).

Figure 4. OxLDLs induce platelet phosphoACC in a CD36-dependent manner. Washed platelets (4.0×10^8/mL) from healthy volunteers were (A) treated with the following selected cytokines (IL1β, IL6, IL10, IL17A, and TNFα) and (B) stimulated with thrombin, collagen, ADP, coxLDL or moxLDL prior to lysis. Time course (C) and dose response (D) curve of effect of moxLDL on phosphoACC. (E) Platelets were pre-treated with 0.2 U/mL anti-CD36 antibody (FA6-152) (FA6 Ab) or an isotype control (control Ab) for 15 minutes before stimulation with moxLDL. (F) Platelets were stimulated with varying concentrations of a specific CD36 ligand ($OxPC^{CD36}$) for 5 minutes prior to lysis. All experiments were carried out at least four times. Thrombin-stimulated platelets were used as a positive control. Gelsolin was the loading control. Representative western blots are shown, with quantification of western blots represented in the right-hand panels. Data expressed as mean ± SEM. Significance was determined by a 2-tailed Student's *t*-test (A, B, and E) or 1-way ANOVA with Bonferroni post-hoc analysis (B-thrombin, D, and F). *P<0.05, **P<0.01, ***P<0.001 compared with unstimulated platelets. Ab: antibody, coxLDL: copper-oxidized LDL, IL1β: interleukin-1beta, IL6: interleukin-6, IL10: interleukin-10, IL17A: interleukin-17A, moxLDL: myeloperoxidase-oxidized LDL, $OxPC^{CD36}$: oxidized choline glycerophospholipids, Thr: thrombin, TNFα: tumor necrosis factor-alpha.

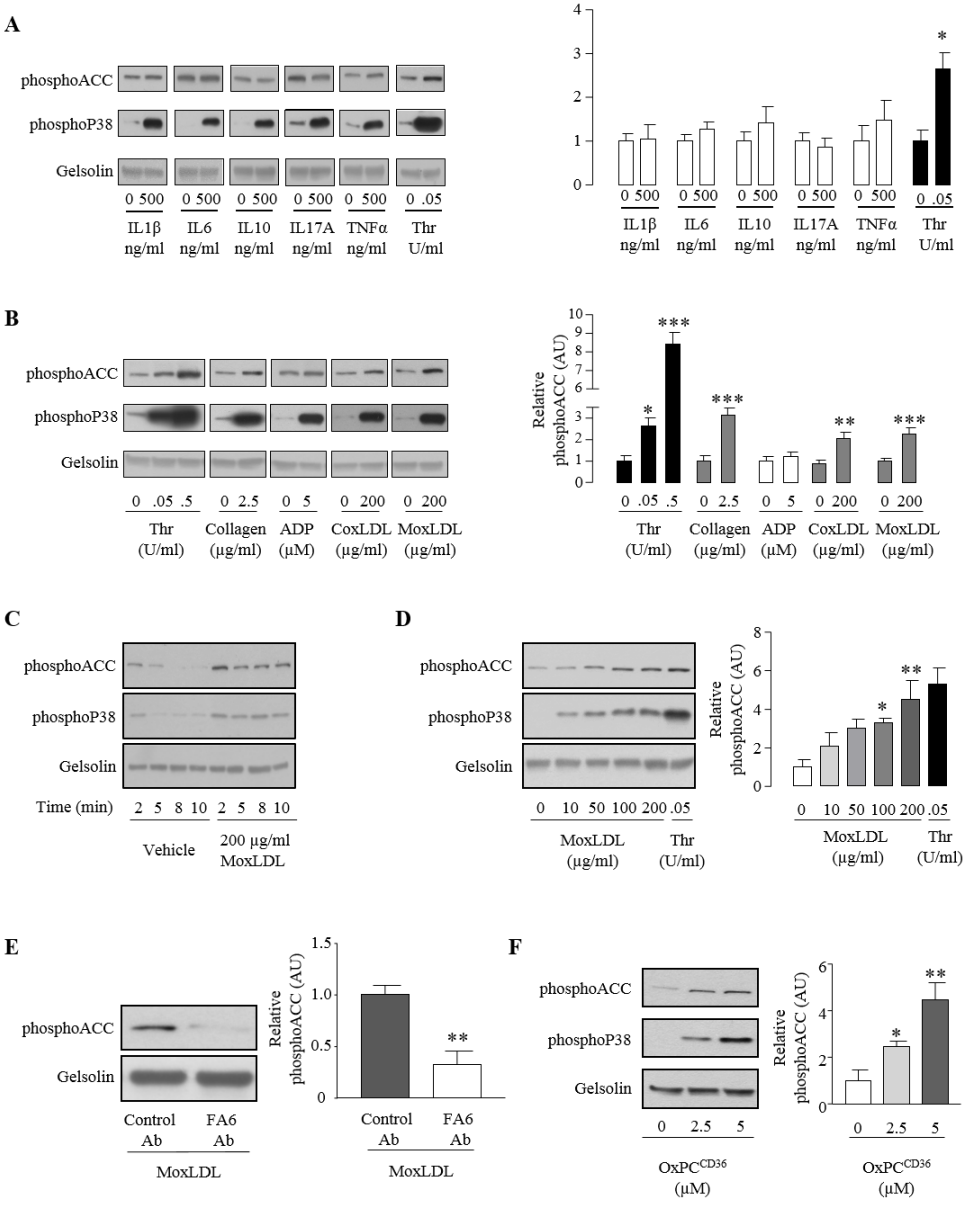
A
phosphoACC
phosphoP38
Gelsolin
0 500 0 500 0 500 0 500 0 500 0 .05
IL1β ng/ml
IL6 ng/ml
IL10 ng/ml
IL17A ng/ml
TNFα ng/ml
Thr U/ml
B
phosphoACC
phosphoP38
Gelsolin
0 .05 .5 0 2.5 0 5 0 200 0 200
Thr (U/ml)
Collagen (µg/ml)
ADP (µM)
CoxLDL (µg/ml)
MoxLDL (µg/ml)
Relative phosphoACC (AU)
C
phosphoACC
phosphoP38
Gelsolin
Time (min) 2 5 8 10 2 5 8 10
Vehicle
200 µg/ml MoxLDL
D
phosphoACC
phosphoP38
Gelsolin
0 10 50 100 200 .05
MoxLDL (µg/ml)
Thr (U/ml)
Relative phosphoACC (AU)
E
phosphoACC
Gelsolin
Control Ab
FA6 Ab
MoxLDL
Relative phosphoACC (AU)
F
phosphoACC
phosphoP38
Gelsolin
0 2.5 5
OxPC^CD36 (µM)
Relative phosphoACC (AU)

Table 3: Laboratory parameters associated with increased platelet phosphoACC in CAD patients (>0.5 AU threshold).		
Variable	**OR (95% CI)**	**P value**
D-dimer (log-transformed)	0.62 (0.20-1.94)	0.41
TATc (log-transformed)	0.93 (0.53-1.62)	0.80
F1.2 (log-transformed)	0.45 (0.11-1.76)	0.25
HsCRP (log-transformed)	1.00 (0.58-1.71)	0.99
Total cholesterol (mg/dL)	1.00 (0.99-1.00)	0.95
TG (mg/dL)	**1.00 (1.00-1.01)**	**0.048**
HDL (mg/dL)	**0.97 (0.96-1.00)**	**0.043**
TG/HDL-C ratio (log-transformed)	**3.97 (1.25-12.61)**	**0.019**

Table 3. Statistical significance when P<0.05. F1.2: fragment1+2, HDL: high-density lipoprotein, hsCRP: high sensitivity C-reactive protein, TATc: thrombin anti-thrombin complex, TG: triglycerides, TG/HDL-C ratio: triglyceride/high-density lipoprotein cholesterol ratio.

4.5 Lipidomic profiling of circulating platelets and metabolic regulation of intraplatelet TG levels by phosphoACC in CAD patients

We investigated the impact of ACC phosphorylation/inhibition on platelet lipid regulation via a lipidomic study. To this end, we selected platelet lysates from 31 patients displaying the lowest and highest phosphoACC levels. Baseline characteristics of these are provided in Online Table 1. We first showed that diabetes and, more importantly, plasma TG levels were independently associated with up-regulation of intraplatelet TG lipid species (Figure 5A). Of the 490 TG lipid species detected within platelets, 253 (52%) were significantly up-regulated (Figure 5A) when plasma TG levels increased. Contrarily, increased phosphoACC was highly associated with down-regulation of 66 (14%) intraplatelet TGs (Figure 5B and Online Table 2). This was confirmed by lipid class enrichment analysis revealing a

significant proportion of down-regulated lipid species belonging to TG class in platelets of patients with high phosphoACC levels (OR: 27.0, 95%CI: 7.1-228.3, P<0.001) (Online Figure 7). Furthermore, we characterized changes in fatty-acid-chain composition of TGs. Increased platelet phosphoACC was associated with down-regulation of TGs containing 14 carbons (C14:0, myristic acid) (Figure 5C). These findings support that circulating platelets interact with the hyperlipidemic environment in atherosclerosis and, more importantly, that ACC phosphorylation/inhibition affects endogenous platelet lipid content, by regulating TG lipid species and their fatty-acid-chain composition.

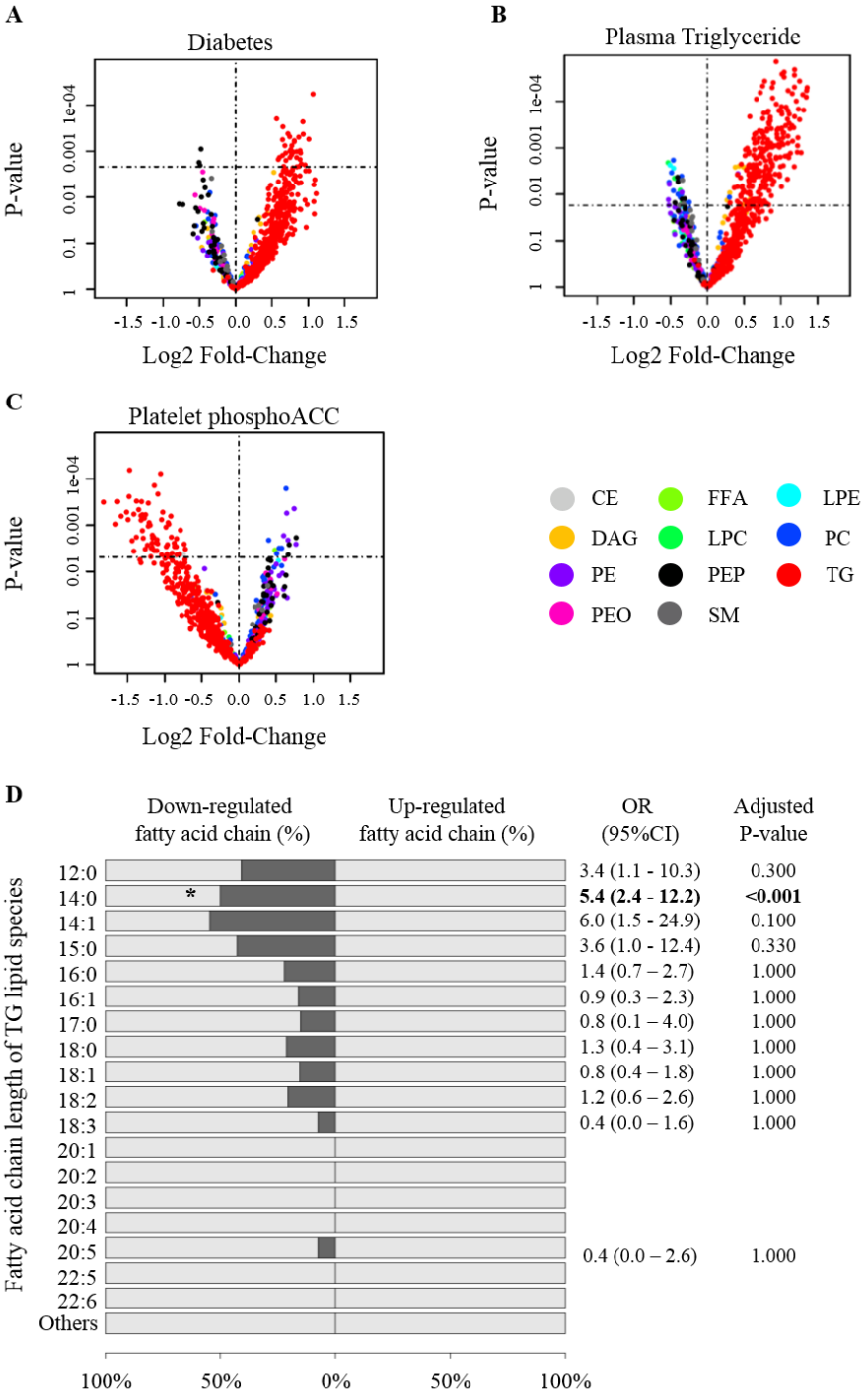
A
Diabetes
P-value
1
0.1
0.01
0.001
1e-04
-1.5 -1.0 -0.5 0.0 0.5 1.0 1.5
Log2 Fold-Change
B
Plasma Triglyceride
P-value
1
0.1
0.01
0.001
1e-04
-1.5 -1.0 -0.5 0.0 0.5 1.0 1.5
Log2 Fold-Change
C
Platelet phosphoACC
P-value
1
0.1
0.01
0.001
1e-04
-1.5 -1.0 -0.5 0.0 0.5 1.0 1.5
Log2 Fold-Change
CE
DAG
PE
PEO
FFA
LPC
PEP
SM
LPE
PC
TG
D
Down-regulated fatty acid chain (%)
Up-regulated fatty acid chain (%)
OR (95%CI)
Adjusted P-value
Fatty acid chain length of TG lipid species
12:0
14:0
14:1
15:0
16:0
16:1
17:0
18:0
18:1
18:2
18:3
20:1
20:2
20:3
20:4
20:5
22:5
22:6
Others
*
3.4 (1.1 - 10.3)
5.4 (2.4 - 12.2)
6.0 (1.5 - 24.9)
3.6 (1.0 - 12.4)
1.4 (0.7 – 2.7)
0.9 (0.3 – 2.3)
0.8 (0.1 – 4.0)
1.3 (0.4 – 3.1)
0.8 (0.4 – 1.8)
1.2 (0.6 – 2.6)
0.4 (0.0 – 1.6)
0.4 (0.0 – 2.6)
0.300
<0.001
0.100
0.330
1.000
1.000
1.000
1.000
1.000
1.000
1.000
1.000
100%
50%
0%
50%
100%

Figure 5. PhosphoACC regulates TG lipid species in platelets of CAD patients. (A-C) Volcano plot representations of the 865 lipid species detected in platelets by lipidomic profiling. Log fold-changes and P values were calculated from the multivariate regression model. Lipids above the horizontal dotted line were up- or down-regulated with significant adjusted P values. Relationship between diabetic status (A), plasma TG levels (B), platelet phosphoACC (C) and intraplatelet lipid species content. (D) Class enrichment analysis of fatty-acid-chain constituents of TG lipid species in platelets with respect to increased phosphoACC. Bars (dark gray) represent the percentage of down-regulated fatty acid-containing TG. Odds ratio (OR) and adjusted P values derived from Fisher's exact test are shown. CE: cholesterol ester, CI: confidence interval, DAG: diacylglycerol, FFA: free fatty acid, LPC: lysophosphatidylcholine, PE: phosphatidylethanolamine, LPE: lysophosphatidylethanolamine, OR: odds ratio, PC: phosphatidylcholine, PEO: plasmenyl phosphatidylethanolamine, PEP: plasmalogen phosphatidylethanolamine, SM: sphingomyelin, TG: triglycerides.

5. DISCUSSION

This study highlights that platelet phosphoACC is a risk marker in patients with suspected CAD and provides additional evidence of an interplay between platelets and lipids in atherosclerosis. We demonstrate a clear relationship between platelet phosphoACC and CAC Agatston score severity, and acute coronary events in CAD. oxLDL participates in increasing phosphoACC in circulating platelets via a CD36-dependent pathway. ACC phosphorylation/inhibition impacts endogenous platelet lipid synthesis by regulating TG lipid species (central illustration).

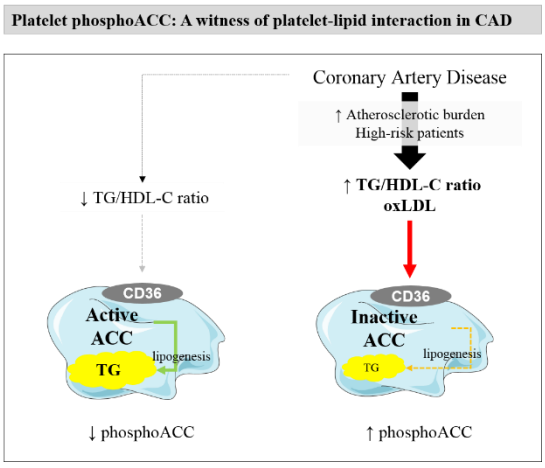

5.1 Platelet phosphoACC and risk assessment

Despite the LDL-C-lowering drugs and platelet inhibitors currently available, substantial residual risk remains [260], and many patients should be given more aggressive treatment [250, 261]. These patients must be identified by measurable risk markers. Our study brings platelet phosphoACC to the fore as a potential marker for identifying high-risk patients. More importantly, higher phosphoACC states were detected in platelets of ACS patients, even if treated with aspirin, $P2Y_{12}$ inhibitors, or statins. The long-term influence of therapeutic strategies on platelet phosphoACC remains to be determined in this high-risk population.

Numerous studies have reported that high on-treatment platelet reactivity and platelet activation indices reveal high-risk patients in CAD population [262]. Particularly, increased circulating activated platelets, evidenced by monocyte- or neutrophil-platelet aggregates or P-selectin expression, can be detected in high-risk patients versus normal subjects. However, this increase is marginal and involves a small proportion of the total platelet pool [263-265]. In our study, AMPK-ACC signalling activation was mostly observed in resting platelets. The absence of PKC substrate phosphorylation, a sign of platelet activation [266], supports the theory that increased phosphoACC and platelet activation are unrelated. Even if thrombin is the principal agonist of platelet AMPK activation *ex vivo* [29], we found no association between ThG markers and phosphoACC. Therefore, platelet phosphoACC is not caused by thrombin-induced platelet activation in patients. Our findings thus suggest that platelets of high-risk CAD patients

exhibit altered metabolic phenotypes characterized by activation of AMPK-ACC signalling, independent of platelet activation state.

5.2 Lipid-platelet interaction

Changes in LDL phenotypes, like tendency to aggregate, oxidative status, or size and density, influence cardiovascular risk and can determine residual post-treatment risk [267, 268]. In line with previous studies [254], our work further supports that this atherogenic environment influences platelet phenotype in CAD. As a novel mechanistic finding, we found a significant positive correlation between platelet phosphoACC and TG/HDL-C ratio, a marker of a pro-atherogenic lipid profile, including small LDL particles known to be more oxidizable [258, 259]. Based on our data, oxLDL mediates, at least in part, the phosphoACC increase in CAD patients. This is supported by: (i) our *ex vivo* data showing that oxLDL induces phosphoACC in platelets from healthy volunteers; (ii) clinical correlation between oxLDL levels and platelet phosphoACC in the ACCTHEROMA cohort. PhosphoACC in response to oxLDL occurs downstream of CD36. Numerous *in vitro* studies suggested that oxLDL binds to platelet CD36 and induces activatory signalling, including the recruitment of Src family kinases Fyn and Lyn [269], cytoskeleton rearrangement [107], and NADPH oxidase 2 [109]. Additionally, CD36 is an established receptor for platelet interaction with atherogenic environments, and CD36 expression variability may determine platelet reactivity and thrombotic risk [101, 251].

5.3 ACC and platelet lipid content

Given the central role of ACC in lipid biosynthesis, we performed lipidomic profiling to investigate the impact of its phosphorylation/inhibition on lipid content. Plasma TG levels were associated with an up-regulation of TG lipid species in platelets of CAD patients, highlighting the strong interaction between platelets and plasma lipids. Our results corroborate recent data revealing platelet lipid content to be altered in ACS patients [254]. We further demonstrated that increased platelet phosphoACC in high-risk CAD patients is strongly associated with platelet TG down-regulation, reflecting the inhibitory impact of phosphoACC on platelet lipid synthesis. Similar findings were reported in hepatocytes, where liver-specific pharmacological inhibition of ACC lowered lipogenesis and reduced liver TG [270]. The down-regulation of fatty acid chains containing 14 carbons (C14:0, myristic acid) provides further evidence that endogenous platelet lipid synthesis is altered upon ACC phosphorylation. In line with our data, ACC inhibition in cancer cells decreases *de novo* fatty acid synthesis, leading to a reduction in fatty acids containing 14 to 18 carbons [271]. To our knowledge, this is the first study to report the impact of ACC phosphorylation/inhibition on the regulation of lipid content in circulating platelets of CAD patients.

5.4 Study limitations

First, phosphoACC was determined using immunoblotting in whole platelet lysates. Given the circulating platelets' heterogeneity [272], it is still unclear whether increased phosphoACC occurs in the entire platelet

population or a platelet subgroup only. Moreover, in this setting, platelets must be purified before phosphoACC is measured, and quantitative assessment of phosphoACC remains challenging. However, we employed a more quantitative method, ECLIA, to confirm the phosphoACC increase. Second, phosphoACC was measured in arterial blood samples, which may be of limited use in routine clinical practice for outpatient clinics. Of note, we found that phosphoACC signal was fairly similar in arterial and peripheral venous blood in a patient subset. Third, the ACCTHEROMA trial was a single-center trial, with a limited patient number. While the sample size allowed us to fully address our primary endpoint, *i.e.*, increase in phosphoACC in CAD patients, it proved difficult to evaluate the impact of phosphoACC in predicting adverse events during follow-up owing to the small number of events. Nevertheless, patients exhibiting high phosphoACC (>0.5 AU) tended to have a worse prognosis compared to those exhibiting low phosphoACC (HR: 2.45 [0.82-7.31], p=0.09), reinforcing our hypothesis. Multicenter studies may be required to validate the prognostic impact of increased phosphoACC in peripheral blood and determine signal variability over time, as with LDL cholesterol [267].

5.5 Conclusions

Our study identifies platelet phosphoACC as a risk stratification marker that reflects the interaction between pro-atherogenic lipids and circulating platelets. In CAD patients, phosphoACC contributed to regulating endogenous lipid synthesis. We recently provided new insights into AMPK-ACC signalling's key role in regulating platelet lipid composition and function

using a genetic mouse model. The absence of phosphoACC (and inhibition) by AMPK in platelets resulted in increased phospholipid content, with enhanced platelet reactivity and thrombus formation. It is tempting to speculate that increased phosphoACC is a counter-regulatory mechanism limiting lipogenesis and platelet reactivity in CAD patients within a pro-atherogenic environment.

6. CLINICAL PERSPECTIVES

6.1 Competency in medical knowledge

The circulating platelets of high-risk CAD patients exhibit altered metabolic phenotypes characterized by phosphorylation and inhibition of acetyl-CoA carboxylase (ACC), the first committed enzyme of the fatty-acid biosynthesis pathway. Platelet ACC phosphorylation is thus a potential marker for risk stratification in suspected CAD patients, indicating an interplay between platelets and atherogenic lipids.

6.2 Translational outlook 1

Additional studies are needed to further define the role of endogenous lipogenesis in the control of platelet function.

6.3 Translational outlook 2

Large multicenter studies must investigate whether individual platelet phenotypes, including ACC phosphorylation, influences major adverse outcomes in coronary artery disease.

7. SUPPLEMENTAL MATERIALS

7.1 Supplemental Material and Methods

7.1.1 Reagents and Materials

Apyrase (#A6132), bovine thrombin (#T6634), ADP (#A2754), horse radish peroxidase (HRP)-conjugated anti-rabbit antibodies (#A0545), hematoxylin (#MHS32) and oil-red-O (#O0625) were purchased from Sigma. Eptifibatide (Integrilin) was obtained from GlaxoSmithKline. Collagen (#ABP-COL-1, equine tendon type 1) was obtained from American Biochemical and Pharmaceutical Ltd. Anti-phosphoACC (S79) (#3661), anti-phosphoP38 MAPK (T180/Y182) (#4511), anti-gelsolin (#12953) and anti-phosphoPKC substrate (#2261) antibodies were obtained from Cell Signaling. Bovine serum albumin (BSA) (#8076) was purchased from Roth. GOLD 96-well streptavidin SECTOR plates (#L15SA-5) and goat anti-rabbit sulfo-tag secondary antibody (#R32AB5) were purchased from MSD. A cocktail of protease and phosphatase inhibitors was purchased from Thermo Fisher Scientific. IL1β (#78034), IL6 (#78050), IL10 (#78024), IL17A (#78032), and TNFα (#78068) cytokines were purchased from STEMCELL Technologies. Oxidized choline glycerophospholipids ($OxPC^{CD36}$- KOdia-PC, CAS 439904) were purchased from Santa Cruz Biotechnology. Anti-CD36 (FA6-152, ab17044) and the corresponding isotype control (ab18449) antibodies were purchased from Abcam.

LDL preparation and oxidation

Native low-density lipoproteins (LDLs) were isolated from the plasma of healthy donors by means of sequential density gradient ultracentrifugation. LDL concentration was adjusted to 1mg/mL in phosphate-buffered saline (PBS). Copper-oxidized LDLs (coxLDLs) were obtained by treating native LDLs (1mg/mL) with 10µM $CuSO_4$ for 24 hours at 37°C. The reaction was stopped on ice with 25µM butylated hydroxytoluene (Sigma-Aldrich, St. Louis, MO, USA) [273]. Myeloperoxidase-oxidized LDLs (moxLDLs) were produced by mixing 1.6mg of native LDL with PBS containing 4mM HCl, 250nM myeloperoxidase, 1mM H_2O_2 and 3.4mM EDTA for 4 hours at 37°C [273, 274]. OxLDL and moxLDL were desalted in RPMI-1640 medium without glutamine (Lonza, Belgium) using PD-10 desalting columns (GE Healthcare, Little Chalfont, Buckinghamshire, UK). OxLDL and moxLDL were sterilized using sterile filters (0.2µm), resuspended in Tyrode's buffer and stored in the dark at 4°C. Concentrations of both types of oxidized LDL were determined using the Lowry method [275].

7.1.2 Clinical Cohort

7.1.2.1 Patients were classed as follows:

- Non-significant coronary artery disease (NS-CAD) if stenosis less than 50% or displayed irregularities
- Significant CAD (S-CAD) or acute coronary syndrome (ACS) classifications depended on the clinical presentation of the patient and the presence of

stenosis of more than 50%. S-CAD included patients with chronic stable chest pain for more than 1 month or patients with valvular disease or heart failure. ACS included patients with unstable angina (*de novo* chest pain for < 1 month, resting angina or worsening symptoms without high sensitivity [hs]-troponin T elevation); non-ST segment elevation myocardial infarction (NSTEMI) (requiring changes in cardiac markers, including hs-troponin T elevation above the 99th percentile in addition to recent chest pain and/or ECG changes); or ST segment elevation myocardial infarction (STEMI) treated by primary angioplasty.

7.1.2.2 Eligibility criteria

7.1.2.2.1 Inclusion criteria

- Patients > 18 years old
- Signed informed consent
- Angiography scheduled within the following 3 days, whatever the indication

7.1.2.2.2 Exclusion criteria

- Patients not able to sign the informed consent form
- Patients on anticoagulation therapy (oral or parenteral) for any reason, including heparins, fondaparinux, vitamin K antagonists, or novel oral anticoagulants
- Hemophilia or other coagulopathy
- Abnormal platelet count (< 1.5 x 10^5/µL or > 4 x 10^5/µL)
- Active neoplasia or chronic inflammatory disease
- Patients with a life expectancy of less than 3 years

- Heart transplant patients
- Active hepatitis B or C, or HIV patients
- Any contraindication to coronary angiography

7.1.2.3 Study endpoints

7.1.2.3.1 Primary endpoint

To demonstrate an increase in platelet ACC phosphorylation (phosphoACC) in CAD patients.

7.1.2.3.2 Secondary endpoints

- To correlate platelet phosphoACC with thrombin generation (ThG) markers in diseased patients.
- To determine factors predictive of increased platelet phosphoACC in the study population.
- To establish the importance of coronary and extra-coronary atherosclerotic burden in mediating an increase in platelet phosphoACC.

7.1.2.4 Estimated sample size before inclusion

Based on our preliminary data, we determined that an enrolment of 102 patients would provide a power of 80% at a significance level of 5% for detecting a difference of 0.15 AU in platelet phosphoACC in CAD patients.

7.1.3 Multidetector computed tomography (MDCT)

To assess global (coronary and extra-coronary) atherosclerotic plaque burden, we performed thoraco-abdominal MDCT with prospective ECG-gating in a randomly selected subgroup of patients (n=68). At least one

patient per day scheduled for a morning angiogram underwent MDCT for calcium scoring. Scans were taken with a 256-slice multidetector-row CT scanner (Brilliance iCT 256; Philips Healthcare, Cleveland, Ohio, USA) with 3.0mm slice collimation, 120kV tube voltage and 100mAs tube current using a prospectively gated “step and shoot” protocol. Coronary artery calcification (CAC) was expressed by means of the Agatston score using calcium scoring software (Philips Healthcare) with a threshold of 130 HU. The degree of CAC was classified as mild (Agatston score < 100), moderate (between 100 and 400), or severe (> 400) [276]. An extra-coronary calcification score (AoC) was measured from the aortic root (excluding the aortic valve) to the common iliac artery in all patients. The AoC score was divided into tertiles for analysis.

7.1.4 Blood sampling and analysis

7.1.4.1 Human platelet isolation

Blood samples were drawn into citrated tubes (citrate phosphate dextrose adenine, S-Monovette, Sarstedt) after the sheath had been inserted at the catheterization laboratory but before any drugs had been administered. Platelet-rich plasma (PRP) was obtained by 20 minutes’ centrifugation at 330 × g. Platelets were then counted with a Cell-Dyn Emerald (Abbott) and pelleted by centrifugation at 400 × g for 10 minutes in apyrase (0.5 U/mL) and eptifibatide (4µg/mL). The platelet pellets were either immediately lyzed (400,000 platelets/µL) or stored frozen (-80°C) along with plasma samples .

7.1.4.2 Western blot analysis

The platelet pellets were lyzed in Laemmli buffer (50mM Tris-HCl, pH 6.8, 10% (v/v) glycerol, 2% (w/v) SDS, 0.01% (w/v) bromophenol blue, and 6.25% (v/v) β-mercaptoethanol). Protein extracts from whole platelet lysates for each patient were separated on polyacrylamide gels (Criterion TGX, Bio-Rad). The membranes were probed with phosphoACC (1:1000), gelsolin (1:40 000), phosphoP38, or phosphoPKC substrate (1:10 000) antibodies. HRP-conjugated anti-rabbit (1:20 000) antibodies were diluted in 5% bovine serum albumin. Band intensities were quantified using Image J (National Institutes of Health, Bethesda, MD, USA).

7.1.4.3 Electrochemiluminescence analysis (ECLIA)

To facilitate the quantitative assessment of platelet phosphoACC in patients, we optimized the ECLIA technique from MSD. Since ACC contains biotin, phosphoACC quantification was based on the interaction between streptavidin and its biotin group. GOLD 96-well streptavidin SECTOR plate wells (MSD) were blocked for 1 hour, washed and incubated with protein extracts (1µg/µL) from the patients' platelets, which had been previously lyzed in 50mM Tris-HCl, pH 7.5, 1mM EGTA, 1mM EDTA, 1% Triton X 100, 0.27M sucrose, 0.1% β-mercaptoethanol, 0.1% SDS and a cocktail of protease and phosphatase inhibitors (1:100). The plate was incubated at room temperature with shaking for 1 hour. After washing, primary rabbit anti-phosphoACC antibody was added (1:250) and incubated overnight at 4°C with shaking. After washing, goat anti-rabbit sulfo-tag secondary antibody (1:250) was added and incubated at room temperature with

shaking for 1 hour. The plates were read on the SECTOR Imager 2400 (Meso Scale Discovery) immediately after the read buffer had been added. A positive control of washed platelets from healthy volunteers stimulated with thrombin (0.5 U/mL) for 2 minutes was used as a benchmark in all experiments.

7.1.4.4 ThG, oxLDL and platelet reactivity measurement

ThG was assessed in citrated plasma by measuring D-dimer levels using the automated latex-enhanced immunoassay (HemosIL D-dimer HS, Werfen, Milan, Italy), and thrombin anti-thrombin complex (TATc) and fragment 1.2 (F1.2) using the ELISA method (Siemens Healthcare Diagnostics), according to the manufacturers' protocols. OxLDL levels were measured using the ELISA method with the 4E6 monoclonal antibody (Mercodia, Uppsala, Sweden). Platelet reactivity was also evaluated in all patients by the multiple electrode platelet aggregometry method (Multiplate® Analyzer, Roche Diagnostics).

7.1.4.5 Platelet lipid extraction and analysis

Lipids were extracted using the methyl-tert-butyl ether (MTBE) method [277, 278]. Platelets were transferred to a 2mL Eppendorf vial to which 100µL of water and 100µL of an Internal Standard Mix (Sciex, Nieuwekerk aan den Ijsel, Netherlands) were added. Next, 160µL of methanol and 500µL of MTBE were added. The extracts were then shaken at room temperature for 30 minutes. Then, 200µL of water was added, after which the samples were briefly vortexed and then centrifuged at 16 100 × g

for 3 minutes. The upper organic layer (400µL) was then transferred to a fresh glass vial. Another 500µL of MTBE, 100µL of methanol and 100µL of water were added to the original Eppendorf vials and the extraction was repeated. The combined organic extracts were concentrated under a gentle stream of nitrogen and reconstituted in 250µL of running buffer (10mM ammonium acetate in 50:50 dichloromethane:methanol).

Lipidomic analysis was carried out using the commercial Lipidyzer platform according to the manufacturer's instructions (Sciex) [230]. Lipid analysis was performed in flow-injection mode. The lipid classes were separated using differential mobility spectroscopy [230], followed by tandem mass spectrometric lipid species analysis on a QTrap 5500 (Sciex) in multiple reaction monitoring mode. The lipid species were identified and quantified based on characteristic mass spectrometric transitions. The Lipidyzer software automatically calculated lipid species concentrations. All samples were analyzed in a randomized fashion. Control and fortified plasma samples were analyzed daily as quality controls. The relative standard deviations (RSD) of the quality control samples were below 15% for all lipid classes, except for sphingomyelin, where a RSD of 25% was observed.

7.1.5 Experimental dataset

7.1.5.1 Atherosclerotic mouse model

We studied platelet phosphoACC in 20 to 24-week-old female SR-B1$^{flox/flox}$/ApoE$^{-/-}$ hypercholesterolemic mice. The animals were randomized to receive either 24 weeks of standard chow diet or 12 weeks of a chow diet

followed by 12 weeks of a Western diet (1.25% cholesterol, 16% cocoa butter, U8220 version 151, Safe, Augy, France), while 24-week-old female C57BL6 mice were similarly randomized as above and were used as controls. On the day of sacrifice, the mice were bled under ketamine and xylazine anesthesia from the retro-orbital plexus. Blood was processed for platelet isolation as described below. All animals were kept in a 12:12 hour light/dark cycle with free access to food and water. Animal procedures and protocols were approved by local authorities (Comité d'éthique facultaire pour l'expérimentation animale, 2012/UCL/MD/003 and 2016/UCL/MD/027) and performed in accordance with the "Guide for the Care and Use of Laboratory Animals" published by the US National Institutes of Health (publication no. 85-23, revised 1996).

7.1.5.2 Murine platelet preparation

Blood was collected in EDTA-K tubes (Sarstedt) containing citrate-dextrose solution (1:8), apyrase (1 U/mL) and eptifibatide (4µg/mL). PRP was obtained by centrifugation at 100 × g for 5 minutes. Platelets were counted with a Cell-Dyn Emerald (Abbott). After centrifugation at 400 × g for 5 minutes, platelet pellets were lyzed in Laemmli buffer for Western blotting (400,000 platelets/µL).

7.1.5.3 Murine atherosclerosis analysis

Murine hearts and aortic roots were isolated, embedded in optimum cutting temperature (OCT) compound (Tissue-Tek, Sakura, Torrance, CA, USA) and frozen to quantify atherosclerosis at the aortic sinus. Cryostat

sections (10μm) were then cut, fixed with 4% formaldehyde, stained with 0.3% oil-red-O and counterstained with hematoxylin. Lesion sizes were quantified using a Leica SCN400 image analysis program and calculated by dividing the surface area of the lesion by the total surface area of the vessel.

7.1.5.4 Ex vivo human platelet signalling

7.1.5.4.1 Human platelet preparation

Blood from healthy volunteers was processed as previously described [253]. Platelet pellets were washed in modified Tyrode's buffer (135mM NaCl, 12mM $NaHCO_3$, 2.9mM KCl, 0.3mM Na_2HPO_4, 1mM $MgCl_2$, 10mM Hepes, 5mM D-glucose, 0.35% bovine serum albumin, pH 7.4, 37°C) before being suspended to a density of 4.0 x 10^5 platelets/μL. Platelets were treated with selected cytokines for 5 minutes at 37°C and stimulated (in 2mM Ca^{2+}) with thrombin, collagen or ADP for 2 minutes at 37°C, or coxLDL or moxLDL for 5 minutes at 37°C (as stated in the figure legends), prior to lysis with Laemmli buffer for western blot analysis. Gelsolin was used as the loading control.

7.2 Supplemental Figures and Tables

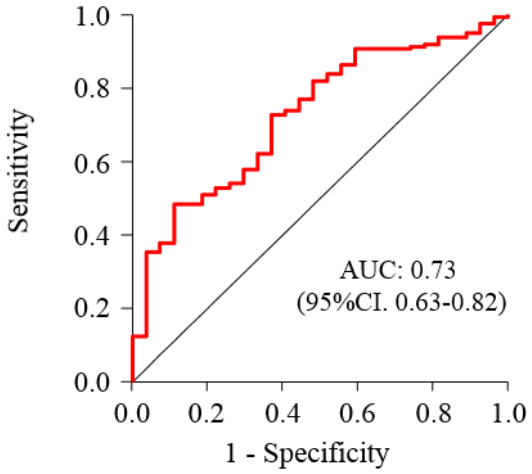

Online Figure 1. ROC curve analysis of platelet phosphoACC (CAD vs N-CAD). ROC curve analysis of platelet phosphoACC (CAD vs. N-CAD) to estimate the optimal threshold (0.5 AU) for a maximal sensitivity (48 %) and specificity (90 %). AUC: area under the curve, CAD: coronary artery disease, CI: confidence interval, N-CAD: absence of coronary artery disease, ROC: receiver operating characteristic.

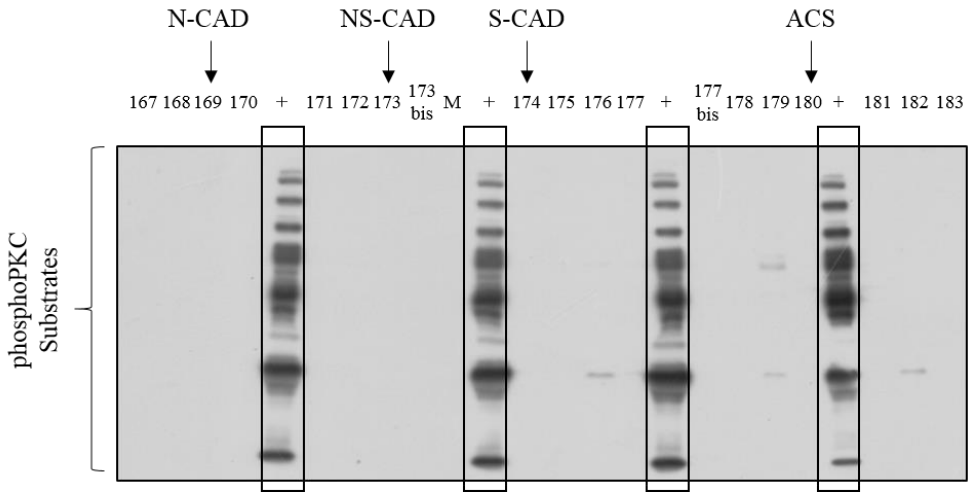

Online Figure 2. PKC substrates phosphorylation in ACCTHEROMA cohort. Representative western blot of platelet phosphoPKC substrates of 17 consecutive patients (their corresponding phosphoACC is shown in Figure 3A). +, positive controls corresponding to washed platelets from healthy volunteer, stimulated *ex-vivo* with thrombin 0.5 U/ml for 2 min. ACS: acute coronary syndrome, CAD: coronary artery disease, M: molecular weight marker, N-CAD: absence of coronary artery disease, NS-CAD: coronary artery disease without significant stenosis, phosphoPKC substrates: phosphorylation of protein kinase C substrates, S-CAD: coronary artery disease with at least one lesion > 50 %.

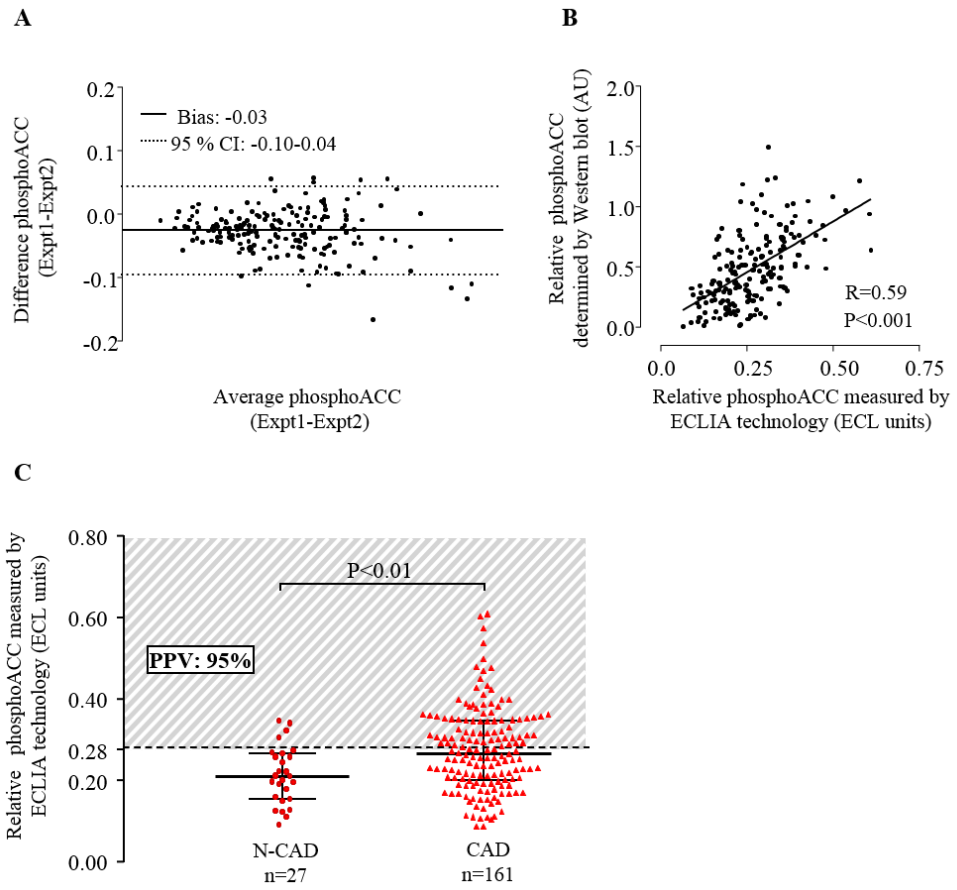

Online Figure 3. Detection of platelet phosphoACC by electrochemiluminescence. (A) Bland-Altmann analysis of two separate quantifications (Expt1-Expt2) of phosphoACC by electrochemiluminescence. (B) Correlation between western blot quantifications and electrochemiluminescence results for platelet phosphoACC (R=Spearman coefficient). (C) Electrochemiluminescence quantification of platelet phosphoACC in N-CAD and CAD patients. PPV of optimal threshold (0.28 ECL units for a sensitivity of 47 % and specificity of 85 %) for CAD is indicated on the graph. Red dots (N-CAD, reference population) or triangles (CAD patients) represent individual values. Medians with interquartile range are presented. AU: arbitrary unit, CAD: coronary artery disease, CI: confidence interval, ECL: electrochemiluminescence, ECLIA: electrochemiluminescence immunoassay, Expt: experiment, N-CAD: absence of coronary artery disease, PPV: positive predictive value.

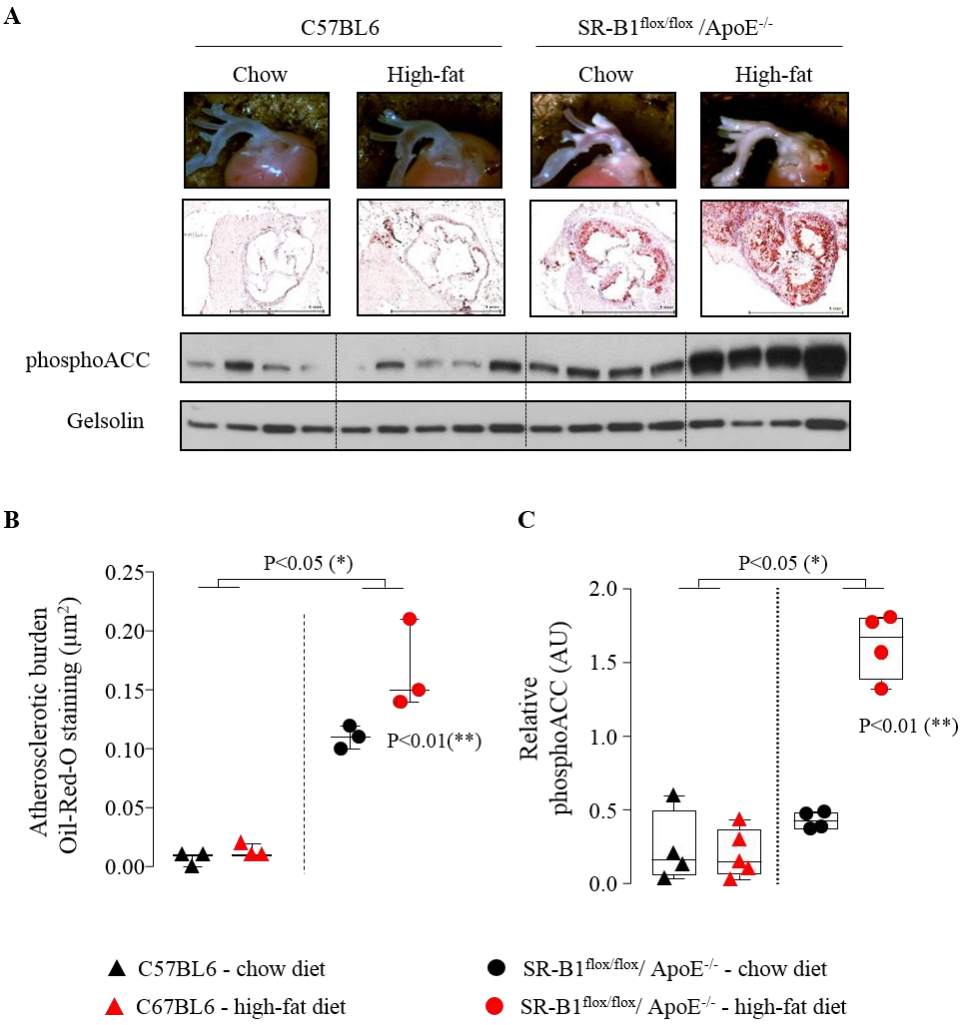

Online Figure 4. Increased platelet phosphoACC in atherosclerotic mice. (A-C) Female SR-B1$^{flox/flox}$/ApoE$^{-/-}$ (dot) and control C57BL6 (triangle) mice received either chow diet for 24 weeks (black symbols) or 12 weeks chow diet followed by 12 weeks western diet (red symbols) before sacrifice. Atherosclerotic burden was evaluated by Oil-Red-O staining of the aortic root (A, B) and platelet phosphoACC by western blot (A, C). (A) Top two panels: representative pictures of the aortic root (top) and of Oil-Red-O staining after cross section of the aortic root, scale bars indicate 1 mm (bottom). Bottom two panels: representative western blot of platelet phosphoACC. Gelsolin was used as loading control. Quantifications of Oil-Red-O staining (B) and phosphoACC (C) are shown. Data are represented as median and interquartile rage (B) or Box plot (C). (*) denotes statistical difference between C57BL6 and SR-B1$^{flox/flox}$/ApoE$^{-/-}$ (**) denotes statistical differences between SR-B1$^{flox/flox}$/ApoE$^{-/-}$ under high fat diet compared to all other groups. AU: arbitrary unit.

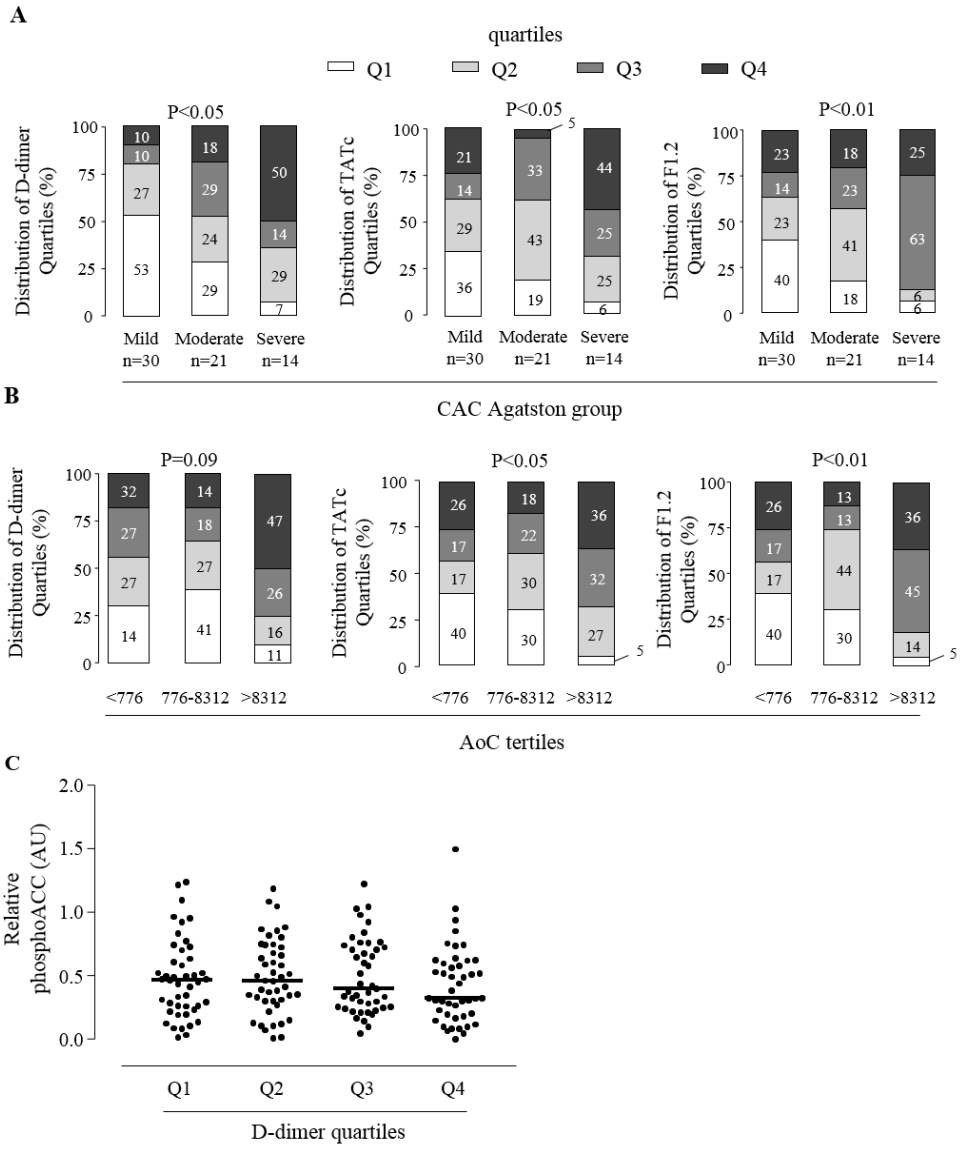

Online Figure 5. Association between thrombin generation markers and the severity of atherosclerotic burden. (A, B) Distribution of D-dimers, TATc and F1.2 quartiles among CAC Agatston score groups (A) or AoC score tertiles (B). CAC was classified as mild, moderate or severe if the CAC Agatston score was below 100, between 100-400 or above 400, respectively. (C) Correlation between D-dimer quartiles and platelet phosphoACC in the entire cohort (P=ns). Black dots represent individual values. Medians are presented. AoC: extra-coronary calcification score, AU: arbitrary unit, CAC: coronary artery calcification, F1.2: fragment 1.2, Q: quartile, TATc: thrombin anti-thrombin complex.

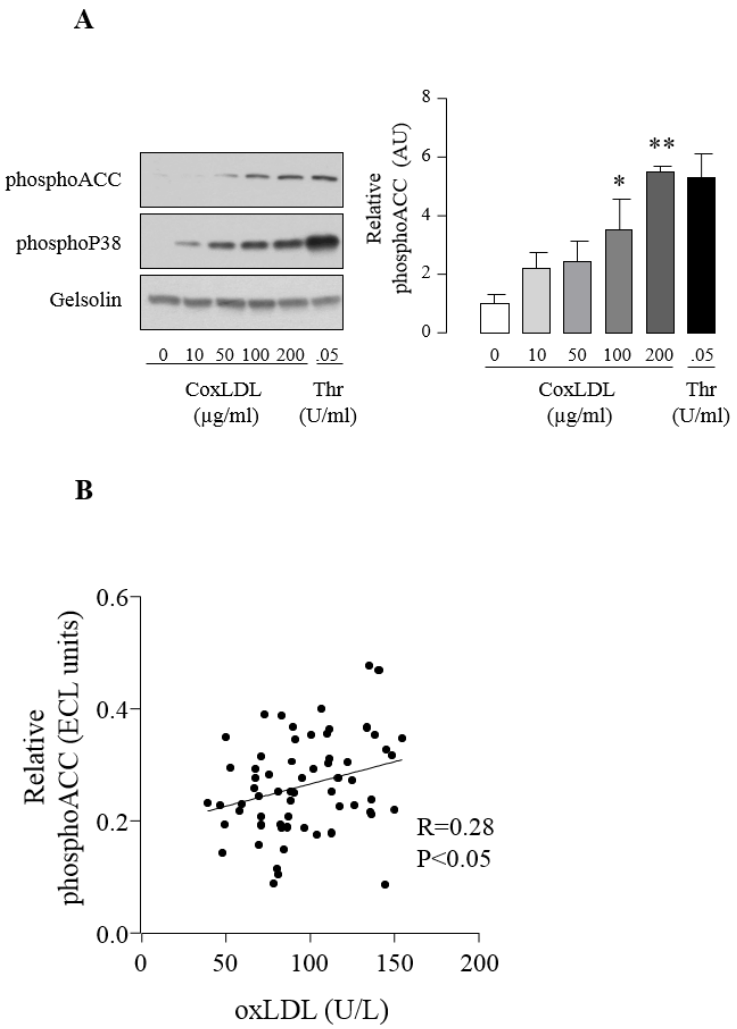

Online Figure 6. Platelet phosphoACC-induced by OxLDL and CoxLDL. (A) Platelet phosphoACC and phosphoP38 were detected in washed platelets from healthy volunteers, after treatment with varying concentrations of CoxLDL (10-200 µg/ml) for 5 min or with thrombin (0.05 U/ml) for 2 min, which was used as reference. Gelsolin was used as loading control. Representative western blots and quantifications are shown. Data are expressed as mean±SEM. Significance was determined by 1-way ANOVA with bonferroni post hoc analysis. *P<0.05, **P<0.01, relative to unstimulated platelets. (B) Correlation between platelet phosphoACC and oxLDL levels in the statin-free CAD population (R=Pearson coefficient). AU: arbitrary unit, CAD: coronary artery disease, CoxLDL: copper-oxidized low-density lipoprotein, ECL: electrochemiluminescence, oxLDL: oxidized low-density lipoprotein, Thr: thrombin

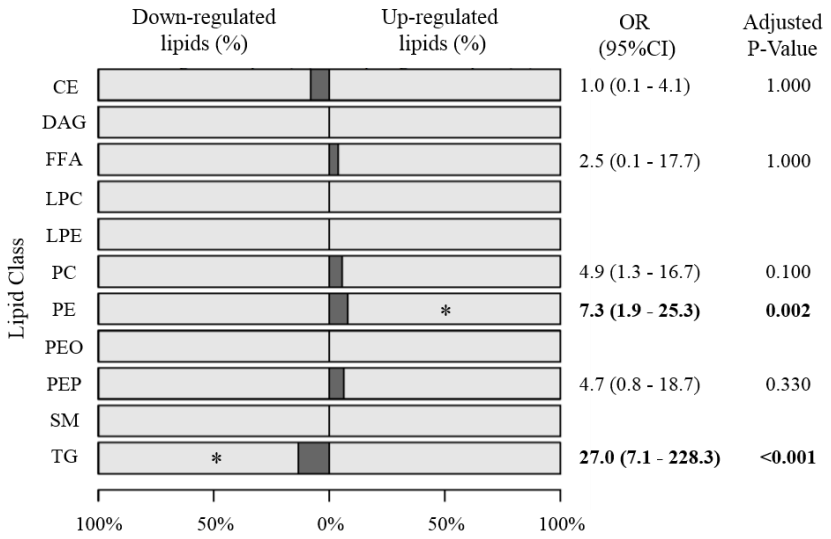

Online Figure 7. Lipid class enrichment analysis from the lipidomic study. Bars (dark grey) represent lipid classes with differentially regulated lipid species with respect to increased platelet phosphoACC. * denotes classes with significantly up- or down-regulated lipid species. OR and adjusted P-value derived from Fisher's exact test are represented. CE: cholesterol ester, CI: confidence interval, DAG: diacylglycerol, FFA: free fatty acid, LPC: lysophosphatidylcholine, LPE: lysophosphatidylethanolamine, OR: odds ratio, PC: phosphatidylcholine, PE: phosphatidylethanolamine, PEO: plasmenyl phosphatidylethanolamine, PEP: plasmalogen phosphatidylethanolamine, SM: sphingomyelin, TG: triglycerides

Online Table 1. Baseline characteristics of the lipidomics cohort				
	All N = 31	Low phosphoACC N = 12	High phosphoACC N = 19	P
Clinical Characteristics				
Age, years	61.4 ± 10.6	56.2 ± 10.4	64.7 ± 9.5	0.025*
Male sex, n (%)	19 (61.3)	6 (50)	13 (68.4)	0.31
BMI, kg/m²	28.4 ± 4.2	27.3 ± 4.7	29.1 ± 3.9	0.25
Hypertension, n (%)	15 (48.4)	5 (41.7)	9 (52.6)	0.55
Smoking, n (%)	18 (58.1)	8 (66.7)	10 (52.6)	0.44
Diabetes, n (%)	6 (19.4)	1 (8.3)	5 (26.3)	0.22
Prior history of CAD, n (%)	10 (32.3)	0 (0)	10 (52.6)	0.002
- MI, n (%)	7 (22.6)	0 (0)	7 (36.8)	0.017
- PCI, n (%)	10 (32.3)	0 (0)	10 (32.3)	0.002
- CABG, n (%)	1 (3.2)	0 (0)	1 (5.3)	0.42
Aortic valve disease, n (%)	3 (9.7)	2 (16.7)	1 (5.3)	0.30
Mitral valve disease, n (%)	2 (6.5)	2 (16.7)	0 (0)	0.07
ACS, n (%)	12 (38.7)	0 (0)	12 (63.2)	<0.001
Lab results				
Creatinine, (mg/dL)	1.0 (0.8-1.2)	0.9 (0.8-1.3)	1.0 (0.9-1.2)	0.68
CRI, n (%)	2 (6.5)	2 (16.7)	0 (0)	0.07
Total cholesterol, (mg/dL)	167 ± 47	175 ± 66	163 ± 34	0.51
LDL, (mg/dL)	95 ± 40	102 ± 49	91 ± 34	0.46
Triglycerides, (mg/dL)	125 ± 54	98 ± 44	141 ± 53	0.034*
Medication				
ACEi/ARB, n (%)	13 (41.9)	4 (33.3)	9 (47.4)	0.44
Beta-blockers, n (%)	14 (45.2)	5 (41.7)	9 (47.4)	0.76
Lipid-lowering treatment, n (%)	18 (58.1)	4 (33.3)	14 (73.7)	0.027
Aspirin, n (%)	23 (74.2)	6 (50)	17 (89.5)	0.014
Dual antiplatelet therapy, n (%)	6 (19.4)	0 (0)	6 (31.6)	0.030
- Clopidogrel, n (%)	2 (6.5)	0 (0)	2 (10.5)	0.24
- Ticagrelor, n (%)	3 (9.7)	0 (0)	3 (15.8)	0.15
- Prasugrel, n (%)	1 (3.2)	0 (0)	1 (5.3)	0.42
Platelet phosphoACC	0.8 (0.1-1.0)	0.10 (0.08-0.13)	0.96 (0.85-1.03)	<0.001

Online Table 1. Values are mean ± SD, n (%) or median (IQR). ACEi/ARB: angiotensin converting enzyme inhibitor/angiotensin receptor blocker, ACS: acute coronary syndrome, BMI: body mass index, CABG: coronary artery bypass graft, CAD: coronary artery disease, CRI: chronic renal insufficiency, hsCRP: high sensitivity C reactive protein, LDL: low-density lipoprotein, MI: myocardial infarction, PCI: percutaneous coronary intervention, P: P value. Statistical differences between groups are denoted as * between low- and high-phosphoACC.

Online Table 2. List of the significantly down-regulated TG lipid species in platelets with increased phosphoACC.

Lipid Species	N data	Log FC	P	Adj P
TAG40.0.FA16.0	23	-1.383	0.002	0.038
TAG42.0.FA14.0	30	-1.657	0.001	0.027
TAG42.0.FA16.0	31	-1.824	0.000	0.025
TAG42.1.FA14.0	20	-1.351	0.000	0.025
TAG42.1.FA16.0	26	-1.262	0.003	0.042
TAG42.1.FA18.1	28	-1.493	0.001	0.025
TAG44.0.FA14.0	31	-1.588	0.001	0.025
TAG44.0.FA16.0	31	-1.438	0.002	0.038
TAG44.0.FA18.0	30	-1.301	0.001	0.031
TAG44.1.FA12.0	31	-1.416	0.004	0.043
TAG44.1.FA14.0	31	-1.635	0.000	0.025
TAG44.1.FA14.1	18	-1.041	0.004	0.047
TAG44.1.FA16.0	31	-1.319	0.001	0.025
TAG44.1.FA16.1	31	-1.289	0.002	0.038
TAG44.1.FA18.1	31	-1.480	0.000	0.025
TAG44.2.FA12.0	20	-1.162	0.002	0.038
TAG44.2.FA16.0	31	-1.380	0.000	0.025
TAG44.2.FA16.1	21	-0.866	0.003	0.041
TAG44.2.FA18.1	29	-1.417	0.001	0.025
TAG44.2.FA18.2	31	-1.514	0.001	0.025
TAG44.3.FA18.2	14	-0.915	0.001	0.025
TAG45.0.FA14.0	29	-1.320	0.001	0.025
TAG45.0.FA15.0	27	-1.311	0.000	0.025
TAG45.0.FA16.0	31	-1.472	0.000	0.025
TAG45.1.FA15.0	18	-1.139	0.000	0.025
TAG45.1.FA16.0	24	-0.945	0.001	0.027
TAG45.1.FA18.1	23	-0.983	0.001	0.028
TAG46.0.FA14.0	31	-1.171	0.002	0.040
TAG46.0.FA16.0	31	-1.140	0.004	0.043
TAG46.0.FA18.0	31	-1.232	0.003	0.040
TAG46.1.FA14.1	31	-1.167	0.003	0.042
TAG46.1.FA18.0	30	-1.301	0.001	0.025
TAG46.1.FA18.1	31	-1.180	0.003	0.042
TAG46.2.FA14.0	31	-1.273	0.001	0.025
TAG46.2.FA18.1	31	-1.209	0.001	0.027
TAG46.2.FA18.2	31	-1.188	0.005	0.050
TAG46.3.FA14.0	20	-1.148	0.002	0.038
TAG46.3.FA14.1	16	-0.802	0.004	0.047
TAG46.3.FA16.0	26	-0.900	0.004	0.047
TAG46.3.FA16.1	26	-0.844	0.003	0.041
TAG46.3.FA18.1	30	-1.222	0.001	0.028
TAG46.3.FA18.2	30	-1.196	0.001	0.027
TAG46.4.FA18.2	16	-1.056	0.000	0.025
TAG47.0.FA14.0	29	-0.968	0.004	0.047
TAG47.0.FA15.0	31	-1.103	0.002	0.038
TAG47.0.FA16.0	31	-1.166	0.002	0.038
TAG47.0.FA17.0	31	-0.787	0.001	0.031
TAG47.1.FA14.0	31	-1.106	0.004	0.043
TAG47.1.FA15.0	31	-1.116	0.002	0.040
TAG47.1.FA16.0	31	-1.094	0.003	0.040
TAG47.1.FA16.1	31	-0.839	0.002	0.038
TAG47.1.FA17.0	24	-0.910	0.002	0.038
TAG47.1.FA18.1	31	-1.257	0.001	0.025
TAG47.2.FA14.0	26	-1.026	0.001	0.025
TAG47.2.FA15.0	29	-1.091	0.000	0.025
TAG47.2.FA16.1	30	-1.222	0.000	0.025
TAG47.2.FA18.1	30	-0.954	0.001	0.027
TAG47.2.FA18.2	29	-1.042	0.001	0.025
TAG48.0.FA18.0	31	-0.932	0.005	0.050
TAG48.2.FA18.2	31	-0.962	0.003	0.040
TAG48.3.FA16.0	31	-0.976	0.005	0.048
TAG49.0.FA15.0	31	-0.836	0.004	0.047
TAG49.2.FA18.2	31	-0.977	0.003	0.041
TAG49.3.FA18.3	25	-0.871	0.002	0.040
TAG50.2.FA18.0	31	-0.722	0.003	0.042
TAG50.4.FA14.1	31	-0.737	0.003	0.040

Online Table 2. Analysis was performed by a multivariate logistic regression model. Statistical significance was determined using the Benjamini-Hochberg correction procedure with a false discovery rate < 0.05. TG lipid species are arranged from top to bottom in order of increasing number of carbons in the TG structure. Only TG with significantly adjusted P values (<0.05) are shown (n=66). Adj P: adjusted P value, FC: fold-change, n: number of data analyzed, P: P value

.

GENERAL DISCUSSION AND PERSPECTIVES

1. ACETYL-COA CARBOXYLASE, A NEW REGULATOR OF PLATELET FUNCTION

Lipids are essential for platelet structure, signalling and energy storage and their contribution to platelet physiological functions has been well highlighted in different models displaying impaired lipid generation. For example, inhibition of platelet *de novo* lipogenesis by cerulenin, a pharmacological inhibitor of the FAS, decreases platelet granule secretion, aggregation and their accumulation into thrombi [130, 131, 279]. Similarly, genetic invalidation of PLA_2, responsible for phospholipid cleavage, decreases platelet aggregation, granules secretion and alters haemostasis [139, 140]. Given the increasing interest on the role of lipid species in platelet function, it is crucial to better characterize the molecular pathways involved in their synthesis. In this regard, we analyzed the role of ACC, the enzyme catalyzing the rate-limiting step of *de novo* lipogenesis, on lipid content and platelet functions. We demonstrate that basal ACC activity influences the pool, and therefore availability, of AA-containing membrane phospholipids and by this way, modulates subsequent TXA_2 generation, platelet secretion upon collagen stimulation and thrombus formation. This result importantly highlights the notion that any factors modulating ACC basal activity is susceptible to influence platelet regulation and affect haemostasis and/or thrombosis.

1.1 Genetic variants in acetyl-CoA carboxylase genes

Various single nucleotide polymorphisms (SNPs) have been identified in human ACC1 and ACC2 genes and are clearly associated to pathologies such as type 2 diabetes-associated nephropathy [280] and cancers [281, 282]. Among these SNPs, it has been shown that SNP rs11871275 is associated with increased ACC protein levels [281] and more interestingly, that SNP rs2268388 is not only linked to increased ACC mRNA and protein expression levels but also to higher hepatic TG content [280]. Similarly to humans, pork and cattle also display SNPs in ACC genes, which have been shown to alter either muscle or milk fatty acid composition [283, 284]. All together these studies highlight that genetic variations in ACC genes exist and that they affect cell metabolism and lipid content. The impact on platelets has never been investigated in this context. Our work allows us to postulate that the presence of SNPs in the ACC genes might modify platelet lipid content and reactivity in health and/or disease.

1.2 Acetyl-CoA carboxylase in atherosclerosis

Given that ACC phosphorylation/inhibition increases in thrombin-stimulated platelets *in vitro* [29], we hypothesized that this correlation could also apply to a clinical situation associated with thrombin generation such as atherosclerosis. We showed that ACC phosphorylation does not only increase in CAD patients along with the severity of the disease, but that it also regulates the content of platelet TG species. Supporting our own data, similar results have been obtained in other tissues. Liver TG content is

reduced in response to pharmacological ACC inhibitors [285, 286] or in mice carrying a specific deletion in liver ACC1 [235].

A modification of platelet TG content might impact platelet reactivity in CAD patients. Indeed, it has been shown that TG can modulate platelet function, even though their role as anti- or pro-stimulatory molecule is controversial. Stoetzer et al. indicate that platelets incubated *in vitro* with medium- and long-chains TG display enhanced P-selectin expression, both under basal and stimulated conditions [287]. Confirming these data, increase in circulating TG, induced either by a specific meal in human volunteers [288] or by a hypercholesterolemic diet in rats [289], stimulates P-selectin expression [288, 289], as well as platelet aggregation and TXA_2 secretion [289]. In contrast, platelets from patients with familial hypertriglyceridemia show decreased aggregation and TXA_2 generation in response to collagen [290]. In addition, infusion in humans of lipid mixtures containing different concentrations of TG, reduces *in vitro* platelet aggregation [291]. Therefore, further investigations are needed in order to define the precise impact of ACC-dependent increase in platelet TG on platelet functions and thrombus formation in an atherosclerotic context. In this regard, a perspective of this work is to generate chimeric mice by transferring ACC WT or ACC DKI bone marrow to irradiated ApoE KO recipient mice. Mice survival as well as thrombus growth and stability will be evaluated. Interestingly, ApoE KO mice have been shown to display increase in circulating oxLDL [292] and TG [293], as observed in CAD patients, and would therefore be a good model for studying the role of platelet ACC phosphorylation in atherosclerosis.

2. ACETYL-COA CARBOXYLASE: A NEW ANTIPLATELET TARGET?

Since we showed that sustained basal ACC activity in platelets promotes thrombus formation, inhibiting ACC could represent a potential new therapeutic target for treating excessive platelet activation. This perspective is particularly attractive as ACC is involved in many pro-thrombotic diseases such as diabetes, metabolic syndrome and cancer [294], in which platelets are not only over-activated but also critically participate in the progression of the disease. The idea of inhibiting ACC is therefore appealing as it would not only target cancer cells or tumors metabolism but it would also act on platelet reactivity and potentially reduce their deleterious effects.

ACC inhibitors have already been tested in preliminary studies in animal models and have demonstrated a protective role in the progression of diabetes [295] and metabolic syndrome [296] by reducing ectopic lipid deposition and improving insulin sensitivity. Similar effects have been observed on cancer regression. In this context, ACC inhibition decreases lipid synthesis, which is essential for tumor growth and viability [271, 297]. However, none of these works have analyzed platelet reactivity, which might be decreased given the role of ACC on platelet function. It would therefore be tempting to speculate that modifications of platelet lipid content and functions contribute to the beneficial effects of ACC inhibitors on diseases regression. Due to the positive impact of ACC inhibition in preclinical animal models, increasing attempts are being made to design safe, well-tolerated and specific ACC inhibitors [298, 299]. However, the identification of compounds fulfilling these criteria and that can be tested in human trials

remains a challenge. One compound has been shown to reduce *de novo* lipogenesis and stimulate fatty acid oxidation after a single oral dose in Phase I clinical trial [298]. However, the trial was not pursued probably due to poor pharmaceutical properties of the molecule [286]. Pfizer tested the compound PF-05175157 both in Phase I and Phase II studies, involving type 2 diabetes patients [300]. However, the trial was discontinued because of an unspecified adverse event [300]. More promising, NDI-010976, a recently developed allosteric inhibitor of both ACC1 and ACC2, was shown to be well tolerated and to successfully inhibit hepatic *de novo* lipogenesis in Phase I study [301]. It is now under investigation in Phase II for the treatment of NAFLD and non-alcoholic steatohepatitis. Nevertheless, several potential hurdles in the development of ACC inhibitors for human therapy need to be highlighted [294]. First of all, it has been demonstrated that hypothalamic malonyl-CoA negatively regulates food intake [302], indicating that the decrease in malonyl-CoA in response to ACC inhibition may increase food consumption. Secondly, inhibiting ACC might influence glucose-induced insulin secretion by the pancreas [303]. Finally, increasing fatty acid oxidation in the heart could lead to contractile dysfunction and ischemic injury [304]. As a consequence, the prospect of success of ACC inhibition in the clinic remains uncertain.

3. ACETYL-COA CARBOXYLASE, A ROLE BEYOND LIPID METABOLISM?

Similarly to phosphorylation on serine/threonine and tyrosine residues, proteins can be reversibly acetylated on their lysine. Protein acetylation is a

dynamic process, regulated by the balance between lysine acetyltransferases (KATs), which catalyze the binding of acetyl groups, using acetyl-CoA as donor, and by lysine deacetylases (KDACs) [305], which remove the acetyl group. KATs can be classified into three main groups: GNAT, p300/CBP and MYST [305], whereas KDACs belong to two distinct families, having different catalytic mechanisms: Zn^{2+}-dependent histone deacetylases (HDACs) and NAD^{+}-dependent sirtuin deacetylases (SIRTs) [305]. Both KDACs are mainly expressed in the nucleus and the cytoplasm. It has been shown that platelets express the KAT p300, which is activated upon stimulation with collagen [306], and the KDACs HDAC6 and SIRT2 [307], resulting in over 200 proteins being acetylated on more than 500 lysine residues [306]. Even though acetylated proteins are involved in diverse functions such as cytoskeleton reorganization and signal transduction, a large proportion of them (45 %) are metabolic enzymes with roles in glycolysis, TCA cycle and oxidative phosphorylation [306]. Given the number of acetylated platelet proteins, it is not surprising that altering acetylation levels affects many platelet functions, including *in vitro* and *ex vivo* (under flow) aggregation, spreading, granules secretion, and cytosolic Ca^{+2} levels [306, 308].

Protein acetylation depends on the intermediary metabolite acetyl-CoA which is also used by ACC for *de novo* lipogenesis. As a consequence, the two processes compete for the same pool of acetyl-CoA. The link between carbon metabolism and protein acetylation has been highlighted in several papers showing that global protein acetylation is largely influenced by ACC activity. Genetic inhibition of hepatic ACC promotes global liver protein

acetylation [309] and ACC inhibition, either by the pharmacological inhibitor TOFA [310, 311] or by protein knock down [311], increases the acetylation levels of proteins in cancer cells.

Given the associations between protein acetylation and platelet functions on the one hand and protein acetylation and ACC activity on the other hand, it would be worth analyzing the impact of altered ACC phosphorylation on platelet protein acetylation. If similarly to other cell types, ACC controls platelet protein acetylation, we could speculate that, besides modifying lipid content, alteration of ACC phosphorylation would impact protein acetylation and thereby constitute an additional mechanism by which ACC regulates platelet functions.

ANNEXES

blood®
Regular Article

PLATELETS AND THROMBOPOIESIS

AMPK-ACC signaling modulates platelet phospholipids content and potentiates platelet function and thrombus formation

Sophie Lepropre,[1,*] Shakeel Kautbally,[1,*] Marie Octave,[1] Audrey Ginion,[1] Marie-Blanche Onselaer,[1,2] Gregory R. Steinberg,[3] Bruce E. Kemp,[4,5] Alexandre Hego,[6] Odile Wéra,[6] Sanne Brouns,[7] Frauke Swieringa,[7] Martin Giera,[8] Victor M. Darley-Usmar,[9] Jérôme Ambroise,[10] Bruno Guigas,[11,12] Johan Heemskerk,[7] Luc Bertrand,[1] Cécile Oury,[6] Christophe Beauloye,[1,13,#] and Sandrine Horman[1,#]

[1]Pôle de Recherche Cardiovasculaire, Institut de Recherche Expérimentale et Clinique, Université catholique de Louvain, Brussels, Belgium; [2]Institute of Cardiovascular Sciences, College of Medical and Dental Sciences, University of Birmingham, Birmingham, United Kingdom; [3]Division of Endocrinology and Metabolism, Departments of Medicine and Biochemistry and Biomedical Sciences, McMaster University, Hamilton, Ontario, Canada; [4]St. Vincent's Institute of Medical Research and Department of Medicine, University of Melbourne, Fitzroy, VIC, Australia; [5]Mary MacKillop Institute for Health Research, Australian Catholic University, Fitzroy, VIC, Australia; [6]Laboratory of Thrombosis and Hemostasis and Valvular Heart Disease, GIGA-Cardiovascular Sciences, Department of Cardiology, Université de Liège, CHU Sart-Tilman, Liège, Belgium; [7]Department of Biochemistry, Cardiovascular Research Institute Maastricht, University of Maastricht, Maastricht, the Netherlands; [8]Center for Proteomics and Metabolomics, Leiden University Medical Center, Leiden, the Netherlands; [9]Department of Pathology, UAB Mitochondrial Medicine Laboratory, Center for Free Radical Biology, University of Alabama at Birmingham, Birmingham, AL; [10]Centre de Technologies Moléculaires Appliquées, Institut de Recherche Expérimentale et Clinique, Université catholique de Louvain, Brussels, Belgium; [11]Department of Parasitology, Leiden University Medical Center, Leiden, the Netherlands; [12]Department of Cell and Chemical Biology, Leiden University Medical Center, Leiden, the Netherlands; and [13]Division of Cardiology, Cliniques Universitaires Saint-Luc, Université catholique de Louvain, Brussels, Belgium

KEY POINTS

- **AMPK-ACC signaling in platelets is a key mechanism regulating primary hemostasis and arterial thrombosis.**
- **AMPK-ACC signaling controls collagen-induced TXA_2 generation and dense granule release by modulating platelet phospholipid content.**

AMP-activated protein kinase (AMPK) α1 is activated in platelets on thrombin or collagen stimulation, and as a consequence, phosphorylates and inhibits acetyl-CoA carboxylase (ACC). Because ACC is crucial for the synthesis of fatty acids, which are essential for platelet activation, we hypothesized that this enzyme plays a central regulatory role in platelet function. To investigate this, we used a double knock-in (DKI) mouse model in which the AMPK phosphorylation sites Ser79 on ACC1 and Ser212 on ACC2 were mutated to prevent AMPK signaling to ACC. Suppression of ACC phosphorylation promoted injury-induced arterial thrombosis in vivo and enhanced thrombus growth ex vivo on collagen-coated surfaces under flow. After collagen stimulation, loss of AMPK-ACC signaling was associated with amplified thromboxane generation and dense granule secretion. ACC DKI platelets had increased arachidonic acid-containing phosphatidylethanolamine plasmalogen lipids. In conclusion, AMPK-ACC signaling is coupled to the control of thrombosis by specifically modulating thromboxane and granule release in response to collagen. It appears to achieve this by increasing platelet phospholipid content required for the generation of arachidonic acid, a key mediator of platelet activation. (*Blood*. 2018;00(00):1-13)

Introduction

A growing body of evidence shows that lipids are essential in regulating platelet functions. Indeed, the platelet exhibits a complex array of more than 5000 distinct lipid species, with more than 700 responding to thrombin activation.[1] Given this increased focus on the role of lipid species in platelet function, it is imperative to understand the molecular basis of their regulation during platelet activation. Acetyl-CoA carboxylase (ACC) is a good candidate because of its established role as a central regulator of fatty acid metabolism.[2] ACC catalyzes acetyl-CoA carboxylation to form malonyl-CoA. Its 2 isoforms, ACC1 and ACC2, have distinct cellular distributions.[3] ACC1 is present in the cytosol and synthesizes malonyl-CoA for de novo lipogenesis,[4] whereas ACC2 is localized on the outer mitochondrial membrane and generates malonyl-CoA, which inhibits fatty acid transport into mitochondria for oxidation.[5,6] ACC is a bona fide substrate of AMP-activated protein kinase (AMPK), and its phosphorylation is typically used as a marker of AMPK activation in cells and tissues, including platelets.[7-9] AMPK phosphorylates ACC1/2 on serine residues (Ser79/212), leading to suppression of ACC activity.[10,11] We have previously reported that AMPKα1 is activated in platelets upon thrombin stimulation, and increases the phosphorylation of myosin regulatory light chains, cofilin, and vasodilator-stimulated phosphoprotein.[7] These cytoskeletal proteins are critical for triggering platelet shape change and the centralization of secretory granules during platelet activation.[12] However, the effect of AMPK-mediated ACC phosphorylation on platelet function has never been investigated.

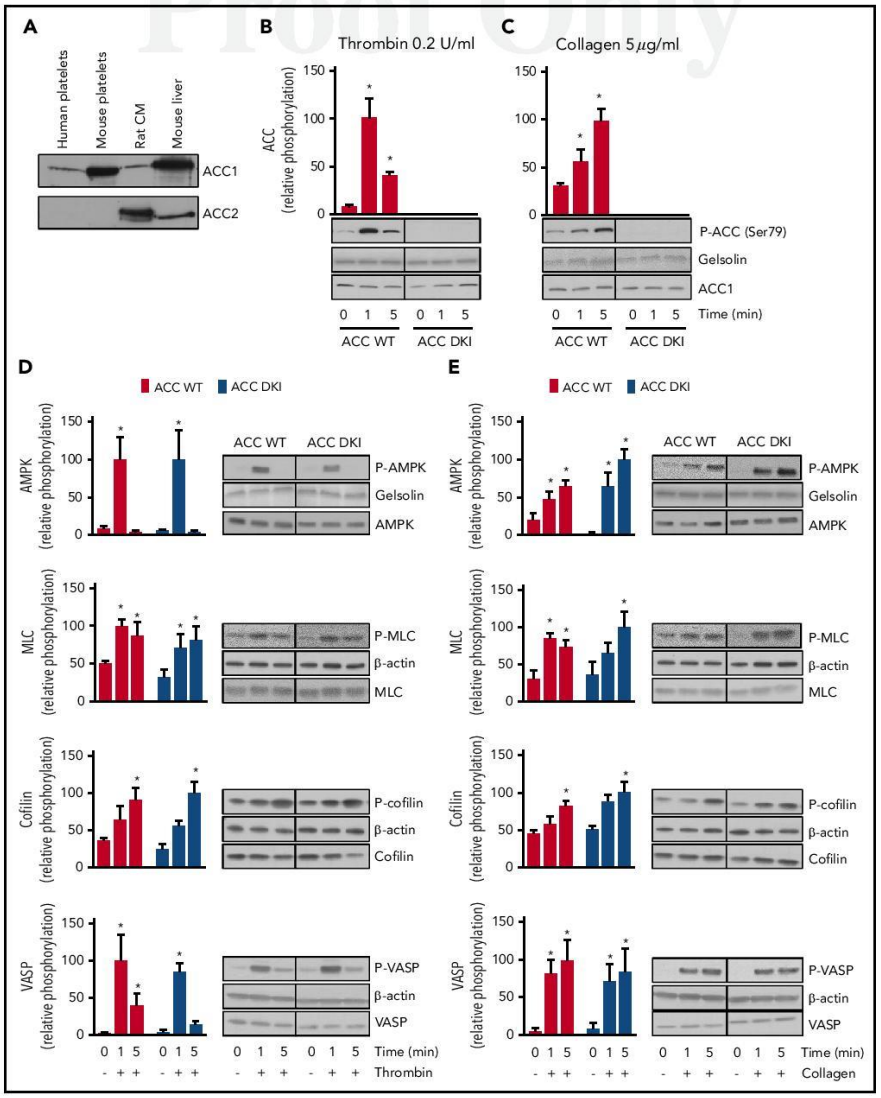

Figure 1. Lack of AMPK-ACC phosphorylation does not affect AMPK signaling or phosphorylation of cytoskeletal proteins. (A) Washed murine and human platelets were lysed and subjected to western blotting for ACC1 or ACC2 isoform expression analysis. Isolated rat cardiomyocytes (CM) and mouse liver extracts served as positive controls for the detection of ACC2 and ACC1, respectively. (B-E) ACC WT and ACC DKI platelets were stimulated with 0.2 U/mL thrombin (B,D) or 5 μg/mL collagen (C,E) for the indicated times. Whole-platelet lysates were subjected to western blotting and probed with Ser79 phosphorylated ACC Ab (B,C), Thr172 phosphorylated AMPK, Ser19 phosphorylated myosin light chain (MLC), Ser3 phosphorylated cofilin and Thr278 phosphorylated vasodilator-stimulated phosphoprotein (VASP) Abs (D,E). Gelsolin and β-actin were used as loading controls. Quantification and representative western blotting are systematically shown. The solid lines on the western blots indicate that samples were run on the same gel

Fatty acids fulfill at least 3 main roles: structural, signaling, and energy storage. Phospholipids (PL) are the major structural lipids in platelets. Upon platelet activation, reorganization of the plasma membrane PL facilitates shape change and filopodia and lamellipodia formation,[13] as well as granule secretion[14] or microvesicle formation. In addition to this structural role, PL provide substrates for phospholipases A (PLA) or C (PLC) to generate bioactive species, including phosphatidylinositides, 1,2-diacylglycerol (DAG), inositol 1,4,5-trisphosphate, and eicosanoids/prostaglandins.[1] These secondary mediators are crucial for the tight regulation of platelet activation.[15-17]

Finally, lipids contribute to platelet energy metabolism. In the basal state, platelets are more oxidative than glycolytic,[18,19] and lipid oxidation contributes to at least one-third of the total oxygen consumed by mitochondria.[18,20,21] Mitochondrial lipid oxidation increases on thrombin stimulation to cope with the energetic demands of platelet activation,[20,22] a process that is supported by the enhanced availability of eicosanoids released from the membrane PL through the action of Ca^{2+}-dependent cytosolic phospholipase A_2 ($cPLA_2$).[1]

Clearly, the signaling needed to coordinate these diverse functions of PL metabolism is important to define. In the current study, we hypothesized that ACC controls key aspects of platelet function using mice with alanine knock-in mutations in both ACC1 (at Ser79) and ACC2 (at Ser212; ACC double knock-in [ACC DKI] mice). These mice harbor functional ACC and AMPK, but express a mutant form of ACC that can no longer be inhibited by AMPK phosphorylation, resulting in a persistent active form of the enzyme.[2]

Here, we report that blood from ACC DKI mice have increased thrombus formation on collagen-coated surfaces or after vascular injury. The underlying mechanisms involve elevated levels of arachidonic acid (AA)-containing phosphatidylethanolamine plasmalogen (PEP) lipids in ACC DKI platelets compared with wild-type (WT), increasing thromboxane A_2 (TXA_2) generation and granule secretion after platelet stimulation with collagen. Although mitochondrial fatty acid oxidation is important in thrombin-dependent platelet activation, we found that AMPK-ACC signaling had no effect on platelet bioenergetics.

These findings highlight a novel metabolic regulatory pathway in platelets that influences thrombus formation by modulating the content of specific PL, which generates key mediators of platelet activation.

Methods

Mice

ACC1/2 DKI mice have been described previously.[2] WT mice served as controls. Eight- to 16-week-old male mice were studied. Animal procedures and protocols were approved by local authorities (Comité d'éthique facultaire pour l'expérimentation animale, 2012/UCL/MD/003 and 2016/UCL/MD/027) and performed in accordance with the Guide for the Care and Use of Laboratory Animals, published by the National Institutes of Health (NIH Publication No. 85-23, revised 1996).

Platelet preparation

Murine platelet Mice were bled under ketamine and xylazine anesthesia from the retro-orbital plexus. Blood was collected in 1/6 citrate-dextrose solution with apyrase 1 U/mL. PRP was obtained by centrifugation at 800*g* for 5 seconds, followed by 5 minutes at 100*g*. It was washed by adding 2 volumes of citrate-dextrose with apyrase 1 U/mL. The platelets were pelleted by centrifugation at 400*g* for 5 minutes and resuspended to a density of $2.5 \times 10^5/\mu L$ (unless stated otherwise) in modified Tyrode's buffer. Platelets were counted with Cell-Dyn Emerald. They were stimulated with agonists in the presence of 2 mM $CaCl_2$.

Flow chamber assay

Blood was collected from the retro-orbital plexus into 48 μM D-Phenylalanyl-prolyl-arginyl Chloromethyl Ketone, 5 U/mL heparin, and 40 U/mL fragmin. Samples of 400 μL were flowed over type I collagen-coated (100 μg/mL), vWF-binding protein (12.5 μg/mL) and laminin (50 μg/mL)-coated or vWF-binding protein (12.5 μg/mL), laminin (50 μg/mL), and rhodocytin (250 μg/mL)-coated coverslips mounted on a transparent, parallel plate flow chamber (50 μm depth, 3 mm width, and 20 mm length), at a shear rate of 1000 s^{-1} for 3.5 minutes, as described.[23] Alternatively, samples were preincubated with 20 μM ticagrelor for 10 minutes or the corresponding vehicle (dimethyl sulfoxide) and flowed over type I collagen-coated coverslips, as described earlier. Activated platelets in thrombi were poststained with fluorescein isothiocyanate-labeled anti-P-selectin antibody (Ab; 1:40), PE-labeled JON/A Ab against the active conformation of αIIbβ3 (1:20), or Alexa Fluor 647-annexin A5 (1:200), all diluted in Tyrode's buffer. Labeling was undertaken for 2 minutes (stasis), after which unbound Abs were removed by perfusion with Tyrode's buffer. Brightfield phase-contrast and fluorescence images were recorded by a non-confocal 2-camera system. Surface coverage was analyzed by ImagePro software (Media Cybernetics).[24]

Ferric chloride-induced thrombosis

Carotid arteries were injured in anesthetized mice by topical application of 10% ferric chloride ($FeCl_3$) for 5 minutes, as described previously.[25] Briefly, exogenous carboxyfluorescein succinimidyl ester-labeled platelets were injected into the jugular vein of anesthetized mice, and fluorescence was recorded by BX61WI microscope (Olympus). Digital images were captured every 2 minutes for a total of 24 minutes.

Untargeted lipidomics

Lipidomics analysis was carried out on the commercial Lipidyzer platform, according to the manufacturer's instructions (Sciex).[26] The amount of platelets needed to obtain consistent results was evaluated before application of the commercial platform. Lipid analysis was performed in flow-injection mode, separating lipid classes by differential mobility spectroscopy,[26] followed by tandem mass spectrometry of lipid species with QTrap 5500 in multiple reaction monitoring mode. Lipid species were identified

Figure 1 (continued) but were not contiguous. The results are expressed as means ± standard error of the mean (SEM; at least 3 experiments for each condition). *Values statistically different from respective untreated platelets; $P \leq .05$. Analysis was performed by 2-way analysis of variance (ANOVA). See also supplemental Figure 1 and supplemental Table 1.

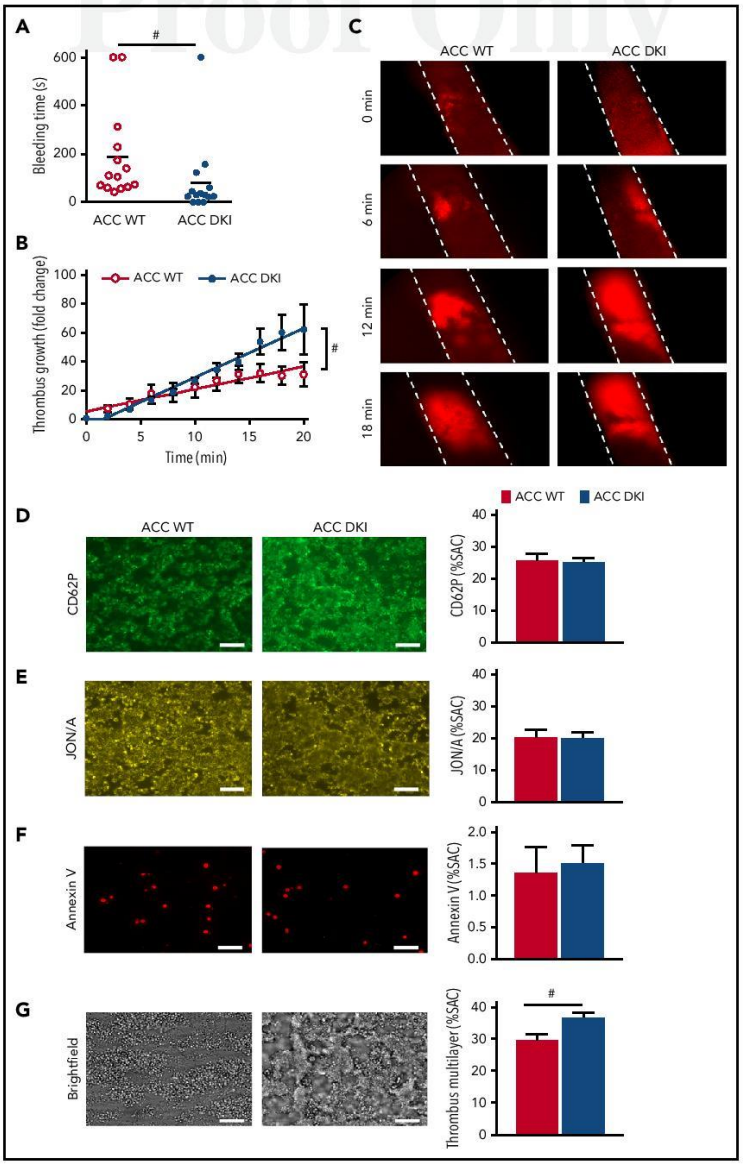

and quantified on the basis of characteristic mass spectrometric transitions. Commercial Lipidyzer software automatically calculated lipid species concentrations. All samples were analyzed in a randomized fashion. Control plasma samples, as well as fortified plasma samples, were assessed daily as quality controls. Relative standard deviations of quality control samples were below 15% for all lipid classes, except for sphingomyelin, for which a relative standard deviation of 25% was noted.

A detailed description of the reagents and the methods is provided in supplemental Methods, available on the *Blood* website.

Results

Lack of AMPK-ACC phosphorylation does not affect AMPK signaling or cytoskeletal protein phosphorylation

ACC WT and ACC DKI mice have comparable erythrocyte, leukocyte, and platelet counts in whole blood (supplemental Table 1). Expression levels of the major platelet surface receptors, αIIbβ3, GPIbα, the collagen receptor GPVI, and the protease-activated receptor-3 and protease-activated receptor-4, were equivalent in ACC WT and ACC DKI platelets (supplemental Figure 1A-B).

ACC1, but not ACC2, was detected in both human and murine platelets (Figure 1A). Consistent with previous observations,[7] 0.2 U/mL thrombin (Figure 1B) or 5 μg/mL collagen (Figure 1C) induced phosphorylation on Ser79 of ACC in platelets from WT mice with maximal effects after 1 and 5 minutes, respectively. As expected, no Ser79 ACC phosphorylation was detected in either basal or thrombin- or collagen-treated ACC DKI platelets (Figure 1B-C). ACC1 mutation did not influence AMPK activation, reflected by Thr172 phosphorylation (Figure 1D-E). In addition, thrombin- or collagen-induced phosphorylation of known AMPK cytoskeletal targets, myosin light chain, cofilin, and vasodilator-stimulated phosphoprotein were similar between ACC DKI and ACC WT platelets(Figure 1D-E), as well as platelet-spreading and lamellipodia/filopodia formation after platelet immobilization on fibrinogen-coated coverslips (supplemental Figure 1C-H). These data confirm that although ACC phosphorylation was impaired, AMPK signaling was unaltered in ACC DKI platelets.

ACC DKI mice display enhanced primary hemostasis and thrombosis

The effect of AMPK-mediated ACC phosphorylation on hemostasis and thrombosis was evaluated in vivo. No spontaneous bleeding or thrombotic event was observed in 91 ACC DKI young mice (up to 4 months) or 19 ACC DKI older mice (at least 9 months old). However, median tail bleeding time was significantly shorter in ACC DKI mice than in their WT counterparts (ACC DKI: 82 ± 42 seconds vs ACC WT: 188 ± 51 seconds; $P < .05$; Figure 2A). We then investigated the role of ACC phosphorylation on arterial thrombosis in vivo, in the collagen-dependent carotid artery thrombosis model, in response to a 10% $FeCl_3$ application. Arterial thrombus formation was monitored in real time by intravital fluorescence microscopy (Figure 2B-C). The rate of thrombus growth was significantly increased in ACC DKI mice compared with the WT animals. The fold change increase in thrombus growth during a 20-minute period after arterial injury was 62.4 ± 17.4 for ACC DKI mice vs 31.3 ± 8.2 for ACC WT mice relative to baseline (Figure 2B). These data demonstrate that AMPK-ACC signaling is a key mechanism regulating primary hemostasis and arterial thrombosis in vivo.

Lack of AMPK-ACC signaling favors thrombus formation during perfusion on collagen in flow conditions

We next examined thrombus formation ex vivo, using a flow chamber system. Whole blood from ACC WT and DKI mice was perfused at an intermediate shear rate of 1000 s^{-1}, on 3 different coated surfaces containing collagen, laminin, or vWF-binding peptide in the absence or presence of rhodocytin.[24] Brightfield images were captured to assess overall platelet adhesion and thrombus formation. Platelet activation was simultaneously monitored by infusing fluorescently labeled anti-CD62P Ab as a marker of α-granule secretion, JON/A Ab to measure αIIbβ3 activation, and annexin V to analyze phosphatidylserine externalization, reflecting platelet procoagulant activity.

On collagen-coated coverslips, the surface area covered by adherent platelets and their activation state (Figure 2D-F) were similar between the 2 genotypes. However, buildup of multilayered platelet thrombi was increased with ACC DKI blood compared with WT (Figure 2G), indicating that AMPK-ACC signaling affects mechanisms involved in the secondary formation of platelet aggregates on collagen. Of note, no differences in platelet adhesion and activation processes were observed between ACC DKI and WT blood perfused on laminin and vWF-BP in the absence or presence of rhodocytin (data not shown).

ACC DKI platelets display increased dense granule secretion and thromboxane generation on collagen stimulation

To further decipher the mechanisms responsible for the gain-of-function phenotype of ACC DKI mice on thrombus formation, we studied the effect of a lack of AMPK-mediated ACC phosphorylation on washed platelet reactivity. First, we investigated

Figure 2. ACC DKI mice display enhanced primary hemostasis and thrombosis. (A) Tail bleeding times of ACC WT and ACC DKI mice in saline at 37°C. Individual values are plotted on the graph (n = 14 in each group). Bars indicate means. *$P \leq .05$. Data were analyzed by the Mann-Whitney test. (B,C) ACC WT and ACC DKI mice were subjected to in vivo $FeCl_3$-induced thrombosis of carotid arteries (10% $FeCl_3$, 5 min). Thrombus formation was monitored by analyzing exogenous carboxyfluorescein succinimidyl ester-labeled platelet accumulation by intravital microscopy and recording videos (fluorescence) of microscopic images every 2 minutes. (B) Thrombus growth kinetics was evaluated by dividing the area of the thrombus at time (t) by the area of the same thrombus at time 0, defined as the time at which the thrombus first reaches 100 μm. Thrombus growth is expressed as means ± SEM per group at different times with fitted regression lines (at least 6 mice/group). Slopes are statistically different on the basis of significant interaction (*$P \leq .05$) between slope and group in a linear model, with group, time, and their interaction as covariates. (C) Representative fluorescence microscopy images at 0, 6, 12, and 18 minute after $FeCl_3$ application. (D-G) Whole blood from ACC WT and ACC DKI mice was perfused over collagen-coated surfaces (100 μg/mL) at a shear rate of 1000 s^{-1}. Exposure of P-selectin was evaluated by staining with CD62P Ab (D), αIIbβ3 integrin activation by JON/A Ab (E) and phosphatidylserine externalization by Annexin V (F). Thrombus formation was assessed on brightfield images taken 3.5 minutes after initial blood perfusion (G). Representative images appear on the left. Scale bars represent 20 μm. Histograms indicate quantification of surface area covered (SAC) by P-selectin (D), activated αIIbβ3 (E), Annexin V (F)-positive platelets or multilayered platelet thrombi (G). The results are expressed as means ± SEM (at least 4 mice/group). *$P \leq .05$. Data were analyzed by the Mann-Whitney test.

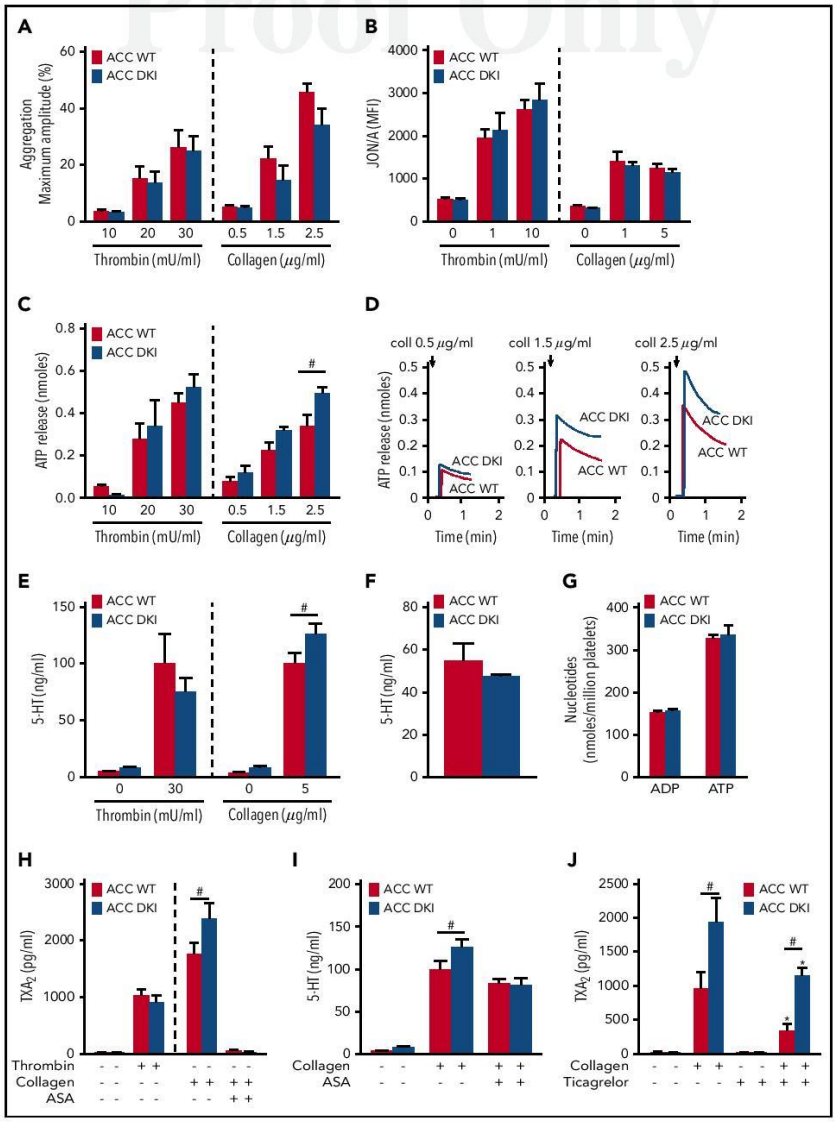

Figure 3. ACC DKI platelets display increased dense granule secretion and thromboxane generation on collagen stimulation. (A) Washed platelets were stimulated with thrombin or collagen at the indicated concentrations, and light transmission was measured (Chrono-Log). Aggregation is expressed as the maximal percentage of light transmitted. The dashed line represents separate analyses. The results are expressed as means ± SEM (at least 4 experiments for each condition). (B) αIIbβ3 activation (binding of JON/A) was analyzed by flow cytometry in washed ACC WT and DKI platelets stimulated with thrombin for 8 minutes or collagen for 30 minutes at the indicated concentrations. The dashed line represents separate analyses. The results are expressed as mean fluorescence intensity (MFI) ± SEM (at least 4 experiments for each condition). (C,D) Washed

the effect of thrombin or collagen on αIIbβ3 inside-out activation by analyzing platelet aggregation. ACC DKI platelets aggregated normally at low and high concentrations of thrombin or collagen (Figure 3A; supplemental Figure 2A). Accordingly, thrombin- or collagen-induced activation of αIIbβ3, detected by JON/A Ab, was normal (Figure 3B). Integrin αIIbβ3-mediated clot retraction consistently showed no differences between ACC WT and ACC DKI platelets after thrombin stimulation (supplemental Figure 2B-C).

In addition to αIIbβ3 activation, TXA_2 generation and ADP released from dense granules are important players in collagen-induced platelet aggregate formation under flow[27,28] and in thrombus formation in vivo.[29,30] Interestingly, the lack of AMPK-ACC signaling amplified dense granule release, specifically in response to collagen. Indeed, a significant 30% increase of ATP (Figure 3C-D) and serotonin secretion (Figure 3E) was detected after collagen stimulation in ACC DKI platelets compared with WT, but not in response to thrombin (Figure 3C,E). To further conclude that this increase was related to secretion rather than to augmented packaging of dense granules, we measured total ADP, ATP, and serotonin content in platelet extracts and found no difference between genotypes (Figure 3F-G). Regarding α-granule secretion, P-selectin surface exposure was similar between ACC WT and ACC DKI platelets (supplemental Figure 3A). However, platelet factor 4 (PF4) secretion was potentiated on collagen stimulation in ACC DKI platelets (supplemental Figure 3B), although total PF4 levels in α-granules showed no change (supplemental Figure 3C), indicating that the ACC DKI phenotype seems also associated with increased
Q:10 α-granule secretion, at least those containing PF4.

Lack of AMPK-ACC signaling potentiated TXA_2 generation in response to collagen (Figure 3H), independent of any change in basal cyclooxygenase 1 expression or activity (supplemental Figure 4A-B). To evaluate the connection between ACC DKI-related increased TXA_2 generation and dense granule secretion, collagen-stimulated ACC DKI platelets were pretreated with 1 mM aspirin before assessment of serotonin secretion. As expected, cyclooxygenase 1 inhibition by aspirin almost completely abolished collagen-induced TXA_2 generation (Figure 3H). In this condition, collagen failed to further enhance serotonin secretion in ACC DKI compared with WT platelets (Figure 3I), demonstrating that the increase in dense granule secretion observed in ACC DKI platelets depends on TXA_2 synthesis. The increased TXA_2 generation in ACC DKI platelets did not result from the enhanced dense granule release induced by collagen, as ticagrelor, a P2Y12 inhibitor, preserved TXA_2 potentiation in ACC DKI platelets (Figure 3J). More interestingly, whole-blood flow perfusion experiments over type I collagen showed that ticagrelor completely abolished the increased thrombus buildup in ACC DKI blood compared with WT, demonstrating the key implication of dense granule secretion in the enhanced thrombus formation (Figure 4A-B).

In addition to thrombin and collagen, ACC WT and ACC DKI platelets were also treated with increasing concentrations of ADP, U46619, rhodocytin, an agonist of the C-type lectin such as receptor-2, or collagen-related peptide, a specific GPVI agonist. For all agonists and concentrations tested, ACC DKI platelets aggregated normally (supplemental Figure 5A-B), and there was no difference in ATP released from dense granules (supplemental Figure 5C). These data reinforce the conclusion that the effect of AMPK-ACC signaling on TXA_2 generation and dense granule secretion is specific to platelet response to collagen. Moreover, these results reveal that collagen increases TXA_2 generation in ACC DKI platelets, most likely through a mechanism involving the α2β1 integrin, which is compatible with the enhancing role of this integrin in GPVI-dependent thrombus stability via TXA_2 production.[31]

Taken together, these results indicate that the absence of AMPK-ACC signaling in collagen-stimulated platelets elicits increased TXA_2 generation and, subsequently, enhanced granule secretion. These events might contribute to exacerbated thrombus growth via a mechanism that is independent of an altered αIIbβ3 activation.

Lack of AMPK-ACC signaling does not affect lipid oxidation, but results in an increased AA-containing PL pool

To test whether persistent activation of ACC in platelets may affect platelet bioenergetics, we measured the thrombin- or collagen-dependent increase in mitochondrial function in ACC WT and ACC DKI platelets. As illustrated in Figure 5A-F, extracellular flux analysis showed that platelet basal oxygen consumption rate (OCR) was similar between ACC WT and DKI mice, and similar to reported studies in the literature.[1,20] As expected, thrombin stimulated OCR (Figure 5A-B), which has been shown to be a result of increased mitochondrial lipid oxidation.[1,20] The oxidative phosphorylation component was further assessed by injecting oligomycin, a complex V inhibitor, which led to an expected decrease in OCR. ATP-linked respiration was not

Figure 3 (continued) ACC WT and DKI platelets were stimulated with thrombin or collagen at the indicated concentrations in the presence of Luciferase-Luciferin reagent, and ATP release was measured in a Lumi-aggregometer. (C) The dashed line represents separate analyses. The results are expressed as mean amount of ATP released (nmoles) ± SEM (at least 4 experiments for each condition). $^{\#}P \leq .05$ between ACC WT and DKI platelets. The data underwent 2-way ANOVA. (D) Representative traces of ATP secretion after 0.5 μg/mL, 1.5 μg/mL, and 2.5 μg/mL collagen stimulation. (E) Washed platelets ($30 \times 10^3/\mu L$) were stimulated with 30 mU/mL thrombin or 5 μg/mL collagen for 5 minutes, and serotonin (5-HT) was measured in the supernatant by ELISA kit. The dashed line represents separate analyses. The results are normalized to ACC WT-stimulated platelets and are expressed as means ± SEM (at least 3 experiments for each condition). $^{\#}P \leq .05$ between ACC WT and DKI platelets. The data underwent 2-way ANOVA. (F) Washed platelets ($7.5 \times 10^3/\mu L$) were centrifuged, the pellet was lysed, and serotonin (5-HT) was assayed in the lysate. The results are expressed as means ± SEM (n = 3). (G) Washed platelets were centrifuged, the pellet was lysed, and ADP and ATP content assayed in the lysate by reverse-phase high-performance liquid chromatography. Results are expressed as means ± SEM (n = 3). (H) Washed platelets were stimulated with 100 mU/mL thrombin alone or preincubated or not for 45 minutes with 1 mM aspirin (ASA), and stimulated with 5 μg/mL collagen. TXA_2 was measured in the supernatant by ELISA. The dashed line represents separate analyses. The results are expressed as means ± SEM (at least 3 experiments for each condition). $^{\#}P \leq .05$ between ACC WT and DKI platelets. The data underwent 2-way ANOVA. (I) Washed platelets were preincubated or not for 45 minutes with 1 mM ASA and stimulated with 5 μg/mL collagen. Serotonin (5-HT) was measured in the supernatant by ELISA. The results are expressed as means ± SEM (at least 3 experiments for each condition). $^{\#}P \leq .05$ between ACC WT and DKI platelets. The data were assessed by 2-way ANOVA. (J) Washed platelets were preincubated with 30 μM ticagrelor or the corresponding vehicle (dimethyl sulfoxide) for 30 minutes and stimulated with 5 μg/mL collagen for 5 minutes. TXA_2 was measured in the supernatant by ELISA. The results are expressed as means ± SEM (n = 4). $^{*}P \leq .05$ relative to respective untreated platelets, $^{\#}P \leq .05$ between ACC WT and ACC DKI platelets. The data underwent 2-way ANOVA. See also supplemental Figures 1-5.

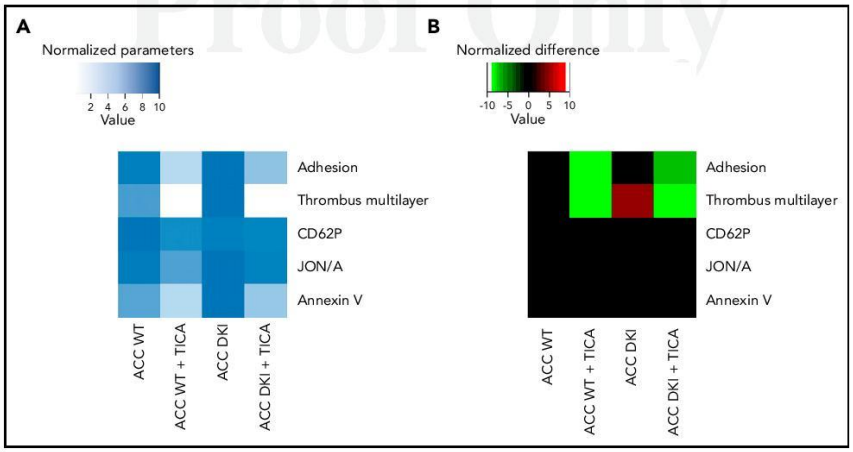

Figure 4. Increased thrombus formation in ACC DKI mice is prevented by P2Y12 inhibition. (A-B) Whole-blood flow perfusion experiments were performed with collagen type I as platelet-adhesive substrate. Where indicated, autocrine effects were blocked by preincubation with 20 μM ticagrelor (TICA) or vehicle (dimethyl sulfoxide) for 10 minutes. Microscopic images were analyzed for indicated parameters, and per parameter normalized on scale from 0 to 10.[24] (A) Heat map of normalized parameters. (B) Subtraction heat map of normalized differences compared with WT mice, filtered for changes with $P \leq .05$.

different in ACC DKI platelets compared with WT platelets. Carbonyl cyanide *p*-trifluoromethoxyphenylhydrazone, a proton-ionophore, then induced maximal OCR and a corresponding decrease in maximal respiration and reserve capacity on thrombin stimulation, as a result of the mobilization of endogenous metabolic substrates to cope with increased energetic demands. This occurred to a similar extent in platelets from both genotypes (Figure 5A-B). Finally, antimycin A and rotenone, complex III/I inhibitors, totally inhibited mitochondrial-induced OCR. Proton leak was unchanged in all groups (Figure 5A-B). It has not been previously reported that collagen also stimulates mitochondrial function using this approach. As shown in Figure 5C-D, collagen stimulates OCR with similar characteristics to thrombin. Taken together, these data indicate that in platelets, AMPK-ACC signaling is not playing a major role in mitochondrial respiration, both basally and in the presence of thrombin or collagen. The comparable impact of Etomoxir, a carnitine palmitoyltransferase-1 inhibitor, on the ACC WT and ACC DKI platelet mitochondrial bioenergetics further supports the conclusion that platelets from both genotypes similarly rely on fatty acids to produce ATP (Figure 5E-F).

Q:11

To investigate whether the gain-of-function of ACC DKI platelets relies on a modified lipid content, we undertook a quantitative lipidomic analysis of resting and stimulated platelets. Isolated ACC DKI and ACC WT platelets were either left unstimulated or activated with 25 μg/mL collagen, 0.3 U/mL thrombin, or a mix of both. The lipids classes analyzed included different PL (PE, PEP, plasmenyl phosphatidylethanolamine, phosphatidylcholine [PC], lysophosphatidylethanolamine, lysophosphatidylcholine), sphingomyelin, cholesteryl esters, free fatty acids, DAG, and triglycerides.[32]

In agreement with previous data,[33] class enrichment analysis indicated that collagen significantly upregulated lipid species among free fatty acids (31%), lysophosphatidylcholine (57%), lysophosphatidylethanolamine (38%), and DAG (21%) lipid classes, in both ACC WT and ACC DKI platelets (Figure 6A; supplemental Table 2). Enrichment of free fatty acids and DAG was also observed in response to thrombin alone (supplemental Figure 6A) and to a combination of thrombin and collagen (supplemental Figure 6B). More important, loss of AMPK-ACC signaling resulted in enrichment of upregulated lipid species among PEP lipid classes (28%), independent of the basal or simulated condition (Figure 6B; supplemental Table 3). Indeed, an increase in lipid species among PEP was strongly associated with lack of ACC phosphorylation (odds ratio, 48 [14-217]; Figure 6B). ACC DKI also displayed an increment of downregulated lipid species among cholesteryl esters (38%) and PC (14%; Figure 6B). Given that ACC DKI platelets show increased TXA_2 generation, we specifically focused our data analysis on AA-containing PEP and PC, the 2 PL classes particularly containing differentially regulated lipids. Relevant PEP species with side-chains 16:0/20:4 and 18:1/20:4 were significantly increased in ACC DKI platelets (Figure 6C). We showed that they, respectively, contributed 18.9% and 7.3% to the total reservoir of AA-containing PL (Figure 6D). In contrast, PC species with side-chains 18:2/20:4 and 14:0/20:4 were decreased (Figure 6C) and marginally accounted for 0.8% and 0.4%, respectively, of all AA-containing PL (Figure 6D). Taken together, upregulated AA-containing PEP in ACC DKI platelets clearly supports the enhanced TXA_2 formation observed in this condition. Of note, the AMPK-ACC signaling did not influence platelet palmitate uptake (supplemental Figure 7A). Moreover, collagen-induced TXA_2 production was not modulated by extracellular fatty acid availability in ACC WT or ACC DKI platelets (supplemental Figure 7B).

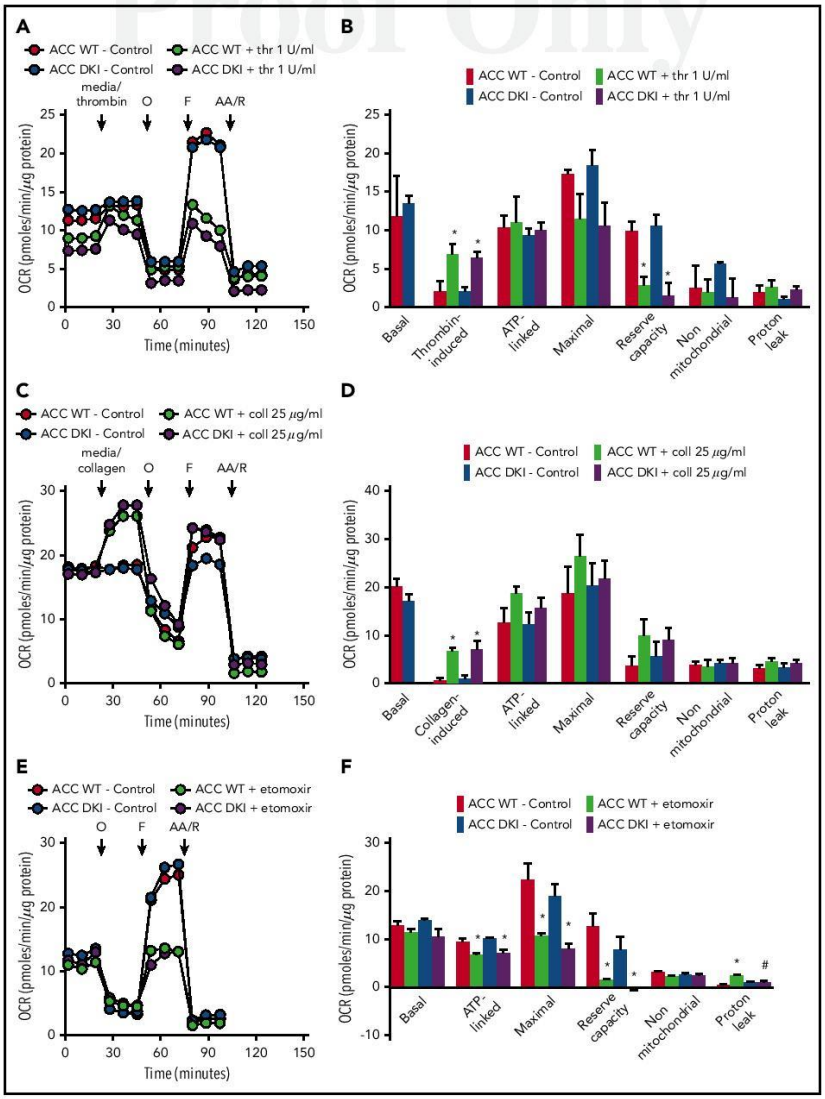

Figure 5. Lack of ACC phosphorylation does not affect oxidative metabolism. (A-F) Oxygen consumption rate (OCR) was measured in washed platelets pretreated or not with Etomoxir (25 μM) (E,F) for 1 hour before bioenergetic measurements. OCR was assessed under basal conditions, after injection of media alone or 1 U/mL thrombin (A,B) or 0.25 μg/mL collagen (C,D) or followed by treatment with 1 μM oligomycin (O), 0.1 μM carbonyl cyanide *p*-trifluoromethoxyphenylhydrazone (F), and a mix of 1 μM antimycin A (AA) and 1 μM rotenone (R). (A,C,E) Representative OCR profiles with thrombin (A) and collagen stimulation (C) or Etomoxir treatment (E). (B,D) Mitochondrial function was assessed by calculating basal, thrombin-induced (B) or collagen-induced (D), ATP-linked, maximal, nonmitochondrial, reserve capacity and proton leak OCR. In addition, bioenergetics measurements were assessed in Etomoxir-treated platelets (F). The results are expressed as means ± SEM (at least n = 3). *$P \leq .05$ relative to respective untreated platelets, #$P \leq .05$ between ACC WT and ACC DKI platelets. The data underwent 2-way ANOVA.

Q:16
Q:17

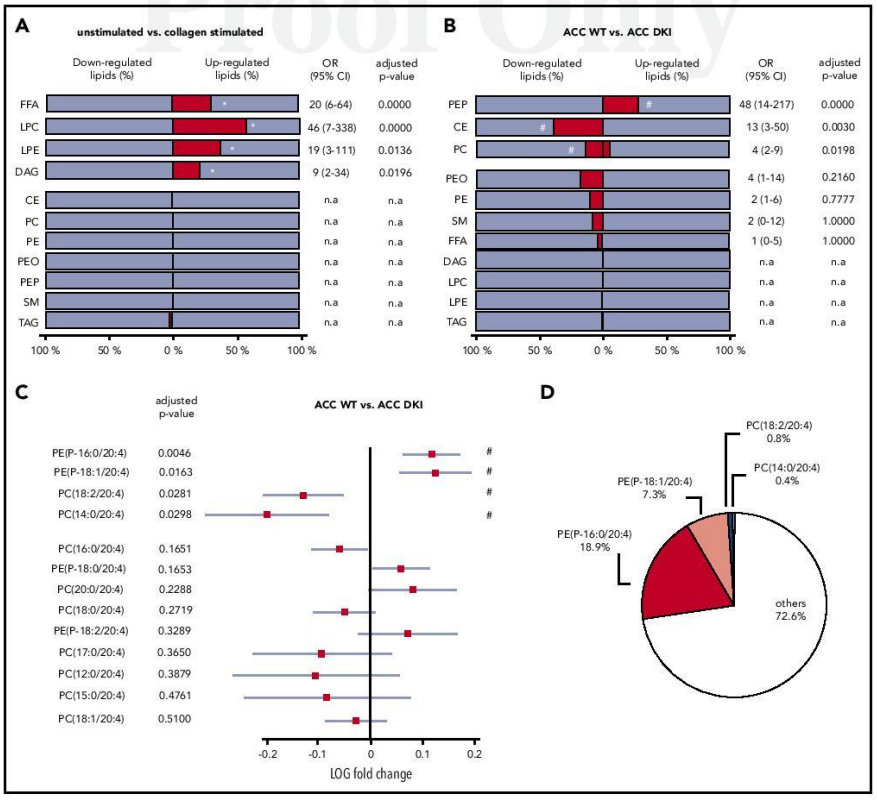

Figure 6. Lack of AMPK-ACC signaling results in an increased AA-containing PL pool. (A,B) The percentage (dark gray bar) of down- or upregulated lipid species relative to the whole lipid class was calculated in collagen-stimulated platelets relative to unstimulated platelets (A) or ACC DKI relative to ACC WT platelets (B). The different lipid classes are arranged from top down in order of increasing adjusted *P* values. (A) *Adjusted $P \leq .05$ between collagen-stimulated platelets and unstimulated platelets (n = 3). (B) #$P \leq .05$ between ACC DKI and WT platelets (n = 3). Multivariate regression analysis was performed. OR, odds ratio; CI, confidence interval; n.a., not applicable (if no change or if change is OR < 1). (C) Comparison of AA-containing PEP and PC between ACC DKI and WT platelets. The data are presented as log fold change (squares) relative to ACC WT platelets and with 95% CI (horizontal lines). Statistical significance was based on false discovery rate *P* values (adjusted *P* values). The different lipid species are arranged from top down in order of increasing adjusted *P* values. Multivariate regression analysis was performed. #$P \leq .05$ between ACC WT and ACC DKI platelets. (D) Proportions of PE(P-16:0/20:4), PE(P-18:1/20:4), PC(18:2/20:4), and PC(14:0/20:4) relative to all AA-containing PL were evaluated in ACC WT platelets. See also supplemental Figure 6 and 7 and supplemental Table 2 and 3.

Discussion

Lipids play fundamental roles in platelets, but little is known about the effect of endogenous lipid metabolism on platelet functions and subsequent thrombosis. To assess the importance of endogenous lipid synthesis on platelet function, we characterized a mouse model carrying a genetic mutation that prevents the AMPK-induced phosphorylation of ACC, the first rate-limiting enzyme of lipid synthesis.[2] We have shown that ACC1 is the predominant isoform in murine and human platelets. These data are consistent with transcriptomic and proteomic analyses that demonstrate ACC1 but not ACC2 transcript and protein expression in platelets.[34,35] In accordance with the primary role of ACC1 in lipogenesis, ACC DKI platelets display modified PL content rather than altered lipid oxidation. Indeed, no difference in oxygen consumption, which relies on endogenous lipid oxidation,[20] is observed between ACC WT and ACC DKI platelets under both basal conditions and on thrombin or collagen treatment. Consistent with our results, liver-specific inactivation of ACC1 resulted in reduced de novo fatty acid synthesis without alteration of fatty acid oxidation.[36]

In the first series of experiments, we demonstrated that bleeding time is shorter in ACC DKI mice and thrombosis is increased in vivo and ex vivo under flow on collagen. Second, platelet functions were analyzed and the results indicate that ACC DKI

platelets exhibit enhanced dense granule secretion in response to collagen, attributed to exacerbated TXA_2 generation. Finally, untargeted lipidomics revealed that lack of AMPK-ACC signaling was associated with an increase in some AA-containing PEP, leading to TXA_2 enrichment. Our findings highlight the critical role of platelet endogenous lipid synthesis in thrombosis and hemostasis, a concept that is supported by a recent study showing that a genetic deletion of acid sphingomyelinase, which converts sphingomyelin to ceramide, leads to an alteration of platelet lipidome, which in turn causes dysregulated granule secretion and in vitro thrombus formation.[37]

Thrombosis induced by $FeCl_3$ in the carotid artery is a widely used model that can provide valuable information about the effect of genetic modifications on platelet functions. However, it has a number of limitations regarding the underlying mechanisms that induce thrombus formation, notably about the relative roles of tissue factor and thrombin.[38-41] Recently, several studies reported that plasma proteins and blood cells, including platelets, aggregate because their negatively charged proteins bind to positively charged iron species.[42,43] Altogether, these results indicate that $FeCl_3$-induced thrombosis relies on complex multifaceted, incompletely elucidated, mechanisms.

Collectively, the data presented here demonstrate that AMPK-induced ACC1 phosphorylation in platelets does not control lipid oxidation but, rather, regulates cellular lipid content. Intriguingly, we expect that an increase in AA-containing PL, as observed in ACC DKI platelets, would provide more substrates for mitochondrial respiration in response to thrombin.[1] However, we could not find any modifications of platelet mitochondrial oxygen consumption, indicating some degree of compartmentalization and suggesting that increased PEP16:0/20:4 and 18:1/20:4 in ACC DKI platelets do not significantly contribute to overall platelet bioenergetics.

The view that TXA_2 and dense granules are of central importance in triggering thrombus formation but not platelet activation on collagen surfaces has been advanced in previous studies.[27,28] In addition, the relationship between TXA_2 and dense granule secretion has been clearly established.[15,44,45] Our work not only confirms this link in ACC DKI platelets but also underlines that excessive thrombus formation is not systematically associated with an alteration of αIIbβ3-dependent platelet aggregation. This disconnection has been recently reported[37] and supports the notion that additional cell surface molecules participate in platelet/platelet interactions and support thrombus growth.[46,47] Therefore, based on the core-shell thrombosis model of,[48,49] we postulate that lack of AMPK-ACC signaling might potentiate platelet recruitment to the shell structure through increased TXA_2 and ADP secretion, augmenting thrombosis through mechanisms independent of αIIbβ3. In addition, increased PF4 secretion might possibly contribute to a rise in thrombus growth in ACC DKI mice.

Interestingly, the effect of AMPK-ACC signaling on TXA_2 generation and platelet dense granule secretion is collagen-specific. This is in agreement with previous data showing that different mechanisms of AA-containing PL breakdown are operating in response to collagen or thrombin. Indeed, although AA release by thrombin is dependent on $cPLA_2$,[1,50] collagen-induced AA generation involves $cPLA_2$, the low-molecular-weight secreted PLA_2 ($sPLA_2$) and the Ca^{2+}-independent cytosolic PLA_2 ($iPLA_2$).[51] In line with these observations, thrombin and collagen differentially degrade AA-containing PL, depending on the nature of the PL.[37,52] For instance, thrombin is more potent at cleaving AA-containing PI and phosphatidylserine than collagen, whereas the latter is 2 times more efficient toward AA-containing PEP.[52] These data reinforce our observations and help us to understand the specific response or responses of ACC DKI platelets to collagen.

Importantly, ACC phosphorylation could be detected, even in the absence of any agonist stimulation, in platelets from both healthy mice and volunteers.[7] This has been confirmed by comparing ACC phosphorylation between ACC WT and ACC DKI platelets under basal conditions. A sustained change in basal ACC phosphorylation was sufficient to induce a decrease in PL, suggesting that ACC phosphorylation already affects lipid composition in resting platelets before activation.

In conclusion, our work provides new insights into the contribution of endogenous lipid synthesis to platelet functions. It reveals that sustained modulation of ACC phosphorylation in platelets can modify specific AA-containing PL content and influence platelet reactivity to collagen. This finding might have far-reaching clinical relevance in the pathological context of diseases such as atherosclerosis. Indeed, this is now being tested in a clinical trial demonstrating that basal ACC phosphorylation dramatically increases in platelets of patients with coronary artery disease (ACCTHEROMA Clinical Trial identifier: NCT03034148). How and whether such a pathway is involved in regulating platelet function in this context remain to be determined.

Acknowledgments

The authors thank Pierre Sonveaux (Pole of Pharmacology, Institut de Recherche Expérimentale et Clinique, Université catholique de Louvain, Brussels, Belgium) for his help with extracellular flux analysis of mitochondrial function.

This work was supported by grants from Fonds National de la Recherche Scientifique et Médicale (FNRS, Belgium), Action de Recherche Concertée de la Communauté Wallonie-Bruxelles, Belgium (ARC 13/18-051, ARC 16-21), and Fondation Louvain, Belgium, and with unrestricted grants from Bayer and Astra Zeneca. S.L. and S.K. were supported by FNRS, S.L. and M.-B.O. were supported by Bourse Salus Sanguinis (Université catholique de Louvain, Belgium). M.O. and O.W. have a FRIA fellowship (FNRS, Belgium). B.E.K is supported by the National Health and Medical Research Council and the Victorian Government Operational Infrastructure Support Scheme. S.B. and J.H. are supported by the Interreg Euregio Meuse-Rhine program Polyvalve. S.H. is research associate, and L.B. and C.O. are senior research associates at FNRS, Belgium. C.B. was a clinical master specialist at FNRS, Belgium. Q:13

Authorship

Contribution: S.L., M.-B.O., L.B., C.O., C.B., and S.H. provided conceptualization; V.M.D.-U. provided methodology; M.G., J.A., and B.G. provided formal analysis; S.L., S.K., M.O., A.G., M.-B.O., A.H., O.W., S.B., F.S., M.G., and J.H. performed the investigation; G.R.S., B.E.K., and C.O. provided resources; S.L., V.M.D.-U., C.B., and S.H., wrote the original draft and performed a review; and C.B. and S.H. performed supervision.

Conflict-of-interest disclosure: The authors declare no competing financial interests.

ORCID profile: M.G., 0000-0003-1684-1894. Q:A2

Correspondence: Sandrine Horman, Pôle de Recherche Cardiovasculaire, Institut de Recherche Expérimentale et Clinique, Université catholique de

Q:14 Louvain, 55, Avenue Hippocrate, 1200 Brussels, Belgium; e-mail: sandrine.horman@uclouvain.be.

*S.L. and S.K. contributed equally to this study and are joint first authors.

#C.B. and S.H. contributed equally to this study and are joint last authors.

Footnotes

Submitted 4 February 2018; accepted 8 July 2018. Prepublished online as *Blood* First Edition paper, 17 July 2018; DOI 10.1182/blood-2018-02-831503.

The publication costs of this article were defrayed in part by page charge payment. Therefore, and solely to indicate this fact, this article is hereby marked "advertisement" in accordance with 18 USC section 1734.

REFERENCES

1. Slatter DA, Aldrovandi M, O'Connor A, et al. Mapping the human platelet lipidome reveals cytosolic phospholipase A2 as a regulator of mitochondrial bioenergetics during activation. *Cell Metab*. 2016;23(5):930-944.

Q:15 2. Fullerton MD, Galic S, Marcinko K, et al. Single phosphorylation sites in Acc1 and Acc2 regulate lipid homeostasis and the insulin-sensitizing effects of metformin. *Nat Med*. 2013;19(12):1649-1654.

3. Iverson AJ, Bianchi A, Nordlund AC, Witters LA. Immunological analysis of acetyl-CoA carboxylase mass, tissue distribution and subunit composition. *Biochem J*. 1990;269(2):365-371.

4. Abu-Elheiga L, Matzuk MM, Kordari P, et al. Mutant mice lacking acetyl-CoA carboxylase 1 are embryonically lethal. *Proc Natl Acad Sci USA*. 2005;102(34):12011-12016.

5. Abu-Elheiga L, Brinkley WR, Zhong L, Chirala SS, Woldegiorgis G, Wakil SJ. The subcellular localization of acetyl-CoA carboxylase 2. *Proc Natl Acad Sci USA*. 2000;97(4):1444-1449.

6. Wakil SJ, Abu-Elheiga LA. Fatty acid metabolism: target for metabolic syndrome. *J Lipid Res*. 2009;50(Suppl):S138-S143.

7. Onselaer MB, Oury C, Hunter RW, et al. The Ca(2+) /calmodulin-dependent kinase kinase β-AMP-activated protein kinase-α1 pathway regulates phosphorylation of cytoskeletal targets in thrombin-stimulated human platelets. *J Thromb Haemost*. 2014;12(6):973-986.

8. Randriamboavonjy V, Isaak J, Frömel T, et al. AMPK α2 subunit is involved in platelet signaling, clot retraction, and thrombus stability. *Blood*. 2010;116(12):2134-2140.

9. Signorello MG, Leoncini G. Activation of CaMKKβ/AMPKα pathway by 2-AG in human platelets. *J Cell Biochem*. 2018;119(1):876-884.

10. Munday MR, Campbell DG, Carling D, Hardie DG. Identification by amino acid sequencing of three major regulatory phosphorylation sites on rat acetyl-CoA carboxylase. *Eur J Biochem*. 1988;175(2):331-338.

11. Carling D, Zammit VA, Hardie DG. A common bicyclic protein kinase cascade inactivates the regulatory enzymes of fatty acid and cholesterol biosynthesis. *FEBS Lett*. 1987;223(2):217-222.

12. Pula G, Schuh K, Nakayama K, Nakayama KI, Walter U, Poole AW. PKCdelta regulates collagen-induced platelet aggregation through inhibition of VASP-mediated filopodia formation. *Blood*. 2006;108(13):4035-4044.

13. Bettache N, Baisamy L, Baghdiguian S, Payrastre B, Mangeat P, Bienvenue A. Mechanical constraint imposed on plasma membrane through transverse phospholipid imbalance induces reversible actin polymerization via phosphoinositide 3-kinase activation. *J Cell Sci*. 2003;116(Pt 11):2277-2284.

14. Koseoglu S, Meyer AF, Kim D, et al. Analytical characterization of the role of phospholipids in platelet adhesion and secretion. *Anal Chem*. 2015;87(1):413-421.

15. Stefanini L, Roden RC, Bergmeier W. CalDAG-GEFI is at the nexus of calcium-dependent platelet activation. *Blood*. 2009;114(12):2506-2514.

16. Münzer P, Walker-Allgaier B, Geue S, et al. PDK1 Determines Collagen-Dependent Platelet Ca2+ Signaling and Is Critical to Development of Ischemic Stroke In Vivo. *Arterioscler Thromb Vasc Biol*. 2016;36(8):1507-1516.

17. Nocella C, Carnevale R, Bartimoccia S, et al. Lipopolysaccharide as trigger of platelet aggregation via eicosanoid over-production. *Thromb Haemost*. 2017;117(8):1558-1570.

18. Guppy M, Abas L, Neylon C, et al. Fuel choices by human platelets in human plasma. *Eur J Biochem*. 1997;244(1):161-167.

19. Chacko BK, Kramer PA, Ravi S, et al. Methods for defining distinct bioenergetic profiles in platelets, lymphocytes, monocytes, and neutrophils, and the oxidative burst from human blood. *Lab Invest*. 2013;93(6):690-700.

20. Ravi S, Chacko B, Sawada H, et al. Metabolic plasticity in resting and thrombin activated platelets. *PLoS One*. 2015;10(4):e0123597.

21. Nguyen QL, Corey C, White P, et al. Platelets from pulmonary hypertension patients show increased mitochondrial reserve capacity. *JCI Insight*. 2017;2(5):e91415.

22. Akkerman JW, Holmsen H. Interrelationships among platelet responses: studies on the burst in proton liberation, lactate production, and oxygen uptake during platelet aggregation and Ca2+ secretion. *Blood*. 1981;57(5):956-966.

23. Mattheij NJ, Gilio K, van Kruchten R, et al. Dual mechanism of integrin αIIbβ3 closure in procoagulant platelets. *J Biol Chem*. 2013;288(19):13325-13336.

24. de Witt SM, Swieringa F, Cavill R, et al. Identification of platelet function defects by multi-parameter assessment of thrombus formation. *Nat Commun*. 2014;5(1):4257.

25. Musumeci L, Kuijpers MJ, Gilio K, et al. Dual-specificity phosphatase 3 deficiency or inhibition limits platelet activation and arterial thrombosis. *Circulation*. 2015;131(7):656-668.

26. Lintonen TP, Baker PR, Suoniemi M, et al. Differential mobility spectrometry-driven shotgun lipidomics. *Anal Chem*. 2014;86(19):9662-9669.

27. Kuijpers MJ, Schulte V, Bergmeier W, et al. Complementary roles of glycoprotein VI and alpha2beta1 integrin in collagen-induced thrombus formation in flowing whole blood ex vivo. *FASEB J*. 2003;17(6):685-687.

28. Lecut C, Schoolmeester A, Kuijpers MJ, et al. Principal role of glycoprotein VI in alpha2-beta1 and alphaIIbbeta3 activation during collagen-induced thrombus formation. *Arterioscler Thromb Vasc Biol*. 2004;24(9):1727-1733.

29. Graham GJ, Ren Q, Dilks JR, Blair P, Whiteheart SW, Flaumenhaft R. Endobrevin/VAMP-8-dependent dense granule release mediates thrombus formation in vivo. *Blood*. 2009;114(5):1083-1090.

30. Vilahur G, Casaní L, Badimon L. A thromboxane A2/prostaglandin H2 receptor antagonist (S18886) shows high antithrombotic efficacy in an experimental model of stent-induced thrombosis. *Thromb Haemost*. 2007;98(3):662-669.

31. Kuijpers MJ, Pozgajova M, Cosemans JM, et al. Role of murine integrin alpha2beta1 in thrombus stabilization and embolization: contribution of thromboxane A2. *Thromb Haemost*. 2007;98(5):1072-1080.

32. Berod L, Friedrich C, Nandan A, Freitag J. De novo fatty acid synthesis controls the fate between regulatory T and T helper 17 cells. *Nat Med*. 2014;20(11):1327-1333

33. Turini ME, Holub BJ. Eicosanoid/thromboxane A2-independent and -dependent generation of lysoplasmenylethanolamine via phospholipase A2 in collagen-stimulated human platelets. *Biochem J*. 1993;289(Pt 3):641-646.

34. Rowley JW, Oler AJ, Tolley ND, et al. Genome-wide RNA-seq analysis of human and mouse platelet transcriptomes. *Blood*. 2011;118(14):e101-e111.

35. Burkhart JM, Vaudel M, Gambaryan S, et al. The first comprehensive and quantitative analysis of human platelet protein composition allows the comparative analysis of structural and functional pathways. *Blood*. 2012;120(15):e73-e82.

36. Mao J, DeMayo FJ, Li H, et al. Liver-specific deletion of acetyl-CoA carboxylase 1 reduces hepatic triglyceride accumulation without affecting glucose homeostasis. *Proc Natl Acad Sci USA*. 2006;103(22):8552-8557.

37. Peng B, Geue S, Coman C, et al. Identification of key lipids critical for platelet activation by comprehensive analysis of the platelet lipidome [published online ahead of print 21 May 2018]. *Blood*. doi:.

38. Li W, Gigante A, Perez-Perez MJ, et al. Thymidine phosphorylase participates in platelet signaling and promotes thrombosis. *Circ Res*. 2014;115(12):997-1006.

39. Massberg S, Gawaz M, Grüner S, et al. A crucial role of glycoprotein VI for platelet recruitment to the injured arterial wall in vivo. *J Exp Med*. 2003;197(1):41-49.

40. Konstantinides S, Ware J, Marchese P, Almus-Jacobs F, Loskutoff DJ, Ruggeri ZM. Distinct antithrombotic consequences of platelet glycoprotein Ibalpha and VI deficiency in a mouse model of arterial thrombosis. *J Thromb Haemost*. 2006;4(9):2014-2021.

41. Eckly A, Hechler B, Freund M, et al. Mechanisms underlying FeCl3-induced arterial thrombosis. *J Thromb Haemost*. 2011;9(4):779-789.

42. Ciciliano JC, Sakurai Y, Myers DR, et al. Resolving the multifaceted mechanisms of the ferric chloride thrombosis model using an interdisciplinary microfluidic approach. *Blood*. 2015;126(6):817-824.

43. Barr JD, Chauhan AK, Schaeffer GV, Hansen JK, Motto DG. Red blood cells mediate the onset of thrombosis in the ferric chloride murine model. *Blood*. 2013;121(18):3733-3741.

44. Naik MU, Patel P, Derstine R, et al. Ask1 regulates murine platelet granule secretion, thromboxane A2 generation, and thrombus formation. *Blood*. 2017;129(9):1197-1209.

45. Rinder CS, Student LA, Bonan JL, Rinder HM, Smith BR. Aspirin does not inhibit adenosine diphosphate-induced platelet alpha-granule release. *Blood*. 1993;82(2):505-512.

46. Prévost N, Woulfe DS, Jiang H, et al. Eph kinases and ephrins support thrombus growth and stability by regulating integrin outside-in signaling in platelets. *Proc Natl Acad Sci USA*. 2005;102(28):9820-9825.

47. Nanda N, Bao M, Lin H, et al. Platelet endothelial aggregation receptor 1 (PEAR1), a novel epidermal growth factor repeat-containing transmembrane receptor, participates in platelet contact-induced activation. *J Biol Chem*. 2005;280(26):24680-24689.

48. Stalker TJ, Traxler EA, Wu J, et al. Hierarchical organization in the hemostatic response and its relationship to the platelet-signaling network. *Blood*. 2013;121(10):1875-1885.

49. Stalker TJ, Welsh JD, Tomaiuolo M, et al. A systems approach to hemostasis: 3. Thrombus consolidation regulates intrathrombus solute transport and local thrombin activity. *Blood*. 2014;124(11):1824-1831.

50. Yoda E, Rai K, Ogawa M, et al. Group VIB calcium-independent phospholipase A2 (iPLA2γ) regulates platelet activation, hemostasis and thrombosis in mice. *PLoS One*. 2014;9(10):e109409.

51. Wong DA, Kita Y, Uozumi N, Shimizu T. Discrete role for cytosolic phospholipase A(2) alpha in platelets: studies using single and double mutant mice of cytosolic and group IIA secretory phospholipase A(2). *J Exp Med*. 2002;196(3):349-357.

52. Takamura H, Narita H, Park HJ, Tanaka K, Matsuura T, Kito M. Differential hydrolysis of phospholipid molecular species during activation of human platelets with thrombin and collagen. *J Biol Chem*. 1987;262(5):2262-2269.

BIBLIOGRAPHY

1. Kaushansky, K., et al., *Thrombopoietin, the Mp1 ligand, is essential for full megakaryocyte development.* Proc Natl Acad Sci U S A, 1995. **92**(8): p. 3234-8.
2. Tijssen, M.R. and C. Ghevaert, *Transcription factors in late megakaryopoiesis and related platelet disorders.* J Thromb Haemost, 2013. **11**(4): p. 593-604.
3. Vitrat, N., et al., *Endomitosis of human megakaryocytes are due to abortive mitosis.* Blood, 1998. **91**(10): p. 3711-23.
4. Schulze, H., et al., *Characterization of the megakaryocyte demarcation membrane system and its role in thrombopoiesis.* Blood, 2006. **107**(10): p. 3868-75.
5. Cramer, E.M., et al., *Ultrastructure of platelet formation by human megakaryocytes cultured with the Mpl ligand.* Blood, 1997. **89**(7): p. 2336-46.
6. Lefrancais, E., et al., *The lung is a site of platelet biogenesis and a reservoir for haematopoietic progenitors.* Nature, 2017. **544**(7648): p. 105-109.
7. Schmitt, A., et al., *Of mice and men: comparison of the ultrastructure of megakaryocytes and platelets.* Exp Hematol, 2001. **29**(11): p. 1295-302.
8. Thon, J.N. and J.E. Italiano, *Platelets: production, morphology and ultrastructure.* Handb Exp Pharmacol, 2012(210): p. 3-22.
9. White, J.G. and C.C. Clawson, *The surface-connected canalicular system of blood platelets--a fenestrated membrane system.* Am J Pathol, 1980. **101**(2): p. 353-64.
10. White, J.G., *Effects of colchicine and Vinca alkaloids on human platelets. I. Influence on platelet microtubules and contractile function.* Am J Pathol, 1968. **53**(2): p. 281-91.
11. Handagama, P., et al., *Endocytosis of fibrinogen into megakaryocyte and platelet alpha-granules is mediated by alpha IIb beta 3 (glycoprotein IIb-IIIa).* Blood, 1993. **82**(1): p. 135-8.
12. Nurden, A.T. and P. Nurden, *The gray platelet syndrome: clinical spectrum of the disease.* Blood Rev, 2007. **21**(1): p. 21-36.
13. Deppermann, C., et al., *The Nbeal2(-/-) mouse as a model for the gray platelet syndrome.* Rare Dis, 2013. **1**: p. e26561.
14. Heijnen, H. and P. van der Sluijs, *Platelet secretory behaviour: as diverse as the granules ... or not?* J Thromb Haemost, 2015. **13**(12): p. 2141-51.
15. Li, R. and S.L. Diamond, *Detection of platelet sensitivity to inhibitors of COX-1, P2Y(1), and P2Y(1)(2) using a whole blood microfluidic flow assay.* Thromb Res, 2014. **133**(2): p. 203-10.
16. Turner, N.A., J.L. Moake, and L.V. McIntire, *Blockade of adenosine diphosphate receptors P2Y(12) and P2Y(1) is required to inhibit platelet aggregation in whole blood under flow.* Blood, 2001. **98**(12): p. 3340-5.

17. Wolf, K., et al., *Partially Defective Store Operated Calcium Entry and Hem(ITAM) Signaling in Platelets of Serotonin Transporter Deficient Mice.* PLoS One, 2016. **11**(1): p. e0147664.
18. Smith, S.A., et al., *Polyphosphate modulates blood coagulation and fibrinolysis.* Proc Natl Acad Sci U S A, 2006. **103**(4): p. 903-8.
19. Morrissey, J.H. and S.A. Smith, *Polyphosphate as modulator of hemostasis, thrombosis, and inflammation.* J Thromb Haemost, 2015. **13 Suppl 1**: p. S92-7.
20. Smith, S.A., et al., *Polyphosphate exerts differential effects on blood clotting, depending on polymer size.* Blood, 2010. **116**(20): p. 4353-9.
21. Gahl, W.A., et al., *Genetic defects and clinical characteristics of patients with a form of oculocutaneous albinism (Hermansky-Pudlak syndrome).* N Engl J Med, 1998. **338**(18): p. 1258-64.
22. King, S.M., et al., *Platelet dense-granule secretion plays a critical role in thrombosis and subsequent vascular remodeling in atherosclerotic mice.* Circulation, 2009. **120**(9): p. 785-91.
23. Graham, G.J., et al., *Endobrevin/VAMP-8-dependent dense granule release mediates thrombus formation in vivo.* Blood, 2009. **114**(5): p. 1083-90.
24. Ravi, S., et al., *Metabolic plasticity in resting and thrombin activated platelets.* PLoS One, 2015. **10**(4): p. e0123597.
25. Jackson, S.P. and S.M. Schoenwaelder, *Procoagulant platelets: are they necrotic?* Blood, 2010. **116**(12): p. 2011-8.
26. Coenen, D.M. and T.G. Mastenbroek, *Platelet interaction with activated endothelium: mechanistic insights from microfluidics.* Blood, 2017. **130**(26): p. 2819-2828.
27. Ruggeri, Z.M. and G.L. Mendolicchio, *Adhesion mechanisms in platelet function.* Circ Res, 2007. **100**(12): p. 1673-85.
28. Aslan, J.E. and O.J. McCarty, *Rho GTPases in platelet function.* J Thromb Haemost, 2013. **11**(1): p. 35-46.
29. Onselaer, M.B., et al., *The Ca(2+) /calmodulin-dependent kinase kinase beta-AMP-activated protein kinase-alpha1 pathway regulates phosphorylation of cytoskeletal targets in thrombin-stimulated human platelets.* J Thromb Haemost, 2014. **12**(6): p. 973-86.
30. Flaumenhaft, R., et al., *The actin cytoskeleton differentially regulates platelet alpha-granule and dense-granule secretion.* Blood, 2005. **105**(10): p. 3879-87.
31. Golebiewska, E.M., et al., *Syntaxin 8 regulates platelet dense granule secretion, aggregation, and thrombus stability.* J Biol Chem, 2015. **290**(3): p. 1536-45.

32. Konopatskaya, O., et al., *Protein kinase C mediates platelet secretion and thrombus formation through protein kinase D2.* Blood, 2011. **118**(2): p. 416-424.
33. van den Bosch, M.T., A.W. Poole, and I. Hers, *Cytohesin-2 phosphorylation by protein kinase C relieves the constitutive suppression of platelet dense granule secretion by ADP-ribosylation factor 6.* J Thromb Haemost, 2014. **12**(5): p. 726-35.
34. Stalker, T.J., et al., *Hierarchical organization in the hemostatic response and its relationship to the platelet-signaling network.* Blood, 2013. **121**(10): p. 1875-85.
35. Muthard, R.W., et al., *Fibrin, gamma'-fibrinogen, and transclot pressure gradient control hemostatic clot growth during human blood flow over a collagen/tissue factor wound.* Arterioscler Thromb Vasc Biol, 2015. **35**(3): p. 645-54.
36. Kuijpers, M.J., et al., *Complementary roles of glycoprotein VI and alpha2beta1 integrin in collagen-induced thrombus formation in flowing whole blood ex vivo.* Faseb j, 2003. **17**(6): p. 685-7.
37. Lecut, C., et al., *Principal role of glycoprotein VI in alpha2beta1 and alphaIIbbeta3 activation during collagen-induced thrombus formation.* Arterioscler Thromb Vasc Biol, 2004. **24**(9): p. 1727-33.
38. Shen, J., et al., *Coordination of platelet agonist signaling during the hemostatic response in vivo.* Blood Adv, 2017. **1**(27): p. 2767-2775.
39. Brass, L.F., et al., *Regulating thrombus growth and stability to achieve an optimal response to injury.* J Thromb Haemost, 2011. **9 Suppl 1**: p. 66-75.
40. Wannemacher, K.M., et al., *Diminished contact-dependent reinforcement of Syk activation underlies impaired thrombus growth in mice lacking Semaphorin 4D.* Blood, 2010. **116**(25): p. 5707-15.
41. Brass, L.F., L. Zhu, and T.J. Stalker, *Minding the gaps to promote thrombus growth and stability.* J Clin Invest, 2005. **115**(12): p. 3385-92.
42. Heemskerk, J.W., E.M. Bevers, and T. Lindhout, *Platelet activation and blood coagulation.* Thromb Haemost, 2002. **88**(2): p. 186-93.
43. Preissner, K.T., L. Zwicker, and G. Muller-Berghaus, *Formation, characterization and detection of a ternary complex between S protein, thrombin and antithrombin III in serum.* Biochem J, 1987. **243**(1): p. 105-11.
44. Altes, A., et al., *Hemostatic disturbances in acute ischemic stroke: a study of 86 patients.* Acta Haematol, 1995. **94**(1): p. 10-5.
45. Law, D.A., et al., *Integrin cytoplasmic tyrosine motif is required for outside-in alphaIIbbeta3 signalling and platelet function.* Nature, 1999. **401**(6755): p. 808-11.

46. Xu, X.R., G.M. Yousef, and H. Ni, *Cancer and platelet crosstalk: opportunities and challenges for aspirin and other antiplatelet agents.* Blood, 2018. **131**(16): p. 1777-1789.
47. Cho, M.S., et al., *Platelets increase the proliferation of ovarian cancer cells.* Blood, 2012. **120**(24): p. 4869-72.
48. Janowska-Wieczorek, A., et al., *Microvesicles derived from activated platelets induce metastasis and angiogenesis in lung cancer.* Int J Cancer, 2005. **113**(5): p. 752-60.
49. Velez, J., et al., *Platelets promote mitochondrial uncoupling and resistance to apoptosis in leukemia cells: a novel paradigm for the bone marrow microenvironment.* Cancer Microenviron, 2014. **7**(1-2): p. 79-90.
50. Bottsford-Miller, J., et al., *Differential platelet levels affect response to taxane-based therapy in ovarian cancer.* Clin Cancer Res, 2015. **21**(3): p. 602-10.
51. Varon, D. and E. Shai, *Role of platelet-derived microparticles in angiogenesis and tumor progression.* Discov Med, 2009. **8**(43): p. 237-41.
52. Ho-Tin-Noe, B., et al., *Platelet granule secretion continuously prevents intratumor hemorrhage.* Cancer Res, 2008. **68**(16): p. 6851-8.
53. Golebiewska, E.M. and A.W. Poole, *Secrets of platelet exocytosis - what do we really know about platelet secretion mechanisms?* Br J Haematol, 2013. **165**(2): p. 204-216.
54. Franco, A.T., A. Corken, and J. Ware, *Platelets at the interface of thrombosis, inflammation, and cancer.* Blood, 2015. **126**(5): p. 582-8.
55. Kune, G.A., S. Kune, and L.F. Watson, *Colorectal cancer risk, chronic illnesses, operations, and medications: case control results from the Melbourne Colorectal Cancer Study.* Cancer Res, 1988. **48**(15): p. 4399-404.
56. Algra, A.M. and P.M. Rothwell, *Effects of regular aspirin on long-term cancer incidence and metastasis: a systematic comparison of evidence from observational studies versus randomised trials.* Lancet Oncol, 2012. **13**(5): p. 518-27.
57. Bibbins-Domingo, K., *Aspirin Use for the Primary Prevention of Cardiovascular Disease and Colorectal Cancer: U.S. Preventive Services Task Force Recommendation Statement.* Ann Intern Med, 2016. **164**(12): p. 836-45.
58. Crescente, M. and L. Menke, *Eicosanoids in platelets and the effect of their modulation by aspirin in the cardiovascular system (and beyond).* 2018.
59. Cho, M.S., et al., *Role of ADP receptors on platelets in the growth of ovarian cancer.* Blood, 2017. **130**(10): p. 1235-1242.
60. Wang, Y., et al., *Platelet P2Y12 is involved in murine pulmonary metastasis.* PLoS One, 2013. **8**(11): p. e80780.

61. Ballerini, P., et al., *P2Y12 Receptors in Tumorigenesis and Metastasis.* Front Pharmacol, 2018. **9**: p. 66.
62. Schneider, S.W., et al., *Shear-induced unfolding triggers adhesion of von Willebrand factor fibers.* Proc Natl Acad Sci U S A, 2007. **104**(19): p. 7899-903.
63. Bryckaert, M., et al., *Of von Willebrand factor and platelets.* Cell Mol Life Sci, 2015. **72**(2): p. 307-26.
64. Berndt, M.C., et al., *The vascular biology of the glycoprotein Ib-IX-V complex.* Thromb Haemost, 2001. **86**(1): p. 178-88.
65. Harper, M.T. and A.W. Poole, *Diverse functions of protein kinase C isoforms in platelet activation and thrombus formation.* J Thromb Haemost, 2010. **8**(3): p. 454-62.
66. Stefanini, L., R.C. Roden, and W. Bergmeier, *CalDAG-GEFI is at the nexus of calcium-dependent platelet activation.* Blood, 2009. **114**(12): p. 2506-14.
67. Romo, G.M., et al., *The glycoprotein Ib-IX-V complex is a platelet counterreceptor for P-selectin.* J Exp Med, 1999. **190**(6): p. 803-14.
68. Vanhoorelbeke, K., et al., *Inhibition of platelet glycoprotein Ib and its antithrombotic potential.* Curr Pharm Des, 2007. **13**(26): p. 2684-97.
69. Lopez, J.A., et al., *Bernard-Soulier syndrome.* Blood, 1998. **91**(12): p. 4397-418.
70. Savage, B., M.H. Ginsberg, and Z.M. Ruggeri, *Influence of fibrillar collagen structure on the mechanisms of platelet thrombus formation under flow.* Blood, 1999. **94**(8): p. 2704-15.
71. Nieswandt, B. and S.P. Watson, *Platelet-collagen interaction: is GPVI the central receptor?* Blood, 2003. **102**(2): p. 449-61.
72. Mammadova-Bach, E., et al., *Platelet glycoprotein VI binds to polymerized fibrin and promotes thrombin generation.* Blood, 2015. **126**(5): p. 683-91.
73. Onselaer, M.B., et al., *Fibrin and D-dimer bind to monomeric GPVI.* Blood Adv, 2017. **1**(19): p. 1495-1504.
74. Matus, V., et al., *An adenine insertion in exon 6 of human GP6 generates a truncated protein associated with a bleeding disorder in four Chilean families.* J Thromb Haemost, 2013. **11**(9): p. 1751-9.
75. Akiyama, M., et al., *Presence of platelet-associated anti-glycoprotein (GP)VI autoantibodies and restoration of GPVI expression in patients with GPVI deficiency.* J Thromb Haemost, 2009. **7**(8): p. 1373-83.
76. Nuyttens, B.P., et al., *Platelet adhesion to collagen.* Thromb Res, 2011. **127 Suppl 2**: p. S26-9.
77. Inoue, O., et al., *Integrin alpha2beta1 mediates outside-in regulation of platelet spreading on collagen through activation of Src kinases and PLCgamma2.* J Cell Biol, 2003. **160**(5): p. 769-80.

78. Deckmyn, H., S.L. Chew, and J. Vermylen, *Lack of platelet response to collagen associated with an autoantibody against glycoprotein Ia: a novel cause of acquired qualitative platelet dysfunction.* Thromb Haemost, 1990. **64**(1): p. 74-9.
79. Nieuwenhuis, H.K., et al., *Human blood platelets showing no response to collagen fail to express surface glycoprotein Ia.* Nature, 1985. **318**(6045): p. 470-2.
80. Coughlin, S.R., *Thrombin signalling and protease-activated receptors.* Nature, 2000. **407**(6801): p. 258-64.
81. Coughlin, S.R., *Protease-activated receptors in hemostasis, thrombosis and vascular biology.* J Thromb Haemost, 2005. **3**(8): p. 1800-14.
82. Vu, T.K., et al., *Molecular cloning of a functional thrombin receptor reveals a novel proteolytic mechanism of receptor activation.* Cell, 1991. **64**(6): p. 1057-68.
83. Vu, T.K., et al., *Domains specifying thrombin-receptor interaction.* Nature, 1991. **353**(6345): p. 674-7.
84. Klages, B., et al., *Activation of G12/G13 results in shape change and Rho/Rho-kinase-mediated myosin light chain phosphorylation in mouse platelets.* J Cell Biol, 1999. **144**(4): p. 745-54.
85. Soh, U.J., et al., *Signal transduction by protease-activated receptors.* Br J Pharmacol, 2010. **160**(2): p. 191-203.
86. Tseng, A.S., et al., *Clinical Review of the Pharmacogenomics of Direct Oral Anticoagulants.* Cardiovasc Drugs Ther, 2018.
87. Mundell, S.J., et al., *Rapid resensitization of purinergic receptor function in human platelets.* J Thromb Haemost, 2008. **6**(8): p. 1393-404.
88. Gachet, C., C. Leon, and B. Hechler, *The platelet P2 receptors in arterial thrombosis.* Blood Cells Mol Dis, 2006. **36**(2): p. 223-7.
89. Raslan, Z. and K.M. Naseem, *The control of blood platelets by cAMP signalling.* Biochem Soc Trans, 2014. **42**(2): p. 289-94.
90. Hattori, M. and E. Gouaux, *Molecular mechanism of ATP binding and ion channel activation in P2X receptors.* Nature, 2012. **485**(7397): p. 207-12.
91. Toth-Zsamboki, E., et al., *P2X1-mediated ERK2 activation amplifies the collagen-induced platelet secretion by enhancing myosin light chain kinase activation.* J Biol Chem, 2003. **278**(47): p. 46661-7.
92. Oury, C., et al., *Overexpression of the platelet P2X1 ion channel in transgenic mice generates a novel prothrombotic phenotype.* Blood, 2003. **101**(10): p. 3969-76.
93. Hirata, T., et al., *Two thromboxane A2 receptor isoforms in human platelets. Opposite coupling to adenylyl cyclase with different sensitivity to Arg60 to Leu mutation.* J Clin Invest, 1996. **97**(4): p. 949-56.

94. Ginsberg, M.H., A. Partridge, and S.J. Shattil, *Integrin regulation.* Curr Opin Cell Biol, 2005. **17**(5): p. 509-16.
95. Niiya, K., et al., *Increased surface expression of the membrane glycoprotein IIb/IIIa complex induced by platelet activation. Relationship to the binding of fibrinogen and platelet aggregation.* Blood, 1987. **70**(2): p. 475-83.
96. Nurden, A.T., *Glanzmann thrombasthenia.* Orphanet J Rare Dis, 2006. **1**: p. 10.
97. Estevez, B., B. Shen, and X. Du, *Targeting integrin and integrin signaling in treating thrombosis.* Arterioscler Thromb Vasc Biol, 2015. **35**(1): p. 24-9.
98. Lafuente, E.M., et al., *RIAM, an Ena/VASP and Profilin ligand, interacts with Rap1-GTP and mediates Rap1-induced adhesion.* Dev Cell, 2004. **7**(4): p. 585-95.
99. Stritt, S., et al., *Rap1-GTP-interacting adaptor molecule (RIAM) is dispensable for platelet integrin activation and function in mice.* Blood, 2015. **125**(2): p. 219-22.
100. Durrant, T.N., M.T. van den Bosch, and I. Hers, *Integrin alphaIIbbeta3 outside-in signaling.* Blood, 2017. **130**(14): p. 1607-1619.
101. Ghosh, A., et al., *Platelet CD36 surface expression levels affect functional responses to oxidized LDL and are associated with inheritance of specific genetic polymorphisms.* Blood, 2011. **117**(23): p. 6355-66.
102. Silverstein, R.L., *Type 2 scavenger receptor CD36 in platelet activation: the role of hyperlipemia and oxidative stress.* Clin Lipidol, 2009. **4**(6): p. 767.
103. Hoosdally, S.J., et al., *The Human Scavenger Receptor CD36: glycosylation status and its role in trafficking and function.* J Biol Chem, 2009. **284**(24): p. 16277-88.
104. Yoshida, H. and R. Kisugi, *Mechanisms of LDL oxidation.* Clin Chim Acta, 2010. **411**(23-24): p. 1875-82.
105. Yang, M., et al., *Platelet CD36 promotes thrombosis by activating redox sensor ERK5 in hyperlipidemic conditions.* Blood, 2017. **129**(21): p. 2917-2927.
106. Berger, M., et al., *Dyslipidemia-associated atherogenic oxidized lipids induce platelet hyperactivity through phospholipase Cgamma2-dependent reactive oxygen species generation.* Platelets, 2018: p. 1-6.
107. Wraith, K.S., et al., *Oxidized low-density lipoproteins induce rapid platelet activation and shape change through tyrosine kinase and Rho kinase-signaling pathways.* Blood, 2013. **122**(4): p. 580-9.
108. Johnson, G.J., et al., *The critical role of myosin IIA in platelet internal contraction.* J Thromb Haemost, 2007. **5**(7): p. 1516-29.
109. Magwenzi, S., et al., *Oxidized LDL activates blood platelets through CD36/NOX2-mediated inhibition of the cGMP/protein kinase G signaling cascade.* Blood, 2015. **125**(17): p. 2693-703.

110. Zhu, W., et al., *Gut Microbial Metabolite TMAO Enhances Platelet Hyperreactivity and Thrombosis Risk.* Cell, 2016. **165**(1): p. 111-124.
111. Zhu, W., et al., *Flavin monooxygenase 3, the host hepatic enzyme in the metaorganismal trimethylamine N-oxide-generating pathway, modulates platelet responsiveness and thrombosis risk.* J Thromb Haemost, 2018. **0**(0).
112. Yano, J.M., et al., *Indigenous bacteria from the gut microbiota regulate host serotonin biosynthesis.* Cell, 2015. **161**(2): p. 264-76.
113. Jackel, S., et al., *Gut microbiota regulate hepatic von Willebrand factor synthesis and arterial thrombus formation via Toll-like receptor-2.* Blood, 2017. **130**(4): p. 542-553.
114. Hahn, C. and M.A. Schwartz, *Mechanotransduction in vascular physiology and atherogenesis.* Nat Rev Mol Cell Biol, 2009. **10**(1): p. 53-62.
115. Chistiakov, D.A., et al., *Mechanisms of foam cell formation in atherosclerosis.* J Mol Med (Berl), 2017. **95**(11): p. 1153-1165.
116. Bessueille, L. and D. Magne, *Inflammation: a culprit for vascular calcification in atherosclerosis and diabetes.* Cell Mol Life Sci, 2015. **72**(13): p. 2475-89.
117. Agatston, A.S., et al., *Quantification of coronary artery calcium using ultrafast computed tomography.* J Am Coll Cardiol, 1990. **15**(4): p. 827-32.
118. Smid, M., et al., *Thrombin generation in the Glasgow Myocardial Infarction Study.* PLoS One, 2013. **8**(6): p. e66977.
119. Lisman, T., *Platelet-neutrophil interactions as drivers of inflammatory and thrombotic disease.* Cell Tissue Res, 2018. **371**(3): p. 567-576.
120. Obermayer, G., T. Afonyushkin, and C.J. Binder, *Oxidized low-density lipoprotein in inflammation-driven thrombosis.* J Thromb Haemost, 2018. **16**(3): p. 418-428.
121. Davi, G. and C. Patrono, *Platelet activation and atherothrombosis.* N Engl J Med, 2007. **357**(24): p. 2482-94.
122. Lindemann, S., et al., *Activated platelets mediate inflammatory signaling by regulated interleukin 1beta synthesis.* J Cell Biol, 2001. **154**(3): p. 485-90.
123. Gawaz, M., H. Langer, and A.E. May, *Platelets in inflammation and atherogenesis.* J Clin Invest, 2005. **115**(12): p. 3378-84.
124. Vasina, E., et al., *Platelets and platelet-derived microparticles in vascular inflammatory disease.* Inflamm Allergy Drug Targets, 2010. **9**(5): p. 346-54.
125. Giesen, P.L., et al., *Blood-borne tissue factor: another view of thrombosis.* Proc Natl Acad Sci U S A, 1999. **96**(5): p. 2311-5.
126. von Bruhl, M.L., et al., *Monocytes, neutrophils, and platelets cooperate to initiate and propagate venous thrombosis in mice in vivo.* J Exp Med, 2012. **209**(4): p. 819-35.

127. Pillai, V.G., et al., *Human neutrophil peptides inhibit cleavage of von Willebrand factor by ADAMTS13: a potential link of inflammation to TTP.* Blood, 2016. **128**(1): p. 110-9.
128. Dolegowska, B., A. Lubkowska, and L. De Girolamo, *Platelet lipidomic.* J Biol Regul Homeost Agents, 2012. **26**(2 Suppl 1): p. 23S-33S.
129. Dobner, P. and B. Engelmann, *Low-density lipoproteins supply phospholipid-bound arachidonic acid for platelet eicosanoid production.* Am J Physiol, 1998. **275**(5 Pt 1): p. E777-84.
130. Sim, D.S., J.R. Dilks, and R. Flaumenhaft, *Platelets possess and require an active protein palmitoylation pathway for agonist-mediated activation and in vivo thrombus formation.* Arterioscler Thromb Vasc Biol, 2007. **27**(6): p. 1478-85.
131. Zhang, J., et al., *Dynamic Cycling of t-SNARE Acylation Regulates Platelet Exocytosis.* J Biol Chem, 2018.
132. Majerus, P.W., M.B. Smith, and G.H. Clamon, *Lipid metabolism in human platelets. I. Evidence for a complete fatty acid synthesizing system.* J Clin Invest, 1969. **48**(1): p. 156-64.
133. Deykin, D. and R.K. Desser, *The incorporation of acetate and palmitate into lipids by human platelets.* J Clin Invest, 1968. **47**(7): p. 1590-602.
134. O'Donnell, V.B., R.C. Murphy, and S.P. Watson, *Platelet lipidomics: modern day perspective on lipid discovery and characterization in platelets.* Circ Res, 2014. **114**(7): p. 1185-203.
135. Simon, C.G., Jr., S. Chatterjee, and A.R. Gear, *Sphingomyelinase activity in human platelets.* Thromb Res, 1998. **90**(4): p. 155-61.
136. Min, S.H. and C.S. Abrams, *Regulation of platelet plug formation by phosphoinositide metabolism.* Blood, 2013. **122**(8): p. 1358-65.
137. Murakami, M., et al., *Recent progress in phospholipase A(2) research: from cells to animals to humans.* Prog Lipid Res, 2011. **50**(2): p. 152-92.
138. Slatter, D.A., et al., *Mapping the Human Platelet Lipidome Reveals Cytosolic Phospholipase A2 as a Regulator of Mitochondrial Bioenergetics during Activation.* Cell Metab, 2016. **23**(5): p. 930-44.
139. Yoda, E., et al., *Group VIB calcium-independent phospholipase A2 (iPLA2gamma) regulates platelet activation, hemostasis and thrombosis in mice.* PLoS One, 2014. **9**(10): p. e109409.
140. Wong, D.A., et al., *Discrete role for cytosolic phospholipase A(2)alpha in platelets: studies using single and double mutant mice of cytosolic and group IIA secretory phospholipase A(2).* J Exp Med, 2002. **196**(3): p. 349-57.
141. Shankar, H., et al., *P2Y12 receptor-mediated potentiation of thrombin-induced thromboxane A2 generation in platelets occurs through regulation of Erk1/2 activation.* J Thromb Haemost, 2006. **4**(3): p. 638-47.

142. Kramer, R.M., et al., *p38 mitogen-activated protein kinase phosphorylates cytosolic phospholipase A2 (cPLA2) in thrombin-stimulated platelets. Evidence that proline-directed phosphorylation is not required for mobilization of arachidonic acid by cPLA2.* J Biol Chem, 1996. **271**(44): p. 27723-9.
143. Grouse, L.H., et al., *Surface-activated bovine platelets do not spread, they unfold.* Am J Pathol, 1990. **136**(2): p. 399-408.
144. Bettache, N., et al., *Mechanical constraint imposed on plasma membrane through transverse phospholipid imbalance induces reversible actin polymerization via phosphoinositide 3-kinase activation.* J Cell Sci, 2003. **116**(Pt 11): p. 2277-84.
145. Salaun, C., D.J. James, and L.H. Chamberlain, *Lipid rafts and the regulation of exocytosis.* Traffic, 2004. **5**(4): p. 255-64.
146. Koseoglu, S., et al., *Analytical characterization of the role of phospholipids in platelet adhesion and secretion.* Anal Chem, 2015. **87**(1): p. 413-21.
147. Niggli, V., *Structural properties of lipid-binding sites in cytoskeletal proteins.* Trends Biochem Sci, 2001. **26**(10): p. 604-11.
148. Wang, Y., et al., *Platelets lacking PIP5KIgamma have normal integrin activation but impaired cytoskeletal-membrane integrity and adhesion.* Blood, 2013. **121**(14): p. 2743-52.
149. Kam, J.L., et al., *Phosphoinositide-dependent activation of the ADP-ribosylation factor GTPase-activating protein ASAP1. Evidence for the pleckstrin homology domain functioning as an allosteric site.* J Biol Chem, 2000. **275**(13): p. 9653-63.
150. Gilmore, A.P. and K. Burridge, *Regulation of vinculin binding to talin and actin by phosphatidyl-inositol-4-5-bisphosphate.* Nature, 1996. **381**(6582): p. 531-5.
151. Bodin, S., H. Tronchere, and B. Payrastre, *Lipid rafts are critical membrane domains in blood platelet activation processes.* Biochim Biophys Acta, 2003. **1610**(2): p. 247-57.
152. Locke, D., et al., *Lipid rafts orchestrate signaling by the platelet receptor glycoprotein VI.* J Biol Chem, 2002. **277**(21): p. 18801-9.
153. Shrimpton, C.N., et al., *Localization of the adhesion receptor glycoprotein Ib-IX-V complex to lipid rafts is required for platelet adhesion and activation.* J Exp Med, 2002. **196**(8): p. 1057-66.
154. Quinton, T.M., et al., *Lipid rafts are required in Galpha(i) signaling downstream of the P2Y12 receptor during ADP-mediated platelet activation.* J Thromb Haemost, 2005. **3**(5): p. 1036-41.
155. Moscardo, A., et al., *The association of thromboxane A2 receptor with lipid rafts is a determinant for platelet functional responses.* FEBS Lett, 2014. **588**(17): p. 3154-9.

156. Kasahara, K., et al., *Clot retraction is mediated by factor XIII-dependent fibrin-alphaIIbbeta3-myosin axis in platelet sphingomyelin-rich membrane rafts.* Blood, 2013. **122**(19): p. 3340-8.
157. Lee, S.B., et al., *Decreased expression of phospholipase C-beta 2 isozyme in human platelets with impaired function.* Blood, 1996. **88**(5): p. 1684-91.
158. Zheng, Y., et al., *Restoration of responsiveness of phospholipase Cgamma2-deficient platelets by enforced expression of phospholipase Cgamma1.* PLoS One, 2015. **10**(3): p. e0119739.
159. Adler, D.H., et al., *Inherited human cPLA(2alpha) deficiency is associated with impaired eicosanoid biosynthesis, small intestinal ulceration, and platelet dysfunction.* J Clin Invest, 2008. **118**(6): p. 2121-31.
160. Duvernay, M.T., et al., *Platelet Lipidomic Profiling: Novel Insight into Cytosolic Phospholipase A2alpha Activity and Its Role in Human Platelet Activation.* Biochemistry, 2015. **54**(36): p. 5578-88.
161. Quach, M.E., W. Chen, and R. Li, *Mechanisms of platelet clearance and translation to improve platelet storage.* Blood, 2018. **131**(14): p. 1512-1521.
162. Clark, S.R., et al., *Characterization of platelet aminophospholipid externalization reveals fatty acids as molecular determinants that regulate coagulation.* Proc Natl Acad Sci U S A, 2013. **110**(15): p. 5875-80.
163. Alonzo, M.T., et al., *Platelet apoptosis and apoptotic platelet clearance by macrophages in secondary dengue virus infections.* J Infect Dis, 2012. **205**(8): p. 1321-9.
164. Fidler, T.P., et al., *Deletion of GLUT1 and GLUT3 Reveals Multiple Roles for Glucose Metabolism in Platelet and Megakaryocyte Function.* Cell Rep, 2017. **20**(4): p. 881-894.
165. Newton, A.C., *Protein kinase C: structure, function, and regulation.* J Biol Chem, 1995. **270**(48): p. 28495-8.
166. Thomas, C.P., et al., *Phospholipid-esterified eicosanoids are generated in agonist-activated human platelets and enhance tissue factor-dependent thrombin generation.* J Biol Chem, 2010. **285**(10): p. 6891-903.
167. Li, Z., et al., *Two waves of platelet secretion induced by thromboxane A2 receptor and a critical role for phosphoinositide 3-kinases.* J Biol Chem, 2003. **278**(33): p. 30725-31.
168. Naik, M.U., et al., *Ask1 regulates murine platelet granule secretion, thromboxane A2 generation, and thrombus formation.* Blood, 2017. **129**(9): p. 1197-1209.
169. Vito, C.D., et al., *Platelet-derived sphingosine-1-phosphate and inflammation: from basic mechanisms to clinical implications.* Platelets, 2016. **27**(5): p. 393-401.

170. Palur Ramakrishnan, A.V., et al., *Platelet activating factor: A potential biomarker in acute coronary syndrome?* Cardiovasc Ther, 2017. **35**(1): p. 64-70.
171. Kramer, P.A., et al., *A review of the mitochondrial and glycolytic metabolism in human platelets and leukocytes: Implications for their use as bioenergetic biomarkers.* Redox Biol, 2014. **2**: p. 206-10.
172. Papp, B., et al., *Simultaneous presence of two distinct endoplasmic-reticulum-type calcium-pump isoforms in human cells. Characterization by radio-immunoblotting and inhibition by 2,5-di-(t-butyl)-1,4-benzohydroquinone.* Biochem J, 1992. **288 (Pt 1)**: p. 297-302.
173. Redondo, P.C., et al., *Collaborative effect of SERCA and PMCA in cytosolic calcium homeostasis in human platelets.* J Physiol Biochem, 2005. **61**(4): p. 507-16.
174. Heijnen, H.F., et al., *Thrombin stimulates glucose transport in human platelets via the translocation of the glucose transporter GLUT-3 from alpha-granules to the cell surface.* J Cell Biol, 1997. **138**(2): p. 323-30.
175. Ferreira, I.A., et al., *Glucose uptake via glucose transporter 3 by human platelets is regulated by protein kinase B.* J Biol Chem, 2005. **280**(38): p. 32625-33.
176. Fidler, T.P., et al., *Glucose Transporter 3 Potentiates Degranulation and Is Required for Platelet Activation.* Arterioscler Thromb Vasc Biol, 2017. **37**(9): p. 1628-1639.
177. Murer, E.H., *Clot retraction and energy metabolism of platelets. Effect and mechanism of inhibitors.* Biochim Biophys Acta, 1969. **172**(2): p. 266-76.
178. Misselwitz, F., V.L. Leytin, and V.S. Repin, *Effect of metabolic inhibitors on platelet attachment, spreading and aggregation on collagen-coated surfaces.* Thromb Res, 1987. **46**(2): p. 233-40.
179. Scott, R.B., *Activation of glycogen phosphorylase in blood platelets.* Blood, 1967. **30**(3): p. 321-30.
180. Guppy, M., et al., *Fuel choices by human platelets in human plasma.* Eur J Biochem, 1997. **244**(1): p. 161-7.
181. Bressler, N.M., M.J. Broekman, and A.J. Marcus, *Concurrent studies of oxygen consumption and aggregation in stimulated human platelets.* Blood, 1979. **53**(2): p. 167-78.
182. Corona de la Pena, N., et al., *Glycoprotein Ib activation by thrombin stimulates the energy metabolism in human platelets.* PLoS One, 2017. **12**(8): p. e0182374.
183. Holmsen, H., K.L. Kaplan, and C.A. Dangelmaier, *Differential energy requirements for platelet responses. A simultaneous study of aggregation, three secretory processes, arachidonate liberation, phosphatidylinositol*

breakdown and phosphatidate production. Biochem J, 1982. **208**(1): p. 9-18.
184. Peerschke, E.I., *Maintenance of GPIIb-IIIa avidity supporting "irreversible" fibrinogen binding is energy-dependent.* J Lab Clin Med, 1999. **134**(4): p. 398-404.
185. Ishikura, H., N. Takeyama, and T. Tanaka, *Effects of 2-tetradecylglycidic acid on rat platelet energy metabolism and aggregation.* Biochim Biophys Acta, 1992. **1128**(2-3): p. 193-8.
186. Willoughby, S.R., et al., *Inhibition of long-chain fatty acid metabolism does not affect platelet aggregation responses.* Eur J Pharmacol, 1998. **356**(2-3): p. 207-13.
187. Vasta, V., et al., *Glutamine transport and enzymatic activities involved in glutaminolysis in human platelets.* Biochim Biophys Acta, 1995. **1243**(1): p. 43-8.
188. Vasta, V., et al., *Glutamine utilization in resting and stimulated platelets.* J Biochem, 1993. **114**(2): p. 163-6.
189. Lanyon-Hogg, T., et al., *Dynamic Protein Acylation: New Substrates, Mechanisms, and Drug Targets.* Trends Biochem Sci, 2017. **42**(7): p. 566-581.
190. Dowal, L., et al., *Proteomic analysis of palmitoylated platelet proteins.* Blood, 2011. **118**(13): p. e62-73.
191. Huang, E.M., *Agonist-enhanced palmitoylation of platelet proteins.* Biochim Biophys Acta, 1989. **1011**(2-3): p. 134-9.
192. Israels, S.J. and E.M. McMillan-Ward, *Palmitoylation supports the association of tetraspanin CD63 with CD9 and integrin alphaIIbbeta3 in activated platelets.* Thromb Res, 2010. **125**(2): p. 152-8.
193. Canobbio, I., et al., *Targeting of the small GTPase Rap2b, but not Rap1b, to lipid rafts is promoted by palmitoylation at Cys176 and Cys177 and is required for efficient protein activation in human platelets.* Cell Signal, 2008. **20**(9): p. 1662-70.
194. Muszbek, L., E. Racz, and M. Laposata, *Posttranslational modification of proteins with fatty acids in platelets.* Prostaglandins Leukot Essent Fatty Acids, 1997. **57**(4-5): p. 359-66.
195. Schick, P.K. and J. Walker, *The acylation of megakaryocyte proteins: glycoprotein IX is primarily myristoylated while glycoprotein Ib is palmitoylated.* Blood, 1996. **87**(4): p. 1377-84.
196. Tong, L., *Structure and function of biotin-dependent carboxylases.* Cell Mol Life Sci, 2013. **70**(5): p. 863-91.
197. Abu-Elheiga, L., et al., *The subcellular localization of acetyl-CoA carboxylase 2.* Proc Natl Acad Sci U S A, 2000. **97**(4): p. 1444-9.

198. Abu-Elheiga, L., et al., *Mutant mice lacking acetyl-CoA carboxylase 1 are embryonically lethal.* Proc Natl Acad Sci U S A, 2005. **102**(34): p. 12011-6.
199. Abu-Elheiga, L., et al., *Continuous fatty acid oxidation and reduced fat storage in mice lacking acetyl-CoA carboxylase 2.* Science, 2001. **291**(5513): p. 2613-6.
200. Wakil, S.J. and L.A. Abu-Elheiga, *Fatty acid metabolism: target for metabolic syndrome.* J Lipid Res, 2009. **50 Suppl**: p. S138-43.
201. Wang, C., et al., *The acetyl-CoA carboxylase enzyme: a target for cancer therapy?* Expert Rev Anticancer Ther, 2015. **15**(6): p. 667-76.
202. Brownsey, R.W., et al., *Regulation of acetyl-CoA carboxylase.* Biochem Soc Trans, 2006. **34**(Pt 2): p. 223-7.
203. Hardie, D.G., *Regulation of fatty acid and cholesterol metabolism by the AMP-activated protein kinase.* Biochim Biophys Acta, 1992. **1123**(3): p. 231-8.
204. Davies, S.P., A.T. Sim, and D.G. Hardie, *Location and function of three sites phosphorylated on rat acetyl-CoA carboxylase by the AMP-activated protein kinase.* Eur J Biochem, 1990. **187**(1): p. 183-90.
205. Ha, J., et al., *Critical phosphorylation sites for acetyl-CoA carboxylase activity.* J Biol Chem, 1994. **269**(35): p. 22162-8.
206. Munday, M.R., et al., *Identification by amino acid sequencing of three major regulatory phosphorylation sites on rat acetyl-CoA carboxylase.* Eur J Biochem, 1988. **175**(2): p. 331-8.
207. Cho, Y.S., et al., *Molecular mechanism for the regulation of human ACC2 through phosphorylation by AMPK.* Biochem Biophys Res Commun, 2010. **391**(1): p. 187-92.
208. Abu-Elheiga, L., et al., *Human acetyl-CoA carboxylase 2. Molecular cloning, characterization, chromosomal mapping, and evidence for two isoforms.* J Biol Chem, 1997. **272**(16): p. 10669-77.
209. Fullerton, M.D., et al., *Single phosphorylation sites in Acc1 and Acc2 regulate lipid homeostasis and the insulin-sensitizing effects of metformin.* Nat Med, 2013. **19**(12): p. 1649-54.
210. O'Neill, H.M., et al., *AMPK phosphorylation of ACC2 is required for skeletal muscle fatty acid oxidation and insulin sensitivity in mice.* Diabetologia, 2014. **57**(8): p. 1693-702.
211. O'Neill, H.M., et al., *Skeletal muscle ACC2 S212 phosphorylation is not required for the control of fatty acid oxidation during exercise.* Physiol Rep, 2015. **3**(7).
212. Zordoky, B.N., et al., *AMPK-dependent inhibitory phosphorylation of ACC is not essential for maintaining myocardial fatty acid oxidation.* Circ Res, 2014. **115**(5): p. 518-24.

213. Signorello, M.G. and G. Leoncini, *Activation of CaMKKbeta/AMPKalpha pathway by 2-AG in human platelets.* J Cell Biochem, 2017. **119**(1): p. 876-884.
214. Randriamboavonjy, V., et al., *AMPK alpha2 subunit is involved in platelet signaling, clot retraction, and thrombus stability.* Blood, 2010. **116**(12): p. 2134-40.
215. Rowley, J.W., et al., *Genome-wide RNA-seq analysis of human and mouse platelet transcriptomes.* Blood, 2011. **118**(14): p. e101-11.
216. Burkhart, J.M., et al., *The first comprehensive and quantitative analysis of human platelet protein composition allows the comparative analysis of structural and functional pathways.* Blood, 2012. **120**(15): p. e73-82.
217. Randriamboavonjy, V., et al., *Metformin reduces hyper-reactivity of platelets from patients with polycystic ovary syndrome by improving mitochondrial integrity.* Thromb Haemost, 2015. **114**(3): p. 569-78.
218. Sakamoto, K., et al., *Activity of LKB1 and AMPK-related kinases in skeletal muscle: effects of contraction, phenformin, and AICAR.* Am J Physiol Endocrinol Metab, 2004. **287**(2): p. E310-7.
219. Iverson, A.J., et al., *Immunological analysis of acetyl-CoA carboxylase mass, tissue distribution and subunit composition.* Biochem J, 1990. **269**(2): p. 365-71.
220. Carling, D., V.A. Zammit, and D.G. Hardie, *A common bicyclic protein kinase cascade inactivates the regulatory enzymes of fatty acid and cholesterol biosynthesis.* FEBS Lett, 1987. **223**(2): p. 217-22.
221. Pula, G., et al., *PKCdelta regulates collagen-induced platelet aggregation through inhibition of VASP-mediated filopodia formation.* Blood, 2006. **108**(13): p. 4035-44.
222. Munzer, P., et al., *PDK1 Determines Collagen-Dependent Platelet Ca2+ Signaling and Is Critical to Development of Ischemic Stroke In Vivo.* Arterioscler Thromb Vasc Biol, 2016. **36**(8): p. 1507-16.
223. Nocella, C., et al., *Lipopolysaccharide as trigger of platelet aggregation via eicosanoid over-production.* Thromb Haemost, 2017. **117**(8): p. 1558-1570.
224. Chacko, B.K., et al., *Methods for defining distinct bioenergetic profiles in platelets, lymphocytes, monocytes, and neutrophils, and the oxidative burst from human blood.* Lab Invest, 2013. **93**(6): p. 690-700.
225. Nguyen, Q.L., et al., *Platelets from pulmonary hypertension patients show increased mitochondrial reserve capacity.* JCI Insight, 2017. **2**(5): p. e91415.
226. Akkerman, J.W. and H. Holmsen, *Interrelationships among platelet responses: studies on the burst in proton liberation, lactate production, and oxygen uptake during platelet aggregation and Ca2+ secretion.* Blood, 1981. **57**(5): p. 956-66.

227. Mattheij, N.J., et al., *Dual mechanism of integrin alphaIIbbeta3 closure in procoagulant platelets.* J Biol Chem, 2013. **288**(19): p. 13325-36.
228. de Witt, S.M., et al., *Identification of platelet function defects by multi-parameter assessment of thrombus formation.* Nat Commun, 2014. **5**: p. 4257.
229. Musumeci, L., et al., *Dual-specificity phosphatase 3 deficiency or inhibition limits platelet activation and arterial thrombosis.* Circulation, 2015. **131**(7): p. 656-68.
230. Lintonen, T.P., et al., *Differential mobility spectrometry-driven shotgun lipidomics.* Anal Chem, 2014. **86**(19): p. 9662-9.
231. Vilahur, G., L. Casani, and L. Badimon, *A thromboxane A2/prostaglandin H2 receptor antagonist (S18886) shows high antithrombotic efficacy in an experimental model of stent-induced thrombosis.* Thromb Haemost, 2007. **98**(3): p. 662-9.
232. Kuijpers, M.J., et al., *Role of murine integrin alpha2beta1 in thrombus stabilization and embolization: contribution of thromboxane A2.* Thromb Haemost, 2007. **98**(5): p. 1072-80.
233. Berod, L., et al., *De novo fatty acid synthesis controls the fate between regulatory T and T helper 17 cells.* Nat Med, 2014. **20**(11): p. 1327-33.
234. Turini, M.E. and B.J. Holub, *Eicosanoid/thromboxane A2-independent and -dependent generation of lysoplasmenylethanolamine via phospholipase A2 in collagen-stimulated human platelets.* Biochem J, 1993. **289 (Pt 3)**: p. 641-6.
235. Mao, J., et al., *Liver-specific deletion of acetyl-CoA carboxylase 1 reduces hepatic triglyceride accumulation without affecting glucose homeostasis.* Proc Natl Acad Sci U S A, 2006. **103**(22): p. 8552-7.
236. Peng, B., et al., *Identification of key lipids critical for platelet activation by comprehensive analysis of the platelet lipidome.* Blood, 2018.**132**(5): p. e1-e12
237. Li, W., et al., *Thymidine phosphorylase participates in platelet signaling and promotes thrombosis.* Circ Res, 2014. **115**(12): p. 997-1006.
238. Massberg, S., et al., *A crucial role of glycoprotein VI for platelet recruitment to the injured arterial wall in vivo.* J Exp Med, 2003. **197**(1): p. 41-9.
239. Konstantinides, S., et al., *Distinct antithrombotic consequences of platelet glycoprotein Ibalpha and VI deficiency in a mouse model of arterial thrombosis.* J Thromb Haemost, 2006. **4**(9): p. 2014-21.
240. Eckly, A., et al., *Mechanisms underlying FeCl3-induced arterial thrombosis.* Journal of Thrombosis and Haemostasis, 2011. **9**(4): p. 779-789.
241. Ciciliano, J.C., et al., *Resolving the multifaceted mechanisms of the ferric chloride thrombosis model using an interdisciplinary microfluidic approach.* Blood, 2015. **126**(6): p. 817-24.

242. Barr, J.D., et al., *Red blood cells mediate the onset of thrombosis in the ferric chloride murine model.* Blood, 2013. **121**(18): p. 3733-41.
243. Rinder, C.S., et al., *Aspirin does not inhibit adenosine diphosphate-induced platelet alpha-granule release.* Blood, 1993. **82**(2): p. 505-12.
244. Prevost, N., et al., *Eph kinases and ephrins support thrombus growth and stability by regulating integrin outside-in signaling in platelets.* Proc Natl Acad Sci U S A, 2005. **102**(28): p. 9820-5.
245. Nanda, N., et al., *Platelet endothelial aggregation receptor 1 (PEAR1), a novel epidermal growth factor repeat-containing transmembrane receptor, participates in platelet contact-induced activation.* J Biol Chem, 2005. **280**(26): p. 24680-9.
246. Stalker, T.J., et al., *A systems approach to hemostasis: 3. Thrombus consolidation regulates intrathrombus solute transport and local thrombin activity.* Blood, 2014. **124**(11): p. 1824-31.
247. Takamura, H., et al., *Differential hydrolysis of phospholipid molecular species during activation of human platelets with thrombin and collagen.* J Biol Chem, 1987. **262**(5): p. 2262-9.
248. Mastenbroek, T.G., et al., *Acute and persistent platelet and coagulant activities in atherothrombosis.* J Thromb Haemost, 2015. **13 Suppl 1**: p. S272-80.
249. Merlini, P.A., et al., *Persistent activation of coagulation mechanism in unstable angina and myocardial infarction.* Circulation, 1994. **90**(1): p. 61-8.
250. Eikelboom, J.W., et al., *Rivaroxaban with or without Aspirin in Stable Cardiovascular Disease.* N Engl J Med, 2017. **377**(14): p. 1319-1330.
251. Podrez, E.A., et al., *Platelet CD36 links hyperlipidemia, oxidant stress and a prothrombotic phenotype.* Nat Med, 2007. **13**(9): p. 1086-95.
252. Dyck, J.R., et al., *Phosphorylation control of cardiac acetyl-CoA carboxylase by cAMP-dependent protein kinase and 5'-AMP activated protein kinase.* Eur J Biochem, 1999. **262**(1): p. 184-90.
253. Lepropre, S., et al., *AMPK-ACC signaling modulates platelet phospholipids content and potentiates platelet function and thrombus formation.* Blood, 2018.
254. Chatterjee, M., et al., *Regulation of oxidized platelet lipidome: implications for coronary artery disease.* Eur Heart J, 2017. **38**(25): p. 1993-2005
255. Stacklies, W., et al., *pcaMethods--a bioconductor package providing PCA methods for incomplete data.* Bioinformatics, 2007. **23**(9): p. 1164-7.
256. Benjamini, Y. and Y. Hochberg, *Controlling the False Discovery Rate: A Practical and Powerful Approach to Multiple Testing.* Journal of the Royal Statistical Society, 1995. **57**(1): p. 289-300.

257. Beaulieu, L.M., et al., *Interleukin 1 receptor 1 and interleukin 1beta regulate megakaryocyte maturation, platelet activation, and transcript profile during inflammation in mice and humans.* Arterioscler Thromb Vasc Biol, 2014. **34**(3): p. 552-64.
258. Hanak, V., et al., *Accuracy of the triglyceride to high-density lipoprotein cholesterol ratio for prediction of the low-density lipoprotein phenotype B.* Am J Cardiol, 2004. **94**(2): p. 219-22.
259. Harmon, M.E., et al., *Associations of Circulating Oxidized LDL and Conventional Biomarkers of Cardiovascular Disease in a Cross-Sectional Study of the Navajo Population.* PLoS One, 2016. **11**(3): p. e0143102.
260. Kaasenbrood, L., et al., *Distribution of Estimated 10-Year Risk of Recurrent Vascular Events and Residual Risk in a Secondary Prevention Population.* Circulation, 2016. **134**(19): p. 1419-1429.
261. Sabatine, M.S., et al., *Evolocumab and Clinical Outcomes in Patients with Cardiovascular Disease.* N Engl J Med, 2017. **376**(18): p. 1713-1722.
262. Gurbel, P.A., et al., *Platelet function monitoring in patients with coronary artery disease.* J Am Coll Cardiol, 2007. **50**(19): p. 1822-34.
263. Michelson, A.D., et al., *Circulating monocyte-platelet aggregates are a more sensitive marker of in vivo platelet activation than platelet surface P-selectin: studies in baboons, human coronary intervention, and human acute myocardial infarction.* Circulation, 2001. **104**(13): p. 1533-7.
264. Linden, M.D., et al., *Indices of platelet activation and the stability of coronary artery disease.* J Thromb Haemost, 2007. **5**(4): p. 761-5.
265. Stellos, K., et al., *Platelet-bound P-selectin expression in patients with coronary artery disease: impact on clinical presentation and myocardial necrosis, and effect of diabetes mellitus and anti-platelet medication.* J Thromb Haemost, 2010. **8**(1): p. 205-7.
266. Konopatskaya, O., et al., *PKCalpha regulates platelet granule secretion and thrombus formation in mice.* J Clin Invest, 2009. **119**(2): p. 399-407.
267. Ruuth, M., et al., *Susceptibility of low-density lipoprotein particles to aggregate depends on particle lipidome, is modifiable, and associates with future cardiovascular deaths.* Eur Heart J, 2018. **39**(27): p. 2562-2573.
268. Laufs, U. and O. Weingartner, *Pathological phenotypes of LDL particles.* Eur Heart J, 2018. **39**(27): p. 2574-2576.
269. Chen, K., et al., *A specific CD36-dependent signaling pathway is required for platelet activation by oxidized low-density lipoprotein.* Circ Res, 2008. **102**(12): p. 1512-9.
270. Kim, C.W., et al., *Acetyl CoA Carboxylase Inhibition Reduces Hepatic Steatosis but Elevates Plasma Triglycerides in Mice and Humans: A Bedside to Bench Investigation.* Cell Metab, 2017. **26**(2): p. 394-406 e6.

271. Svensson, R.U., et al., *Inhibition of acetyl-CoA carboxylase suppresses fatty acid synthesis and tumor growth of non-small-cell lung cancer in preclinical models.* Nat Med, 2016. **22**(10): p. 1108-1119.
272. Ibrahim, H., et al., *Detection and quantification of circulating immature platelets: agreement between flow cytometric and automated detection.* J Thromb Thrombolysis, 2016. **42**(1): p. 77-83.
273. Calay, D., et al., *Copper and myeloperoxidase-modified LDLs activate Nrf2 through different pathways of ROS production in macrophages.* Antioxid Redox Signal, 2010. **13**(10): p. 1491-502.
274. Delporte, C., et al., *Impact of myeloperoxidase-LDL interactions on enzyme activity and subsequent posttranslational oxidative modifications of apoB-100.* J Lipid Res, 2014. **55**(4): p. 747-57.
275. Lowry, O.H., et al., *Protein measurement with the Folin phenol reagent.* J Biol Chem, 1951. **193**(1): p. 265-75.
276. Greenland, P., et al., *Coronary Calcium Score and Cardiovascular Risk.* J Am Coll Cardiol, 2018. **72**(4): p. 434-447.
277. Matyash, V., et al., *Lipid extraction by methyl-tert-butyl ether for high-throughput lipidomics.* J Lipid Res, 2008. **49**(5): p. 1137-46.
278. Giera, M., et al., *Lipid and lipid mediator profiling of human synovial fluid in rheumatoid arthritis patients by means of LC-MS/MS.* Biochim Biophys Acta, 2012. **1821**(11): p. 1415-24.
279. Matsushima, Y., et al., *Inhibition by the antilipogenic antibiotic cerulenin of thrombin-induced activation of human platelets.* Thromb Res, 1988. **49**(1): p. 79-90.
280. Ma, L., et al., *An ACACB variant implicated in diabetic nephropathy associates with body mass index and gene expression in obese subjects.* PLoS One, 2013. **8**(2): p. e56193.
281. Jiang, H., et al., *Genetic variants in de novo lipogenic pathway genes predict the prognosis of surgically-treated hepatocellular carcinoma.* Sci Rep, 2015. **5**: p. 9536.
282. Sinilnikova, O.M., et al., *Haplotype-based analysis of common variation in the acetyl-coA carboxylase alpha gene and breast cancer risk: a case-control study nested within the European Prospective Investigation into Cancer and Nutrition.* Cancer Epidemiol Biomarkers Prev, 2007. **16**(3): p. 409-15.
283. Matsumoto, H., et al., *The SNPs in the ACACA gene are effective on fatty acid composition in Holstein milk.* Mol Biol Rep, 2012. **39**(9): p. 8637-44.
284. Munoz, M., et al., *Survey of SSC12 Regions Affecting Fatty Acid Composition of Intramuscular Fat Using High-Density SNP Data.* Front Genet, 2011. **2**: p. 101.

285. Kim, C.W., et al., *Acetyl CoA Carboxylase Inhibition Reduces Hepatic Steatosis but Elevates Plasma Triglycerides in Mice and Humans: A Bedside to Bench Investigation.* Cell Metab, 2017. **26**(2): p. 394-406.e6.
286. Harriman, G., et al., *Acetyl-CoA carboxylase inhibition by ND-630 reduces hepatic steatosis, improves insulin sensitivity, and modulates dyslipidemia in rats.* Proc Natl Acad Sci U S A, 2016. **113**(13): p. E1796-805.
287. Stoetzer, C., et al., *Olive Oil-Based Lipid Emulsions Do Not Influence Platelet Receptor Expression in Comparison to Medium and Long Chain Triglycerides In vitro.* Lipids, 2016. **51**(11): p. 1241-1248.
288. Broijersen, A., et al., *Alimentary lipemia enhances the membrane expression of platelet P-selectin without affecting other markers of platelet activation.* Atherosclerosis, 1998. **137**(1): p. 107-13.
289. da Motta, N.A. and F.C. de Brito, *Cilostazol exerts antiplatelet and anti-inflammatory effects through AMPK activation and NF-kB inhibition on hypercholesterolemic rats.* Fundam Clin Pharmacol, 2016. **30**(4): p. 327-37.
290. Pedreno, J., et al., *Platelet function in patients with familial hypertriglyceridemia: evidence that platelet reactivity is modulated by apolipoprotein E content of very-low-density lipoprotein particles.* Metabolism, 2000. **49**(7): p. 942-9.
291. Aviram, M. and R.J. Deckelbaum, *Intralipid infusion into humans reduces in vitro platelet aggregation and alters platelet lipid composition.* Metabolism, 1989. **38**(4): p. 343-7.
292. Kato, R., et al., *Transient increase in plasma oxidized LDL during the progression of atherosclerosis in apolipoprotein E knockout mice.* Arterioscler Thromb Vasc Biol, 2009. **29**(1): p. 33-9.
293. Zhang, W.J., et al., *Dietary alpha-lipoic acid supplementation inhibits atherosclerotic lesion development in apolipoprotein E-deficient and apolipoprotein E/low-density lipoprotein receptor-deficient mice.* Circulation, 2008. **117**(3): p. 421-8.
294. Tong, L. and H.J. Harwood, Jr., *Acetyl-coenzyme A carboxylases: versatile targets for drug discovery.* J Cell Biochem, 2006. **99**(6): p. 1476-88.
295. Glund, S., et al., *Inhibition of acetyl-CoA carboxylase 2 enhances skeletal muscle fatty acid oxidation and improves whole-body glucose homeostasis in db/db mice.* Diabetologia, 2012. **55**(7): p. 2044-53.
296. Harwood, H.J., Jr., et al., *Isozyme-nonselective N-substituted bipiperidylcarboxamide acetyl-CoA carboxylase inhibitors reduce tissue malonyl-CoA concentrations, inhibit fatty acid synthesis, and increase fatty acid oxidation in cultured cells and in experimental animals.* J Biol Chem, 2003. **278**(39): p. 37099-111.

297. Luo, J., et al., *Acetyl-CoA carboxylase rewires cancer metabolism to allow cancer cells to survive inhibition of the Warburg effect by cetuximab.* Cancer Lett, 2017. **384**: p. 39-49.
298. Griffith, D.A., et al., *Decreasing the rate of metabolic ketone reduction in the discovery of a clinical acetyl-CoA carboxylase inhibitor for the treatment of diabetes.* J Med Chem, 2014. **57**(24): p. 10512-26.
299. Luo, D.X., et al., *Targeting acetyl-CoA carboxylases: small molecular inhibitors and their therapeutic potential.* Recent Pat Anticancer Drug Discov, 2012. **7**(2): p. 168-84.
300. Bourbeau, M.P. and M.D. Bartberger, *Recent advances in the development of acetyl-CoA carboxylase (ACC) inhibitors for the treatment of metabolic disease.* J Med Chem, 2015. **58**(2): p. 525-36.
301. Stiede, K., et al., *Acetyl-coenzyme A carboxylase inhibition reduces de novo lipogenesis in overweight male subjects: A randomized, double-blind, crossover study.* Hepatology, 2017. **66**(2): p. 324-334.
302. Lane, M.D., et al., *Role of malonyl-CoA in the hypothalamic control of food intake and energy expenditure.* Biochem Soc Trans, 2005. **33**(Pt 5): p. 1063-7.
303. An, J., et al., *Hepatic expression of malonyl-CoA decarboxylase reverses muscle, liver and whole-animal insulin resistance.* Nat Med, 2004. **10**(3): p. 268-74.
304. Sambandam, N. and G.D. Lopaschuk, *AMP-activated protein kinase (AMPK) control of fatty acid and glucose metabolism in the ischemic heart.* Prog Lipid Res, 2003. **42**(3): p. 238-56.
305. Choudhary, C., et al., *The growing landscape of lysine acetylation links metabolism and cell signalling.* Nat Rev Mol Cell Biol, 2014. **15**(8): p. 536-50.
306. Aslan, J.E., et al., *Lysine acetyltransfer supports platelet function.* J Thromb Haemost, 2015. **13**(10): p. 1908-17.
307. Latorre, A. and A. Moscardo, *Regulation of Platelet Function by Acetylation/Deacetylation Mechanisms.* Curr Med Chem, 2016. **23**(35): p. 3966-3974.
308. Moscardo, A., et al., *The histone deacetylase sirtuin 2 is a new player in the regulation of platelet function.* J Thromb Haemost, 2015. **13**(7): p. 1335-44.
309. Chow, J.D., et al., *Genetic inhibition of hepatic acetyl-CoA carboxylase activity increases liver fat and alters global protein acetylation.* Mol Metab, 2014. **3**(4): p. 419-31.
310. Galdieri, L., et al., *Activation of AMP-activated Protein Kinase by Metformin Induces Protein Acetylation in Prostate and Ovarian Cancer Cells.* J Biol Chem, 2016. **291**(48): p. 25154-25166.

311. Rios Garcia, M., et al., *Acetyl-CoA Carboxylase 1-Dependent Protein Acetylation Controls Breast Cancer Metastasis and Recurrence.* Cell Metab, 2017. **26**(6): p. 842-855.e5.